

LIQUEFACTION PATHWAYS OF BITUMINOUS AND SUBBITUMINOUS COALS AND THEIR INTERMEDIATES

Robert A. Keogh, Liguang Xu, Scott Lambert,
and Burtron H. Davis

Center for Applied Energy Research
University of Kentucky
3572 Iron Works Pike
Lexington, KY 40511

Keywords: Liquefaction, Pathway, Coal

ABSTRACT

Thermal liquefaction studies of a number of high volatile bituminous coals suggest that these coals have a common liquefaction pathway. Verification of this pathway was confirmed using a single coal and a number of reaction conditions. The addition of a catalyst did not alter the observed thermal pathway. The thermal and catalytic liquefaction pathway obtained for a subbituminous coal was significantly different from the one obtained for the bituminous coals. To investigate ways to alter the bituminous coal liquefaction pathway, the intermediates, asphaltenes and preasphaltenes, were prepared, isolated and liquefied in batch reactors to determine their conversion pathway.

INTRODUCTION

Historically, lumped parameter kinetic models have been used successfully to describe industrially significant processes such as catalytic cracking (1), catalytic reforming (1), and condensation polymerization (2). The same approach has been used in the description of the various liquefaction processes (3,4). A physically realistic and technically viable lumped parameter kinetic model for liquefaction would be of considerable value in the development of pathways, mechanism, and the scale-up of the liquefaction processes.

In the work presented here, the solubility classes obtained from the liquefaction products of the coals were lumped into the following parameters: (a) oils plus gases (O+G), (b) asphaltenes plus preasphaltenes (A+P) and (c) insoluble organic matter (IOM). The lumped parameters used for the liquefaction products obtained from the intermediates asphaltenes and preasphaltenes were: (a) O+G, (b) asphaltenes, and (c) preasphaltenes plus IOM. The lumped parameters were plotted on a triangular diagram for interpretation.

EXPERIMENTAL

The description of the coals used in these study has been given in detail elsewhere (5). All of the liquefaction experiments using the coals were performed in 50 mL batch autoclaves using a hydrogen atmosphere and tetralin as the solvent. Details of the liquefaction runs and the analytical methods used have been described elsewhere (5).

The liquefaction of the intermediates were performed in 25 mL batch autoclaves using the same procedures as those used for the coals.

The intermediates, asphaltenes and preasphaltenes, were obtained from the liquefaction of a Western Kentucky #9 coal and a heavy petroleum resid which contained no asphaltenes. The coal/resid slurry was run in the CAER 1/8 tpd pilot plant using a 1 ℓ CSTR, a reaction temperature of 385°C, a 40 minute residence time and a hydrogen pressure of 2000 psig. The products used for the separation of the asphaltenes and preasphaltenes were obtained from the hot, low pressure separator upon reaching steady state conditions. The intermediates were separated into the solubility classes using the same method as was used in the batch microautoclave experiments. The coal conversion obtained during the steady state operation was 76 wt.% (daf).

RESULTS AND DISCUSSION

The solubility class distributions obtained from the thermal liquefaction of 69 bituminous coals using a single residence time (15 min.) and three reaction temperatures (385°C, 427°C, 445°C) are plotted on a triangle plot in Figure 1. The data suggested a common liquefaction pathway for these coals. The pathway was verified by using a set of reaction temperatures and residence times such that the entire range of conversions were obtained for a single coal (Western Kentucky #6). The data obtained from these experiments are shown in Figure 2. The data in Figure 2 confirmed the thermal pathway suggested from the single residence time data.

The pathway shown in Figure 2 indicates two distinct stages. In the initial coal dissolution stage, the intermediates (asphaltenes plus preasphaltenes) increase with increasing coal conversion. During this stage of coal dissolution, the oil plus gas yields remain fairly constant. It should be noted that the gas produced during this stage of coal dissolution contributes only a small amount to the lumped parameter (O+G). The second stage of the pathway begins after the coal has reached a maximum in conversion (and A+P yield). In this stage the coal conversion remains fairly constant and the major reactions are the conversion of A+P to O+G.

The data obtained from these coals suggest that if a set of conditions could be found which would change the initial stage of the thermal pathway, the process would produce more of the desirable products (oils). One possible method would be to use a catalyst to change the selectivity. A number of catalysts were studied using the Western Kentucky #6 coal. The data obtained from some of these experiments are shown in Figure 3. As can be seen in this figure, the catalytic pathway is similar to the thermal pathway shown in Figure 2. The addition of the catalysts did not change the pathway; however, the catalysts did increase the rate of the production of the intermediates.

Thermal and catalytic data were obtained for a subbituminous Wyodak coal to investigate the effect of rank on the observed pathway. These data are shown in Figure 4. As can be seen in this figure, the pathway obtained is significantly different from the one obtained for the bituminous coals. In the initial and dissolution stage of the pathway, both the A+P and O+G yields increase with coal conversion. In the second stage of the pathway, similar to the pathway of the bituminous coals, the major reaction appears to be

the conversion of A+P and O+G with a small concurrent increase in coal conversion. Also similar to the bituminous coal data, the thermal and catalytic pathway of the Wyodak coal are similar.

The intermediates (asphaltenes and preasphaltenes) were produced, separated and checked for purity to further investigate the pathway of the bituminous coals. The intermediates, both separately and a 50/50 wt.% mixture, were reacted using similar conditions to those used for the coals. The thermal pathway of these samples are shown in Figure 5. The thermal pathway of the coal-derived asphaltenes, as expected, indicates the primary reaction is the conversion of the asphaltenes to oils plus gases. Again, the contribution of the gases to the lumped parameter is small. It appears from these data that the conversion of the asphaltenes follows a similar path both during coal conversion and during the conversion of the isolated intermediate solubility fraction.

The thermal conversion pathway of the preasphaltene intermediate, also shown in Figure 5, was somewhat unexpected. The pathway indicates that the oils are formed slightly faster from the preasphaltenes, presumably through the asphaltene intermediate, than the asphaltenes are formed from the preasphaltenes. However, if the unconverted coal (IOM) is subtracted from the coal conversion products, the points for the conversion of coal and preasphaltenes are similar. Thus, it appears that the conversion of the preasphaltenes follow a similar path during coal conversion and the conversion of the isolated solubility fraction.

The thermal pathway observed for the mixture (50/50 wt.%) of asphaltenes and preasphaltenes is also shown in Figure 5. The pathway defined for the mixture indicates that the two reactants are converted independently. The experimental data and the calculated data based on the conversions of the individual asphaltenes and preasphaltenes runs are similar within experimental error.

SUMMARY

It has been shown that high volatile bituminous coals have a similar reaction pathway and that the addition of a catalyst does not significantly change the observed thermal pathway. The pathway for the bituminous coals indicate that to obtain a significant oil yield, a maximum in the intermediate (A+P) yield (and coal conversion) must be obtained. The thermal and catalytic pathway obtained for a Wyodak coal is significantly different. For this coal, an increase in the asphaltene plus preasphaltene and oils plus gases yield parallel the increase in coal conversion in the initial stage. The thermal conversion pathways of the isolated intermediate solubility fractions were similar to those obtained during coal conversion.

ACKNOWLEDGMENT

This work was supported by the Commonwealth of Kentucky and DOE contract No. DE-FC88-PC8806 as part of the Consortium for Fossil Fuel Liquefaction Science (administered by the University of Kentucky).

REFERENCES

1. V. W. Weekman, *AIChE Monograph Series*, **75** (11), (1979).
2. P. J. Flory, "Principles of Polymer Chemistry", Cornell University Press, New York, NY, 1953.
3. S. Weller, M. G. Pelipetz and S. Friedman, *Ind. Eng. Chem.*, **43** (7), 1575 (1951).
4. D. C. Cronauer, Y. T. Shah and R. G. Ruberto, *Ind. Eng. Chem., Proc. Des. Div.*, **17**, 281 (1978).
5. R. A. Keogh, K. Tsai, L. Xu and B. H. Davis, *Energy & Fuels*, **5** (5), 625 (1991).

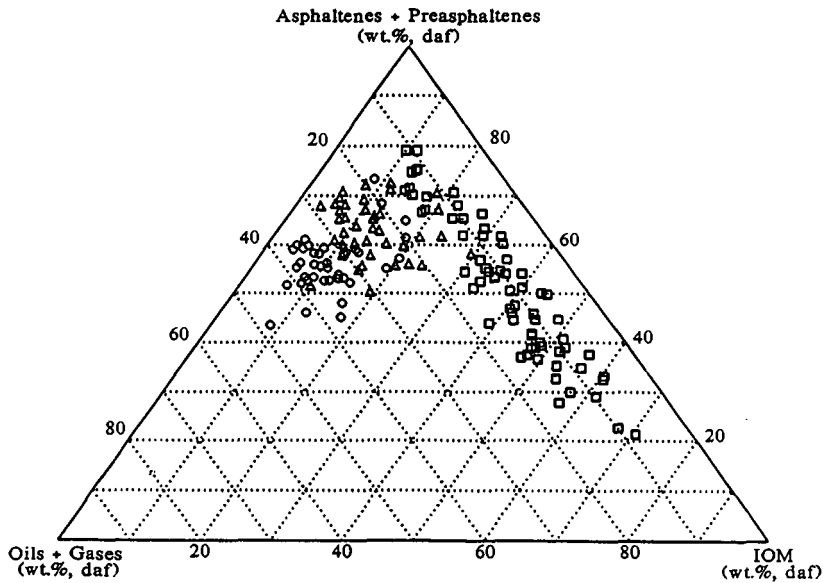


Figure 1. Solubility class distribution of 69 bituminous coals using a 15 minute residence time and three temperatures (\square , 385°C; \triangle , 427°C; \circ , 445°C).

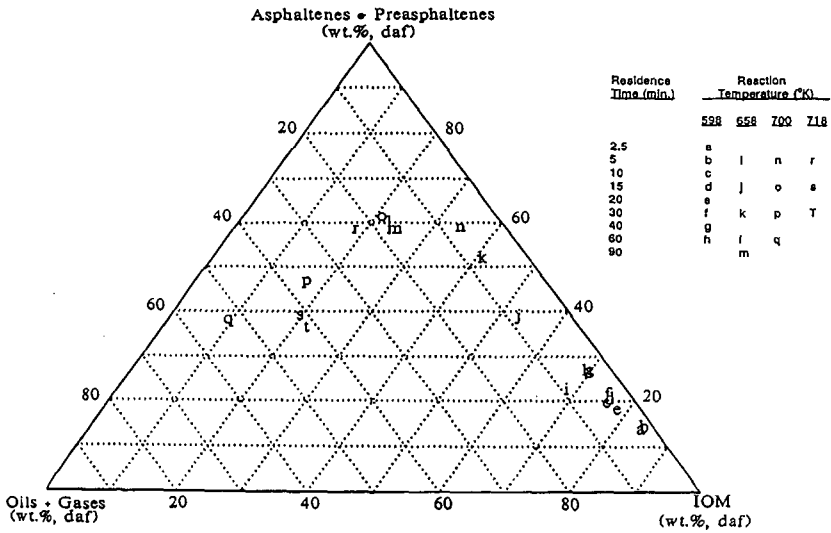


Figure 2. Thermal liquefaction pathway of a Western Kentucky #6 coal.

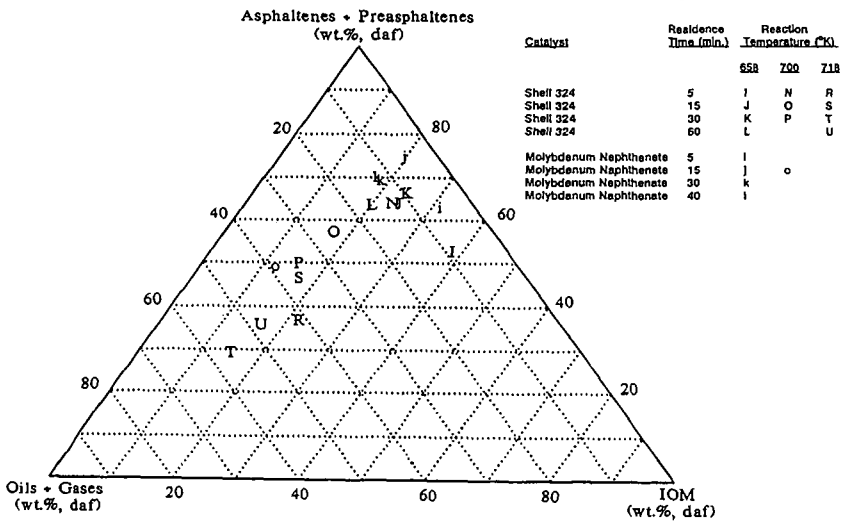


Figure 3. Catalytic liquefaction pathway of a Western Kentucky #6 coal.

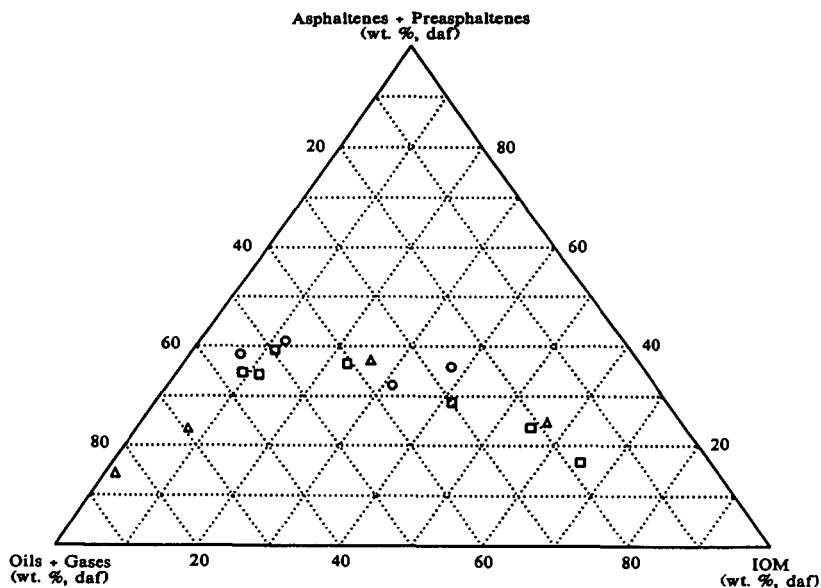


Figure 4. Thermal and catalytic pathway of a Wyodak coal (□, thermal; ○, Fe₂O₃; △, molybdenum naphthenate).

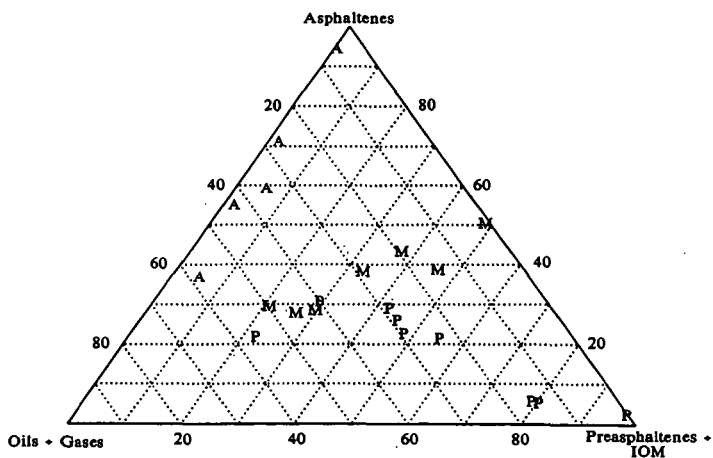


Figure 5. Thermal pathway of bituminous coal-derived asphaltene (A), preasphaltenes (P) and a 50/50 wt.% mixture of asphaltene and preasphaltenes (M).

NEW DIRECTIONS TO PRECONVERSION PROCESSING OF COAL

M. Nishioka, W. Laird, P. Bendale, and R. A. Zell

Viking Systems International, 2070 William Pitt Way, Pittsburgh, PA 15238

Keywords: Coal Liquefaction, High-Temperature Soaking, Coal Associations

INTRODUCTION

Coal structure should be well understood for the effective development of coal liquefaction. A cross-linked three-dimensional macromolecular model has been widely accepted for the structure of coal. Coal liquefaction is being developed based on this model. Recent studies, however, showed that significant portions (far more than generally believed) of coal molecules are physically associated¹. If physical association is dominant, all properties and reactivities in coal liquefaction must be a strong function of intra- and intermolecular (secondary) interactions and molecular weight. It is necessary to reinvestigate a coal conversion procedure based on the associated nature of coal.

Many efforts of chemical pretreatments have been made to cleave chemical bonds by using reagents or high pressure of CO and H₂O etc. Coal changes molecular conformations during soaking/dissolution steps due to relatively strong secondary interactions. This may lead to decrease in dissolution, but this phenomena have often been regarded as retrograde reactions. The stabilization of radical intermediate has been considered to prevent retrograde reactions. These concepts of selective bond cleavages and prevention of retrograde reactions are based on the network model.

If a large portion of coal is associated, coal may be dissolved to a great degree. It is expected that largely dissolved coal can easily be converted to liquid. However, dissolution has not been an easy task, as shown by many researchers for a long time. If coal/coal complexes with high molecular weight are replaced with molecules with low molecular weight, coal may be dissolved to more extent. Associated coal is regarded as material with broad molecular weight distribution. Reactivity of these material may be different. Fractions with different molecular weight may be treated separately to produce desired fractions, if possible. These are the major features considered in this paper based on the associated molecular nature of coal.

In this paper, a new concept of coal preconversion is shown on the basis of these propositions. Two subjects are focused on: (1) maximizing dissolution of associated coal without additional chemicals and (2) step-wise conversion of associated coal with broad molecular weight distribution. For these purposes, the following procedure has been tested: two-step soaking at 350-400°C, followed by isolation of oil, and then liquefaction of residue. This enabled to lower liquefaction severity, to decrease the gas yield, and to increase the oil yield. Some of these results and the future perspective of two-stage liquefaction will be discussed.

EXPERIMENTAL

Coal samples were obtained from the DOE Coal Bank at Pennsylvania State University.

Illinois no. 6 coal (DECS-2) was used as received, and Smith Roland coal (DECS-8) was washed with 2N HCl² and dried before use. A coal liquid derived from Illinois no. 6 coal obtained from the Wilsonville pilot plant³ was used. All the reagents and solvents were obtained from Aldrich Chemical Co. (Milwaukee, WI) and Fisher Scientific (Pittsburgh, PA), and HPLC-grade solvents were used without further purification.

Two reactors, a 250 ml autoclave (Model 4576; Parr Instrument CO., Moline, IL, USA) and 27 ml microreactors fabricated, were used. These reactors were evacuated and purged with nitrogen five times after charging a coal sample and a solvent. The autoclave was heated approximately at 8°C min⁻¹ to required temperature, and controlled to $\pm 3^\circ\text{C}$, while agitating with the autoclave stirrer (500 rev min⁻¹). Microreactors were heated in a fluidized sand bath (Model SBL-2; Techne Corp., Princeton, NJ) which was controlled within $\pm 1.0^\circ\text{C}$ of the set point. The shaker (Model 75; the Burrell Corp., Pittsburgh, PA) was modified to shake the microreactor horizontally at 320 rev min⁻¹. Mixtures in the reactor attained the set point within 5 min, when the reactor was being immersed into the sand bath.

After reactions, the mixtures were filtered and Soxhlet-extracted with cyclohexane, toluene and tetrahydrofuran (THF) for 24 h, respectively, and then these samples were dried under vacuum at 95°C overnight. The amounts of THF solubles (TS), toluene solubles (ToS) and cyclohexane solubles (CyS) were determined from the mass of the respective insolubles. Produced gas was generally included in the CyS yield.

Gas was collected with a sample bag after cooling the autoclave, and analyzed with gas chromatography by the University of Pittsburgh Applied Research Center (Pittsburgh, PA). Approximate gas yields were calculated on the assumption that the amount of nitrogen does not change before and after reactions.

RESULTS AND DISCUSSION

Coal dissolution and liquefaction

The effect of soaking temperature on liquefaction was compared at 200°C and at 350°C. Illinois no. 6 coal was liquefied at 430°C for 1 h after soaking at these temperatures. The yields of TS were the same for these runs, but the yields of ToS and CyS were 5% higher for the samples soaked at 350°C than for that at 200°C. The coal was mildly refluxed in pyridine for 24 h, followed by the removal of the solvent, and liquefied at 430°C. The conversion was compared to that liquefied under the same condition but using the raw coal. The yield of CyS increased about 10% by soaking in pyridine. Other related results are available. An increase in conversion at 427°C was observed when a coal/coal liquid mixture was soaked at 277-322°C for 10 min⁴. Preswelling with THF and tetraammoniumhydroxide, followed by removal of solvents, enhanced hydroliquefaction yields at 400°C^{5,6}. These results show that disintegrated coals lead to high conversions in liquefaction.

Optimum temperature of the high temperature soaking was around 350°C as shown in *Figure 1*. However, the CyS (or oil) yield was still low (35%) at 350°C. The two-step wise soaking was further tested to increase an oil yield. Soaking at 350°C, followed by soaking at 400°C, gave the 50% oil yield (Run 10 in *Figure 2*), but soaking at 200°C, followed by soaking at 400°C, was not effective and led to the yield of more than 100%

because of incorporation of the coal liquid used as a solvent (Run 11).

The effect of radical initiators on the high-temperature soaking and liquefaction were investigated in the recent works^{7,8}. Although it has widely been accepted that radicals cause retrograde reactions, the addition of radical initiators did not have the expected negative effect and the slightly positive effect in the high-temperature soaking (350-400°C). The addition of H₂O₂ at the high-temperature soaking increased the 5% oil yield under low pressure hydrogen gas (Run 12)⁸. The addition of small amount of water alone gave the similar change in conversion in the high-temperature soaking. Therefore, a small amount of water or hydrogen peroxide solution may be added to improve the high-temperature soaking.

The two-step high-temperature soaking at 350°C and 400°C gave the 50% of cyclohexane solubles as shown above. This implies that slow heating is better than fast heating on coal conversion. The autoclave was heated up relatively slowly (at 8°C min⁻¹). The effect of heating rate, therefore, was investigated using the microreactor which was relatively fast heated up in the sand bath. The reactor was heated from room temperature to 430°C in 0.5 h and held at 430°C for 2 h (Run 13). For Run 14, the mixture was reacted under the same condition, but heated with a step-wise heating before reaction (at 350°C for 0.5 h and at 400°C for 0.5 h), and then held at 430°C for 1 h. The total heating-up time from room temperature to 350°C, from 350°C to 400°C and from 400°C to 430°C was 0.5 h. So, the total residence time including heating-up was 2.5 h. For Run 15, the mixture was slowly heated from 130°C to 430°C and held at 430°C for 1 h. The total duration of heating-up and reaction time was also controlled to 2.5 h. Although the coal was reacted at 430°C for the longest time for Run 13, coal conversion was the lowest among three Runs. The oil yield was enhanced about 10% by these programmed heatings. These results shows that the programmed heating or step-wise high-temperature soaking was important for coal conversion. Song *et al.*⁹ recently reported the effect of the temperature-programmed liquefaction of low rank coals. Montana subbituminous coal was converted to 5-10% more (THF solubles) by slow heating compared to rapid heating.

Coal fractions and liquefaction

Another important factor to decrease a gas yield is suggested on the basis of the associated molecular nature of coal. Hydrocarbons with lower molecular weight generally produce more gas by thermal pyrolysis. Hydrocarbons with higher molecular weight will be decomposed under more severe conditions under which more gas will be produced from hydrocarbons with lower molecular weight. The associated structural model of coal can be regarded as material with broad molecular weight distribution. Therefore, coal with different molecular weight should be treated separately, if possible.

A low molecular weight fraction may be separated after dissolution of coal, and a remaining high molecular weight fraction may selectively be liquefied. Here, pyridine solubles and insolubles were separately liquefied to compare their conversions under the same condition (Runs 16 and 17). Approximately the same oil yield was obtained from pyridine solubles and insolubles (Figure 3). Furthermore, cyclohexane insolubles from Run 10 was examined. The 50% oil yield was obtained even from this fraction (Run 18).

The liquefaction characteristics of the soluble and insoluble components has recently

been reviewed and studied¹⁰. The dissolution and hydrogen consumption rates of a pyridine extracted coal and a whole coal were similar for West Kentucky coal (80% carbon, daf)¹¹. Whereas, a significant decrease in liquefaction conversions was observed when a coal was extracted with pyridine for Illinois no. 6 coal¹². Warzinski and Holder¹⁰ found the retrogressive behavior in conversion for pyridine extract part of Illinois no. 6 coal. Although it is difficult to conclude the effect of the soluble and insoluble components from these results, it seems that the reactivity of residues or high molecular weight components is not so poor as that of low molecular weight components.

The associated molecular nature and liquefaction

It was shown that a large portion of coal can be dissolved by the high-temperature soaking in the coal liquid, and the programmed or step-wise heating is preferred to enhance an oil yield. The highly dissolved coal was liquefied to a larger extent. Further, it was suggested that coal with a broad molecular weight distribution should be separated into an oil fraction after dissolution, and that only residue should be liquefied at the following step. From these results, a new concept is proposed to increase an oil yield and decrease a gas yield as shown in the block diagram (*Figure 4*). Coal is soaked in a recycle oil at 350°C and at 400°C. Gas and oil are recovered by vacuum distillation, and the bottom fraction is fed to a liquefaction section and liquefied under low pressure hydrogen at a relatively low temperature.

The proposed procedure was tested using an autoclave. The DECS-2 coal was soaked in the coal liquid under nitrogen at 350°C and at 400°C for 1 h, respectively. The oil fraction was extracted with cyclohexane, and the cyclohexane insoluble portion was liquefied under low pressure of hydrogen (2.8 MPa) at 430°C for 1 h (Run 20). For comparison, the coal was soaked in the coal liquid at 200°C for 1 h, and then the mixture was liquefied under the same condition for 2 h (Run 19). In these Runs, gas yields were analyzed. *Figure 5* shows these results. It is notable that the CyS (or oil) yield increased 30% and the gas yield decreased 15%.

DECS-8 (subbituminous) coal was also examined with the same procedure. As the ionic forces are relatively strong and abundant in low rank coals², it is an important step to weaken the ionic forces before the high-temperature soaking. Although it has been known that acid washing enhances the conversion of low rank coal¹³⁻¹⁶, the details on acid washing have not clearly been explained. Here, 2N HCl washing² was used to weaken the ionic forces in the coal before the high-temperature soaking. The coal was soaked in the coal liquid at 350°C and at 400°C for 1 h, respectively. Cyclohexane insolubles from the soaked coal was similarly liquefied at 430°C for 1 h (Run 22). As the acid washed coal was dried, the dried DECS-8 coal was soaked at 200°C for 1 h and then liquefied at 430°C for 2 h for comparison (Run 21). Again, more than 30% increase in the oil yield and 20% decrease in the gas yield was observed by the procedure (*Figure 5*).

CONCLUSIONS

An improved coal liquefaction concept was reinvestigated for the current two-stage process on the basis of the associated molecular nature of coal. Since a significant portion of coal molecules are physically associated as pointed in our recent paper, physical dissolution

should be considered more. The step-wise high-temperature soaking was a simple and effective method for coal dissolution. Larger dissolution made liquefaction severity lower. Broad molecular weight distribution in the associated coal was another important factor. The selective reaction of fractions with high molecular weight which were isolated after the high-temperature soaking made gas yield lower. Tests with using an autoclave by the concept shown in Figure 5 enabled to produce 30% more oil and 15-20% less gas yields. It is expected that the procedure will result in great cost down in coal liquefaction.

ACKNOWLEDGEMENT

This work was supported by the U.S. Department of Energy under Contract DE-AC22-91PC91041.

REFERENCES

- 1 Nishioka, M. *Fuel* 1992, 71, 941
- 2 Nishioka, M., Gebhard, L. and Silbernagel, B. G. *Fuel* 1991, 70, 341
- 3 Gollakota, S. V., Lee, J. M. and Davies, O. *Fuel Proc. Tech.* 1989, 22, 205
- 4 Wham, R. M. *Fuel* 1987, 66, 283
- 5 Joseph, J. T. *Fuel* 1991, 70, 139
- 6 Joseph, J. T. *Fuel* 1991, 70, 459
- 7 Nishioka, M., Laird, W. and Bendale, P. *Fuel* submitted
- 8 Nishioka, M. and Laird, W. *Fuel* submitted
- 9 Song, C., Schobert, H. H. and Hatcher, P. G. *Energy & Fuels* 1992, 6, 328
- 10 Warzinski, R. P. and Holder, G. D. *Fuel* 1992, 71, 993
- 11 Whitehurst, D. D., Farcasiu, M., Mitchell, T. O. and Dickert, J. J. Jr. Electric Power Research Institute Report EPRI AF-480, Palo Alto, CA, 1077, pp. 7-2-7-10
- 12 Seth, M. PhD Thesis University of California Berkeley, Berkeley, CA, 1980
- 13 Schafer, H. N. S. *Fuel* 1970, 49, 197
- 14 Mochida, I., Shimohara, T., Korai, Y., Fujitsu, H. and Takeshita, K. *Fuel* 1983, 62, 659
- 15 Serio, M. A., Solomon, P. R., Kroo, E., Bassilakis, R., Malhotra, R. and McMillen, D. *Am. Chem. Soc. Div. Fuel Chem. Prepr.* 1990, 35(1), 61
- 16 Joseph, J. T. and Rorrai, T. R. *Fuel* 1992, 71, 75

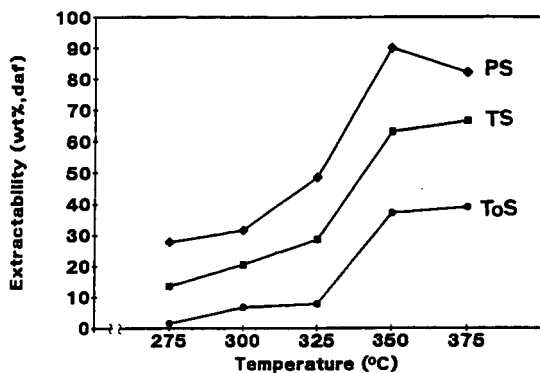


Figure 1 The effect of soaking temperature on extractability (DECS-2 coal, 0.35 MPa N_2 , 1.5h)

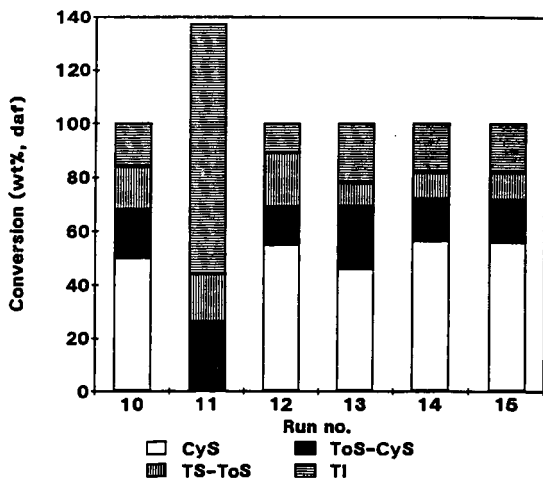


Figure 2 The effect of step-wise soaking on extractability for DECS-2 coal under N_2 , except for Run 12 (Conditions: Run 10; 350°C(1h)/430°C(1h), Run 11; 200°C(1h)/430°C(1h); Run 12; 350°C(1h)/430°C(1h) with H_2O_2 (3000 ppm) and H_2 (1.4 MPa), Run 13; 430°C(2.5h), Run 14; 350°C(0.5h)/400°C(0.5h)/430°C(1h), Run 15; 130°C to 430°C at 3.5°C min^{-1} , followed by 430°C(1h))

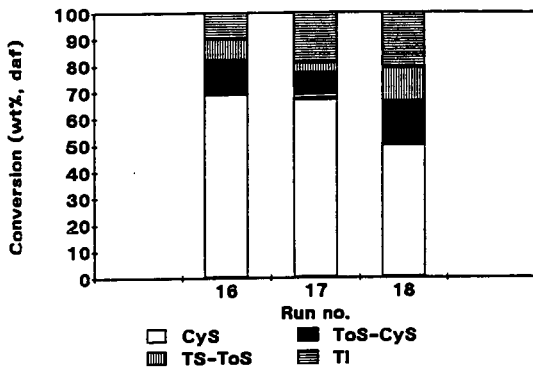


Figure 3 Coal fractions and their conversions at 430°C for 1 h with 2.8 MPa of H₂ ((Run 16; DECS-2/PS, Run 17; DECS-2/PI, Run 18; Cyclohexane insolubles from Run 10)

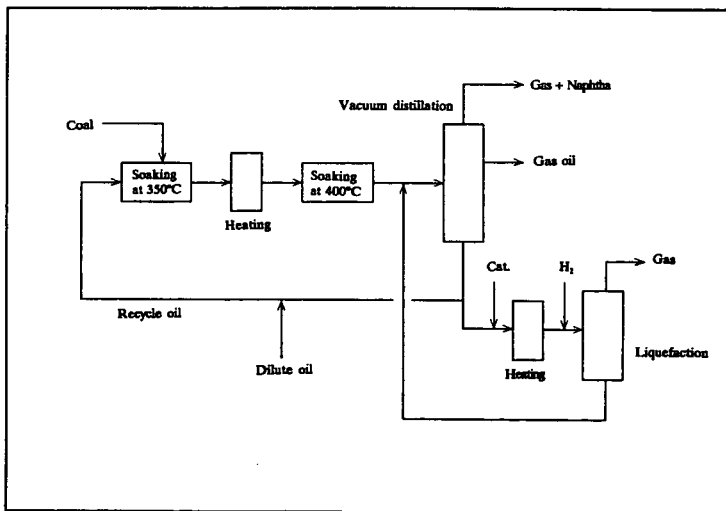


Figure 4 Block diagram of the proposed coal liquefaction concept

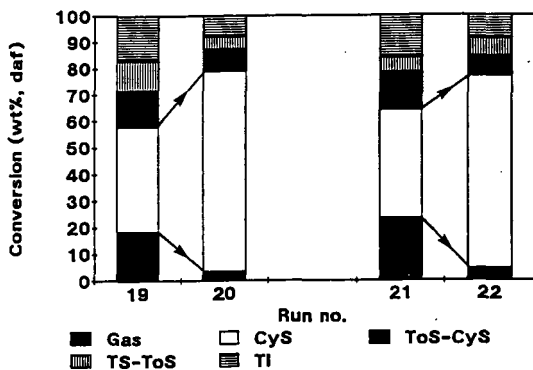


Figure 5 Coal conversion by the proposed procedure for DECS-2 coal (Runs 19 and 20) and DECS-8 coal (Runs 21 and 22) (Run 19; 200°C(1h)/430°C(2h), Run 20; calculation from Runs 10 and 18, Runs 20 and 21 under the same conditions as Runs 19 and 20, see the text in detail)

Effects of Thermal and Solvent Pretreatments on the Elastic Properties of Coal

Yongseung Yun and Eric M. Suuberg
Division of Engineering, Brown University
Providence, RI 02912

(Keywords: Elastic property, Dynamic Mechanical Analysis, Pretreatment)

INTRODUCTION

It is now well established that thermal pretreatment in a range of temperatures lower than those needed for pyrolysis can significantly affect the penetrability and swellability of coals. This suggests that judicious use of heat together with effective swelling solvents for coal, can affect mass transport of reagents or catalysts into or out of the coal, during the early stages of liquefaction.

The present study is concerned with the effects of heat/solvent pretreatments on the elastic constants of the coal network structure. This, in turn, tells one about how the non-covalent interactions in coal are being broken down. Studies of the elastic properties of coal are nothing new [e.g. 1-10]. Because of the compressibility of coal, the application of mercury porosimetry to pore characterization in coal has involved careful corrections, so that the actual pore size distribution could be calculated [1,11,12]. However, the limitation caused by compressibility of bulk coal structure can be an advantage in revealing the structural changes during pretreatment processes and in establishing a suitable elastic model for macromolecular coal structure.

It is known that dynamic mechanical methods are ca. 1000 times more sensitive for detecting molecular relaxations such as the glass transition temperature, T_g , than are differential scanning calorimetry (DSC)/differential thermal analysis (DTA) techniques [13]. Weller and Wert [7-10] have extensively applied the torsion pendulum technique, one of the dynamic mechanical methods, for elucidating the elastic properties of coal in the temperature range below 200 °C. They employed square rods cut from whole coal. Since the relevant temperature range for the structural relaxation by heat is generally higher than 200°C, we decided to study the thermal structural relaxation at temperatures higher than 200°C by employing dynamic mechanical analysis (DMA). This technique involves constant amplitude oscillation of the solid to determine stress-strain properties.

EXPERIMENTAL

A DuPont 982 DMA was employed for mechanical analysis. A detailed description of the equipment has been given elsewhere [13,14]. The sample for the DMA was prepared by pressing the as-received coal powder (-100 mesh) obtained from the Argonne Premium Sample Bank with a press normally used for making FTIR sample pellets, at 15 kpsi for 6-12 hr, which results in a sample of ca. 4 mm thickness with 12.8 mm diameter.

Slippage of the samples from the clamps inside the DMA, especially during oscillation in the high temperature range (>300°C), was noted to be a main cause for irreproducibility, and special care was taken to make certain that the sample was tightly clamped. The pelletizing process used here clearly creates a solid tablet of different macroscopic mechanical properties than the original solid. The choice to work with samples prepared in this way was dictated by a desire to continue to use the Argonne Premium Coal Samples, that are generally only available in powdered form. The gross macroscopic

mechanical properties of such pellets, e.g. tensile modulus, will clearly be different from those of a sample prepared, for example, by cutting a chunk from a virgin block of coal. In fact, any samples cut directly from coal could still be subject to naturally occurring heterogeneities in the coal, and thus mechanical properties are in that case still subject to large variations, depending upon the nature of the tests. This is not important for present purposes, because our goal is not to make use of macroscopic mechanical properties. Rather, we are here only interested in changes on the molecular level that manifest themselves as changes in a particular property.

For purposes of comparison, we examined the changes revealed by DMA in the context of changes earlier noted using thermal techniques, such as DSC and solvent swelling techniques. The detailed procedures for obtaining DSC and solvent swelling results have been reported earlier [15,16].

RESULTS AND DISCUSSION

Raw DMA results are obtained as the frequency of oscillation and the damping signal. The frequency of oscillation is directly related to an elastic modulus of the sample, whereas the energy needed to maintain constant amplitude oscillation is a measure of damping within the sample [14]. Normally, the modulus is resolved into storage and loss moduli. The storage modulus corresponds to the perfectly elastic component whereas the loss modulus represents the perfectly viscous component. The dimensionless ratio of loss/storage components is defined as the damping factor, $\tan \delta$.

The tensile storage modulus, in absolute value, is comparable to what might be encountered in some polymer samples. We caution against placing too much emphasis on this absolute value, because of the issues related to pressing samples from powder. Instead, it is features that are clearly visible in the $\tan \delta$ or loss modulus spectra that are of significance. It is the changes in storage modulus E' and loss modulus E'' , and their ratio, $\tan \delta = E''/E'$ that convey significant information about microscopic change in the material being tested. Both E'' and $\tan \delta$, for example, are used to reveal glass transitions as maxima in the spectra. Physically, E' represents the elastic energy storage capacity of the material, whereas E'' represents the energy lost as heat due to dissipation. Many other transitions, in addition to a glass transition, can cause changes in E'' . Thus this parameter is a sensitive indicator of a change in the ability of molecular segments to move, relative to one another. It is this property we choose to focus on here. It should be also emphasized that in a transition, such as a glass transition, the storage modulus will normally show a slow continuous decline, whereas the loss modulus (and thus $\tan \delta$) will show a distinct peak. This is what makes use of this modulus preferable for detecting transition.

In Figure 1, the first transition is seen near 60°C, for different samples of wet, as-received Pittsburgh high volatile bituminous coal. This transition is normally not visible in DSC, because it is buried beneath the water evaporation peak. The position of this peak is sensitive to the presence of moisture, as is seen from Figure 2. This behavior is typical of the effects of a "plasticizing agent" in a polymer. The molecular motions of the coal chains are enhanced at low temperatures when water is present, and internal hydrogen bonding of the coal itself is suppressed by the opportunity to hydrogen bond with a solvent (in this case, water).

The large peak that is revealed by $\tan \delta$ above 200°C coincides with a transition shown both by DSC analysis of this coal and by a change in tetrahydrofuran (THF) swellability (see Figure 3). This transition involves an irreversible relaxation of the coal structure [16,17].

Figure 4 illustrates the behavior of Upper Freeport medium volatile bituminous coal in DMA. The tensile storage modulus exhibits a continuous decline with temperature, except for two regions of more

rapid decline in modulus. The loss modulus, and thus $\tan \delta$, both suggest that there is a low temperature event, again probably associated with moisture in the coal, at below 100°C. The main relaxation of structure starts to occur from 240°C, as observed in both tensile storage modulus and $\tan \delta$. This observation augments the DSC and solvent swelling results (see Figure 5) for the same coal, in that Upper Freeport coal showed the characteristics of a relaxed coal structure such as increased swellability in solvents and endothermic peak. In the DSC, the coal exhibited a distinct endothermic peak centered around 350°C which was started from around 310°C, whereas solvent swellability increased significantly above 250°C. It is thus confirmed by DMA that solvent swelling is a more sensitive indicator of irreversible structural relaxation than is DSC.

CONCLUSIONS

Two bituminous coals were subjected to DMA analysis and the results were compared our earlier reported DSC and solvent swelling results. Results from different techniques appear to point to the same basic conclusions with regard to transitions, although there are subtle differences between the results of different techniques. The transition related to coal moisture is more visible in DMA and solvent swelling techniques than in DSC analysis. DMA confirms that solvent swellability is a more sensitive index of macromolecular changes than is DSC. The importance of observations made by several different techniques in order to discern transitions accurately has been noted. This study confirms the usefulness of applying different techniques simultaneously for this purpose.

We noticed that good reproducibility in DMA depends upon the reproducibility of forming pellets, in our case. A main problem was small cracks generated while the pellet was released from the press. We are further pursuing these problems in order to obtain a better description of transitions and elastic properties of coal.

ACKNOWLEDGEMENTS The work reported here was financially supported by the Department of Energy Contract No. DE-AC22-91PC91027 and grant DE-FG22-90PC90308.

REFERENCES

1. Van Krevelen, D.W. In *Coal*; Elsevier, New York, 1981; Chapter XX.
2. Hiorns, F.J. *Fuel* **1953**, *32*, 113.
3. Terry, N.B. *Fuel* **1958**, *37*, 309.
4. Morgans, W.T.A.; Terry, N.B. *Fuel* **1958**, *37*, 201.
5. Hall, P.J.; Marsh, H.; Thermas, K.M., unpublished results, University of Newcastle-Upon-Tyne, 1988.
6. Brenner, D. *Prepr. Pap.-Am. Chem. Soc., Div. Fuel Chem.* **1986**, *31(1)*, 17.
7. Weller, M.; Wert, C. *Fuel* **1984**, *63*, 891.
8. Wert, C.A.; Weller, M.; Caulfield, D. *J. Appl. Phys.* **1984**, *56(9)*, 2453.
9. Wert, C.A.; Weller, M. *J. Appl. Phys.* **1982**, *53(10)*, 6505.
10. Weller, M.; Wert, C. *Int. Conf. on Coal Science* **1987**, 65.
11. Toda, Y.; Toyoda, S. *Fuel* **1972**, *51*, 199.
12. Debelak, K.A.; Schrod, J.T. *Fuel* **1979**, *58*, 732.
13. Wetton, R.E. *Polymer Testing* **1984**, *4*, 117.
14. Gill, P.S.; Lear, J.D.; Leckenby, J.N. *Polymer Testing* **1984**, *4*, 131.
15. Yun, Y.; Suuberg, E.M. *Prepr. Pap.-Am. Chem. Soc., Div. Fuel Chem.* **1992**, *37(2)*, 856.
16. Yun, Y.; Suuberg, E.M. *Fuel* **1993**, in press.
17. Yun, Y.; Suuberg, E.M. *Energy & Fuels* **1992**, *6*, 328.

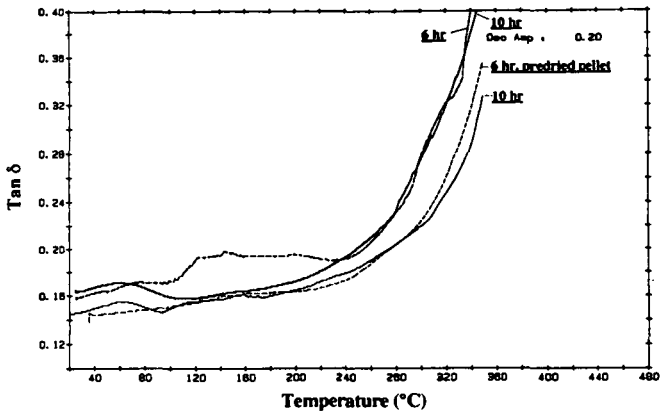


Figure 1. Tan δ DMA spectra obtained from 4 °C/min scans of as-received and predried (up to 200°C at 4 °C/min) Pittsburgh No. 8 coal pellet samples. Pellets were made from -100 mesh powder after pressed at 15 kpsi for the duration as specified in the figure.

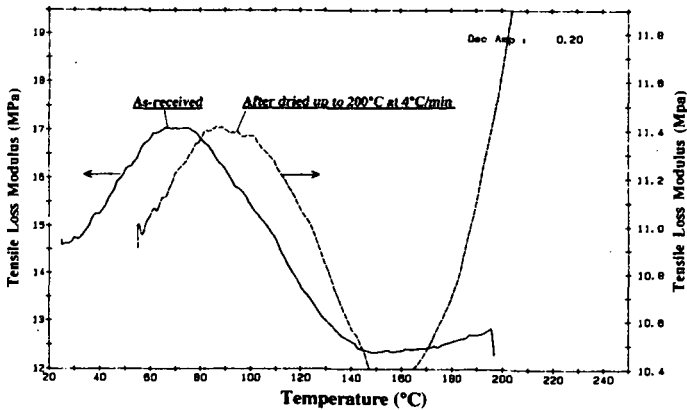


Figure 2. Effect of sample drying on tensile loss modulus obtained at 4°C/min for Pittsburgh No. 8 coal. Sample pellets were made from -100 mesh powder pressed at 15 kpsi for 10 hr.

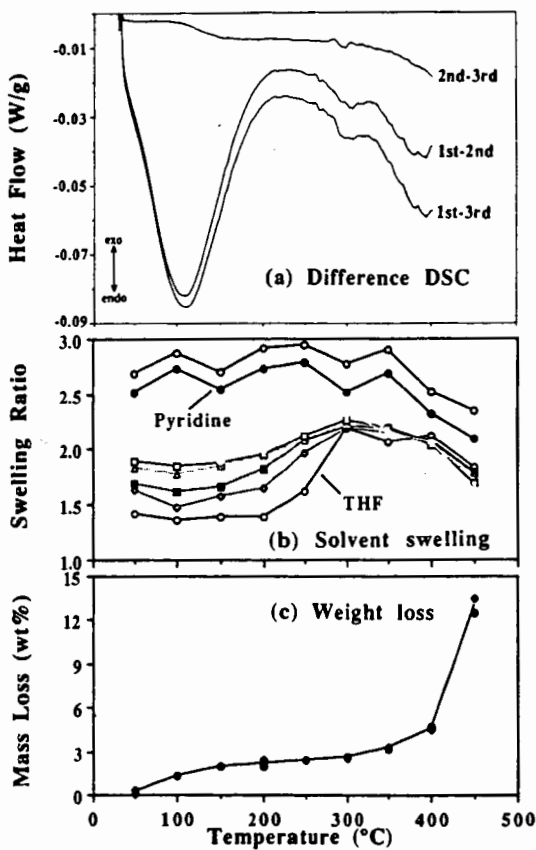


Figure 3. Difference DSC thermograms as well as profiles of solvent swelling ratio and weight loss obtained at 8 °C/min from -100 mesh Pittsburgh No. 8 coal powder (swelling time: \square , 5 hr; \circ , 1 day; \blacksquare , 2 days; \blacktriangle , 4 days; \square , 5 days; \bullet , 6 days).

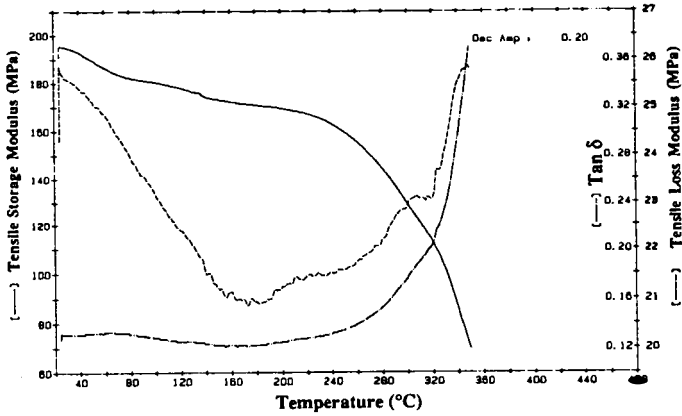


Figure 4. DMA scan of the Upper Freeport medium volatile bituminous coal obtained at 4°C/min. Sample pellet was made from -100 mesh powder pressed at 15 kpsi for 12 hr.

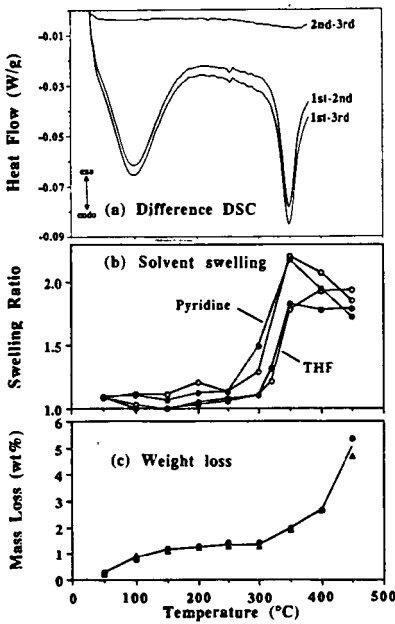


Figure 5. Difference DSC thermograms as well as profiles of solvent swelling ratio and weight loss obtained at 8°C/min from -100 mesh Upper Freeport coal powder (swelling time: ○, 5 hr; ●, 7 days).

Assessment of Small Particle Iron Oxide Catalyst for Coal Liquefaction

Richard Anderson, Edwin N. Givens and Frank Derbyshire
University of Kentucky Center for Applied Energy Research
3572 Iron Works Pike, Lexington, KY 40511-8433

Keywords: Coal liquefaction, iron oxide, catalysis

Introduction

Current efforts to lower the cost of producing coal liquids are concentrated on the use of low-rank coal feedstocks, and dispersed catalysts to promote coal dissolution in the first stage of a two-stage process. Molybdenum and iron are the most commonly investigated catalyst metals, and precursors of both can be converted to an active sulfide catalyst under liquefaction conditions.¹ Although iron catalysts are less active, they are preferred for reasons of economy. A great deal of research has been spent in attempting to understand the chemistry of liquefaction in the presence of iron catalysts. It has also been demonstrated that the use of powdered iron catalysts has allowed the liquefaction of subbituminous coals which could not otherwise be processed². Nevertheless, the activity of these catalysts is still much less than desired and means to enhance their activity are under investigation.

The catalyst activity is determined principally by its composition and the extent of its dispersion with the coal or coal-solvent slurry. The catalyst dispersion is dependent upon the form and mode of addition of the catalyst precursor. High activities are reportedly favored by catalysts introduced as oil-soluble organometallic precursors such as naphthenates and carbonyls.^{3,4,5} The results of some studies, however, indicate that even with these precursors, quite large crystallites or agglomerates can be formed during liquefaction and hence the potentially high dispersion is not maintained. There is some evidence to suggest that, if introduced as fine particulates, there is less tendency for agglomeration. Iron particles of about 50 nm mean diameter synthesized by a flame pyrolysis technique appeared to have retained their particle size and shape during presulfiding and coal liquefaction.^{6,7} Other work has shown that FeS is more active as a colloid than in powder form.⁸ A number of studies have reported enhanced catalytic activity by using methods of preparation that introduce nanometer size iron catalysts.^{9,10,11,12}

The work presented in this paper is concerned principally with a systematic evaluation of the effect of reaction parameters on the catalytic conversion of a subbituminous coal using a commercially produced nanometer size iron oxide catalyst. The work is part of a DOE program to evaluate process concepts that can alone, or in concert, significantly improve process economics. In order to make realistic assessments, studies have been made using process recycle oil from the Wilsonville Advanced Coal Liquefaction Research and Development Facility and Black Thunder subbituminous coal.

Materials

Reagents - Reagents were purchased as follows: Practical grade dimethyl disulfide (DMDS) from Fluka AG; 99% purity UV grade tetralin, high purity tetrahydrofuran (THF), and high purity pentane were Burdick & Jackson Brand from Baxter S/P; UHP 6000# hydrogen was supplied by Air Products and Chemicals, Inc. Coal, coal derived liquids and iron oxide used at the Wilsonville Advanced Coal Liquefaction Research and Development Facility were supplied by CONSOL, Inc.

Coal - Black Thunder subbituminous coal was ground to -200 mesh, riffled and stored under nitrogen at 4°C in a refrigerator.

Recycle oil - A reconstituted recycle oil was used in this program that had been produced at Wilsonville in runs where the plant was in the distillate production mode with all residual materials being recycled to extinction except for the organic matter occluded in the ash reject.¹³ The Wilsonville recycle oil, taken from Run 262 while operating on Black Thunder Coal, contained 43.8 wt% 1050°F distillate, 36.6 wt% residual organic material, 9.2 wt% cresol insolubles and 10.4 wt% ash.

The fractions that were used to form the recycle oil contained significant concentrations of both molybdenum and iron which were being added as catalysts in Run 262. The ashy resid contained 3.3 wt% iron plus 300 ppm molybdenum. The distillate contained only 200 ppm of iron and 2 ppm of molybdenum. It is assumed that these metals possess some indeterminate residual catalytic activity. However, in this research, these effects are integrated into the "thermal" baseline.

Catalysts - Two iron oxide catalyst precursors were used in this study. One was a sample of the iron oxide used at Wilsonville in Run 262 (WIO) while the other was a sample of superfine iron oxide (SFIO) provided by MACH I, Inc., King of Prussia, Pennsylvania. The latter has a bulk density 1/26th that of the WIO (.052 vs. 1.37 g/ml), and a very high surface area (318 vs. 9 m²/g for WIO).

Experimental

Equipment and Procedures - In a typical experiment 3 grams of coal, 5.4 grams of recycle oil, catalyst and DMDS (2.4 moles S/mole Fe added as catalyst) were added to the reactor. The reactor was sealed, pressurized with hydrogen to 1000 psig, and leak tested. Reactions were carried out in a fluidized sandbath set at the specified temperature while the reactor was continuously agitated at a rate of 400 cycles per minute. At the termination of the reaction period, the reactor was quenched to ambient temperature in a room temperature sand bath. The gaseous products were collected and analyzed by gas chromatography. A solvent separation technique, which is described in detail elsewhere,¹⁴ was used to separate both reactants and products. The solid-liquid products were scraped from the reactor using THF and the mixture was extracted in a Soxhlet apparatus for 18 hours. The THF insoluble material, which was comprised of IOM and ash, was dried (80°C/25 mm Hg) and weighed. The THF solubles were concentrated by removing excess THF in a rotary evaporator to which a 50:1 excess volume of pentane was added to precipitate the preasphaltenes and asphaltenes (PA+A). The mixture was placed in an ultrasonic bath for 3 minutes to facilitate the precipitation process before filtering off the PA+A. The PA+A fraction was dried and weighed. This then separates the product into oils, PA+A and IOM plus ash.

Material Balance and Product Yield Computational Methods - The calculation of the yield of products differs somewhat from those reported elsewhere, in that the feed is comprised of the multiple individual Wilsonville recycle oil fractions in addition to coal and catalyst. The product distribution was determined using this same fractionation scheme assuming complete recovery of the ash plus catalyst. In this method the iron is presumed to convert to pyrrhotite and the weight of catalyst reporting to the ash fraction is calculated as the corresponding weight of Fe_{0.9}S. By this method water produced during liquefaction is included in the oils fraction. Experimentally, complete recovery of ash and catalyst was demonstrated. Net product

yields are calculated by subtracting the amount of material contained in the feed fractions from the corresponding amounts found in the product fractions. The total of the net products equals the amount of maf coal in the feed and reflects the net make (or loss) of each of the solubility fractions while coal conversion equals 100 minus the yield of IOM.

Experimental Design - A major portion of the research reported here has been concerned with a detailed investigation of the influence of the reaction variables during coal liquefaction in the presence of added SFIO. An experimental approach was adopted that would maximize the amount of information gathered in a given series of experiments and provide a data set from which to draw valid comparisons. A full 2⁴ factorial experimental design was developed following the method described by Box, Hunter, and Hunter.¹⁵ The main effects and interactions of reaction temperature, catalyst concentration, and sulfur concentration were determined separately for each of several dependent variables including THF conversion, hydrogen consumption, CO+CO₂, hydrocarbon gas, oil and PA+A yields. This technique is particularly applicable to complex reaction systems, such as coal liquefaction, where the reaction mixture is comprised of recycle oil, which itself is a composite of three process materials, coal, catalyst and hydrogen.

Because of the high concentration of metals in the recycle oil, iron oxide concentrations were selected which could have a clearly discernible effect on coal liquefaction, ranging from 1 to 4 wt% Fe on as-fed coal. Added sulfur was selected to explore a wide range of S/Fe atomic ratios, with the centerpoint at 2:1. The reaction temperatures were 390 and 440°C, centered at 415°C.

Results

Comparison of Heavy Distillate and Recycle oil - Liquefaction of Black Thunder Coal in Wilsonville heavy 1050°F distillate at 415°C for 60 minutes gave 95 wt% THF conversion and 35.8 wt% oil yield with the addition of 1.1 wt% iron as WIO and excess DMDS for its conversion to pyrrhotite (see Table 1). The added iron catalyst had a significant effect on THF conversion and the yield of pentane solubles. Based upon previous results, distillate would exhibit little reactivity under these conditions and would not complicate the analysis of coal reactivity.¹⁶

However, coal liquefaction in the Wilsonville recycle oil produced THF conversions which regularly exceeded 100%. In a thermal run, without any added iron oxide, the THF conversion was in excess of 100%, and the oil yield was in excess of the yields observed in the run with distillate alone. The difference between the two solvents was that the recycle oil contained ashy material taken from the vacuum flash unit at Wilsonville and a smaller amount of deashed resid taken from the ROSE-SR deashing unit. The unusually high level of THF conversion and high oil yield indicated that the recycle oil IOM was being converted to soluble product.

Coal Conversion in Wilsonville recycle oil - Liquefaction of Black Thunder coal in the Wilsonville recycle oil, without added catalyst, showed steadily increasing THF conversion, oil and gas make with increasing reaction time at 415°C (see Table 2). The increases parallel the changes in yield obtained with added 1.1 wt% iron as WIO. The main effect of the catalyst was to produce a higher oil yield after 60 minutes. The results are in agreement with experimental data from pilot plant runs at Wilsonville, in which the addition of sulfided iron

oxide caused an appreciable increase in conversion.¹⁷

In both thermal and catalytic cases, the CO and CO₂ are formed at short times, and the yields increased only slightly between 15 to 60 minutes. In comparison, the hydrocarbon gas yield increased from 0.5 to 1.9 wt%. Much of this increase in hydrocarbon gas yield comes from the conversion of recycle oil.

Influence of Nanometer Size Iron Oxide (SFIO) - Sulfided iron oxide particles in the size range 50-80 nm, that were prepared by high temperature thermal oxidation, have been reported to show high activity for coal liquefaction.⁶ The catalytic effect has been attributed to the high surface area and small particle size of the pyrrhotite formed upon sulfiding in the presence of coal where the pyrrhotite particles retain the small particle size of the oxide precursor.¹⁸ The SFIO, whose very high surface area is consistent with nanometer size particles, may also, upon sulfiding, give rise to small particle, high surface area liquefaction catalysts.

The addition of SFIO, at a loading of 2.5 wt% iron on maf coal, produced 11 wt% more oils than in the thermal case (see Table 3). In addition there were slight increases in THF conversion and yield of hydrocarbon gases. These data represent the mid-point of the ranges for each of the three variables. The results of the comparison illustrate the potential advantage of processing with SFIO catalyst.

Impact of Reaction Variables on Liquefaction with SFIO - The R squared values for each dependent variable that was selected indicate the degree of fit by the linear model coefficients as shown in Table 4. Values for the coefficients for each of the simple linear models are summarized in Table 5. The P-value of each coefficient is shown in parentheses.

Of the independent factors, temperature has the strongest overall effect, as seen by the magnitude of the coefficients for THF conversion, hydrogen consumption, and the yields of oil and PA+A; the oil yield increases and PA+A decreases with increasing temperature. Increasing the catalyst concentration produces moderate effects on THF conversion, hydrogen consumption, and enhances the PA+A yield. However, there is no apparent effect of catalyst concentration on oil yield. It must be stressed that only two levels of catalyst concentration have been examined and the zero concentration case is not included: as shown in Table 3, the addition of catalyst significantly improves the oil yield over the thermal case. The effects of added sulfur are small, producing a weak negative coefficient with respect to THF conversion, and a negative coefficient with oil yield.

The average increase in oil yield obtained in the three centerpoint experiments was 11% over the thermal case. This is consistent with the increase of 10 wt% in oil yield predicted by the 2³ factorial design experiments and lends confidence to the linear model.

The addition of 1.1 wt% added iron as WIO, which was the ratio used in the Wilsonville plant, gave 5% more oil than in the thermal case, which agrees closely with the results observed at Wilsonville.¹⁷ The linear model predicts that SFIO at the lower concentration level (1.1 wt% Fe) will produce 15% higher oil yield than in the thermal case, with a decrease to the observed 11% gain at the center point due to the effect of added sulfur (see Table 6). However, the experimental check of this predicted outcome gave only 8% more oil than the thermal case. The catalytic activity of the SFIO for both oil formation and coal

conversion is greater than the corresponding activity of the WIO.

The negative effect of sulfur on THF conversion and on oil yield was unexpected based upon the results of Das Gupta, et al.,¹⁹ on the liquefaction of an iron deficient Indian coal. They found, through a non-linear parameter estimation procedure, that adding sulfur up to a S/Fe atomic ratio of 8 improved conversion. In this system adding sulfur at a S/Fe atomic ratio between 0.6 to 7.4 was detrimental. This effect could be related to adverse side reactions caused by the presence of excess sulfur.

The negative interaction between temperature and SFIO concentration for oil yield indicates that thermal effects begin to dominate catalytic effects at the higher temperature. Also, in addition to thermal conversion of PA+A, the magnitude of the catalyst coefficient for the PA+A model (4.80 vs. 4.08 for THF conversion) suggests that catalytic TOM dissolution reports mainly to the PA+A fraction.

References

1. Derbyshire, F. J., *Catalysis in Coal Liquefaction*, IEACR/08, London, UK, IEA Coal Research, 1988, 69pp.
2. Tomlinson, G. C., Gray, D., Neuworth, M. B. and Talib, A., Report SAND85-7238, Albuquerque, NM, USA, Sandia National Laboratories, 105pp.
3. Hawk, C. O., Hiteshue, R. W., *Hydrogenation of Coal in the Batch Autoclave*. Bulletin 6322 Washington, DC, USA, US Department of the Interior, Bureau of Mines, 1965, 42pp.
4. Watanabe, Y., Yamada, O., Fujita, K., Takegami, Y. and Suzuki T., *Fuel*, 1984, 63, 752-755.
5. Suzuki, T., Yamada, O., Then, J. H., Ando, T. and Watanabe, Y., *Proceedings - 1985 ICCS*, Sydney, NSW, Australia, Pergamon Press, 1985, pp205-8.
6. Andres, M., Charcosset, H., Chiche, P., Davignon, L., Djega-Mariadassou, G., Joly, J-P. and Pregermain, S., *Fuel*, 1983, 62, 69-72.
7. Andres, M., Charcosset, H., Chiche, P., Djega-Mariadassou, G., Joly, J-P. and Pregermain, S., *Preparation of catalysts III* (Eds. G. Poncelet and P. Grange), Elsevier, 1983, pp675-682.
8. Nakao, Y., Yokoyama, S., Maekawa, Y. and Kaeriyama, K., *Fuel*, 1984, 63, 721.
9. Cugini, A. V., Utz, B. R., Krastman, D. and Hickey, R. F., *ACS Div. Fuel Chemistry Preprints*, 1991, 36 (1), 91.
10. Hager, G. T., Bi, X-X., Derbyshire, F. J., Eklund, P. C. and Stencel, J. M., *ACS Div. Fuel Chemistry Preprints*, 1991, 36 (4), 1900.
11. Pradhan, V. R., Tierney, J. W., Wender, I. and Huffman, G. P., *Energy and Fuels*, 1991, 5 (3), 497.
12. Huffman, G. P., Ganguly, B., Taghiei, M., Huggins, F. E. and Shah, N., *ACS Div. Fuel Chemistry Preprints*, 1991, 36 (2), 561.
13. Southern Electric International, Inc., *Technical Progress Report*, "Run 260 with Black Thunder Mine Subbituminous Coal", DOE Contract No. DE-AC22-90PC90033 and EPRI Contract No. RP1234-1-2, Document No. DOE/PC90033-16, January 1992.
14. Derbyshire, F., "Advance Coal Liquefaction Concepts for PETC Generic Bench-scale Unit", DOE/PC/91040-9, May 1992.
15. Box, G. E. P., Hunter, W. G. and Hunter, J. S., *Statistics for Experimenters*, John Wiley and Sons, New York (1978).
16. Anderson, R. R. and Bockrath, B. C., *Fuel*, 1984, 63, 329.
17. Southern Electric International, Inc., *Technical Progress Report*, "Integrated Two-Stage Liquefaction of Subbituminous Coal", DOE Contract No. DE-AC22-82PC50041 and EPRI RP1234-1-2,

EPRI AP-5221, Final Report, June 1987, pp 3-7.

18. Djega-Mariadassou, G., Besson, M., Brodzki, D., Charcosset, H., Huu, T. V. and Varloud, J., Fuel Processing Tech, 1986, 12, 143-145.

19. Das Gupta, R., Mitra, J. R., Dutta, B. K., Sharma, U. N., Sinha, A. K. and Mukherjee, D. K., Fuel Proc Tech, 1991, 27, 35.

Table 1. Liquefaction of Black Thunder Coal with Wilsonville Oils^a

	Distillate ^b	Distillate	Composite ^b	Composite
Added Fe, wt% coal	none	1.1	none	1.1
% Yield, maf coal				
Gases	7.3	7.3	6.9	6.9
Oils	24.9	35.8	48.5	53.8
PA+A	54.5	51.9	52.2	45.3
IOM	13.3	5.0	-7.6	-6.0
THF Conv, wt%	86.7	95.0	107.6	106.0
Run No.	281-1	169-2	139-1/ 167-1	142-2/ 189-1

a. 415° C, 1 hour, 1000 psig H₂ cold, 5.4 grams recycle oil, 3.0 grams coal, 2.4 mole sulfur/mole iron.

b. No DMDS added.

Table 2. Liquefaction of Black Thunder Coal in Wilsonville Recycle Oil^a

Yields, wt %	No Catalyst Added			1.1 wt% Fe Added		
	15 min	30 min	60 min	15 min	30 min	60 min
HC Gases	0.5	1.1	1.9	1.1	1.6	2.1
CO+CO ₂	4.5	5.0	5.0	4.4	4.8	4.8
Oils	21.3	36.4	48.5	20.8	36.0	53.8
PA+A	57.6	56.2	52.2	58.1	59.3	45.3
IOM	16.1	1.3	-7.6	15.6	-1.7	-6.0
Coal Conv, wt %	83.9	98.7	107.6	84.4	101.7	106.0
Run Number	148-2	167-2	139-1/ 167-1	176-1	169-1	189-1/ 142-2

a. 415° C, 1000 psig H₂ cold, 5.4 grams recycle oil, 3.0 grams coal, 2.4 mole sulfur/mole Fe

Table 3. Effect of Superfine Iron Oxide on Liquefaction^a

	Thermal	SFIO	Δ
Iron, wt % coal	None	2.5	
Yields, wt% maf coal			
HC Gases	1.9	2.8	0.9
CO+CO ₂	5.0	4.7	-0.3
Oils	48.5	59.1	10.6
PA+A	52.2	43.3	-8.9
IOM	-7.6	-9.9	-2.3
THF Conversion	107.6	109.9	2.3
Run Number	139-1/167-1	174-2/ 190-1/190-3	

a. 415°C, 1 hour, 1000 psig hydrogen cold, 5.4 grams recycle oil, 3.0 grams coal, 2.0 mole sulfur/mole iron.

Table 4. Dependent Variables Evaluated

<u>Effect</u>	<u>Units</u>	<u>R Squared</u>
THF Conv	THF conversion, wt% maf coal	0.926
mg H ₂	H ₂ consumption, mg/g maf coal	0.973
HC Gas	Hydrocarbon gas yield, wt% maf coal	0.969
CO+CO ₂	CO and CO ₂ gas yield, wt% maf coal	0.944
TGas	Total gas yield, wt% maf coal	0.961
Oils	wt% maf coal	0.880
PA+A	wt% maf coal	0.922

Table 5. Summary of Estimated Coefficients^a

	Intercept	T ^b Coeff (P)	X ^b Coeff	S ^b Coeff	TxX ^b Coeff	TxS ^b Coeff	XxS ^b Coeff
THF Conv	107.40	4.54 (.003)	4.08 (.005)	-1.72 (.097)			-1.62 (.113)
mg H ₂	60.28	9.12 (.001)	2.66 (.014)		1.48 (.097)		-1.13 (.181)
HC Gas	3.50	1.86 (.001)		0.29 (.061)			
CO+CO ₂	5.06	0.84 (.001)		-0.20 (.046)			
TGas	8.57	2.71 (.001)					
Oils	58.61	13.87 (.001)		-5.67 (.054)	-4.60 (.100)		
PA+A	40.23	-12.03 (.005)	4.80 (.085)	3.85 (.141)	3.42 (.179)	3.52 (.169)	

- a. All three way interaction coefficients (TxXxS) are small and set equal to zero. Coefficient estimates are for coded variables (-1,0,+1).
- b. T = temperature; X = wt% Fe in SFIO on coal; S = wt% sulfur in DMDS on coal; TxX = two-way interaction of temperature with wt% Fe in SFIO on coal; TxS = two-way interaction of temperature with wt% sulfur in DMDS on coal; XxS = two-way interaction of wt% Fe in SFIO with wt% sulfur in DMDS on coal.

Table 6. Comparison of Wilsonville and Superfine Iron Oxide^a

	Thermal	WIO	Predicted ^b SFIO	Experimental SFIO
Fe, wt % coal	None	1.1	1.1	1.1
Yields, wt% maf coal				
HC Gases	1.9	2.1	2.6	1.2
CO+CO ₂	5.0	4.8	4.9	5.0
Oils	48.5	53.8	63.7	56.9
PA+A	52.2	45.3	35.1	45.1
IOM	-7.6	-6.0	-6.3	-8.2
THF Conv.	107.6	106.0	106.3	108.2
Run Number	139-1/167-1	142-2/189-1	N/A	272-1

- a. 415°C, 1 hour, 1000 psig H₂ cold, 5.4 grams Wilsonville recycle oil, 3.0 grams coal, 2.4 moles sulfur/mole iron.
- b. Predicted from model parameters. All curvature detected at the mid-range conditions is accounted for as resulting from temperature effects.

EFFECT OF A CATALYST ON THE DISSOLUTION OF BLIND CANYON COAL

Robert P. Warzinski
U.S. Department of Energy
Pittsburgh Energy Technology Center
Pittsburgh, PA 15236

Keywords: coal liquefaction, dispersed catalyst, molybdenum hexacarbonyl

INTRODUCTION

The use of catalysts to improve the dissolution and liquefaction of coal dates back to the 1920s. Reviews in this area have been prepared by Weller (1), Derbyshire (2), and Anderson (3). Recently, interest has been renewed in using dispersed catalysts in the early phases of coal liquefaction to improve the quality of the products produced during the initial dissolution and liquefaction of coal. To facilitate the study of dispersed catalysts in laboratory-scale investigations, a particular sample of Blind Canyon coal (denoted DECS-17) that contains very low levels of pyrite (0.04 wt% on a moisture-free basis) has been made available by the Department of Energy through the Penn State Coal Sample Bank. Thus, complications due to inherent catalytic activity associated with pyrrhotites which can be formed from coal pyrite are eliminated and interferences to the characterization of the added catalysts due to native iron and sulfur are reduced.

The purpose of this paper is to define the effects of a molybdenum-containing catalyst on the initial dissolution and conversion of the DECS-17 coal as a function of temperature. To eliminate competing and/or complicating influences of added solvents, the liquefaction tests were performed in the absence of such materials. The catalytic effects on coal conversion and gas uptake were determined by subtraction of thermal data from the corresponding catalytic results at a given temperature. The results provide a picture of the reactivity of the DECS-17 coal and its response to a dispersed liquefaction catalyst.

EXPERIMENTAL

All of the experiments were performed with the DECS-17 Blind Canyon coal from the Penn State Coal Sample Bank. The coal was minus-60 mesh and was riffled prior to use. The elemental analysis (on a dry basis) provided with the coal was as follows: 76.3% carbon, 5.8% hydrogen, 1.3% nitrogen, 0.4% sulfur, 6.6% ash, and 9.7% oxygen (by difference). The moisture content of the as-received coal was 3.7%.

The liquefaction tests were conducted in 316 stainless-steel microautoclaves. The total internal volume, including connecting tubing, of the microautoclave used in most of this work was 49.0 cm³. During the tests, the microautoclave was mounted in a horizontal position and shaken in an arc motion at approximately 360 cycles per minute in a heated, fluidized sand bath.

The microautoclave was charged with 3.3 g of coal and, if used, 0.008 g of molybdenum hexacarbonyl, Mo(CO)₆. The Mo(CO)₆ was used as received from Strem Chemical Company. Purity was given as 98 + % with moisture being the only major contaminant. No special procedures were used to mix the Mo(CO)₆ with the coal; the compound was simply added from a spatula directly to the microautoclave containing the coal sample.

In all of the tests, an initial charge of 1030 psig (7.20 MPa) hydrogen gas containing 3% hydrogen sulfide was added to the microautoclave after it had been pressure tested and purged with nitrogen.

A series of tests were performed of 60 minutes duration at 325°C, 350°C, 375°C, 400°C, and 425°C. A slow heat-up procedure was employed in which the microautoclave was heated along with the sandbath from room temperature to the desired reaction temperature. The longest heat-up time was approximately 60 minutes to reach the highest temperature of 425°C. The temperature was monitored by a thermocouple placed inside the microautoclave. The pressure was monitored by an electronic pressure transducer connected to the microautoclave by a section of 1/8 inch (3.2 mm) stainless-steel tubing. Time, temperature, and pressure were recorded at ten-second intervals by a PC-based data acquisition system.

At the end of the 60-minute reaction period, the microautoclave was rapidly cooled in water. The gaseous contents of the microautoclave were then measured by water displacement and a gas sample was taken. The microautoclave was then opened and the contents removed with tetrahydrofuran (THF). Sonication was used to facilitate cleaning of the microautoclave and dissolution of the products.

The reaction products were extracted with THF using pressure filtration. The THF conversion was calculated by determining the difference in the weight of the starting coal and the insoluble residue. Cyclohexane conversion was similarly determined by adding the THF-soluble material to cyclohexane and performing another pressure filtration to recover the cyclohexane-insoluble residue. The THF and cyclohexane residues were dried at 110°C under vacuum to constant weight. The conversions are reported on a dry, ash-free basis.

RESULTS AND DISCUSSION

To determine the effects of a catalyst in coal liquefaction, it is useful to perform the liquefaction tests without added solvents or vehicles. Previous work has shown that fundamental catalyst investigations tend to be confounded if any solvents are present (1,2). In particular, the use of reactive liquids such as tetralin was found to exert a leveling effect on the influence of the catalyst on the initial conversion of coal (4). Using only coal and hydrogen magnifies the effect of the added catalyst.

In most solvent-free liquefaction work, a benefit is noted for impregnating the catalyst precursor on the coal over adding it as a powder (1,2). This is usually evident by higher conversions for the impregnated samples. To make the liquefaction tests as simple as possible, it was desirable to utilize a catalyst precursor that required few, if any, special preparation procedures to produce an active catalyst during the liquefaction test. Compounds commonly used in coal liquefaction research such as ammonium heptamolybdate, ammonium tetrathiomolybdate, and molybdenum trisulfide only perform well when special procedures are employed either to disperse or impregnate them onto the coal or to introduce them as very small particles.

$\text{Mo}(\text{CO})_6$ is not commonly used as a catalyst precursor in coal liquefaction research. While it has been shown to be an effective precursor (5,6), it is not practical for use on a larger scale. However, certain attributes of $\text{Mo}(\text{CO})_6$ make it desirable for fundamental investigations into catalytic mechanisms relative to coal liquefaction. In particular, the

inherent volatility of $\text{Mo}(\text{CO})_6$ permits it to form an active liquefaction catalyst (MoS_2) in the presence of sulfur with no special preparation, impregnation, or dispersion techniques (4,6). The reactions involved in the transformation of $\text{Mo}(\text{CO})_6$ to MoS_2 appear to take place in the gas phase as the carbonyl sublimates and decomposes. Conversion of $\text{Mo}(\text{CO})_6$ to MoS_2 has been observed to occur at temperatures as low as 100°C in the presence of hydrogen sulfide (7).

Figure 1 shows the effect on the conversion of the DECS-17 coal of simply adding $\text{Mo}(\text{CO})_6$ powder along with coal to the microautoclave. These tests were performed at 425°C using a slow heatup to reaction temperature and an initial charge of 1030 psig (7.20 MPa) hydrogen/3% hydrogen sulfide. Duplicate tests were performed with the raw coal (indicated in Figure 1 at 10 ppm) and with 100 ppm added molybdenum. Six replicate tests were performed at a level of 1000 ppm added molybdenum. The bars associated with the data points in Figure 1 indicate the range of values obtained (the results were identical for the tests with raw coal). Good conversions to both THF and cyclohexane-soluble products are noted at catalyst concentrations of 500 ppm Mo (based on daf coal) or above. These conversions are similar to those obtained with this coal when using a hydrogen-donor solvent in conjunction with more conventional catalyst precursors (8). A pronounced catalytic effect is noted even at molybdenum loadings of 50 to 100 ppm. There does not appear to be much additional benefit of using catalyst loadings above 1000 ppm.

To determine the effect of $\text{Mo}(\text{CO})_6$ on the conversion of DECS-17 coal as a function of temperature, liquefaction tests were performed at 25°C intervals from 325°C to 425°C in the presence and absence of this compound. In the catalytic tests, $\text{Mo}(\text{CO})_6$ was used at a level of 1000 ppm Mo (based on daf coal). Table I summarizes the number of replicate experiments that were performed in each case.

Table I. Number of Duplicate Tests Performed on the DECS-17 Coal.

Reaction Temperature, $^\circ\text{C}$	Number of Tests Performed	
	Thermal Tests	Catalytic Tests
325	2	2
350	4	4
375	3	2
400	4	2
425	4	6

The conversion data for the thermal and catalytic tests are shown in Figures 2A and 2B, respectively. The symbols represent the average conversion value and the bars associated with the symbols indicate the range of values obtained. No bars imply that the variability was less than two percentage points of conversion (the size of the symbols). The figures reveal that greater variability in conversion values was associated with specific conditions. For example, the greatest variabilities were associated with determinations of cyclohexane conversion for the catalytic tests. It was also noted that

the filtration of the THF solution from the catalytic test at 375°C was much more difficult than for the same product at the other temperatures, resulting in greater variability than for the same determination at the other temperatures.

It is evident from the data in Figure 2B that high conversions of the DECS-17 coal are possible with $\text{Mo}(\text{CO})_6$ in the absence of any added solvents or vehicles. The THF and cyclohexane conversions at 425°C are over 90% and 60%, respectively. Similar conversions were previously obtained using $\text{Mo}(\text{CO})_6$ with an Illinois No. 6 coal (6). Both the thermal and catalytic conversions increase with temperature; however, the influence of the catalyst becomes more apparent at higher temperature.

To better illustrate the effect of the catalyst, Figure 3 contains the differences obtained by subtracting the thermal conversions from the corresponding catalytic conversions. Little or no catalytic effect is observed at 325°C. Other data, which are not presented here, show that a catalytic effect is observed at this temperature at longer reaction times. As the reaction temperature increases, there is a corresponding increase in the additional amount of THF conversion due to the effect of the catalyst. The catalytic effect levels as the maximum total conversion is approached (400°C). The greatest increment to the catalytic effect on THF conversion occurs between 350°C to 375°C.

A different trend is observed for cyclohexane conversion. In this case, no activity is observed until the reaction temperature exceeds 375°C, at which point the conversion attributed to the catalyst suddenly increases. In going to 425°C, a smaller increase is noted. Figure 2A shows that the thermal conversion to cyclohexane-soluble materials increases steadily from 325°C to 425°C.

Based on the above data and observations of the resulting products, it appears that the catalyst formed from $\text{Mo}(\text{CO})_6$ plays two separate roles in the liquefaction of the DECS-17 coal. First, it facilitates the dissolution of the coal to heavy products in a manner that parallels increases in reaction temperature. Second, it improves the conversion of these products to lighter, cyclohexane-soluble material. The onset of catalytic activity occurs at a higher temperature for the latter role. At present, it is not clear whether the difference in onset temperatures for the two catalytic functions is due to differences in activation energies for the catalytic reactions responsible for these two roles, or whether the catalyst itself changes in activity as the reaction temperature is increased. Further experiments would be required to differentiate between these effects. One possibility is that the two roles may be explained on the basis of two different chemical functions. That is, THF conversion is catalytically assisted by prevention of retrogressive reactions while cyclohexane conversion is assisted by catalysis of cracking or deoxygenation reactions.

The conversions noted above are calculated by difference using the weights of the insoluble residues collected and thus do not differentiate between the yields of liquid and gaseous products. Figure 4 shows the average production of gaseous products for the thermal and catalytic tests at the various temperatures. It is apparent that most of the gases produced are the result of thermal chemistry. The largest increase in gas production occurs between 400°C and 425°C. Only the production of butane and, to a lesser degree, propane are influenced by the presence of the catalyst. The increased production of these species again points to increased cracking activity, possibly of hydroaromatic ring structures.

Analysis of the quantity and composition of the gas released when the microautoclave was depressurized permitted calculation of the amount of hydrogen consumed during the reactions. Figure 5 compares the increment in conversion with the increment in hydrogen uptake resulting from the addition of the catalyst. The trends are similar to those in Figure 3 and are consistent with two separate roles of the catalyst. The catalytic promotion of hydrogen uptake is associated with a regular corresponding increase in THF conversion. This is not the case for cyclohexane conversion. This indicates that catalytically promoted hydrogen uptake is insufficient in and of itself to produce lighter or less functional liquefaction products. Catalytic influence on cracking or deoxygenation reactions may require higher temperatures.

The total pressure within the microautoclave was also recorded over time for each test. These data were converted to estimates of the moles of gas in the microautoclave using the ideal gas law and an experimentally derived correlation between measured pressure and reactor temperature. Figure 6 depicts the effect of the catalyst on the rate at which the amount of gas present in the microautoclave changed during the liquefaction tests at the different temperatures. The decreases noted in this figure are primarily due to the uptake of hydrogen. The results are averages of at least two sets of experiments and again are determined by subtracting the thermal data from corresponding catalytic data. The abscissa, time, includes the heat-up period and the one hour reaction time. Little influence of the catalyst on the rate of hydrogen uptake is noted at 325°C. A slightly higher rate is observed at 350°C; however, at even higher temperatures a pronounced increase in the rate of hydrogen uptake is noted. The onset of this pronounced catalytic activity occurs at about 370°C. It also appears that a limit for the catalytic influence on hydrogen uptake of about 0.016 moles is approached at 425°C. This is equivalent to 0.011 grams of hydrogen per gram of coal.

SUMMARY

The preliminary work presented here with the DECS-17 Blind Canyon coal shows the importance of utilizing a catalyst in the dissolution and liquefaction of this coal. Under the conditions of the tests reported here, the catalyst appears to have dual roles in the conversion to THF- and cyclohexane-soluble products. The catalyst appears to be active at 350°C with respect to formation of the THF-soluble products; however, no activity is observed with respect to cyclohexane-soluble products until 400°C.

Overall, the data show that high conversions of this coal are possible using only a dispersed catalyst (no added solvents) and hydrogen. In particular, operation at 400°C results in high conversion but with much lower gas production than at 425°C. If one is going to study the effect of a catalyst on the initial dissolution of this coal, it would be advisable to operate at temperatures below 400°C. If interest is in the production of lighter products, then 400°C or higher should be used.

ACKNOWLEDGMENTS

The author would like to thank Richard Hlasnik and Jerry Foster for performing the microautoclave work:

DISCLAIMER

Reference in this report to any specific product, process, or service is to facilitate understanding and does not imply its endorsement or favoring by the United States Department of Energy.

REFERENCES

1. Weller, S. W. Proc., Fourth International Conference on Chemistry and Uses of Molybdenum, H.F. Barry and P.C.H. Mitchell, eds., 1982, 179-186.
2. Derbyshire, F. J. Catalysis in Coal Liquefaction: New Directions for Research; IEA Coal Research: London, 1988.
3. Anderson, L. L. New Trends in Coal Science, Y. Yürüm, ed.; Kluwer Academic Publishers: Boston, 1988.
4. Warzinski, R. P. Proc., U.S. DOE Direct Liquefaction Contractors' Review Meeting, September 24-26, 1990, 320-336.
5. Suzuki, T; Yamada, H; Sears, P. L.; Watanabe, Y. Energy & Fuels 1989, **3**, 707-713.
6. Warzinski, R. P.; Lee, C.-H.; Holder, G. D. The Journal of Supercritical Fluids 1992, **5**, 60-71.
7. Warzinski, R. P. Proc., U.S. DOE Direct Liquefaction Contractors' Review Meeting, September 22-24, 1992, in press.
8. Personal communication from Anthony V. Cugini, U.S. Dept. of Energy, Pittsburgh Energy Technology Center, Pittsburgh, Pennsylvania.

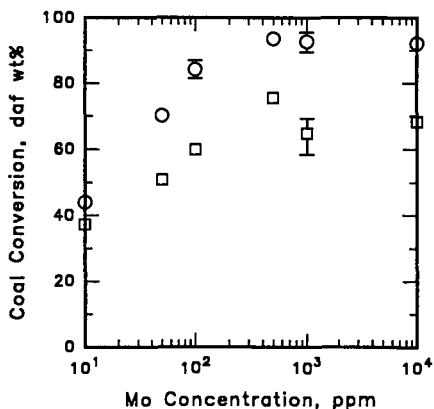


Figure 1. Effect of adding $\text{Mo}(\text{CO})_8$ on the conversion of DECS-17 coal. (○ THF solubility; □ cyclohexane solubility. Data at 10 ppm are for raw coal.)

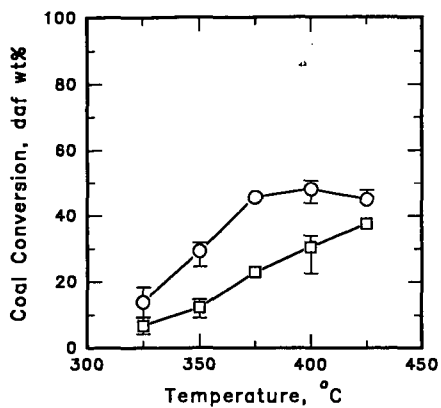


Figure 2A. Conversion results from thermal liquefaction tests. (○ THF solubility; □ cyclohexane solubility)

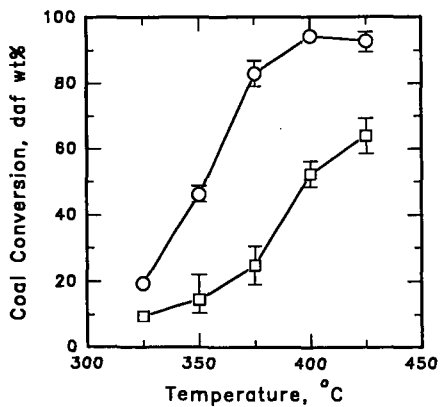


Figure 2B. Conversion results from catalytic liquefaction tests. (○ THF solubility; □ cyclohexane solubility)

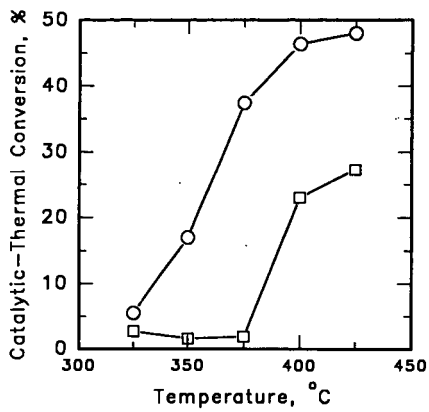


Figure 3. Catalytic-thermal conversions. (O THF solubility; □ cyclohexane solubility)

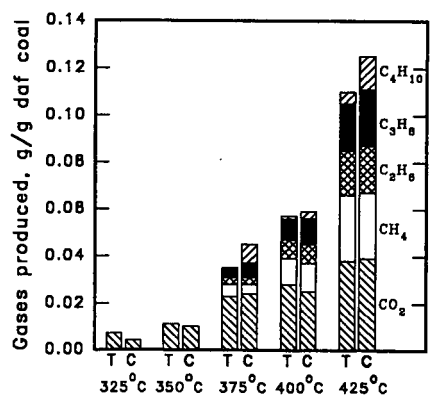


Figure 4. Average gas production for DECS-17 coal for thermal (T) and catalytic (C) tests at different temperatures (shown on abscissa).

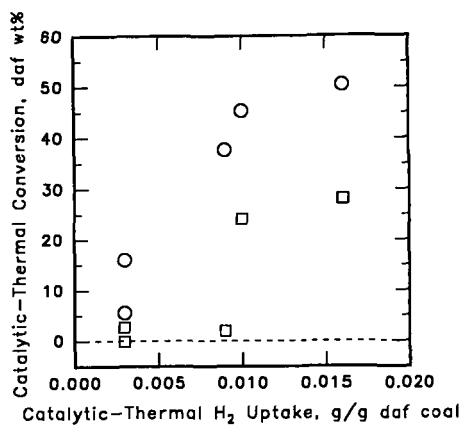


Figure 5. The effect of a catalyst on conversion as a function of the effect of a catalyst on hydrogen uptake. (○ - THF solubility; □ - cyclohexane solubility)

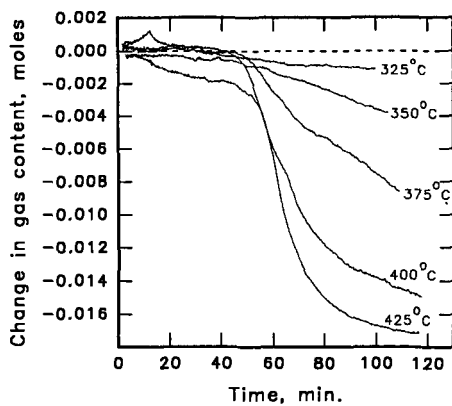


Figure 6. Effect of a catalyst on changes in gas content as a function of time and temperature. Trends are averages of catalytic-thermal data.

EQUILIBRIUM ADSORPTION OF MOLYBDATE BY COAL

K.T. Schroeder, B.C. Bockrath, and M.L. Tate*
U.S. Dept. of Energy, Pittsburgh Energy Technology Center
P.O. Box 10940, Pittsburgh, PA 15236

Keywords: Surface Charge, Catalyst, pH Effects

Abstract: To investigate the effect of solution pH on the adsorption of molybdate, two Argonne Premium coals were equilibrated with aqueous solutions of ammonium heptamolybdate at pH 2 and 4. The extent of molybdate adsorption by the coal was calculated from the decreased concentration of molybdate in solution as determined by atomic absorption. The time necessary to reach equilibrium was always less than 24 hours; the majority of the adsorption occurred within the first hour. The Wyodak coal adsorbed more molybdate with better reproducibility than did the Illinois No.6 coal. The amount of Mo adsorbed by both coals increased with a decrease in the pH of the solution and with increased concentrations of molybdate. The increased adsorption under acidic conditions is consistent with increased positive sites on the coal surface at the lower pH.

Introduction: Electrokinetic studies of coal-water suspensions demonstrate that the surface charge of the coal particle is dependent upon the pH of the solution.¹ At lower pH values, the coal surface becomes positively charged due to protonation of basic sites. For demineralized bituminous coals, the surface usually becomes positively charged below pH 6. Lower rank and oxidized coals have lower isoelectric points; they develop a net positive charge at lower pH levels.

One would expect that the ability to disperse the negatively charged catalyst precursors, such as molybdenum anions, would be affected by the charge on the coal surface. If the coal surface has a net negative charge, the molybdate anion should tend to aggregate at the small localized positive regions. Increasing the number of the positively charged regions would be expected to provide more sites for the precursor to bind. This could lead to a more evenly dispersed catalyst with a smaller particle size.

Experiments with carbon supports indicate that the mechanisms of dispersion can be related to the carbon surface chemistry.² When a number of carbons were treated with molybdate solutions at a pH above their isoelectric points, only small amounts of molybdenum were adsorbed. When the same carbons were treated in the same way at a pH lower than the carbon isoelectric point, considerably larger amounts of molybdenum were adsorbed. The higher molybdenum adsorption at lower pH was taken as evidence that the lower solution pH resulted in a more positively charged carbon particle.

The effect of surface charge on the application of dispersed phase catalysts to coals has been examined only recently.³ Such effects may be important to the art of catalyst impregnation. To investigate the effect of solution pH on the adsorption of molybdate, two Argonne Premium coals were equilibrated with solutions of ammonium heptamolybdate at pH 2 and 4. The results

* M.Tate was a participant in the Professional Internship Program administered by the Oak Ridge Associated Universities, Oak Ridge, Tennessee.

of these studies indicate that control of the pH during catalyst application may lead to more effective impregnation techniques.

Experimental: To a 1 g sample of coal in a 50-mL pyrex centrifuge tube was added 40 mL of a buffered catalyst solution. The slurry was mixed for periods from 0.5 to 24 hours at ambient temperature, then centrifuged. Aliquots (3 mL) were removed for atomic absorption analysis (AA) and the pH was measured. Mixing was then resumed. The solution pH remained relatively constant. The measured pH values over the 3 days of equilibration were 1.90 ± 0.06 for the solution with an initial pH of 1.8 (20 determinations) and 4.14 ± 0.05 for the solution with an initial pH of 4.1 (24 determinations). The average pH of the solutions containing larger amounts of molybdate tended to be slightly higher than those containing lower concentrations, but the difference was always less than 0.1 pH unit.

Coals: The Wyodak and Illinois No.6 coals were obtained from the Argonne Premium Coal sample bank'. Vials were tumbled prior to opening in accord with the Argonne instructions. The coals were pre-equilibrated with the same buffers that were used to prepare the catalyst solutions. Although the purpose of the pre-equilibration was to adjust the pH of the coal surface, it also removed all of the alkali and alkaline earth metal cations Na, K, Mg, and Ca. However, no iron was removed. It was also noted that the Illinois #6 coal samples wetted more easily and formed fewer clumps than did the Wyodak samples.

Catalyst Solutions: Ammonium heptamolybdate tetrahydrate (Fisher, Certified A.C.S.) was used as received to prepare the various concentrations of molybdate in two buffers listed in Table 1. Concentrations are expressed in ppm molybdenum. An additional solution at 6000 ppm formed a white precipitate, presumed to be MoO_3 , after a couple of days. Because of this instability at higher concentrations, experiments were limited to solutions containing 3000 ppm or less.

Buffer Solutions: All solutions were prepared using deionized water which had been deaerated by purging with argon for at least 30 minutes prior to use. An acetate buffer of nominal pH 4 was prepared using acetic acid and sodium acetate. This gave a solution with a measured pH of 4.1. Similarly, a sulfate buffer of nominal pH 2 was prepared using sulfuric acid and sodium sulfate. This gave a solution with a measured pH of 1.8.

Calculations: The molybdate on the coal was calculated from the loss of molybdate from solution according to the equation

$$Mo_{coal,i} = Mo_{coal,i-1} + (Mo_{soln,i-1} - Mo_{soln,i}) \frac{V_{soln,i}}{W_{coal}}$$

where Mo_{coal} is the molybdenum concentration in ppm on the coal, Mo_{soln} is the molybdenum concentration in the solution in ppm, Vol_{soln} is the volume of solution remaining in mL, and W_{coal} is the weight of the coal in grams. It was necessary to take into account the change in volume of the solution with each successive sample i , because the aliquot size was not negligible in comparison to the solution volume. The concentration of molybdate in solution was measured by AA as described below.

AA Analysis: Atomic Absorption (AA) analyses were performed using a Perkin Elmer Model 503 flame atomic absorption spectrophotometer. Ammonium chloride modifier was added to provide a final concentration of 1% in all determinations. The molybdenum

concentration was determined by reference to a linear regression calibration curve derived from four standard solutions ranging from 0 to 10 ppm Mo. Samples which exceeded this range were diluted as needed to fall within the calibrated range.

The agreement of the AA results with the concentrations determined from the weights of molybdate and buffer used in the solution preparations is shown in Table 1. The last column of the Table lists the concentration determined by AA and the fifth column lists the concentration of Mo determined gravimetrically in each of the solutions used in this study. The agreement between the two determinations is very good; the gravimetric determination is always within two standard deviation units of the AA result and is often within one unit. There may be a small bias in one of the methods since the gravimetric determination is always lower than the AA determination, but the difference is considered insignificant for the purpose of these experiments.

The standard deviations and relative standard deviations were derived from a series of control samples analyzed over the several days of the experiment. The magnitudes of the deviations are similar to those found for the AA technique itself. For example, the nominal 600 ppm controls gave a standard deviation of 27 ppm at both pH levels. This compares favorably with the precision of the AA technique of 42 ppm as determined in separate quality assurance experiments. Thus, the solutions themselves were stable with time and precipitation cannot account for the loss of Mo from solution. A false positive was never obtained for blank samples which were also analyzed routinely in single blind experiments.

Results: Aqueous solutions of ammonium heptamolybdate containing up to 3000 ppm molybdenum were allowed to equilibrate with samples of the Argonne Premium Wyodak and Illinois No.6 coals. The loss of molybdate from solution was monitored by AA analyses of aliquots of the supernatant solution. The results obtained using the Wyodak coal at a pH of 2 are shown in Figure 1. Molybdate was adsorbed quickly and equilibration occurred within the first 24 hours. At the lowest initial concentration, 60 ppm, the adsorption of Mo was complete; the supernatant solution contained no detectable Mo after the first hour of contact. At 600 ppm, 90% of the Mo was adsorbed resulting in about 2 g of molybdenum being adsorbed per 100 g of as-received Wyodak coal. Increasing the solution concentration by a factor of 2.5 to 1500 ppm resulted in increased adsorption by a factor of about 2. A further doubling to 3000 ppm resulted in an even smaller incremental increase in adsorption, indicating that the amount of molybdate that can be adsorbed is limited. Inspection of the graphs in Figure 1 suggests that under these conditions the limiting value is in the neighborhood of 5%.

Buffering the solution pH to 4 resulted in less molybdate adsorption, as can be seen in Figure 2. Although increasing the initial Mo concentration from 60 through 600 to 3000 ppm resulted in increased amounts of Mo being adsorbed, the equilibrium values are noticeably lower at this higher pH. For the case at 3000 ppm, equilibration at a pH of 4 resulted in the coal adsorbing 3.4% of its weight in Mo; equilibration at a pH of 2 resulted in 4.3% adsorption by coal. Only at 60 ppm where both solutions were depleted in Mo was the amount adsorbed the same. Thus, lowering the pH of the medium effects a larger adsorption of molybdate from solution.

Different levels of adsorption occurred when a bituminous coal was used. Similar experiments using the Argonne Illinois No.6 coal resulted in the data presented in Figures 3 & 4. In contrast to the rather smooth trends discernible at all Mo concentrations for the Wyodak coal, the results for the Illinois coal contained appreciable scatter at the highest Mo concentration. Despite this scatter, some comparisons between the Wyodak and Illinois coals can be made by focusing on the results obtained at the 60 and 600 ppm concentrations. At these lower initial molybdenum concentrations, a rapid equilibration apparent within the first 24 hours was consistent with the rapid equilibration seen for the Wyodak coal. However, the amount of Mo adsorbed was much smaller than was seen for the lower rank coal. At 60 ppm, the molybdenum adsorbed was barely above the detection limits at a pH of 2 and at the detection limits at a pH of 4. By contrast, the Wyodak coal adsorbed all of the available Mo under similar conditions. At an initial Mo concentration of 600 ppm, the amount of Mo adsorbed by the Illinois No.6 coal is only 10% of that adsorbed by the Wyodak coal. Thus, on a weight basis, the Wyodak coal is 10 times more effective at adsorbing molybdenum anions than is the Illinois coal at a pH of 2. Substituting a pH 4 buffer (Figure 4) for the pH 2 buffer (Figure 3) effected an even greater decrease in Mo adsorption for the Illinois No.6 coal than it did for the Wyodak coal. At the 600 ppm level, the higher pH resulted in the coal adsorbing only 0.13% of its weight in molybdate instead of the 0.51% seen at the lower pH. Thus, the Illinois No.6 coal adsorbs less Mo from solution than does the Wyodak coal and the amount adsorbed is more sensitive to the pH of the aqueous solution.

DISCUSSION: The results obtained for these two coals appear to be consistent with an adsorption mechanism in which molybdate in solution is in equilibrium with surface-bound molybdate. The extent of surface adsorption is expected to depend on both the concentration of molybdenum in solution and the number of adsorption sites available on the coal surface. Because the coal surface develops more net positive charge at the lower pH, more anion binding sites are expected to become available. Thus, both increasing molybdate concentration and decreasing pH are expected to result in more molybdate being removed from solution.

However, the nature of the molybdenum species in solution changes with changes in total concentration of molybdenum(VI) and pH.⁵ For example, at a total Mo(VI) concentration of 50 ppm the predominate species is $\text{Mo}(\text{OH})_6$ at a pH of 2, but MoO_4^{2-} predominates at a pH of 4. At a total Mo(VI) concentration of 2000 ppm the predominate species is $\text{Mo}_2\text{O}_7^{4-}$ at a pH of 2, whereas $\text{HMo}_2\text{O}_7^{3-}$ predominates at a pH of 4. This rich chemistry provides alternate explanations to the observed adsorption trends. Each of these species as well as a number of other minor species may all adsorb with different equilibrium constants. Thus, the details of the adsorption mechanism are not clear.

The adsorption sites on the coals are effected by the solution pH. These sites may reside in the organic portion, the mineral portion, or both portions of the coal. Organic functional groups play an important role in the electrokinetic behavior of coal-water suspensions¹ and the adsorption of molybdate by carbon supports can be related, in part, to the degree of surface oxidation.² Nitrogen heteroatoms, which become positively charged in acid, may also play an important role. It is interesting to note that an atomic Mo to nitrogen ratio of 1 corresponds to a 5

weight % Mo loading on the Wyodak coal. Thus, it is reasonable to suspect that the extent of molybdate adsorption and the pH dependence are related to the organic heteroatom content. Also, mineral matter may play an important role in the adsorption. The protonation of alumina hydroxyl groups is responsible for the creation of adsorption sites for molybdate on catalyst supports.⁶ The clays or other minerals in the coal could behave in a similar fashion.

It is of interest to compare these results with those obtained for some other coal samples. Table 2 compares the results obtained by Abotsi et al.³ with the results obtained here. Since some of the experimental procedures are different, and the coals are not identical, the results are not strictly comparable. The solution concentration used by Abotsi was 4800 ppm whereas our highest concentration was 3000 ppm. However, the main points are readily discernable. There is a fairly large difference in the % Mo adsorbed between the bituminous and subbituminous coals. This may be due to the higher oxygen content of the latter. However, there are also differences within rank. The Montana Rosebud subbituminous coal (PSOC 1493) adsorbed about half as much Mo as did the Wyodak coal. Thus, the nature of the coal is also important to the adsorption mechanism.

CONCLUSIONS: The extent of molybdate adsorption by coal is affected by the nature of the coal and the pH and molybdate concentration of the equilibration solution. Lower pH and higher molybdate concentrations favor molybdate adsorption. Such effects may be important to the art of catalyst impregnation.

ACKNOWLEDGEMENTS: The authors thank Ms. Deborah Hreha and Ms. Jodi Schuster who performed the AA analyses reported in this work and José Solar for many helpful discussions.

DISCLAIMER: Reference in this report to any specific commercial product, process, or service is to facilitate understanding and does not necessarily imply its endorsement or favoring by the U.S. Department of Energy.

REFERENCES

1. Laskowski, J.S.; Parfitt, G.D. *Surfactant Sci. Ser.* 1989, **32**, 279-327.
2. Solar, J.M.; Leon y Leon, C.A.; Osseo-Asare, K. Radovic, L.R. *Carbon* 1990, **28**(2/3), 369-375.
3. Abotsi, G.M.K.; Bota, K.B.; Saha, G. *Energy Fuels* 1992, **6**(6), 779-782.
4. Vorres, K.S. *Energy Fuels* 1990, **4**, 420-426.
5. Cruywagen, J.J.; De Wet, H.F. *Polyhedron* 1988, **7**(7), 547-556.
6. Spanos, N.; Vordonis, L.; Kordulis, Ch.; Lycourghiotis, A. *J. Catal.* 1990, **124**, 301-314.

Table 1. Concentration of Molybdenum in Buffered Solutions					
Nominal pH	Nominal Concentration (ppm Mo)	Ammonium Heptamolybdate (grams)	Amount of Buffer (grams)	Calculated Concentration (ppm Mo)	Concentration Measured by AA (ppm Mo)
4	60	0.0116	100.72	63	66±5 (±8%)
	600	0.1078	100.37	583	598±26 (±4%)
	3000	0.5487	100.20	2960	2968±225 (±8%)
2	60	0.0114	100.60	62	66±5 (±8%)
	600	0.1077	101.46	576	584±27 (±5%)
	1500	0.1325	50.21	1430	1550±71 (±5%)
	3000	0.5484	100.22	2957	3152±175 (±6%)

TABLE 2. Comparison of Molybdate Adsorption for Different Coals			
COAL	pH	% Mo on Coal (Ref. 3)	% Mo on Coal (This Work)
SUBBITUMINOUS	2	2.11	4.1
	4	1.25	3.5
BITUMINOUS	2	0.29	≥0.5
	4	0.19	≥0.3

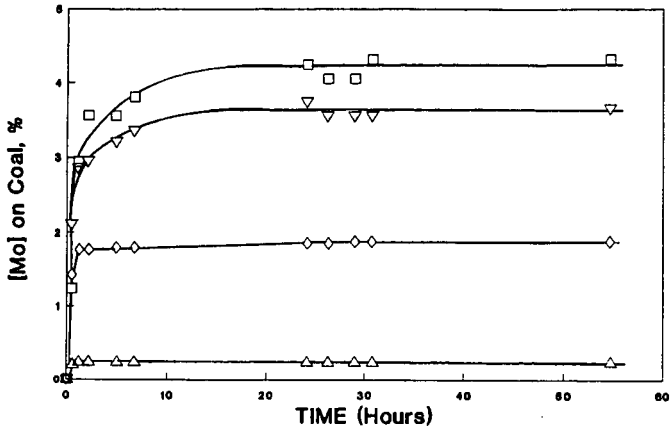


FIGURE 1. Adsorption of Molybdate from Solution by Wyodak Coal at a pH of 2. □ Initial solution concentration = 3000 ppm. ▽ Initial solution concentration = 1500 ppm. ◇ Initial solution concentration = 600 ppm. △ Initial solution concentration = 60 ppm.

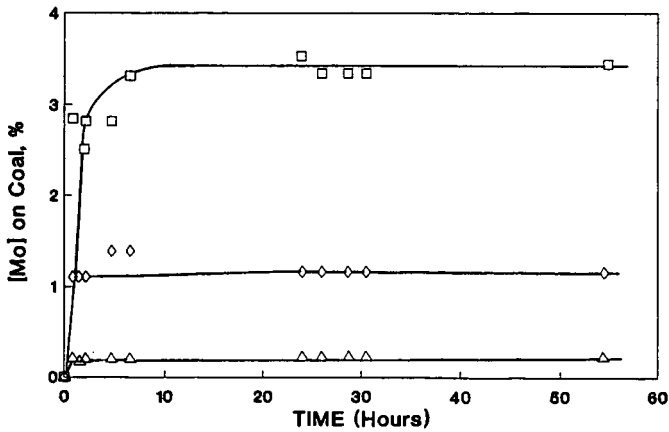


FIGURE 2. Adsorption of Molybdate from Solution by Wyodak Coal at a pH of 4. Symbols the same as on Figure 1.

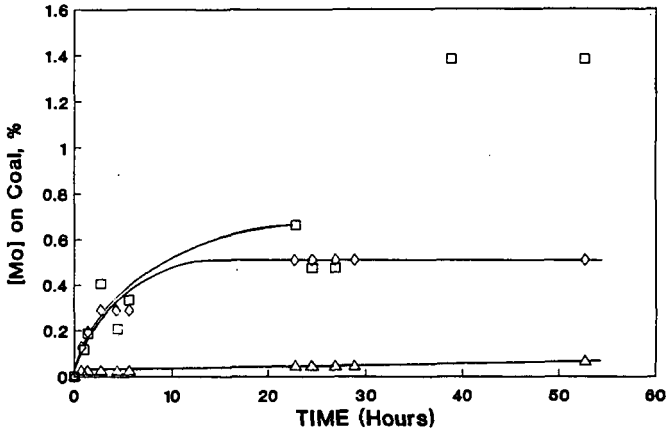


FIGURE 3. Adsorption of Molybdate from Solution by Illinois No.6 Coal at a pH of 2. Symbols the same as on Figure 1.

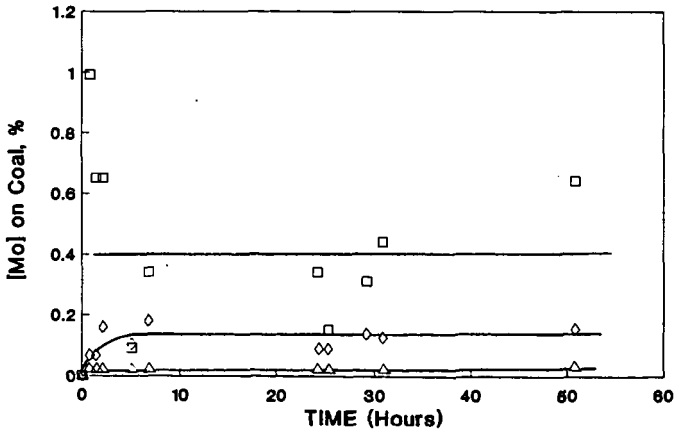


FIGURE 4. Adsorption of Molybdate from Solution by Illinois No.6 Coal at a pH of 4. Symbols the same as on Figure 1.

Empirical Evaluation of Coal Affinity for Various Chemicals

Tetsuo Aida*¹, Shuhsaku Suzuki¹, Masayuki Fujii¹
Masakuni Yoshihara², Teijiro Yonezawa²

¹Department of Industrial Chemistry, Faculty of Engineering in Kyushu
Kinki University

11-6 Kayanomori, Iizuka, Fukuoka 820, JAPAN

²Department of Applied Chemistry, Faculty of Science and Engineering
Kinki University

3-4-1 Kowakae, Higashi-Osaka 577, JAPAN

INTRODUCTION

Coal is a complicated natural product which has several functional groups in its cross-linked macromolecular structure. Because of this fact the diffusion mechanism of the penetrant molecule into the matrix of a solid coal is not so simple. It is quite important to know the affinity between the penetrant molecule and the macromolecular structure of coal for the coal scientists who are challenging to develop efficient chemical transformations of coal such as liquifaction, gasification and etc.. Nevertheless the reliable methodology to determine the affinity has not yet been developed. One of the most practical approach to this goal will be to use the solvent swelling behaviours of coal. Because as it is mostly true that better solvent makes coal better swelling, the equilibrium swelling value(Q-value) of the penetrant may reasonably reflect its affinity to the coal. However, there are some problems in this idea. One of the most critical problems will be how to determine the Q-value of solvents(chemicals) which used to be a solid(crystal) under the measuring condition. Furthermore the steric bulkiness of the penetrant molecule also will provide an aserious error on the net Q-values(1).

Some years ago, we revealed the steric requirement of coal toward the penetrant molecule is significantly relaxed in binary solvent system which is composed with normal solvent such as methanol or DMF and sterically hindered molecule(i.e., triethylamine or HMPA)(2). The mechanism of the relaxation of the steric requirement of coal is considered as follows; the preferential petration of the normal solvent into solid coal makes the coal-solvent gel. Then, the significant expansion of the cross-linked network of coal is induced and thus it makes the bulky molecule easy to penetrate. These findings hinted us to use this swelling system for evaluating the affinity of various chemicals toward coal.

This paper presents the results of the studies on the new methodology to evaluate the coal affinity of various chemicals.

EXPERIMENTAL

The swelling measurements were carried out as described into previous paper(3). Coal, Illinois No.6 coal, used in these studies was from the Ames Laboratory Coal Library. Prior to use, the coal was ground, sized, dried at 110°C overnight under vacuum, and stored under a nitrogen atmosphere. The solvents were distilled by ordinary procedures before use.

This work was supported by the grant from The Japanese Ministry of Education, during 1989-1992.

RESULTS AND DISCUSSION

Swelling of Illinois No. 6 Coal in Various Solvent

Coal swells in the various solvent with the different manners. Figure 1 shows the relation between the equilibrium swelling value of the solvent which were determined by our instrument and its electron donor number(DN). This type of data treatment had been reported by Marzec et al.(4), and they recognized some correlation between them. However as far as the data shown in this Figure, it seems to be quite difficult to find out such correlation. As we discussed before(1), one of the problems in this figure is that the Q-values measured always involve their steric factor, that is, the sterically hindered solvents are restricted the penetration into the macromolecular structure of coal by the steric requirement, probably due to the cross-linking density. If in this Figure we can pick up only the solvents which are not sterically bulky and also have relatively high dielectric constant(>20), the correlation becomes very clear and almost linear as shown in Figure 2. It is quite interesting that the dielectric constant of the penetrant also seems to be one of the key parameters controlling the coal affinity. This fact may suggest that there are the significant contribution to the macromolecular cross-linking structure of coal from relatively weak bonding interactions such as van der Waals, hydrogen bonding, charge transfer bonding and π - π bonding.

Introduction of Coal Affinity Parameter

Although these data shown above suggest the possibility to use the equilibrium swelling value(Q-value) as a convenient scale for evaluating the affinity to the coal, there seems to be at least two big problems, that is, the first of all is how to determine the Q-value of solid chemicals(crystal) by means of the solvent swelling measurement, and the second of all is how to eliminate the steric factor from the observed Q-value.

Table 1 summarizes the swelling behaviours of Illinois No.6 coal in the steric isomers of butylamine. It is obvious that there is a significant steric requirement on their swelling which is reflected not only on the swelling rate(V-value), but also on the Q-value. Thus, the Q-value measured in the neat solvent always involves the contribution from the steric factor. Namely, in order to use the Q-value as a tool for evaluating the coal affinity, we have to find out the methodology to extract the net Q-value from the observed one.

Figure 3 demonstrate the swelling behaviour of Illinois No.6 coal in the binary mixture of the butylamine and methanol. In the case of n-butylamine-methanol system, the observed Q-values have a nice linear relationship versus the concentration. Meanwhile in the mixed system of more sterically bulkier isomers such as sec- and tert-amine a kind of the synergistic effect were observed. It is particularly interesting that the values obtained by the extrapolation(dotted line on the Figure) from the Q-value at the lower concentration region seems to reasonably reflect their own values. We had revealed this phenomena as the relaxation of the steric requirement by the coa-gel formation(2). Now, we may be able to define for the extrapolated values obtained on the Figure to be their potential Q-value(Q_{pot}) which used to be hidden by the steric factor.

If these speculation are correct, we can use this swelling system as a general procedure for evaluating the coal affinity. Namely, as far as the chemicals are soluble in the solvent (reference solvent), gas, liquid even solid or crystal, the potential Q-value(Q_{pot}) must be empirically determined by this method. Furthermore, very fortunately, because of the binary solvent system the steric factor in the observed Q-value can be minimized.

Based on these considerations, we propose a new empirical parameter to evaluate the affinity to the macromolecular structure of coal, as the Coal Affinity Parameter(κ_Q) which is calculated following equation.

$$\kappa_Q = Q_{pot} / Q_{DMF}$$

In this study we have adopted N,N'-dimethylformamide(DMF) as the reference solvent. The reason is that it has a powerful ability to solve many kinds of chemicals even inorganic compounds and it is also easy to purified.

Table 2 summarizes the typical example of Coal Affinity Parameter(κ_Q -value) determined for various chemicals. In these data it is particularly interesting that the β -naphthol(mp 122-123°C), nitrobenzene and maleic anhydride(mp 54-56°C) have higher κ_Q -values than pyridine. These compounds have long been assumed to have reasonably good affinity to coal, but their relative abilities were never compared.

Figure 5 shows the relation between Coal Affinity Parameter(κ_Q -value) and the electron donor number(DN). Surprisingly, a good correlation was observed towards wide range of organic compounds. particularly, a solid(crystal) compound such as ethylenecarbonate(mp.35°C) and a sterically hindered compound such as hexamethylphosphoramide(HMPA) in which coal used to give very small degree of swelling, probably because of the steric hindrance. As previously discussed there seems to be reasonable relationship between coal affinity and electron donor number(DN), and now we can see a similar relation between the Coal Affinity Parameter(κ_Q -value) and DN. Although this methodology proposed may not be a perfect one to evaluate the affinity to coal, but as far as the results shown in this Figure and Table 2, we are very much encouraged to use the κ_Q -value for the study on the chemical transformations of coal.

It will be also interesting to examine the dependency of κ_Q -value on the coal rank or the nature of the reference solvent, which are now underway in our laboratory.

ACKNOWLEDGEMENTS

This research was supported by the grant from the Japanes Ministry of Education(Kagaku Kenkyuhi Hojokin, Juhten Ryouiki Kenkyu) during 1989-1992.

REFERENCES

- (1) T. Aida, K. Fuku, M. Fujii, M. Yoshihara, T. Maeshima, T. G. Squires, *Energy & Fuels*, **5**, 79(1991)
- (2) T. Aida, Y. Shimoura, N. Yamawaki, M. Fujii, T.G. Squires, M. Yoshihara, T. Maeshima, *Prepr. Pap.-Am. Chem. Soc., Div. Fuel Chem.*, **33**, 968(1988)
- (3) T. Aida, T.G. Squires, *Prepr. Pap.-Am. Chem. Soc., Div. Fuel Chem.*, **30**, 95(1985)
- (4) J. Szeliga, A. Marzec, *Fuel*, **62**, 1229(1983)

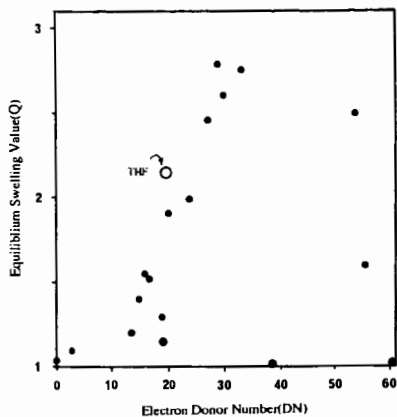


Figure 1 Correlation between Q-value and Electron Donor Number(DN)
(Illinois No. 6 Coal: 60-100mesh; at 20°C)

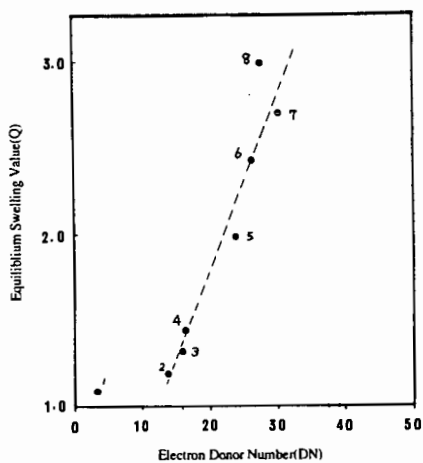


Figure 2 Correlation between Q-value and Electron Donor Number(DN)
(Illinois No. 3 Coal: 60-100mesh; at 20°C)
SOLVENT: 1 nitroethane, 2 acetonitrile, 3 n-butylamine, 4 acetone,
5 trimethylphosphane, 6 DMF, 7 DMSO, 8 N-methylpyrrolidone

Table 1 Solvent Swelling of Illinois No. 6 Coal^a in
Butylamines at 20.0 ± 0.5 °C

amine	V_{ret}^b	Q^c	η_{20}^d cP	CSA ^e
n-butylamine	1.0	2.56	1.54	32.7
isobutylamine	11.9	2.57		32.8
sec-butylamine	5.4	2.41	1.37	33.2
tert-butylamine	599	1.96 ^e	1.48	34.1

^a100-200 US mesh. ^b $V_{ret} = V_{n-Bu} / V_{isomer}$; $V_{n-Bu} = 3.7 \times 10^{-1}$ min⁻¹. ^cMeasured after 10 days' swelling. ^dDetermined by means of Ubbelohde viscometer at 20.00 ± 0.02 °C. ^eSwelling is still continuing.

^e Cross-sectional Area(Å²)

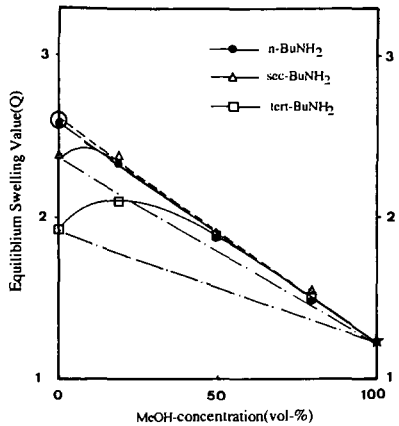


Figure 3 Coal Swelling in Binary mixture (Illinois No. 6 Coal; 60-100mesh; at 20°C)

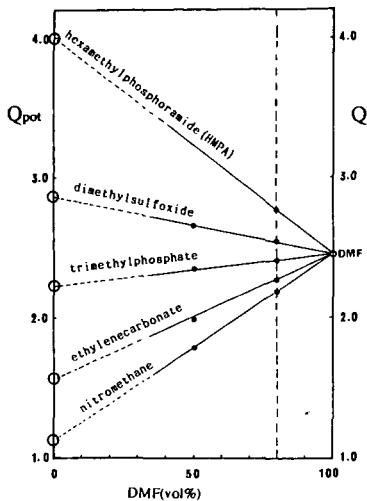


Figure 4 Determination of Potential Q-value (Q_{pot}) (Illinois No. 6 Coal; 60-100mesh; at 20°C)

Table 2 κ_Q -values of various Chemicals (Illinois No. 6 Coal; 60-100mesh; at 20°C)

Chemicals	$^{\circ}\kappa_Q$
nitromethane	0.43
acetonitrile	0.41
n-butyronitrile	0.52
ethylenecarbonate	0.61
acetone	0.68
trimethylphosphate	0.88
DMF	1.00
pyridine	1.08
DMSO	1.14
N-methylpyrrolidinone	1.21
HMPA	1.62
nitrobenzene	1.13
b-naphthol	1.22
maleic anhydride	1.30
benzoic acid	0.80

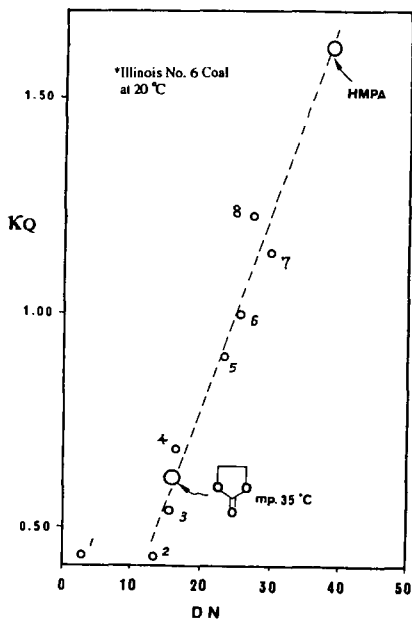


Figure 5 Correlation between K_Q -value and Electron Donor Number(DN)
(Illinois No. 6 Coal; 60-100mesh; at 20°C)

SOLVENT : 1 nitromethane, 2 acetonitrile, 3 n-butyl nitrile, 4 acetone,
5 trimethylphosphate, 6 DMF, 7 DMSO, 8 N-methylpyrrolidone

PROMOTION OF DEUTERIUM INCORPORATION FROM D₂ INTO
COAL MODEL COMPOUNDS BY BENZYLIC RADICALS

Robert D. Guthrie
Buchang Shi
Rustem Sharipov
Department of Chemistry
University of Kentucky
Lexington, KY 40506

Burtron H. Davis
Kentucky Center for Applied Energy Research
3572 Iron Works Pike, Lexington, KY 40511

Keywords: D₂, hydroliquefaction, diphenylethane

INTRODUCTION

A large number of revealing mechanistic investigations have been carried out dealing with the thermolysis of coal and compounds which model its structure. Perhaps because of experimental difficulties, much less attention has been given to the reaction with molecular hydrogen. It seems fair to say that the detailed mechanism by which molecular hydrogen, separately or in combination with "donor solvents", is able to effect the reductive simplification of coal is not completely understood. An obvious approach to following the reaction with H₂ is to substitute D₂. The literature contains ample evidence that deuterium is incorporated into reaction products when thermolysis of coal and coal models is carried out under D₂ gas.¹ It has also been shown that D-labeled substrates, such as tetralin-d₁₂, transfer D atoms back to dihydrogen such that HD is produced from H₂.²

Similarly it is clear that once incorporated into a molecule of organic substrate, transfer of D atoms between molecules is often facile.³ Several mechanisms can be involved in the scrambling process. Molecule-induced homolysis and symmetry-allowed, pericyclic mechanisms have been documented by Brower and Pajak.⁴ A demonstration of radical-promoted exchange was provided by King and Stock⁵ who showed that the presence of species which undergo facile homolysis increases the rate of transfer of deuterium between benzylic positions in different molecules. The mechanisms suggested seem reasonable, however, most of the proposed schemes do not address the question of how the initial transfer from H₂ occurs.

The facility of the scrambling reactions makes the question of how the hydrogen is transferred from H₂ gas into the coal structure in the first place, a particularly difficult one to answer because the initial landing site of the hydrogen atoms is rendered uncertain. Because the H-H bond is quite strong, this initial step would seem likely to be a major obstacle to the process of interest and slower than subsequent events. A scheme put forward by Vernon⁶ proposes hydrogen abstraction from H₂ by benzyl-type radicals. This suggestion was later supported by Shin.⁷ Vernon's suggestion is based on the observation that the cleavage of 1,2-diphenylethane, DPE, gives an increased yield of benzene when the reaction is carried out under H₂. The phenomenon is more pronounced when the reactions are run in the absence of a hydrogen atom donor (tetralin or 9,10-dihydrophenanthrene). It is suggested that benzyl radicals react with dihydrogen, producing toluene and

hydrogen atoms. The hydrogen atoms thus generated are responsible for the hydrogenolysis of the DPE to give benzene. In the presence of hydrogen donor solvents, the benzyl radicals react to give toluene and the production of H atoms is reduced. The latter part of this scheme seems quite reasonable based on the observed facility of reaction between benzyl radicals and compounds with structures similar to donor solvents.⁸ Likewise, the reaction of hydrogen atoms with the aromatic ring of DPE seems reasonable both on energetic grounds and in consideration of the results of Price⁹ who showed that H-atoms generated in the thermolysis of toluene above 500 °C react with toluene to produce CH₃ and H₂ with nearly equal rates. The reaction between benzyl radicals and H₂ seems the most uncertain part of the scheme in that the C-H bond energy of toluene is 85 kcal/mole where as that of H-H is 104 kcal/mole.¹⁰ The reaction of benzyl radical with dihydrogen to form toluene and hydrogen atoms is thus likely to have an activation enthalpy of more than 20 kcal/mole. This would seem to make it an unlikely competitor with various other potential reactions of benzyl radicals which are possible in the system studied.

An additional uncertainty regarding these reactions, is that most of the reported exchange studies using D₂ as a source of deuterium had utilized metal reactor vessels. This raised the question of whether the initial process for introduction of D atoms into the thermolysis milieu might be metal catalyzed. Either the walls of the reaction vessel or metal species contained in common reactor vessel sealants are possible stopover points for D atoms prior to their introduction at the seminal sites for the scrambling process. If these were involved, the well-precedented process of double bond reduction by metal-bound deuterium would then be a likely entry route for D atoms. In cases where liquefaction is accomplished by the deliberate addition of hydrogenation catalysts, this would be the expected mechanism.¹¹ As we wished to understand the noncatalyzed reaction and to use it as a base line for further studies of catalytic agents, we designed and employed a suitable glass reaction vessel.

RESULTS AND DISCUSSION

Using the glass reactor vessel described in the experimental section, we have carried out the thermolysis of 1,2-diphenylethane, DPE, under 2000 psi of D₂ gas at 450 °C. DPE disappeared following a first order rate law as shown in Figure 1. The resultant mixture showed products reported earlier by Poutsma¹² for this reaction in the absence of D₂: toluene, benzene, ethylbenzene, stilbene, 1,1-diphenylethane, phenanthrene and diphenylmethane. We also found what appeared to be diphenylpropane and trace amounts of other materials. For comparison, we carried out the reaction at the same pressure of N₂ and found most of the same products except, as reported by Vernon,⁶ greatly reduced relative amounts of stilbene, benzene and ethylbenzene. These results are shown in Table I.

Representative GC/MS data on the mixture obtained from the D₂ reaction are shown in Table II. The data suggest that deuterium introduction is taking place both at aliphatic positions and in the aromatic rings (note both benzene-d₁ and -d₂ are formed.) To assess the relative amounts of aromatic and aliphatic substitution, the reaction mixture was subjected to gas chromatographic separation and the individual components analyzed by both ²H-NMR and ¹H-NMR. Typical results are shown in Table III.

Interestingly, as seen in Table II, the pattern is very similar for

deuterium distribution in toluene and DPE at low conversion. Later in the reaction, the amount of deuterium in DPE is significantly greater than in toluene. Surprisingly, despite the fact that hydrogen atoms must be supplied in order for DPE to be converted to toluene, the toluene formed at low conversions (in the 8 minute run, ca. 20% of the bibenzyl has been converted to products and about half of this is toluene) contains only about 20% of one atom of D by GC/MS. This can only mean that at least 80% of the benzyl radicals reacting to give toluene do so by removing H atoms, presumably from DPE, rather than D atoms from D₂. Moreover, the fact that at short reaction times, there is already a substantial amount of D in the starting DPE, demands that at least some of the D-substituted toluene arises because it is formed from D-substituted DPE. This strongly suggests that DPE molecules can pick up D atoms without first undergoing homolysis.

If this reasoning is correct, it suggests that the most prominent reaction of the R· + D₂ → R-D + D· type, is that in which R· = 1,2-diphenylethyl radical rather than benzyl radical. This is somewhat surprising in that more highly-substituted radicals are normally viewed as being more stable and consequently less reactive. On the other hand, in the equilibration of species present during reaction conditions, the diphenylethyl radical will achieve higher concentration¹³ which will compensate for its possibly lower reactivity. Further, results to be described later for a new substrate suggest that viewing more highly-substituted radicals as less reactive, may be an oversimplification.

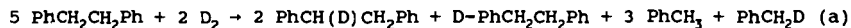
It will be noted that the deuteration pattern for ethylbenzene as seen in Tables I and II, is distinctly different from those of toluene and DPE. If, as is generally accepted,⁶ ethylbenzene is formed by the reaction of 2-phenylethyl radical with a hydrogen source, the results suggest that, being a more reactive radical, the 2-phenylethyl radical is less selective and therefore reacts directly with D₂ to a greater extent than do the more stable benzylic radicals present. Even after only 10% conversion of DPE, about 50% of the ethylbenzene molecules present contain deuterium. A similar situation exists for 1,1-diphenylethane which is believed to arise from 2,2-diphenylethyl radical, believed to be formed by rearrangement.¹² (See Table II.) Unfortunately, we have not yet been able to get reliable GC/MS data for benzene at low conversion because of the problem of getting it cleanly separated from solvent on the GC. We are still working on this.

It has been possible to isolate the more abundant products by preparative GC. We have then determined both ²H and ¹H NMR spectra using DCO₂Me as an internal standard for both spectra. This has allowed us to calculate the relative amounts of GC/MS-determined D atoms which are located at aliphatic vs aromatic sites. These data are shown in Table III for toluene, DPE and ethylbenzene. It is immediately apparent that deuterium is being incorporated at both aliphatic and aromatic sites. Moreover, the D-atom populations at the two types of location would appear to be similar in magnitude. This is consistent with a mechanism in which each aliphatic D atom introduced via R· + D₂ → R-D + D· results in D-atom incorporation in an aromatic ring. More detailed analysis of the recovered DPE suggests that the number of aromatic D atoms exceeds the number of aliphatic D atoms by a factor of between 1.2 and 1.5 (average = 1.4). This would suggest that there is some mechanism for D incorporation at aromatic sites which does not require an aliphatic radical precursor. There are a variety of possibilities, but one of the simplest is the displacement of H atoms by D atoms (probably a two step process such as reactions 4 and 9 in Figure 3). The H atoms thus generated could then react with

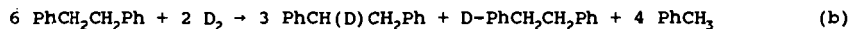
D₂ to generate more D atoms. It is reasonable to expect that if D atoms can displace alkyl radicals from the aromatic ring, the same can happen for H atoms with a five to one statistical advantage. Seeing that the amount of ethylbenzene produced is roughly 10% of the total conversion, it is perhaps reasonable to find a substantial excess of D at aromatic sites.

By computer simulation, we have tried to match the product distribution (including deuterated products) using only the first 8 reactions shown in Figure 3. These account only for the introduction of deuterium into starting DPE and the formation of toluene. We felt if we could get close to an accommodation of the data with this simple scheme, we could then approach the full set of products by elaboration and fine tuning. It will be noticed that the reaction of benzyl radicals with molecular deuterium ($\text{PhCH}_2\cdot + \text{D}_2 \rightarrow \text{PhCH}_2\text{D} + \text{D}\cdot$) has been omitted.

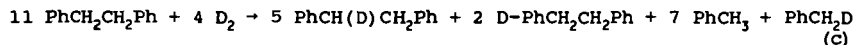
The assumption that only the reactions 1 through 8 are involved leads to the conclusion that the stoichiometry for formation of the major products should be between:



and

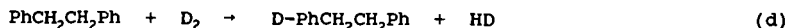


Eq (b) represents the limit in which reaction 2 (Figure 3) becomes so preferred relative to reactions 7 and 8 that all of the toluene formed arises via reaction 2 and thus would contain no D. Eq (a) results from the limit wherein reactions 5 and 6 become unimportant relative to reaction 3 thus maximizing the amount of PhCH₂D produced. If reactions 5, 6, 7 and 8 all participate equally in consuming the adduct, then the intermediate stoichiometry of eq (c) should be found.



Clearly none of these options nor any gradation in between can explain the observed facts. The observed ratio of PhCH₂D and PhCH₃ is not far from the stoichiometry of eq (c), but the experimentally observed ratio of aromatically deuterated DPE to aliphatically deuterated DPE is found experimentally to be rather constant at a value of 1.4. The stoichiometries of eqs (a), (b), or (c) demand that the ratio be between 0.25 and 0.40. Even if a huge isotope effect were assumed favoring reaction 5 over reaction 6, the maximum possible ratio would be 1.0.

Reactions 9 and 10 coupled with reaction 4, constitute a kinetic chain sequence for the introduction of aromatic D without producing aliphatically deuterated DPE. The stoichiometry of this sequence, taken in isolation from the other reactions is simply:



It therefore seems that it should be possible to combine reactions 1 through 10 to approximately match the experimental data by selecting an appropriate set of relative rates. We are working on this proposition at the present time and preliminary results indicate that it will be possible to match the distribution of the major products.

EXPERIMENTAL SECTION

Reaction Procedure. The device shown in Figure 2 (a) consists of a thick glass reaction bulb with a long capillary neck. The reactor is inverted and several glass beads are added followed by solid reactants through the end opposite to the capillary. The reactor is sealed at the constriction Figure 2 (b). The vessel is then suspended in glass wool in the interior of a stainless steel reaction tube having a long neck to house the capillary section of the vessel. The entire apparatus is evacuated, pressured with D₂ gas, closed off and shaken at the desired temperature in a fluidized sand bath. When the reaction is complete, carbon disulfide is added and products removed for analysis using a long syringe needle. In the absence of gas generation within the tube, our observation has been that little or no material is lost from the interior of the bulb. Control experiments in which a hydrogenation catalyst was deliberately added showed complete saturation of aromatic compounds under the reaction conditions.

REFERENCES

1. a. Skowronski, R. P.; Ratto, I. B.; Goldberg, I. B.; Heredy, L. A. Fuel **1984**, 63, 440-448. b. Ratto, J. J. ACS Fuel Chem. Preprints **1979**, 24, 155. c. Goldberg, I. B.; Crowe, H. R.; Ratto, J. J.; Skowronski, P. R.; Heredy, L. A. Fuel **1980**, 59, 133. d. Noor, N. S.; Gaines, A. F. Abbott, J. M. Fuel **1986**, 65, 67-73. e. Kershaw, J. R.; Barrass, G. Fuel **1977**, 56, 455.
2. Cronauer, D. C.; McNeil, D. C.; Ruberto, R. G. Fuel **1982**, 61, 610-619.
3. a. Franz, J. A.; Camaioni, D. M. Fuel **1984**, 63, 213-229. b. Franz, J. A. Fuel **1979**, 58 405-412. c. Aulich, T. R.; Knudson, C. L.; Hawthorne, S. B. Preprints Div. of Fuel Chem., Am. Chem. Soc. **1988**, 33, 368-379. d. Benjamin, B. M.; Douglas, E. C.; Mesmer, S. ibid. **1982**, 27, 1-5.
4. a. Pajak, J.; Brower, K. R. J. Org. Chem. **1986**, 50, 2210-2216. b. Brower, KR.; Pajak, J. ibid., **1984**, 49, 3970-3973.
5. King, H. H.; Stock, L. M. Fuel **1982**, 61, 257-264.
6. Vernon, L. W. Fuel **1980**, 59, 102.
7. Shin, S.-C.; Baldwin, R. M.; Miller, R. L. Energy and Fuels **1989**, 3, 71-76.
8. Bockrath, B.; Bittner, D.; McGrew, J. J. Am. Chem. Soc. **1984**, 106, 135-138.
9. Price, S. J. Can. J. Chem. **1962**, 40 1310.
10. Benson, S. W. J. Chem. Ed. **1965**, 42, 502.
11. a. Chien, P.-L.; Sellers, G. M.; Weller, S. W. Fuel Processing Technology **1983**, 2, 1-9. b. Brammer, S. T.; Weller, S. W. ibid. **1979**, 2, 155-159. c. Patxer, J. F.; Farrauto, R. J.; Montagna, A. A. Ind. Eng. Chem. Process Des. Dev. **1979**, 18, 625-630. d. Davis, K. P.; Garnett, J. L. J. Phys. Chem. **1971**, 75, 1175-1177. e. Davis, K. P.; Farnett, J. L.; O'Keefe, J. H. Chem. Communications **1970**, 1672-1673.

12. a. Poutsma, M. L.; Dyer, C. W. J. Org. Chem. **1982**, *42*, 4903. b. Buchanan, A. C.; Dunstan, T. S. J.; Douglas, E. C.; Poutsma, M. L. J. Am. Chem. Soc. **1986**, *108*, 7703.

13. Livingston, R.; Zeldes, H.; Conradi, M. S. J. Am. Chem. Soc. **1979**, *101*, 4312-4319.

Table I. Product Distribution in the Thermolysis of Diphenylethane at 450° C for 30 Minutes

	Mole % Under D ₂	Wt. % Under D ₂	Mole % Under N ₂	Wt % Under N ₂
1,2-Diphenylethane	23.5	36.6	36.1	47.1
Toluene	47.8	37.1	47.1	31.1
1,2,3,4-Triphenylbutane	0.25	0.8	<0.1	<0.1
Benzene	17.2	9.3	0.9	0.5
Ethylbenzene	8.6	7.7	--	--
1,1-Diphenylethane	1.5	2.3	0.9	1.2
Stilbene	1.3	1.9	12.2	15.8
Phenanthrene	0.8	1.2	<0.3	<0.5
Triphenylpropane	0.8	1.8	0.7	1.9
Diphenylpropane	0.44	0.73	--	--
Diphenylmethane	0.36	0.52	1.4	1.7

Table II. Deuterium Distribution in Products from Thermolysis of Diphenylethane at 450 °C Under D₂

Compound	After 8 min					After 30 min				
	%d ₀	%d ₁	%d ₂	%d ₃	%d ₄	%d ₀	%d ₁	%d ₂	%d ₃	%d ₄
1,2-Diphenyl-ethane	66	28	6	1	-	14	29	29	17	7
Toluene	78	20	2	-	-	45	36	14	4	1
Benzene	54	39	7	-	-	46	41	12	2	-
Ethylbenzene	42	45	12	1	-	18	34	29	14	4
1,1-Diphenyl-ethane	40	43	15	3	-	9	24	30	22	11
Stilbene	70	23	6	-	-	36	33	20	8	3
Phenanthrene						25	34	25	12	4
Diphenyl-methane	67	27	6	-	-	30	33	22	10	4

Table III. Aliphatic vs. Aromatic Deuterium in Products from Thermolysis of 1,2-Diphenylethane under D_2 at $450^\circ C$ by NMR.

Compound	Time (min)	Aromatic D /molecule	Aliphatic D	
			/molecule CH_2	CH_3
1,2-Diphenyl-ethane	8	0.13	0.09	
	30	0.91	0.65	
Toluene	8	0.17		0.18
	30	0.65		0.39
Benzene	30	0.66		
Ethylbenzene	15	0.36	0.18	0.54
	30	0.50	0.28	0.44
	45	1.32	0.54	0.71

Figure 1. First-Order Plot for Conversion of 1,2-Diphenylethane Under D_2 at $450^\circ C$.

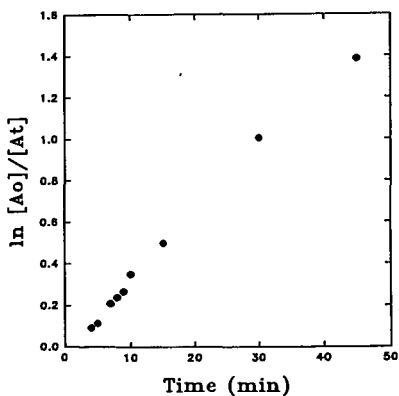


Figure 2. Glass Reaction Vessel for Thermolysis Under D_2 .

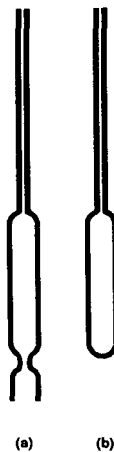
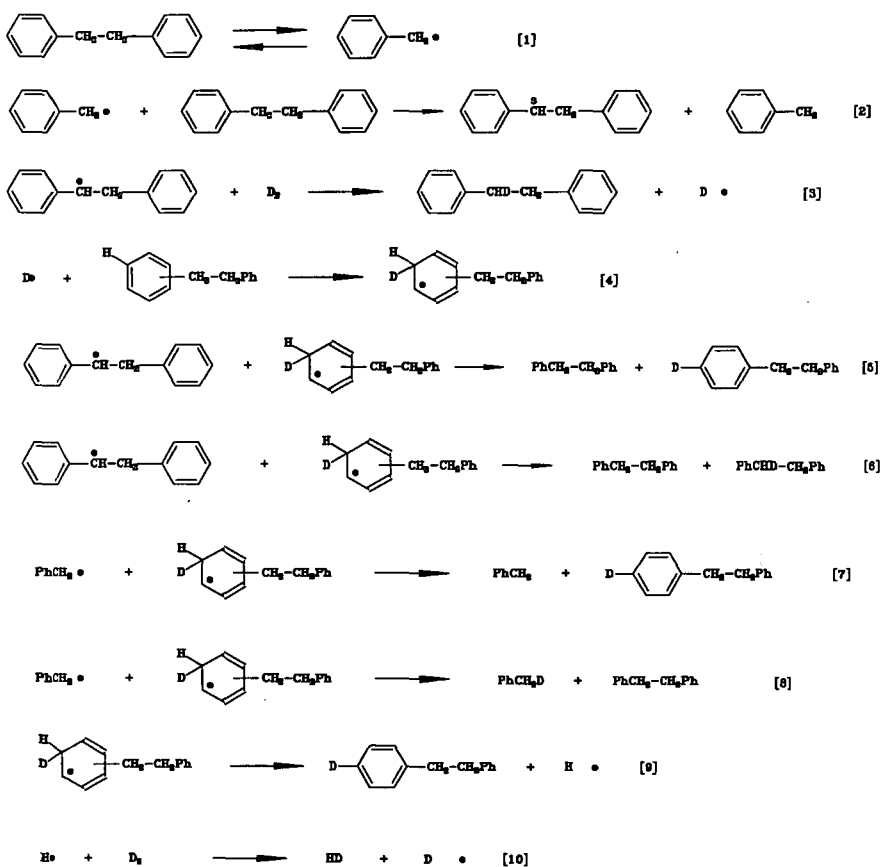


Figure 3. Minimum Steps to Explain Deuterium Distribution Pattern



COAL LIQUEFACTION USING DONOR SOLVENTS HYDROGENATED AT LOW TEMPERATURES*

R.J. Kottenstette and H.P. Stephens
Process Research Department 6212
Sandia National Laboratories
P.O. Box 5800
Albuquerque, NM 87185

Keywords: Hydrogen Donor, Coal Liquefaction, Solvent Quality

Introduction

Direct coal liquefaction proceeds initially through a complex series of bond breaking and hydrogen transfer reactions involving coal and a donor solvent. When the recycle solvent contains high amounts of donor solvent, the requirement for high hydrogen gas pressure in the initial stage of liquefaction is reduced and coal conversion is augmented. Effective tests for hydrogen donating ability of coal derived solvents often consist of GC/MS, proton NMR, catalytic dehydrogenation, as well as microautoclave coal liquefaction testing [1,2,3]. Microautoclave testing is an empirical measure of solvent quality for hydrogen donation using coal, a donor solvent and an inert gas instead of hydrogen. Previous studies [4] have investigated the hydrogen transfer cycle for direct liquefaction using Illinois #6 high volatile bituminous coal and a distillate (650°F-770°F) derived from a coal liquefaction process solvent. The objective of this work is to determine the effects of donor solvent on coal conversions in microautoclave liquefaction experiments performed at 400°C with Wyodak coal. These tests used a heavy distillate solvent that had been hydrogenated with a synthesis gas (50% carbon monoxide:50% hydrogen) mixture and steam at low temperatures (300°C-325°C). The in situ water-gas shift (WGS) reaction provides an alternate source of hydrogen and has the potential of eliminating the need for high purity high pressure hydrogen for solvent hydrogenation. Hydrogenation at low temperatures can lead to increased donor content since larger amounts of hydroaromatics are produced at equilibrium with any given hydrogen pressure. Distillate solvents were hydrogenated at various weight hourly space velocities, using two different catalysts, and used in microautoclave coal liquefaction tests to evaluate solvent pretreatment effects on coal solubility.

Experimental

Materials - Because solvent quality is favorably affected by increasing the aromatic nature of the solvent being fed to the catalytic hydrotreater, and solvent dewaxing has been shown to be an effective means of increasing the aromatic nature of the solvent [5], a heavy distillate and a dewaxed heavy distillate were used. Heavy distillate sample (V1074) from the Wilsonville, Alabama Advanced Integrated Two Stage Liquefaction Facility was provided by CONSOL Inc., Library PA. Dewaxed V1074 distillate was prepared by CONSOL at -5°C from the V1074 heavy distillate using an acetone dewaxing procedure. 1,2,3,6,7,8 hexahydropyrene was purchased from Aldrich Chemical Company with a 99% purity. Reagent grade tetrahydrofuran (THF), pentane, and heptane were purchased from Fischer Scientific. Wyodak subbituminous coal was used as -100 mesh from the Argonne Premium Coal Sample Bank. The NiMo catalyst, was Shell 324M and the platinum catalyst was a hydrous titanium oxide (HTO) compound synthesized in our lab. Hydrogen, carbon monoxide, and nitrogen were UHP grade.

*This work was supported by the U. S. Department of Energy at Sandia National Laboratories under contract DE-AC04-76DP00789.

Apparatus and Procedure

Microflow Reactor Experiments - A fixed bed microflow reactor consisting of liquid and gas feed systems and a stainless steel reactor containing the catalyst bed (0.5" O.D.) was used to hydrogenate heavy distillate and dewaxed heavy distillate. The reactor had an internal volume of 23 cm³ and typically held a 20 gram catalyst charge. These distillate pretreatment experiments consisted of three days of testing for each catalyst and feed combination. The first two days of experiments used the in situ water-gas shift reaction to hydrotreat the distillate. Reactions on the third day used solely hydrogen to test the effect of varying the partial pressure of hydrogen gas upon solvent hydrogen uptake. The reactor tube was first packed with catalyst and then presulfided with a 9% H₂S in hydrogen mixture for four hours at 390°C for the commercial nickel molybdenum on alumina catalyst (NiMo), or pre-reduced in hydrogen at 200°C for the platinum (Pt HTO) catalyst. After catalyst pretreatment, the reactor was pressurized to 1000 psig with a 50:50 mixture of carbon monoxide and hydrogen. The reactor temperature was increased to the operating value while the distillate and a 1:1:1 molar mixture of CO:H₂:H₂O was fed the top of the reactor. Distillate was pumped into the reactor with an Eldex A-30 liquid chromatograph pump and the synthesis gas was metered into the reactor with two Brooks 5850 mass flow controllers. The liquid weight hourly space velocities were varied between 0.4 hr⁻¹ and 0.8 hr⁻¹. Water was fed to the reactor with a Beckman 114M microflow liquid chromatography pump. All reactants flowed downward over the packed bed into a reservoir to separate the gases and liquids. Solvent and gas products were taken from the sample reservoir at the bottom of the reactor during operation. Reactor pressure was maintained with a Circle Seal BPR-7A back pressure regulator, which was located downstream from the liquid separator. Distillates and hydrotreated distillates were also analyzed by high resolution gas chromatography using a Hewlett Packard 5890 GC to qualitatively measure hydrogenation of aromatic compounds.

Microautoclave Experiments - Coal liquefaction tests were used to evaluate donor solvent quality. Hydrogenated solvent was tested in a microautoclave consisting of a 0.75" O.D. Swagelok tubing tee with 40 cm³ of gas volume. Pressure and temperature were measured in the microflow and batch microautoclave reactors with Entran pressure transducers and internal reactor thermocouples. Data acquisition for both the flow and batch reactor systems was accomplished with a personal computer using Labtech Notebook software.

Coal and pretreated solvents representing various hydroprocessing conditions were weighed into the microautoclave reactor. The microautoclaves were sealed and pressurized with nitrogen to 100 psig cold charge to facilitate post reaction gas analysis. The pressurized microautoclaves were then fastened to a wrist-action shaker and immersed in a fluidized sand bath while being shaken at 200 cycles per minute. After a rapid heat up (< 2min.) the microautoclaves were maintained at 400°C for 30 minutes. Following reaction the microautoclaves were cooled to room temperature in water, then depressurized into gas sample bottles and dismantled to recover the reaction products. The gas samples were analyzed for hydrogen, carbon monoxide, carbon dioxide and C₁-C₂ hydrocarbons using a Carle series 400 Gas Chromatograph. Liquid and solids were recovered from the reactor with THF and the THF insolubles were determined by pressure filtration. The THF insolubles were dried and weighed while the THF solubles were rotoevaporated to remove most of the THF. Pentane was then added to these samples to precipitate the preasphaltene/asphaltene material. These solutions were pressure filtered to remove the pentane insolubles. The pentane insolubles were then dried and weighed.

All microautoclave tests were performed with a solvent to coal ratio of 1.5:1. Solvent samples A, B, C and D, shown in Table 1, were produced in the microflow reactor using various catalysts, temperatures and weight hourly space velocities (WHSV). Hydrogen donor (H₆PY) was added to comprise 20 % of the solvent charge for experiments that were designed to test the effect of adding a known amount of a good hydrogen donor. Donor hydrogen was effectively increased in this "composite" solvent by 0.6 wt% (see Table 1).

Model Compound Test - In a series of donor solvent tests which examined the effects of using different levels of hexahdropyrene (H₆PY) alone as the solvent, heptane was used instead of pentane as the precipitating solvent, as shown in Figure 5.

Results and Discussion

The extent of distillate hydrogenation is given in Table 1, which shows elemental analysis results for baseline distillates and hydrotreated products from the microflow reactor. A comparison of samples A and B (from the same reactor run) shows that sample B was hydrogenated to a greater extent than sample A which had a slower space velocity. This is due in part to catalyst deactivation since sample B was obtained earlier in the run when the catalyst bed was fresher. The hydrogenated dewaxed distillates labeled samples C and D compare solvents hydrogenated with different catalysts. The maximum amount of hydrogen increase was 1.0 wt% in the dewaxed distillate (sample D); this distillate was produced at 325°C with the Pt HTO catalyst using only hydrogen gas. This catalyst deactivated to a lesser degree than the NiMo catalyst and was more effective using hydrogen only rather than the in situ water-gas shift reaction. It is believed that the more aromatic dewaxed solvent could be hydrogenated to a greater degree, and this was true for our tests. Figures 1 and 2 show capillary gas chromatograms of the -5°C dewaxed distillate and the hydrotreated distillate. The hydrotreated sample shows a reduction in parent aromatic compounds with an emergence of hydroaromatic products.

Figure 3 shows the product distributions for microautoclave experiments with V1074 (feed), two hydrogenated V1074 distillates (samples A and B), and V1074 + donor solvent (H₆PY) addition. Overall the coal conversion (100-%IOM, Insoluble Organic Matter) increased from 57% to 63% with sample B. Sample B, which had an additional 0.7 wt% hydrogen (over the V1074 amount), gave an increase in pentane solubles from 14% to 25%. The experiment that contained added H₆PY gave 33% pentane soluble material.

Figure 4 shows the product distributions for microautoclave experiments with -5°C dewaxed V1074 (feed), two hydrogenated dewaxed distillates (samples C and D) and dewaxed V1074 with H₆PY addition. The coal conversions increased from 64% to 69% with solvent C. Most notable, however was the increase in pentane solubles with samples C and D. These increased from 0% to 22% and 23% respectively using the hydrotreated solvent. These results show that unhydrogenated dewaxed solvent produced a higher coal conversion than V1074 but little or no oil. The small oil yield for the -5°C dewaxed distillate shows that it is necessary to hydrogenate the more reactive dewaxed solvents to avoid potentially retrogressive conditions that occur when solvent hydrogen is limited. Sample D which had an increase of 1 wt% hydrogen did not perform as well as the H₆PY doped solvent even though the doped solvent had only 0.6 wt% hydrogen. The increase in hydrogen, in sample D, could possibly have been in alicyclic compounds which are poorer donors than hexahdropyrene. Increasing the liquid space velocity could adjust the hydrogenation extent to enhance production of hydrogen donor species in the product when the Pt HTO catalyst is used.

Model Compound Test

Figure 5 shows the product distributions for donor solvent tests which used only hexahydropyrene as the solvent. Coal conversion increases dramatically from 52% to 87% when the hexahydropyrene amount was increased from 0.5g to 1.0g. These addition rates amounted to 10 and 20 mg hydrogen / g dmmf coal respectively. Further addition of H6PY (1.75g H6PY or 35mg H / g dmmf coal) showed little improvement in conversion or heptane solubility over the 1g H6Py addition. This could possibly be due to the relatively mild liquefaction temperature. For comparison the -5°C dewaxed solvent with H6PY addition (Figure 4.) had 15mg of hydrogen / g dmmf coal from the H6PY giving 77% coal conversion.

Conclusions

At 400°C for 30 minutes, coal conversions and pentane/heptane soluble yields increase with increasing solvent hydrogen content during liquefaction using Wyodak coal. Dewaxed V1074 heavy distillate gives higher coal liquefaction conversions than V1074 without dewaxing, yet very little pentane soluble product compared to the V1074 heavy distillate. Hydrogenation of dewaxed heavy distillate is necessary to avoid potentially retrogressive conditions with this solvent since it is a good physical solvent yet produces very little pentane soluble material at these conditions. There is of course a potential to over hydrogenate the solvent by forming alicyclic and naphtheno compounds which would add hydrogen without the benefit of increasing solvent quality. These concerns are especially valid when using low rank coals and solvents with limited hydrogen donating capacity.

Acknowledgments

The authors gratefully acknowledge R. A. Winschel and M. S. Lancet from CONSOL inc. for providing dewaxed solvents for the hydrotreating studies. Experimental contributions from W. K. Hollis of Sandia National Laboratories are also gratefully acknowledged.

References

- 1) C. E. Snape, H. P. Stephens, R. J. Kottenstette and S. R. Moinelo. Proceedings of the 1989 Conference of Coal Science, Vol. 2, p 739.
- 2) J. Delpuech, D. Nicole, M. Le Roux, P. Chiche and S. Pregerman. Fuel, 1986, Vol.65, p 1600.
- 3) R. A. Winschel, G. A. Robbins, and F. P. Burke. Fuel, 1986, Vol.65, p 526.
- 4) H. P. Stephens and R. J. Kottenstette. Preprints of Papers, Amer. Chem. Soc. Div. Fuel Chem. 32 (3), p 377 (1987)
- 5) R. A. Winschell, G. A. Robbins and F. P. Burke. Fuel, 1987, Vol.66, p 654.

Table 1. Elemental analysis of V1074 and -5°C dewaxed hydrotreated distillates

Distillate	WHSV (hr ⁻¹)	Catalyst	Hydrotreating Temp(°C)	%C	% H	Increase in Hydrogen (wt%)
V1074 (feed)	-	-	-	89.5	9.9	-
Sample A	0.46	NiMo	300	88.5	10.1	0.2%
Sample B	0.61	NiMo	300	88.9	10.6	0.7%
V1074+H6PY	-	-	-	-	-	0.6%
-5C Dewax (feed)	-	-	-	90.2	8.6	-
Sample C	0.78	NiMo	325	90.2	8.9	0.3%
Sample D	0.78	Pt HTO	325	89.9	9.6	1.0%
-5C Dewax+H6PY	-	-	-	-	-	0.6%

Figure 1. High resolution gas chromatogram of -5°C dewaxed heavy distillate V1074

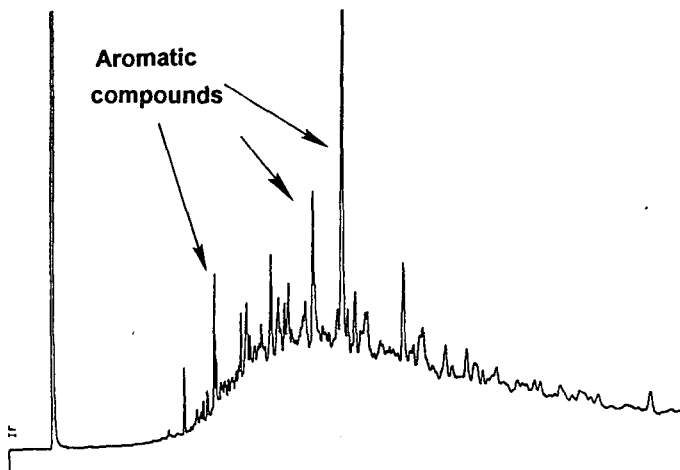


Figure 2. High resolution gas chromatogram of Sample D

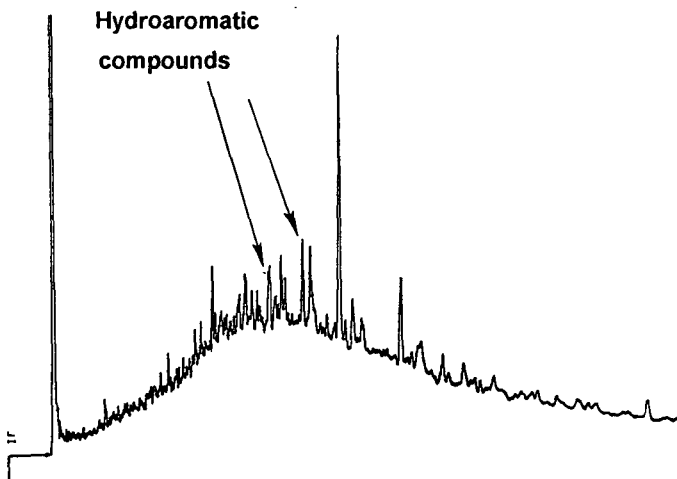


Figure 3. Product distribution for V1074 heavy distillate experiments (Wyodak, 400C, N2, 30 min.)

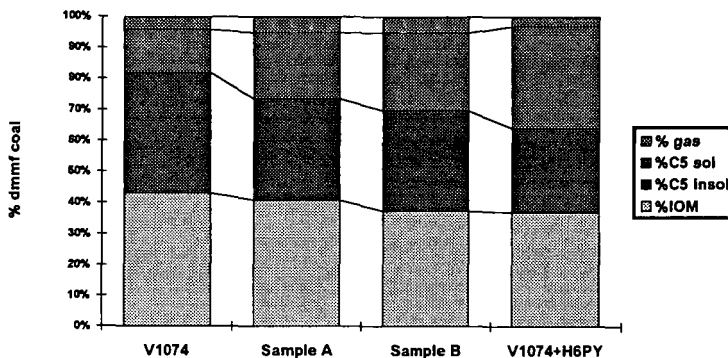


Figure 4. Product distribution for dewaxed V1074 heavy distillate (Wyodak, 400C, N2, 30 min.)

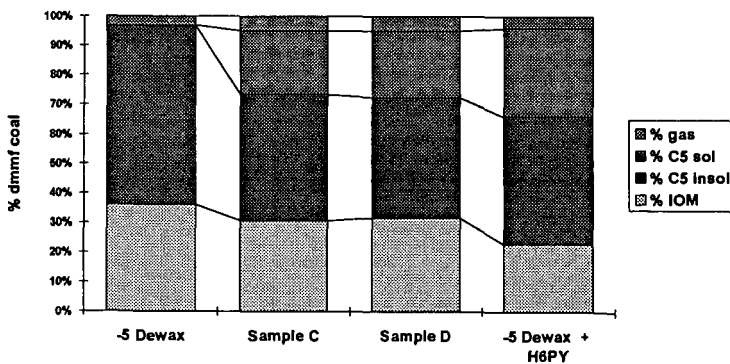
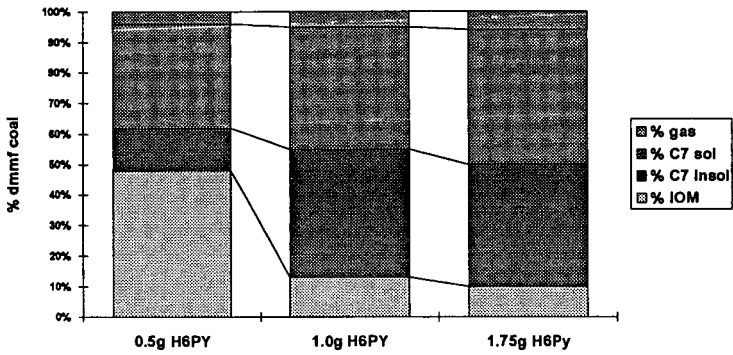


Figure 5. Product distribution for hexahydropyrene donor solvent (Wyodak, 400C, N2, 30 min.)



Bimetallic Ru/Mo Catalyst Particles for HDN of Tetrahydroquinoline

Daniel B. Ryan, Thomas Hinklin, Gregory Reuss, S.-M. Koo[†] and Richard M. Laine, Contribution from the Departments of Materials Science and Engineering, and Chemistry, University of Michigan, Ann Arbor, MI 48109-2136, [†]Depart. of Chemistry and Eng., Hanyang University Seoul, Korea

KEY WORDS: Unsupported RuMo Bimetallic Catalysts, Tetrahydroquinoline Hydrodenitrogenation, Heteropolyanion Catalyst Precursors

ABSTRACT:

Ethanol solutions of the heteropolyanion $H_3PMo_{12}O_{40} \cdot xH_2O$, (Mo-HPA) mixed with $RuCl_3$ were decomposed, at 180°C in the presence of CS_2 and H_2 to form small multimetallic catalyst particles. Previous efforts have demonstrated the synergistic effect of these catalyst systems for Quinoline hydrogenation to THQ and alkylation of THQ by ethanol. The current study extends these efforts to the HDN of THQ in hexadecane.

INTRODUCTION

We have previously shown that alumina supported RuMo and RuCoMo bi- and trimetallic catalysts provide catalytic activities and product selectivities during quinoline (Q) and tetrahydroquinoline (THQ) hydrodenitrogenation (HDN) that are not normally observed with alumina supported, $M'Mo$ ($M' = Co, Ni$) or single metal Mo or Ru catalysts.¹⁻⁷ The RuMo combination of metals appears to offer synergistic behavior during Q and THQ HDN. In particular, the catalysts are sulfur tolerant, even showing enhanced activities in the presence of sulfur compounds. Their activities are 5 to 10 times higher than corresponding $M'Mo$ catalysts for similar weight loadings on identical supports. Moreover, their selectivity towards the formation of propylbenzene vs. propylcyclohexane during Q or THQ HDN is much higher (1:3 product ratios at temperatures of 350°C and H_2 pressures of 400-600 psig at RT).

In an effort to completely delineate this synergistic behavior, we have examined the catalytic activity of RuMo catalysts with Q and THQ under a variety of conditions. Furthermore, we have examined the feasibility of preparing these heterogeneous bimetallic catalysts directly from soluble precursors based on ethanolic solutions of molybdenum heteropolyanion, $H_3PMo_{12}O_{40}$ (Mo-HPA) and $RuCl_3 \cdot xH_2O$ (Ru-Cl).

We find that 1:9 Ru:Mo atomic ratio solutions consisting of 1.0 ml (5.7×10^{-3} M, 5.7×10^{-3} mmol) of $RuCl_3 \cdot xH_2O$ in EtOH with 4.0 ml of 1.1×10^{-3} M in Mo-HPA (4.38×10^{-3} mmol) in EtOH, when heated with 5.0 ml (42 mmol) Q or THQ and 50 μ l of CS_2 for 3 h at 175-200°C decompose uniformly to give 0.3-1.5 μ m dia. RuMo catalyst particles (surface areas typically of 5-9 m^2/g).^{6,7} These bimetallic particles appear to be more catalytically active for Q hydrogenation to THQ than similar particles generated either from Mo-HPA or Ru-Cl under identical conditions.⁷ Furthermore, efforts to promote HDN of

THQ at somewhat higher temperatures in EtOH solutions leads to the N-ethylation of THQ rather than HDN.⁶ Again, the RuMo catalyst is much more effective for N-ethylation than either of the metals alone. N-ethylation was also observed when THQ HDN was attempted in acetonitrile solutions of RuMo. We have now determined that it is possible to conduct THQ HDN to the exclusion of extraneous reactions through the use of hexadecane as solvent. We describe here preliminary efforts to study this reaction.

EXPERIMENTAL

HDN catalysis studies were conducted using hexadecane as solvent and using 1:9 RuMo catalyst particles generated under conditions identical to the Q hydrogenation reactions, at 175°C, but in the absence of Q.⁷ Particle surface areas were 5-6 m²/g. Studies were done with two 250 mg batches of catalyst which were mixed to obtain a uniform catalyst.

Product analyses for all the kinetic studies were performed on a temperature programmed Hewlett-Packard 5890A reporting GC equipped with FID using a 12 m x 0.53 mm x 2.65 μm capillary column packed with 100 % dimethyl polysiloxane gum. The column heating schedule was initiated with a hold at 35°C (2 min) followed by ramping at 7°C/min to 250°C. The eluting gas mixture was H₂/He.

GC-MS studies were performed using an HP 5890 Series II GC, an HP 5970 mass spectrometer, and the HP 5940 MS Chemstation. The capillary column used for product separation was a 12 m x 0.12 mm x 0.33 μm film thickness HP-5 (crosslinked 5% phenyl methyl silicone) capillary column. The temperature for the analysis was held at 50°C for 5 min, then ramped at 4°C/min to 275°C. The eluting gas used was H₂/He.

THQ HDN Kinetic Runs

Typically, 18-20 mg of catalyst are added to a solution of 5.0 ml (42.3 mmol) of THQ mixed with 5.0 ml of hexadecane and 50 μl of decane as internal standard in a quartz lined, Parr General Purpose Bomb reactor with a 34 ml internal volume. The reaction solution is then pressurized to 400 psig with N₂ at RT and depressurized. The process is repeated and then 400 psig with H₂ at RT is added and the reaction is heated, with magnetic stirring, to the desired temperature, e.g 370°C for the studies shown below. At the appropriate times (typically 3, 6, 9, 12 and 15 h) the reactor is cooled in flowing water, depressurized and a sample is taken for GC analysis. The reactions are run to less than 5% conversion so that the initial rates of product formation correspond essentially to zero order in reactant concentration.

RESULTS AND DISCUSSION

Figure 1 shows the standard reaction network for Q HDN.⁸ Propylcyclohexene may arise both from hydrogenation of propylaniline and from deamination of aminopropylcyclohexane, presumed to be an intermediate in DHQ HDN. Propylaniline and DHQ are presumed to derive directly from catalytic reactions of THQ, and propylbenzene and propylcyclohexane are presumed to arise from the catalytic reactions of propylaniline and DHQ respectively; although propylcyclohexane could also derive from propylbenzene.

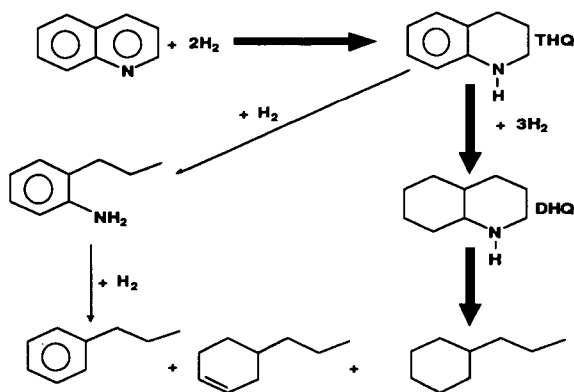


Figure 1. Quinoline HDN Reaction Network

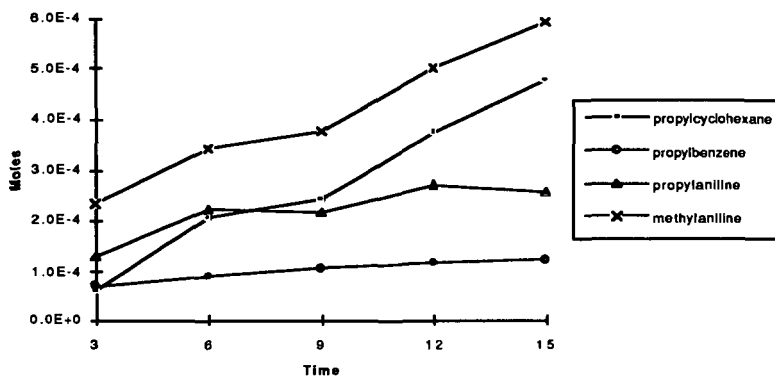
Figure 2 shows a plot of the major bond cleavage products observed at 370°C during RuMo catalyzed HDN of THQ, as a function of time. In Figure 2, the quantities of propylaniline initially produced are not significantly higher than the propylbenzene. Furthermore, [propylcyclohexane] increases significantly with time whereas [propylbenzene] does not. Given that the amount of products produced during the course of the reaction all fall in the 0.1 to 0.8 mmol range and the starting amount of THQ is on the order of 42 mmol, the percent conversion of THQ is of the order of 1%. Normally, the sequential formation of products, as depicted in Figure 1, should not lead to the formation of significant amounts of secondary products such as propylbenzene or propylcyclohexane at conversions of 1%. Thus, these results are rather surprising.

We offer two explanations for these observations, the first is that the catalyst particles are highly porous and that much of the catalysis occurs in the particles' interiors. In this case, the actual concentration of reactants at the catalyst surface would be much higher than it is in solution and secondary products might be expected to escape from the porous body at about the same rate as primary products. Hence the relative concentrations of the two types of products seen by GC would be representative of the mixture in the particle rather than in solution.

The second possibility is that once THQ is bound to the active catalytic site in these unsupported catalyst particles, it remains bound for sufficient periods of time to undergo more than one type of catalytic reaction. This would mean that the site would have a higher affinity for the reaction products and would be able to perform several different types of catalytic operations.

At this point, it is not possible to distinguish between the two possibilities; however, the surface

areas of the particles and the SEM micrographs^{6,7} bely the possibility of a very porous catalyst particle. But the conversions are sufficiently low that it may be that some of this type of porosity exists and is responsible for most of the catalytic activity. Further studies will be required to differentiate between these, or other, possible explanations.



Finally, the appearance of significant quantities of methylaniline, a product of C-C rather than C-N bond hydrogenolysis suggests that there are Ru rich regions on the catalyst particles as this product is more typical of bulk Ru catalyzed HDN of THQ.⁵

ACKNOWLEDGEMENTS

We wish to thank the Department of Energy and the Pittsburgh Energy and Technology Center for generous support of this work through contract no. DE-FG22-90PC90313.

REFERENCES

- Hirschon, A. S.; Wilson, Jr., R. B.; Laine, R. M.; *New J. Chem.*, **1987**, *11*, 543-547.
- Hirschon, A. S.; Wilson, Jr., R. B.; Laine, R. M.; in *Adv. in Coal Chemistry*, Theophrastus Publ, Athens **1988**, p 351.
- Hirschon, A. S.; Wilson Jr., R. B.; Laine, R. M.; *J. Appl. Cat.*, **1987**, *34*, 311-316.
- Laine, R. M.; Hirschon, A. S.; Wilson Jr., R. B.; U.S. Pat. No. 4,716,142 **1987**.
- Hirschon, A. S.; Laine, R. M.; *J. Energy and Fuels*, **1988**, *2*, 292-295.
- Koo, S-M.; Ryan, D. B.; and Laine, R. M.; *Appl. Organomet. Chem.*, **1992**, *6*, 437-448.
- Hoppe, M. L.; Koo, S-M.; Ryan, D. B.; and Laine, R. M.; submitted to *Energy and Fuels*.
- a. Satterfield, C.N.; and Cocchetto, J.F.; *AIChE J.*, **1975**, *21*, 1107-1111. b. Yang, S. H. and Satterfield, C.N., *J. Catal.* **1983**, *81*, 168-178.

Temperature-Programmed Liquefaction of Coals Using Bimetallic Dispersed Catalysts from Organometallic Complexes

Chunshan Song*, Derrick S. Parfitt, and Harold H. Schobert

Fuel Science Program, 209 Academic Projects Building,
The Pennsylvania State University, University Park, PA 16802

Keywords: Bimetallic catalysts, coal, temperature-programmed liquefaction

Introduction

It has been recognized recently that dispersed catalysts are superior to supported catalysts for primary coal liquefaction. Most previous work involved dispersed molybdenum sulfide from a water-soluble salt [Derbyshire, 1988]. Some organometallic compounds including metal carbonyls and naphthenates have also been tested as catalyst precursors [Suzuki et al., 1987; Herrick et al., 1990; Swanson, 1992], which often requires the addition of sulfur compounds [Yamada et al., 1985]. There are some unique advantages of organometallic compounds as catalyst precursors. First, most organometallic compounds are soluble in hydrocarbon solvents and may be used as oil-soluble precursors. Second, as has been demonstrated by Hirschon and Wilson [1991, 1992], some organometallic compounds can be easily decomposed to metal sulfides at low temperatures. The present work is concerned with organometallic precursors which can directly produce metal sulfides upon thermal decomposition.

Little work on bimetallic dispersed catalyst for coal liquefaction has appeared, although previous work on multicomponent catalysts has involved the mixture of two or more inorganic salts [Garg and Givens, 1984; Song et al., 1986, 1991; Sommerfeld et al., 1992]. Related to this work is a general observation from previous investigations that there could be synergistic effects between different metals, and an organometallic precursor may be better than an inorganic one. Our interest in the heteronuclear organometallic compounds was stimulated by the recent book on metal clusters published by Mingos and Wales [1990]. It seemed to us that highly active catalysts might be prepared from some clusters containing metal-metal bonds, especially the "thiocubane" clusters containing two metals such as Fe or Co and Mo in a single molecule.

Two different metals bound together in a single compound should have a more systematic spatial arrangement in the resulting catalytic phase upon thermal decomposition than if two separate compounds were used to introduce the two different metals to a catalytic system. The present work is an exploratory study of bimetallic dispersed metal sulfide catalysts for coal liquefaction, involving the synthesis of the organometallic thiocubane clusters that contain Mo and Co as well as sulfur in a single molecule, and liquefaction of coal impregnated with the precursors under non-programmed and temperature-programmed (TPL) conditions, where the programmed heat-up serves as a step for both catalyst activation and coal pretreatment or preconversion. The advantages of temperature-programmed conditions have been demonstrated in our recent work [Song et al., 1992; Song and Schobert, 1992; Huang et al., 1992].

Experimental

Catalyst Precursors and Coal Samples

Three bimetallic thiocubanes were used as catalytic precursors: $\text{Mo}_2\text{Co}_2\text{S}_4(\text{S}_2\text{CNEt}_2)_2(\text{CH}_3\text{CN})_2(\text{CO})_2$ [MoCo-TC1], $\text{Mo}_2\text{Co}_2\text{S}_4\text{Cp}_2(\text{CO})_2$ [MoCo-TC2], and $\text{Mo}_2\text{Co}_2\text{S}_4(\text{Cp}^{\prime\prime})_2(\text{CO})_2$ [MoCo-TC3], in which Et, Cp and Cp^{''} represent ethyl group, cyclopentadiene, and pentamethylcyclopentadiene, respectively. These thiocubanes were synthesized in our laboratory based on the procedures of Brunner and Watcher [1982] and Halbert et al. [1985]. For comparative examination, bimetallic metal sulfide complex, cobalt bis-tetrathiomolybdate trianion was also synthesized based on the procedure of Pan et al. [1985]. The trianionic compound, $(\text{PPh}_4)_3\text{Co}(\text{MoS}_4)_2$, is designated as MoCo-S.

The U.S. Department of Energy Coal Samples (DECS, #9 and #12) were obtained from the Penn State/DOE Coal Sample Bank. The Montana subbituminous coal (DECS-9, PSOC-1546, < 60 mesh) has the following composition: 24.7% moisture, 4.8% ash, 33.5% volatile matter, and 37.1% fixed carbon on an as-received basis; 76.1% carbon, 5.1% hydrogen, 0.9% nitrogen, 0.3% organic sulfur, and 17.5% oxygen on a dmmf basis. The Pittsburgh #8 bituminous coal (DECS-12, PSOC-1549, < 60 mesh) has the following composition: 2.4% moisture, 10.0% ash, 35.2% volatile matter, and 52.4% fixed carbon on an as-received basis; 84.8% carbon, 5.7% hydrogen, 1.4% nitrogen, 0.7% organic sulfur, and 6.5% oxygen on a dmmf basis. The coals were dried for two hours at 100°C in a vacuum oven before use.

Incipient Wetness Impregnation of Catalyst Precursors

The catalytic precursors were dispersed on to the coal by the incipient wetness impregnation (IWI) method using organic solvents. IWI method was applied to coal in a previous work [Huang et al., 1992]. Because of the difference in the solubility of the organometallic precursors, several solvents including toluene, THF, CHCl_3 and acetonitrile were used for dissolving them. The organic solution of a precursor was intermittently added dropwise to the dried coal in a 100 mL beaker, in a fashion that the wet spots over the coal particles do not touch each other, followed by manual stirring with a glass rod until all signs of wetness disappeared. In order to keep the metal loading from different precursors at a constant level, we first estimated the incipient wetness volume prior to the catalyst impregnation with a given solvent, which means the total volume of the solvent needed to reach the point of incipient wetness: the point when the solution drops begin to remain on the external surface of the coal. The loading for the bimetallic thiocubanes was 0.5-0.6 wt% of molybdenum on the basis of dmmf coal. The impregnated coal sample was dried at 100°C for 2 h in a vacuum oven. IWI method is often used for loading inorganic salts from their aqueous solution on to a catalyst support without [Solar et al., 1991]. It should be noted that the IWI method used in our work is different from conventional one in that we only use certain amount of solution defined by the estimated incipient wetness volume to achieve a constant metal loading.

Liquefaction under SSL and TPL Conditions

All reactions were carried out in 25 mL tubing bomb microautoclaves in a temperature-controlled fluidized sandbath. Each reaction used approximately 3 g dried coal. 1-Methylnaphthalene was used as the reaction solvent (3 g) unless otherwise mentioned. In several experiments tetralin was also used as a hydrogen-donor solvent (3 g) for comparison. The initial H_2 pressure was 7 MPa at room temperature for all the runs. For catalyst screening, single-stage liquefaction (SSL) was performed, where the tubing bomb was rapidly heated to the prescribed temperatures (400-425. °C) for 30 minutes (plus a three minute heat-up period) followed by a rapid quench in cold water bath. Temperature-programmed liquefaction (TPL) had the tubing bomb rapidly heated up to a low temperature (275°C in all the catalytic runs, 200°C in the thermal

runs) and soaked at that temperature for 30 minutes before the temperature was gradually increased (5-7°C/min) to a higher temperature (400°C-425°C) and held there for 30 minutes before rapid quenching with cold water bath. These procedures were established in our recent work [Song and Schobert, 1992; Huang et al., 1992].

The gaseous product was vented after the reaction was complete and the liquid and solid products were washed into a tared ceramic thimble with hexane. The products were separated under a N₂ atmosphere by Soxhlet-extraction using hexane, toluene, and THF in succession. Solvents were removed by rotary evaporation, and the products were dried in vacuum at 100°C for 6 h except for the hexane-solubles. The asphaltene (toluene soluble, but hexane insoluble), preasphaltene (THF soluble, but toluene insoluble), and residue were weighed and the conversion and product distribution were calculated based on dmmf coal. All the runs were repeated at least once or twice to confirm the reproducibility. In most cases, the experimental errors were within ± 2 wt% for conversion, and the average data are reported here.

Results and Discussion

Effects of Precursor Type and Solvents for Impregnation

Table 1 shows the results of liquefaction of the Montana subbituminous coal at 400°C for 30 min. We first prepared and tested Mo₂Co₂S₄(S₂CNEt₂)₂(CH₃CN)₂(CO)₂ [MoCo-TC1], which was first synthesized and used recently by Halbert et al. [1991] in preparing MoCo hydrotreating catalyst. Using MoCo-TC1 impregnated on to DECS-9 coal from acetonitrile, however, showed little catalytic effect for increasing conversion. Replacing CH₃CN with THF for impregnating MoCo-TC1 increased coal conversion relative to the thermal run by 14 wt%, but did not improve oil formation to any significant extent. It seems that the acetonitrile solution and the dithiocarbamate and acetonitrile ligands in MoCo-TC1 can poison the resulting catalyst under the conditions employed. This observation prompted us to prepare the thiocubane which contains no nitrogen in the ligands, leading to the synthesis of Mo₂Co₂S₄Cp₂(CO)₂ [MoCo-TC2], and Mo₂Co₂S₄(Cp'')₂(CO)₂ [MoCo-TC3]. The basic difference between these three thiocubanes is the type of ligands to the Mo [Cp = C₅H₅, Cp'' = C₅Me₅; all the five (ring) carbon atoms are equidistant from the metal atom].

MoCo-TC2 impregnated from toluene afforded much higher conversion and oil yield; it appears to be much more active than MoCo-TC1. MoCo-TC3 exhibited slightly lower catalytic activity compared to MoCo-TC2. It was expected that MoCo-TC2 would afford greater conversion when THF was used as the impregnating solvent, since THF is a better swelling solvent and can penetrate the coal structure, which would improve the dispersion of the resulting Co-Mo bimetallic sulfide catalyst. Surprisingly, the catalytic liquefaction using MoCo-TC2 gave both higher oil yields and total conversion when toluene was used rather than THF. The structure and ligands of MoCo-TC3 and MoCo-TC2 are of the same nature, except that cyclopentadiene in MoCo-TC2 is substituted by pentamethylcyclopentadiene in MoCo-TC3. There was a small increase in the oil yield coupled with a decrease in preasphaltene yield when MoCo-TC3 was used in temperature-programmed liquefaction. Table 2 presents the results of catalytic runs of DECS-9 coal at 425°C. The order of catalytic activity at 425°C is the same as that observed from runs at 400°C: MoCo-TC2 > MoCo-TC3 > MoCo-TC1.

In an attempt to examine the role of bonding between Co and Mo, we further prepared and tested heterometallic cluster of the form Co(MoS₄)₂³⁻ which has distinctly different structure than the above-mentioned thiocubanes. Comparing results in Table 1 and Table 2 reveal that MoCo-S is more active than MoCo-TC1 at both 400 and 425°C but is much less active compared to MoCo-TC2, regardless of the

impregnating solvent.

Table 3 shows the effect of using the catalytic precursors on liquefaction of DECS-12 Pittsburgh #8 bituminous coal. At 400°C, the catalytic effects appear to be enhanced coal conversion to preasphaltene and asphaltene, with little increase in oil production relative to thermal run. At 425°C, using MoCo-TC2 increased total conversion significantly compared to the thermal run; it also promoted oil production moderately. However, increasing temperature from 400°C to 425°C caused decrease in total conversion both in thermal run and catalytic runs. In both cases, MoCo-TC2 was much more active than MoCo-TC1, although the latter was used under better conditions (TPL) than the former (SSL), as we further describe below. This again points to the negative impact of the CH₃CN and S₂CNEt₂ ligands in MoCo-TC1 upon the resulting catalyst in coal liquefaction. Therefore, it appears that an active MoCo bimetallic sulfide catalyst is generated in-situ from MoCo-TC2 during liquefaction. Under comparable conditions the catalyst from MoCo-TC1 is much less active, although an active catalyst could be generated also from this precursor if first decomposed at low temperature followed by venting and purging to remove poisonous compounds and followed by re-charging H₂ gas and heat-up.

By combining Tables 1, 2 and 3 it becomes very clear that MoCo-TC2 is the best precursor and MoCo-TC1 is the worst precursor among the three thiocubanes which differ from each other only in the type of ligands to Mo. Bimetallic sulfide complex MoCo-S also produces a catalyst whose activity is lower than that from MoCo-TC3 at 400°C and close to MoCo-TC3 at 425°C. In MoCo-S, the Co and Mo are bound through sulfur-bridge bonding, but in MoCo-TC2 or TC3, there are direct metal-metal bonds between Co-Mo, Co-Co, and Mo-Mo in addition to the sulfur-bridges. The superiority of MoCo-TC2 over MoCo-S may suggest the importance of direct metal-metal bonding; the differences between the three thiocubanes clearly indicate the importance of ligand type. The solvents used for loading the precursors are also influential. Both toluene and THF were tested for impregnating MoCo-TC2 but the non-polar solvent seems to be better in terms of higher oil yield; the optimum solvent and method for loading catalyst are not known yet. In summary, the above results indicate that both the ligands to the metal species and the type of bonding between the two metals affect the activity of the resulting bimetallic MoCo sulfide catalyst significantly. For a given precursor, the solvent used for catalyst impregnation also affects coal conversion, although the impregnating solvent was removed before reaction.

Effects of Temperature-Programming

The second major task in this study is to optimize the performance of promising catalysts selected from screening tests described above. As a means to increase conversion, the liquefaction of coals impregnated with the precursors was carried out under temperature-programmed (TPL) conditions, where the programmed heat-up serves as a step for both catalyst activation (precursor decomposition to active phase) and coal pretreatment or preconversion.

Table 4 shows the effects of temperature-programming on the catalytic and thermal runs of both DECS-9 and DECS-12 coals. In the presence of either MoCo-TC2 or MoCo-TC3, TPL runs in 1-MN always give higher conversions and higher oil yields than the corresponding SSL runs. At a final reaction temperature of 425°C with 1-MN solvent, TPL runs of both DECS-9 and DECS-12 coals using MoCo-TC2 or TC3 gave 13-15 wt% higher conversions and 5-11 wt% higher oil yields than the corresponding SSL runs. Most of the trends observed from Table 4 can be rationalized based on a general reaction model for liquefaction presented in recent papers [Song et al., 1989, 1991].

The first question that arises is why programmed heat-up is better than rapid heat-up? The superiority of TPL over SSL in catalytic runs with 1-MN solvent could be due to 1) more products from coal after longer residence time irrespective of catalyst, since a programmed heat-up is included in TPL but SSL only involves a very rapid heat-up in about three minutes followed by reaction at 400 or 425°C; 2) due to reactions including precursor decomposition and catalytic reactions during programmed heat-up. The first is not the case, as demonstrated by the fact that in the non-catalytic runs in 1-MN, using temperature programmed heat-up had essentially no impact on the liquefaction of DECS-9, neither on total conversion nor on product distribution, as can be seen from Table 4. The desirable effects of TPL, therefore, are associated with low-temperature catalytic hydrogenation reactions during programmed heat-up.

It is interesting to note from Table 4 that under TPL conditions using 1-MN solvent, increasing final temperature of all the catalytic runs from 400 to 425°C further increased coal conversions and oil yields considerably. In distinct contrast, under SSL conditions, increasing temperature of the catalytic runs (using MoCo-TC₂, TC₃) from 400 to 425°C caused marked decrease in the total conversions, which is a remarkable sign of significant retrogressive reactions. As pointed out in Song et al. [1989], the rate of coal thermal fragmentation is influenced by temperature and heating rate; very fast heating to high temperature would lead to extremely rapid fragmentation of coals that may exceed the capacity or rate of hydrogenation (H-donation) of the system, leading to significant retrogressive crosslinking. It is also likely that under SSL conditions (heating rates, $\geq 100^\circ\text{C}/\text{min}$) very fast radical formation occurs before transformation of MoCo-TC₂ into active phase is completed, resulting in an imbalance between the rate of radical formation and the rate of radical-capping by H from catalyst surface, especially at higher temperature. In TPL runs, however, the catalyst precursor decomposes to form active bimetallic sulfide and the weak linkages are broken and stabilized during programmed heat-up, so that at the time the radical formation becomes considerable at high temperature (425°C), the catalyst is already activated and can provide dissociated hydrogen atom to cap the thermally generated radicals. These mechanistic considerations account for why using MoCo-TC₂ or TC₃ affords further increased conversion and oil yield under TPL conditions but gives decreased conversion under SSL conditions when the final reaction temperature is increased from 400 to 425 °C.

In regards to the catalytic effects associated with solvent, the increases in conversion and oil yield due to catalyst are much higher when using a non-donor 1-MN solvent as compared to the runs using a H-donor tetralin (Table 4). For example, for SSL runs of DECS-9 coal at 400°C, using MoCo-TC₂ increased coal conversion from about 32 to 75 wt% [(75-32)/32 = 134% increase] with 1-MN, and from about 71 to 88 wt% [(88-71)/71 = 24% increase] with tetralin. In the presence of H-donor solvent, the catalytic effects relative to thermal runs appear to be higher in SSL runs than under TPL conditions, as can be seen by comparing the thermal and catalytic runs with tetralin in Table 4.

Conclusions

This work provides a fundamental approach to developing novel bimetallic dispersed catalysts and optimum conditions for coal conversion. We have synthesized and tested several heterometallic complexes consisting of two transition metals [Co, Mo] and sulfur as precursors of bimetallic dispersed catalysts for liquefaction of a subbituminous and a bituminous coal. The results revealed that both the ligands to the metal species and the type of bonding between the two metals affect the activity of the resulting catalyst significantly. Among the M-M' type precursors tested, Mo-Co thiocubane cluster, $\text{Mo}_2\text{Co}_2\text{S}_4(\text{Cp})_2(\text{CO})_2$ [MoCo-TC₂], produced the best catalyst. Loading

of MoCo-TC2 at the level of 0.5 wt% Mo can increase the conversion of the subbituminous coal from 32 to as high as 80 wt%. The performance of the Mo-Co bimetallic catalyst was further enhanced by using temperature programmed heat-up (TPL) conditions. For a final temperature of 425°C, using the programmed conditions with MoCo-TC2 significantly increased the conversions by about 12-13 wt% for both coals, as compared to the non-programmed runs. Further work is now in progress.

Acknowledgements

This project was supported by the US DOE Pittsburgh Energy Technology Center and the US Air Force Wright Laboratory/Aero Propulsion and Power Directorate. We are pleased to thank Mr. W. E. Harrison III and Dr. D. M. Storch of WL, and Dr. S. Rogers of PETC for their support. We gratefully acknowledge Mr. J. McConnie for his assistance in the non-catalytic SSL and TPL experiments. We also wish to thank Dr. A. Davis and Mr. D.C. Glick of PSU for providing the samples and data of the coals from the sample bank, and Dr. A.S. Hirschon of SRI International for providing recent literature information.

References

- Brunner, H.; Wachter, J., *J. Organomet. Chem.* 1982, 240, C41-44.
Derbyshire, F.J.; *Catalysis in Coal Liquefaction*, IEACR/08, IEA Coal Research, London, 1988, 69 pp.
Garg, D.; Givens, E.N.; *Fuel Process. Technol.*, 1984, 8, 123-134.
Halbert, T. R.; Cohen, S. A.; Stieffel, E. I., *Organometallics* 1985, 4, 1689-1690.
Halbert, T.R.; Ho, T. C. Stieffel, E. I.; Chianelli, R. R., Daage, M., *J. Catal.* 1991, 130, 116-119.
Herrick, D. E.; Tierney, J. W.; Wender, I.; Huffamn, G. P.; Huggins, F. E., *Energy & Fuels* 1990, 4, 231-236.
Hirschon, A.S.; Wilson, R.B.; *Am. Chem. Soc. Sym. Ser.*, 1991, 461, 273-283.
Hirschon, A.S.; Wilson, R.B.; *Fuel*, 1992, 71, 1025-1031.
Huang, L.; Song, C.; Schobert, H. H., *Am. Chem. Soc. Div. Fuel Chem. Prepr.*, 1992, 37(1), 223-227.
Mingos, D.M.P.; Wales, D.J., "Introduction to Cluster Chemistry", Prentice Hall: Englewood Cliffs, New Jersey, 1990, 318 pp.
Solar, J.M.; Derbyshire, F.J.; de Beer, V.H.J.; Radovic, L.R.; *J. Catal.*, 1991, 129, 330-342.
Sommerfeld, D.A.; Jaturapitpornsakul, J.; Anderson, L.; Eyring, E.M.; *Am. Chem. Soc. Div. Fuel Chem. Prepr.*, 1992, 37(2), 749-755.
Song, C.; Nomura, M.; Miyake, M.; *Fuel*, 1986, 65, 922-926.
Song, C.; Hanaoka, K.; Nomura, M.; *Fuel*, 1989, 68, 287-292.
Song, C.; Nomura, M.; Ono, T., *Am. Chem. Soc. Div. Fuel Chem. Prepr.* 1991, 36(2), 586-596.
Song, C.; Schobert, H. H.; Hatcher, P. G., *Energy & Fuels*, 1992, 6, 326-328.
Song, C.; Schobert, H. H.; *Am. Chem. Soc. Div. Fuel Chem. Prepr.* 1992, 37(2), 976-983.
Suzuki, T.; Ando, T.; Watanabe, Y., *Energy & Fuels* 1987, 1, 299-300.
Swanson, A.; *Am. Chem. Soc. Div. Fuel Chem. Prepr.* 1992, 37(1), 149-155.
Yamada, O.; Suzuki, T.; Then, J.; Ando, T.; Watanabe, Y.; *Fuel Process. Technol.*, 1985, 11, 297-311.

Table 1. Liquefaction of DECS-9 Montana Subbituminous Coal at 400°C for 30 min

Catalyst precursor	Solvent for catalyst impregn ^a	Reaction solvent ^b	Reaction condition	Oil + Gas dmmf wt%	Asphalt dmmf wt%	Preasph. dmmf wt%	Tot Conv dmmf wt%
None	None	1-MN	SSL	16.0	9.4	6.8	32.2
MoCo-TC1	CH ₃ CN	1-MN	SSL	22.8	4.8	5.2	32.8
MoCo-TC1	THF	1-MN	SSL	18.7	12.8	14.8	46.3
MoCo-TC2	Toluene	1-MN	SSL	32.4	18.0	24.2	74.6
MoCo-TC2	THF	1-MN	SSL	25.8	17.9	23.7	67.4
MoCo-TC3	Toluene	1-MN	TPL	33.8	17.8	19.9	71.5
MoCo-S	CHCl ₃	1-MN	SSL	21.3	12.6	16.0	49.8

a) The impregnating solvent was removed by evaporation in vacuum before reaction.

b) 1-MN was added as reaction solvent after the impregnating solvent was removed.

Table 2. Liquefaction of DECS-9 Montana Subbituminous Coal at 425°C for 30 min

Catalyst precursor	Solvent for catalyst impregn	Reaction solvent	Reaction condition	Oil + Gas dmmf wt%	Asphalt dmmf wt%	Preasph. dmmf wt%	Tot Conv dmmf wt%
None	None	1-MN	SSL	16.7	16.4	13.8	46.9
MoCo-TC1	THF	1-MN	SSL	20.3	9.9	5.7	35.9
MoCo-TC2	Toluene	1-MN	SSL	42.3	14.9	14.8	72.0
MoCo-TC2	THF	1-MN	SSL	36.5	15.5	18.0	70.0
MoCo-TC3	Toluene	1-MN	SSL	36.7	11.9	13.2	61.4
MoCo-S	CHCl ₃	1-MN	SSL	34.9	11.1	13.2	59.2

Table 3. Liquefaction of Pittsburgh #8 Bituminous Coal in 1-MN at 400-425°C

Catalyst precursor	Solvent for catalyst impregn	Reaction temp °C	Reaction condition	Oil + Gas dmmf wt%	Asphalt dmmf wt%	Preasph. dmmf wt%	Tot Conv dmmf wt%
None	None	400	SSL	13.7	20.4	26.8	60.9
MoCo-TC1	THF	400	TPL	9.8	21.9	34.0	65.7
MoCo-TC2	Toluene	400	SSL	14.5	27.8	34.3	76.6
None	None	425	SSL	16.2	19.1	16.1	51.4
MoCo-TC1	THF	425	TPL	16.9	24.6	19.4	60.8
MoCo-TC2	Toluene	425	SSL	21.8	27.7	23.8	73.3

Table 4. Effect of Temperature Programming on Coal Liquefaction Using Bimetallic Thiocubane Precursors MoCo-TC2 and MoCo-TC3**

Catalyst precursor	Solvent for catalyst impregn	Reaction solvent	Reaction condition	Oil + Gas dmmf wt%	Asphalt dmmf wt%	Preasph. dmmf wt%	Tot Conv dmmf wt%
DECS-9 Montana Subbit Coal							
None	400	1-MN	SSL	16.0	9.4	6.8	32.2
None	400	1-MN	TPL	18.9	8.2	7.0	34.1
MoCo-TC2	400	1-MN	SSL	32.4	18.0	24.2	74.6
MoCo-TC2	400	1-MN	TPL	37.0	19.8	22.0	78.7
None	425	1-MN	SSL	16.7	16.4	13.8	46.9
MoCo-TC2	425	1-MN	SSL	42.3	14.9	14.8	72.0
MoCo-TC2	425	1-MN	TPL	46.7	19.5	15.0	81.1
MoCo-TC3	425	1-MN	SSL	36.7	11.9	13.2	61.4
MoCo-TC3	425	1-MN	TPL	46.3	17.5	12.9	76.6
None	400	Tetralin	SSL	29.4	20.6	21.4	71.4
None	400	Tetralin	TPL	34.4	21.1	23.7	79.2
MoCo-TC2	400	Tetralin	SSL	44.1	22.9	21.0	88.1
MoCo-TC2	400	Tetralin	TPL	46.4	25.4	17.4	89.2
DECS-12 Pittsburgh #8 Bitum Coal							
None	400	1-MN	SSL	13.7	20.4	26.8	60.9
MoCo-TC2	400	1-MN	SSL	14.5	27.8	34.3	76.6
MoCo-TC2	400	1-MN	TPL	15.8	28.7	35.4	79.9
None	425	1-MN	SSL	16.3	17.6	16.1	51.4
MoCo-TC2	425	1-MN	SSL	21.8	27.6	23.9	73.3
MoCo-TC2	425	1-MN	TPL	33.1	31.5	23.4	87.9
MoCo-TC2	400	Tetralin	SSL	18.8	32.6	31.0	82.4
MoCo-TC2	400	Tetralin	TPL	21.9	34.2	33.0	89.1

** Impregnated from toluene solution using incipient wetness method.

MILD PRETREATMENT METHODS FOR IMPROVING THE LOW SEVERITY REACTIVITY OF ARGONNE PREMIUM COALS

S. Kelkar, K. Shams, R. L. Miller, and R. M. Baldwin
Chemical Engineering and Petroleum Refining Department
Colorado School of Mines
Golden, Colorado 80401

ABSTRACT

This paper describes results from an on-going coal pretreatment study with the goal of developing simple, inexpensive treatment options to enhance low severity coal dissolution reactivity. Data are presented for two pretreatment methods: 1) ambient treatment with methanol and hydrochloric acid, and 2) aqueous carbonic acid treatment. We have found that ambient pretreatment of eight Argonne coals using methanol and a trace amount of hydrochloric acid improves THF-soluble conversions by 24.5 wt% (maf basis) for Wyodak subbituminous coal and 28.4 wt% for Beulah-Zap lignite with an average increase of 14.9 wt% for liquefaction of the eight coals at 623 K (350°C) reaction temperature and 30 min. reaction time. Pretreatment with methanol and HCl separately indicated that both reagents were necessary to achieve maximum liquefaction improvement. The extent of calcium removal correlated well with reactivity enhancement in these experiments. This effect is attributed to the role of calcium as a catalyst for retrogressive reactions during the initial stages of dissolution. Preliminary treatment results using CO₂/H₂O suggest that the reactivity of bituminous coals such as Illinois #6 can be significantly enhanced with this method but that less improvement is seen for low rank coals such as Wyodak or Beulah-Zap.

INTRODUCTION

Much of the recent research in direct coal liquefaction seeks to develop methods for dissolving coal at lower reaction severity [often defined as temperatures below 623 K (350°C) and pressures in the range of 6.9-10.3 MPa (1000-1500 psi)]. The incentives for developing a viable low severity liquefaction process are numerous; they include: 1) reduced hydrocarbon gas production resulting in reduced feed gas consumption and enhanced hydrogen utilization efficiency; 2) suppressed retrogression of primary coal dissolution products resulting in enhanced distillate and residuum product quality; 3) production of high boiling residuum which is less refractory and thus more amenable to catalytic upgrading in a conventional second-stage hydrocracker; 4) substitution of less expensive off-the-shelf vessels, piping, valves, pumps, etc. in place of expensive, custom-designed units; and 5) less severe slurry handling and materials of construction problems as a result of lower operating temperatures and pressures.

However, as shown schematically in Figure 1, lowering the reaction severity reduces coal conversion reaction rates and liquid product yields unless the intrinsic coal reactivity can be sufficiently enhanced using some method of physical or chemical pretreatment prior to dissolution. Possible methods for reactivity enhancement include: 1) dispersed homogeneous or heterogeneous catalysts, 2) promoters such as basic nitrogen compounds, 3) physical pretreatment of the coal structure, or 4) chemical pretreatment of the coal's inorganic and organic fractions. Generally these methods all improve low severity coal liquefaction reactivity, but for various reasons (use of exotic, expensive, and sometimes hazardous chemical feedstocks; long pretreatment times; and the potential for incorporating undesirable chemical constituents into the coal), none have been seriously considered as a process step in coal liquefaction. The objective of the research described in this paper has been to develop simple, inexpensive coal pretreatment methods using readily available commodity chemicals to enhance low severity liquefaction reactivity of lignites, subbituminous, and bituminous coals.

In the past, chemical treatments including reductive and non-reductive alkylation (1,2), acylation (3), partial oxidation (4), alkali hydrolysis (5), and solvent swelling (6) have been used to disrupt the coal's organic structure, increase solubility in selected solvents, and improve liquefaction reactivity. Selected coal demineralization has also been studied as a method for enhancing liquefaction reactivity. Mochida (7) reported that hydrochloric acid can be used to destroy cationic bridges present in low rank coals, thereby reducing coordination between oxygen-containing functional groups and allowing better contacting between coal and solvent during the initial stages of dissolution. Joseph (8) used ion exchange techniques to remove various cations from Wyodak subbituminous coal and North Dakota lignite. He found that removal of calcium, magnesium, sodium, and potassium from each low rank coal improved high severity [673 K (400°C), 3.5 MPa (500 psig) H₂, 60 min.] liquefaction conversion and product quality. This result was attributed to inhibited hydrogen transfer in the presence of alkaline and alkaline earth cations. Serio (9) also found that ion-exchanged and demineralized low rank coals were more reactive at high reaction severity. He attributed his results to reduced cross-linking of the treated coals during the initial stages of dissolution.

The objective of this paper is to present experimental results from a study in which two pretreatment methods were used to improve intrinsic coal reactivity at low severity liquefaction conditions. Possible explanations for the observed reactivity enhancement will also be discussed.

EXPERIMENTAL PROCEDURE

The entire suite of eight coals from the Argonne Premium Coal Sample Bank was used as the source of feed coals for this study. Ultimate analysis (10) and calcium content (11) data for each coal are listed in Table I. Additional chemical and physical properties of the Argonne coals have been reported (12).

Two methods of coal pretreatment were used in this study. The first method employed a liquid phase technique we developed based on the gas phase alkylation chemistry reported by Sharma (13). Coal was pretreated by suspending 5 g of undried coal in 40 cm³ of methanol and 0.2 cm³ (0.5 vol%) of concentrated hydrochloric acid in a 100 cm³ round bottom flask and continuously stirring the coal/methanol slurry on a magnetic stirring plate for the desired pretreatment time (usually 3 hrs.). The flask was connected to a cooling water condenser to reduce solvent losses by evaporation. Treated coal samples were washed with 500 cm³ aliquots of methanol and centrifuged to remove excess acid and soluble mineral species.

The second pretreatment method was based on a CO₂/H₂O treatment technique reported by Hayashi, et al. (14). Five gram samples of coal were pre-dried at 50°C in vacuum [1.3-2.6 Pa (10-20 millitorr)] for 1 hour and then placed in a 300 cm³ autoclave reactor. Distilled water (100 g) was added to the reactor which was then sealed, flushed with CO₂, and finally pressurized with CO₂ to 600 KPa (87 psig) pressure at ambient temperature. The coal/water slurry was agitated at 1000 rpm for the desired treatment time (usually 2 hours). At the end of each pretreatment run, the reactor was depressurized and the moist coal sample recovered from the slurry by centrifugation. Each sample was washed with 500 cm³ aliquots of distilled water to remove any water-soluble species present in the treated coal.

Coal samples from each pretreatment method were vacuum dried at 298 K (25°C) under 1.3-2.6 Pa (10-20 millitorr) pressure for 24 hrs. Untreated coal samples were vacuum dried at the same conditions prior to use. After drying, all treated and untreated coal samples were stored at room temperature in a vacuum desiccator at 13.3 Pa (0.1 torr) before analysis or liquefaction. Reactor runs were scheduled so that each coal sample was stored for less than 12 hours before use. Portions of each untreated coal and pretreated coal were subjected to elemental analysis and ash analysis, as well as ¹H CRAMPS NMR, ¹³C CP/MAS NMR, FTIR, Mossbauer, and XRD spectroscopy.

Liquefaction experiments were conducted in a 20 cm³ tubing bomb reactor system attached to an agitator and immersed in a fluidized sandbath. Low severity liquefaction conditions were set at 350°C reaction temperature, 6.9 MPa (1000 psig) initial cold hydrogen pressure, and 30 minutes reaction time. Dihydrophenanthrene (DHP) was used as hydrogen donor solvent (2/1 solvent/coal wt. ratio) in these runs. Coal conversion was monitored using THF extraction data corrected for the intrinsic THF solubilities of treated and untreated coals. Solubility measurements were conducted at ambient conditions and consisted of three steps: 1) sonicating the liquid products from the tubing bomb reactor (or feed coal sample) in excess THF for 10 min., 2) centrifuging the mixture at 2000 rpm for 20 min., and 3) decanting THF-soluble products and excess THF from the THF-insoluble residuum. This procedure was repeated at least two times or until no additional THF-soluble products were recovered. Remaining THF-insolubles were dried at 373 K (100°C) for 24 hours to remove residual THF, weighed, and finally ashed. Coal conversion to THF-soluble products was computed on a moisture and ash-free basis correcting for the intrinsic solubility of each feed coal sample. Thus reported changes in coal conversion levels can be attributed solely to inherent differences in low severity coal liquefaction reactivity and not to changes in intrinsic solubility.

RESULTS AND DISCUSSION

Several sets of experiments were completed to evaluate the effectiveness of our pretreatment method in enhancing low severity liquefaction reactivity. In each set of runs, individual reactor experiments were duplicated and in some cases triplicated. Results shown in this paper represent average values of replicated runs; conversion differences of 2.1 wt% or greater (maf basis) represent statistically significant differences in liquefaction reactivity at the 95% confidence level.

Baseline low severity liquefaction reactivity data for the untreated Argonne coals are summarized in Figures 2 and 3. At the conditions studied, three of the high volatile bituminous coals [Illinois #6 (75.0 wt%), Blind Canyon (69.9 wt%), and Pittsburgh #8 (57.0 wt%)] gave the highest THF conversions. Wyodak subbituminous coal was the next most reactive coal (42.0 wt%), while Pocahontas low volatile bituminous coal was the least reactive sample studied (15.6 wt%). These reactivity data follow the generally accepted trends reported for thermal conversion of the Argonne coals (15).

Pretreatment with methanol and 1.5 vol% HCl for three hours at ambient conditions using the procedure described earlier enhanced low severity liquefaction reactivity for all eight Argonne coals. The absolute increase ranged from 24.5 wt% for Wyodak coal and 28.4 wt% for Beulah-Zap lignite to 5.2 wt% for Blind Canyon coal, and averaged 14.9 wt% for the eight coals. No simple trends in reactivity improvement with chemical or physical properties of the coals were obvious, although reactivity of the pretreated low rank coals (Wyodak and Beulah-Zap) increased much more than reactivity of the six bituminous coals.

Although Sharma (13) showed that vapor phase methanol/HCl mixtures would partially alkylate bituminous coals, elemental analyses of the treated coals indicated that little methylation (fewer than 0.1 methyl groups/100 C atoms) had occurred during liquid phase methanol/HCl pretreatment; no evidence of methylation was observed from NMR and FTIR measurements on untreated and treated coal samples. This result was confirmed by replacing methanol with hexane during coal pretreatment; reactivity of hexane/HCl pretreated coals was also enhanced. Since hexane cannot participate in the proposed alkylation chemistry, other effects must also contribute to the observed reactivity enhancement. Several pretreatment experiments were conducted using acetone in place of methanol or hexane and similar reactivity results were obtained. Throughout this portion of the study, we found no obvious trends relating reactivity enhancement, pretreatment solvent properties, and coal properties. Our general conclusion is that any simple organic solvent may be used to conduct the liquid phase pretreatment step.

The effect of CO₂/H₂O pretreatment on low severity liquefaction of the Argonne coals is also shown in Figures 2 and 3. With the exception of Blind Canyon coal, CO₂/H₂O pretreatment significantly enhanced low severity reactivity of each Argonne coal. Interestingly, the extent of enhancement for the two low rank coals (Wyodak and Beulah-Zap) was significantly lower than the enhancement observed using MeOH/HCl pretreatment. Conversely, CO₂/H₂O pretreatment of each bituminous coal except Blind Canyon and Lewiston-Stockton provided greater reactivity enhancement than MeOH/HCl pretreatment.

At this point, we can only speculate on the contrast in reactivity behavior between the two pretreatment methods. We have previously reported (16) that reactivity enhancement using MeOH/HCl pretreatment can be correlated with the extent of calcium removal and that HCl destroys calcium dicarboxylate bridging structures. We also presented model compound evidence (16) that calcium can directly catalyze retrogressive reactions involving coal-derived free radical intermediates during the initial stages of coal dissolution. Thus, it appears that given the reactivity enhancement data shown in Figures 2 and 3, we can tentatively conclude that CO₂/H₂O pretreatment more efficiently removes calcium from coals such as Illinois #6 in which calcium exists predominately as part of a discrete mineral phase, while MeOH/HCl pretreatment more efficiently removes calcium from dicarboxylate bridging structures which predominately occur in low rank coals. Further analyses of pretreated coals and additional model compound experiments are currently underway to help elucidate pretreatment effects on low severity coal liquefaction reactivity.

ACKNOWLEDGMENT

We wish to acknowledge financial support from the U.S. Department of Energy under Contract Nos. DE-AC22-88PC88812 and DE-FG22-90PC90289. Jenefer R. Olds performed the intrinsic solubility analyses for untreated and treated coal samples.

LITERATURE CITED

1. Sternberg, H. and Delle Donne, C.L. *Fuel* 1974, **53**, 172.
2. Liotta, R. *Fuel* 1979, **58**, 724.
3. Hodek, W. and Kolling, G. *Fuel* 1973, **52**, 220.
4. Hessley, R.K. 'Co-Oxidative Depolymerization of Coal,' Final Report for Electric Power Research Institute Project No. 2383-2, June 1985.
5. Mirza, Z.B., Sarkar, M.K. and Sharma, D.K. *Fuel Proc. Tech.* 1984, **2**, 149.
6. Sanada, Y. and Honda, H. *Fuel* 1986, **65**, 295.
7. Mochida, I., Shimohara, T., Korai, Y., Fujitsu, H. and Takeshita, K. *Fuel* 1983, **62**, 659.
8. Joseph, J.T. and Forrai, T.R. *Fuel* 1992, **71**, 75.
9. Serio, M.A., Solomon, P.R., Kroo, E., Bassilakis, R., Malhotra, R., and McMillen, D. *Am. Chem. Soc. Div. Fuel Chem. Prepr.* 1990, **35**(1), 61.
10. Vorres, K.S. *Energy & Fuels* 1990, **4**, 420.
11. Doughten, M.W. and Gillison, J.R. *Energy & Fuels* 1990, **4**, 426.
12. Vorres, K.S. "Users Handbook for the Argonne Premium Coal Sample Program," Argonne National Laboratory, Argonne, Illinois, October 1989.
13. Sharma, D.K., Sarkar, M.K., and Mirza, Z.B. *Fuel* 1985, **64**, 449.
14. Hayashi, J., Takeuchi, K., Kusakabe, K., and Morooka, S. *Fuel* 1990, **70**, 1181.
15. Shin, S.C., Baldwin, R.M. and Miller, R.L. *Energy & Fuels* 1989, **3**, 193.
16. Shams, K., Miller, R.L., and Baldwin, R.M. *Fuel* 1992, **71**, 1015.

Table I
Analysis of Feed Coals

Ultimate Analysis (wt% maf coal)	Wyodak	Beulah-Zap	Ill. #6	Pittsburgh #8
Carbon	68.4	65.9	65.7	75.5
Hydrogen	4.9	4.4	4.2	4.8
Nitrogen	1.0	1.0	1.2	1.5
Sulfur	0.6	0.8	4.8	2.2
Oxygen	16.3	18.2	8.6	6.7
Ash	8.8	9.7	15.5	9.3
Calcium content (wt% maf coal)	1.20	1.54	0.96	0.21
Coal Rank	Subbit.	Lignite	HVB	HVB
Symbol	WY	ND	IL	PITT

Table I (cont.)
Analysis of Feed Coals

Ultimate Analysis (wt% maf coal)	Blind Canyon	Lewiston- Stockton	Upper Freeport	Pocahantas
Carbon	76.9	66.2	74.2	86.7
Hydrogen	5.5	4.2	4.1	4.2
Nitrogen	1.5	1.3	1.4	1.3
Sulfur	0.6	0.7	2.3	0.7
Oxygen	10.8	7.8	4.8	2.3
Ash	4.7	19.8	13.2	4.8
Calcium content (wt% maf coal)	0.41	0.06	0.45	0.45
Coal Rank	HVB	HVB	MVB	LVB
Symbol	UT	WV	UF	POC

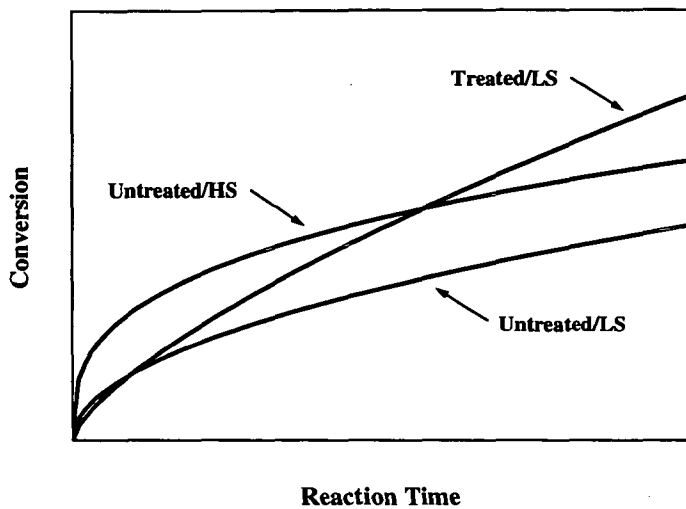


Figure 1 - Schematic Representation of Reactivity Enhancement Using Coal Pretreatment (LS = low reaction severity, HS = high reaction severity)

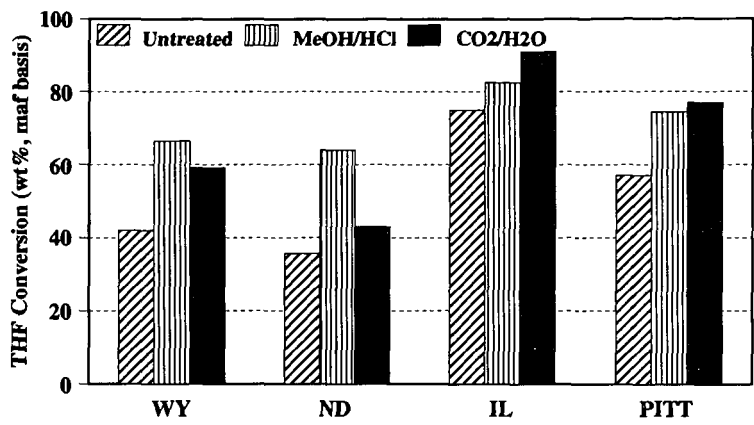


Figure 2 - Effect of Pretreatment with Methanol/Hydrochloric acid and Carbon Dioxide/Water on Low Severity Liquefaction Reactivity of Argonne Coals

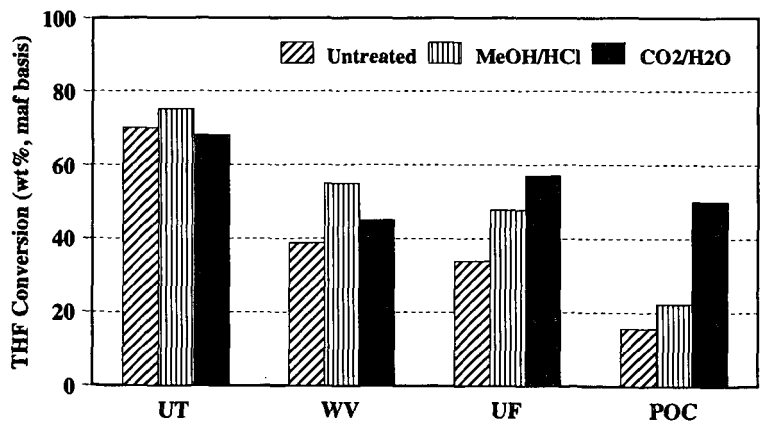


Figure 3 - Effect of Pretreatment with Methanol/Hydrochloric acid and Carbon Dioxide/Water on Low Severity Liquefaction Reactivity of Argonne Coals

DISSOLUTION OF THE ARGONNE PREMIUM
COAL SAMPLES IN STRONG BASE*

R. E. Winans, R. L. McBeth, and J. E. Hunt
Chemistry Division, 9700 S Cass Avenue
Argonne National Laboratory, Argonne, IL 60439

Keywords: Solubilization, Base Hydrolysis, Premium Coals

INTRODUCTION

The objective of this study is to solubilize the Argonne Premium Coal Samples in order to facilitate analysis by mass spectrometry, FTIR and NMR. Earlier, in a search for relatively mild methods for solubilizing coal, we discovered that treating coals with potassium hydroxide in ethylene glycol at 250°C to be quite an effective approach.¹ Under these conditions, secondary reactions which may obscure the distribution of the basic building blocks of the coal structure are not expected to occur. At higher temperatures, such as those used in more traditional liquefaction processes (> 400 °C), secondary reactions such as the formation of polycyclic aromatic and heteroaromatic compounds dominate.

A focus of our approach to characterization of coals is desorption-pyrolysis high resolution CI and EI mass spectrometry and laser desorption mass spectrometry (LDMS). It has been shown by PyMS that the yields and the distribution of products is superior for coal extracts compared to the original whole coals.^{2,3} There appears to be few secondary reactions occurring and many molecules, which are released in analysis of the extract, are trapped in the solid matrix of the coal and never observed. In addition, soluble materials are more amenable to LDMS.⁴

The glycol/KOH system was chosen since in early work up to 93% of the product was soluble for lower-rank bituminous coals.¹ Others have solubilized coals under basic conditions. Ouchi and co-workers⁵ used ethanolic - NaOH at temperatures ranging from 260 °C to 450 °C. More recently, Stock and co-workers have discussed the use of Lochmann's base (potassium tert-butoxide, n-butyl lithium in heptane at reflux) which is especially effective for the higher rank coals.^{6,7} Also, a base hydrolysis is included in a low severity liquefaction scheme devised by Shabtai and co-workers.⁸

Table VII-1. Elemental analyses for the coal samples.

Sample	Name	%C (dmmf)	H	Per 100 Carbons		
				N	S	O
8	Beulah-Zap Lignite	74.1	79.5	1.35	0.36	20.9
2	Wyodak-Anderson SubB	76.0	85.6	1.28	0.23	18.0
3	Herrin hvCB	80.7	77.2	1.51	1.15	13.0
6	Blind Canyon hvBB	81.3	85.7	1.67	0.17	10.8
4	Pittsburgh hvAB	85.0	76.7	1.69	0.40	7.96
7	Lewiston-Stockton hvAB	85.5	76.3	1.62	0.30	8.93
1	Upper Freeport mvB	88.1	66.0	1.55	0.32	6.59
5	Pocahontas lvB	91.8	58.5	1.25	0.21	2.04

EXPERIMENTAL

The following procedure was applied to all eight of the Argonne Premium Coal Samples. Approximately 20 g of coal was stirred in 100 ml concentrated HCl and 100 ml 48% HF under a N₂ atmosphere in a teflon container for at least 48 hours. After dilution to 1.5 l with distilled water, it was filtered through acid-hardened filter paper, the residue was washed off the paper and, subsequently, filtered through a sintered glass funnel, washed acid-free and vacuum dried at 100 °C for 16 hours. An ash determination was made on the dried product.

The demineralized coal was refluxed in pyridine for 10 hours. After cooling, the residue was separated by centrifuging and decantation. The residue was stirred in 5% HCl heated to 80°C for 2 hours, filtered, washed acid-free with distilled water, then methanol and, finally, vacuum dried at 100 °C for 16 hours. The pyridine solution was roto-evaporated to dryness and the pyridine soluble material was treated in the same manner as the insoluble; hot 5% HCl but no methanol rinse.

Ten grams of the pyridine extracted residue was added to a 100 ml solution of 10 g KOH and dissolved in ethylene glycol in a 300 ml stirred Parr reactor. The reaction mixture was heated to 250 °C for 2 hours and cooled. After dilution to 1 l, the mixture was heated to 60 °C and filtered, washed alkaline-free, and the residue vacuum dried at 100 °C for 16 hours.

The residue was then successively extracted by refluxing for 2 hours in hexane, 1:1 benzene-methanol, and pyridine. The filtrates were roto-evaporated to dryness and vacuum dried at 60 °C for 16 hours. The pyridine soluble and insoluble residues were washed as described above with 5% HCl and vacuum dried at 100 °C for 16 hours.

RESULTS AND DISCUSSION

The solubility yields from the KOH in glycol reaction are shown in Figure 1. The pyridine soluble yields are a combination of the yield of pyridine solubles prior to the reaction added to the pyridine solubles produced during the reaction of the extracted coal. This reaction produces (typically less than 1%) of very small, non-polar molecules which would be soluble in hexane. Indigenous molecules of this type would have been removed prior to the reaction by the initial pyridine extraction. Apparently, the extensive bond breaking which occurs at higher temperatures such as in pyrolysis and liquefaction is not taking place under those reaction conditions. In addition, the recovery weights were very close to 100% for all of the samples. Very little sample weight was lost to small molecules or gained from the addition of the solvent to the products.

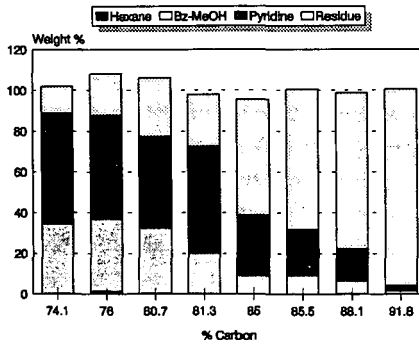


Figure 1. Yields from the ethylene glycol-KOH treatment of the Argonne Premium Coals.

A much more definitive trend is seen for the decrease in soluble product yields as a function of increasing rank than in the previous study.¹ In the original study, surprisingly, only 60% of the lignite products were soluble. However, this lignite coal was highly oxidized and had not been stored under premium conditions as is the case with the present samples. This procedure is obviously very effective for the lower rank coals. There are significant yields of benzene/MeOH solubles in the three lowest rank coals. These mixtures are typically much more amenable to characterization than the pyridine extracts.

There is good correlation with oxygen content as is shown in Figure 2. This is expected since it is likely that cleavage of ether linkages is one of the important mechanisms of solubilization. The Utah coal is much more reactive than expected from its oxygen content. However, this coal tends to be much more reactive than one would expect from its rank, such as in vacuum pyrolysis.² Also, this result implies that oxygen functionality is only partially responsible for the mechanisms of solubilization for this reaction.

The Lochmann's base reaction yields the opposite rank trend compared to the KOH/glycol approach. For the subbituminous coal, which has been methylated, the pyridine solubility increases only to 44% from 35%,⁶

while for the high rank Pocahontas coal (APCS 5), pyridine solubility increases dramatically from 2.5% to 55% upon treatment with the base.⁷ These results suggest that these two different base treatments can be used in parallel to produce a very soluble set of samples for the complete set of Argonne Premium Coal Samples. Mass spectral data from both LDMS and DCIMS, along with FTIR data, are being analyzed for this complete set of samples from the KOH glycol solubilization.

ACKNOWLEDGMENT

This work was performed under the auspices of the Office of Basic Energy Sciences, Division of Chemical Sciences, U.S. Department of Energy, under contract number W-31-109-ENG-38.

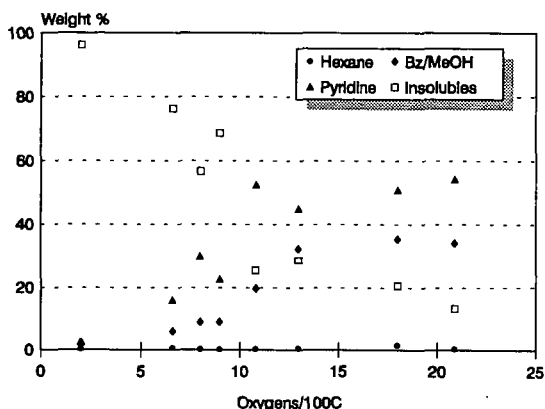


Figure 2. Yields as a function of oxygen content for the ethylene glycol-KOH reaction.

REFERENCES

1. Winans, R.E.; Hayatsu, R.; McBeth, R.L.; Scott, R.G.; Moore, L.P.; Studier, M.H. In *Coal Structure*, Gorbaty and Ouchi, K. Eds.; Adv. Chem. Series 192, ACS, 1981, 161-178.
2. Winans, R.E.; Melnikov, P.E.; McBeth, R.L. *Preprint, Div. Fuel Chem., ACS, 1992, 37(2)*, 693-698.
3. Cagniant, D.; Gruber, R.; Lacordaire-Wilhem, C.; Shulten, H.-R. *Energy Fuels*, 1992, 6, 702-708.
4. Hunt, J.E.; Lykke, K.R.; Winans, R.E. *Preprint, Div. Fuel Chem., ACS, 1992, 36(3)*, 1325-1329.
5. Ouchi, K.; Hosokawa, S.; Maeda, K.; Itoh, H. *Fuel*, 1982, 61, 627-630.
6. Chatterjee, K.; Miyake, M.; Stock, L.M. *Energy Fuels*, 1990, 4, 242-248.
7. Chatterjee, K. Ph.D. Dissertation, The University of Chicago, 1991.
8. Shabtai, J.; Saito, I. *U.S. Patent 4,728,418* (1988).

EFFECT OF CHLOROBENZENE TREATMENT ON THE LOW-SEVERITY LIQUEFACTION OF COALS

Carol A. McArthur, Peter J. Hall and Colin E. Snape

University of Strathclyde, Dept. of Pure & Applied Chemistry, Thomas Graham Building, 295 Cathedral Street, Glasgow G1 1XL, UK

Keywords: Conformational changes, tetralin extraction, hydrogen transfer.

ABSTRACT

Chlorobenzene has the advantage of extracting virtually no organic matter from coals and it has been reported previously, that for the Pittsburgh No. 8 Argonne Premium Coal Sample (APCS), chlorobenzene treatment significantly improved the oil yield as measured by dichloromethane (DCM-solubles) from short contact time hydrogen-donor liquefaction with tetralin (400°C, 15 min.). Similar effects with tetralin have been found for two UK bituminous coals, Point of Ayr and Bentinck, where the yields of DCM-solubles also increased. In contrast, for Wyodak sub-bituminous coal (APCS), pretreatment reduced the yield of DCM-solubles reflecting the vast differences in both liquefaction chemistry and pore structure with bituminous coals. The amounts of hydrogen transferred are broadly similar for the initial and chlorobenzene treated coals strongly suggesting that the improved oil yields arise from limiting char-forming retrogressive reactions rather than cleaving more bonds *per se*. The effect was still evident for Point of Ayr coal when the extraction time was increased from 15 to 60 min., although conversions were considerably higher underlying the importance of the initial contact between coal and solvent. A similar improvement in the oil yield for Point of Ayr coal to that found with tetralin was achieved with hydrogenated anthracene oil which has a boiling range of *ca* 250-450°C and, unlike tetralin, is largely in the liquid phase at 400°C.

INTRODUCTION

Much of the recent literature on the effects of pre-swelling and pre-extracting coals in both polar and non-polar solvents on liquefaction and pyrolysis behaviour⁽¹⁻¹⁰⁾ was briefly reviewed by the authors in an earlier article⁽¹¹⁾. In cases where improved liquefaction yields are achieved, the accessibility of solvents within the highly porous macromolecular structure of coals is undoubtedly improved, particularly during the initial stages of liquefaction where retrogressive reactions need to be avoided. However, unambiguous interpretation of these phenomena in terms of changes in the macromolecular structure of coals is complicated by the fact some organic matter is invariably removed at the same time that conformational changes may be occurring and, in the case of polar solvents and pre-treatments at elevated temperatures, hydrogen bonds are being disrupted. Chlorobenzene has the advantage of extracting virtually no organic matter from coals⁽¹²⁾ but it is non-polar and does not significantly disrupt hydrogen bonds at relatively low temperatures (<150°C). Previous work by one of the authors (PJH)⁽¹³⁾ demonstrated that chlorobenzene treatment markedly

affect mass transfer phenomena in both the Pittsburgh No.8 and Upper Freeport Argonne Premium Coal Samples (APCS) and this prompted an investigation into the effects of the treatment on tetralin extraction and dry hydrogenation (70 bar, with and without a dispersed sulphided molybdenum (Mo) catalyst) for the Pittsburgh No.8 APCS ⁽¹¹⁾.

Tetralin was selected because, although it is clearly not representative of process-derived liquefaction solvents as it can be largely in the vapour phase at 400°C, mass transfer effects may be particularly prevalent for this very reason. Further, a relatively short contact time of 15 min. was used as any conformational effects are likely to be most pronounced during the initial stages of conversion. Indeed, the chlorobenzene treatment significantly improved the oil yields as measured by dichloromethane (DCM)-solubles from both tetralin extraction and non-catalytic dry hydrogenation presumably due to improved accessibility of the tetralin and the hydrogen gas. In marked contrast, reduced yields were obtained in catalytic hydrogenation. However, this was probably due to the macromolecular conformation of the coal being further altered by the procedure used for catalyst addition which involved contacting the coal with methanol before drying at ca 100°C.

The yield of pyridine-solubles from the tetralin extraction was also improved by the chlorobenzene treatment. This finding would appear to be contrary to the recent communication by Larsen and co-workers ⁽¹⁴⁾ who found that the chlorobenzene treatment reduced the yield of pyridine-insolubles in tetralin for the Illinois No. 6 APCS. However, the extraction was conducted at 350°C where the conversions and level of hydrogen transfer are going to be considerably less than at 400°C. Further, only the yield of pyridine-solubles was determined which is less sensitive than the yield of DCM-solubles to hydrogen utilisation as high conversions to pyridine/quinoline-solubles can be achieved with non-donor polynuclear aromatic compound, such as pyrene for some bituminous coals ⁽⁴⁾.

In the continuing investigation into the effects of chlorobenzene treatment on coal conversion phenomena, liquefaction experiments have been conducted on two UK bituminous coals and the Wyodak APCS to address whether the effects of the chlorobenzene treatment found for Pittsburgh No. 8 coal ⁽¹¹⁾ are general and, in cases where improved conversions are achieved with hydrogen-donor solvents, whether more hydrogen transferred. Further, are similar effects likely to occur with other hydrogen-donor and non-donor solvents, for example, hydrogenated anthracene oil (HAO) which, unlike tetralin, is largely in the liquid phase at 400°C?

EXPERIMENTAL

The two UK coals, Point of Ayr (87% dmmf C) and Bentinck (83% dmmf C), and the Wyodak APCS were treated in ca 10 g batches with chlorobenzene under nitrogen for 1 week in a Soxhlet apparatus. The treated coals were then dried *in vacuo* at 50°C as were the original coals prior to the liquefaction experiments. For Point of Ayr coal, the treatment was also carried out with the time reduced from 1 week to 3 hours.

The tetralin extractions were conducted in duplicate on the original and chlorobenzene treated samples, using 1 g of coal and 2 g of tetralin at 400°C for 15 min. as described previously ⁽¹¹⁾, the yields of DCM and pyridine-solubles being determined. In addition, extractions on Point of Ayr coal were carried out with HAO and naphthalene using the

same conditions and an extraction time of 60 min. with tetralin. The amounts of hydrogen donated to the coals from the tetralin during the extractions were calculated from the gas chromatographic-determined mass ratios of tetralin to naphthalene in the recovered DCM solutions.

RESULTS AND DISCUSSION

Tetralin extractions

Tables 1 and 2 list the yields of DCM-solubles, pyridine-solubles/DCM-insolubles and pyridine-insolubles from the tetralin, HAO and naphthalene experiments. For comparison, the results reported previously for Pittsburgh No. 8 coal are included in Table 1. The duplicate tetralin and naphthalene extractions indicate that the repeatability is $ca \pm 1\%$ daf coal. The mean values are presented in Figure 1, together with the concentrations of hydrogen donated for the 15 min. extractions.

The results indicate that chlorobenzene treatment has significantly improved the yield of DCM-solubles for the two UK bituminous coals as found previously for Pittsburgh No.8 coal⁽¹¹⁾. Similarly, the yield of pyridine-insolubles for Bentinck coal has also been reduced (Table 1). It would appear that for the 3 bituminous coals investigated, the increase in the yield of DCM-solubles decreases with increasing rank being smallest for Point of Ayr coal (Figure 1). In contrast, the conversions to DCM and pyridine-solubles for the Wyodak APCS have been reduced considerably (Table 1 and Figure 1). This striking difference in behaviour for the one low-rank coal investigated thus far is attributed to the fact that the macromolecular structures of sub-bituminous coals and lignites are swollen to a considerable extent by the water present and its removal during the chlorobenzene treatment and subsequent drying could well lead to a collapse of the pore structure giving much poorer access to hydrogen-donor solvents. Further, the liquefaction chemistry for bituminous and low-rank coals is quite different during the initial stages of conversion, particularly retrogressive reactions involving coupling of dihydric phenolic moieties being more prevalent in low-rank coals⁽¹⁵⁾.

The concentrations of hydrogen transferred during the tetralin extractions are similar for the initial and the treated coals (Figure 1, expressed on a % daf coal basis). This important finding strongly suggests that the improved oil yields are due to changes in the conformational structure of the bituminous coals allowing better solvent access. This limits the extent of char-forming retrogressive reactions rather than cleaving more bonds *per se* which would result in a greater demand for hydrogen. Indeed, the effect is still evident for Point of Ayr coal with an extraction time of 60 min. (Table 1) although the yield of DCM-solubles and the amount of hydrogen donated are considerably higher underlining the importance of the initial contact achieved between the coal and solvent

Reducing the chlorobenzene treatment time from 1 week to 3 hours had little effect on the conversions indicating that the conformational changes in the macromolecular structure of the coals brought about by the treatment occur on a fast timescale to that of *ca* 3-7 days usually associated with the removal of low temperature solvent extractable material.

HAO and naphthalene extractions

Table 2 indicates that the effect of the chlorobenzene treatment upon HAO extraction of Point of Ayr coal is similar to that for tetralin with the yield of DCM-solubles increasing by *ca* 10% daf coal. The fact that HAO is largely in the liquid rather than the vapour phase at 400°C suggests that mass transfer limitations on controlling the initial rate of conversion are still severe.

The oil yields obtained with non-hydrogen-donor aromatic compounds, such as naphthalene are obviously much lower than with effective donor solvents and this is reflected in the DCM-soluble yields in Table 2. However, as discussed earlier, aromatic compounds can give high conversions to pyridine/quinoline-solubles (*ca* 80% daf basis) for some bituminous coals⁽³⁾ probably with the aid of hydrogen shuttling or radical mediated hydrogen radical transfer in the case of a number of 4 and 5 ring systems, such as pyrene. Table 2 indicates that the chlorobenzene treatment has reduced the yield of pyridine-insolubles for Point of Ayr coal with naphthalene but has had little effect for the lower rank UK bituminous coal, Bentinck. It was reported previously⁽³⁾ for a different sample of Point of Ayr coal that THF extraction lead to significant improvements in primary conversions to pyridine-solubles with both naphthalene and pyrene. In the case of Bentinck coal, it could well be that the primary conversion is limited by the lack of available hydrogen rather than by solvent accessibility.

General discussion

This investigation has reinforced other recent work⁽¹⁻⁷⁾ which has indicated that pre-treatments can greatly enhance liquefaction yields, particularly in relatively low-severity regimes. However, much of the other work was concerned with pre-swelling coals in polar solvents where the dominant effect is undoubtedly the disruption of hydrogen bonding. The increases in oil yield obtained here of 20-25% upon chlorobenzene treatment for the two bituminous coals of lowest rank (Pittsburgh No.8 and Bentinck) are somewhat greater than that of 14% reported by Joseph⁽³⁾ for tetralin extraction (with a hydrogen over-pressure) of an Illinois No.6 coal pre-treated with tetrabutylammonium hydroxide (TBAH). Increases of only 5% were obtained for THF and methanol, but, nonetheless, pre-swelling with both these weakly-basic solvents increased the overall conversions to THF-solubles more than with TBAH. However, their boiling points are considerably lower than that of 132°C for chlorobenzene and, although some disruption of the hydrogen-bonding network in coals would undoubtedly have occurred as the coal swells to a significant extent in these polar solvents, it is uncertain whether the glass transition temperature would have been lowered sufficiently to allow the coal to adopt a lower energy configuration as with chlorobenzene. The nature of the conformational changes have yet to be fully elucidated and are currently being investigated in our laboratory by a combination of DSC, surface area measurements, broadline ¹H NMR and electron microscopy. However, they are clearly different to those induced by polar solvents and could well involve the disruption of non-covalent bonding between aromatic moieties.

There would appear to be considerable scope for improving conversions with process-derived solvents through pretreatments. Although it is clearly impractical to consider the chlorobenzene treatment in terms of a liquefaction process, the fact that it has been shown that the conformational changes can be brought about with a relatively short treatment time (3 hours, Table 1) provides a basis for exploiting such treatments above the glass transition temperatures of bituminous coals with actual process solvents.

ACKNOWLEDGEMENT

The authors thank the British Coal Utilisation Research Association (Contract No. B18) for financial support.

REFERENCES

1. R.M. Wham, *Fuel*, 1987, **66**, 283.
2. N.R. Pollack, G.D. Holder and R.P. Warzinski, *Prepr. Am. Chem. Soc. Div. Fuel Chem.*, 1991, **36(1)**, 15.
3. J.T. Joseph, *Fuel*, 1991, **70**, 139 and 459.
4. C.E. Snape, F.J. Derbyshire, H.P. Stephens, R.J. Kottenstette and N.W. Smith, *Fuel Process. Technol.*, 1990, **24**, 119.
5. J.M. Rincon and S. Cruz, *Fuel*, 1988, **67**, 1162.
6. N.K. Narain, H.R. Appell and B.R. Utz, *Prepr. Am. Chem. Soc. Div. Fuel Chem.*, 1983, **28(1)**, 161.
7. L. Artok, H.H. Schobert, G.D. Mitchell and A. Davis, *Prepr. Am. Chem. Soc. Div. Fuel Chem.*, 1991, **36(1)**, 36.
8. C. Riemer and C.E. Snape *GB Patent No. 2,204,877A*, 1988.
9. J.W. Larsen, T.L. Sams and B.R. Rogers, *Fuel*, 1980, **59**, 666.
10. R.J. O'Brien, J.R. Gibbons and R. Kandiyoti, *Fuel Process. Technol.*, 1987, **15**, 71.
11. C.A. McArthur, S. Mackinnon, P.J. Hall and C.E. Snape, *Prepr. Am. Chem. Soc. Div. Fuel Chem.*, 1992, **37** (San Francisco meeting).
12. M. Nishioka and J.W. Larsen, *Energy and Fuels*, 1990, **4**, 100.
13. P.J. Hall and J.W. Larsen, *Energy and Fuels*, 1991, **5**, 228.
14. J.W. Larsen, M. Azik and A. Korda, *Energy & Fuels*, 1992, **6**, 109.
15. D.S. Ross, B.H. Loo, D.S. Tse and A.S. Hirschon, *Fuel*, 1991, **70**, 289.

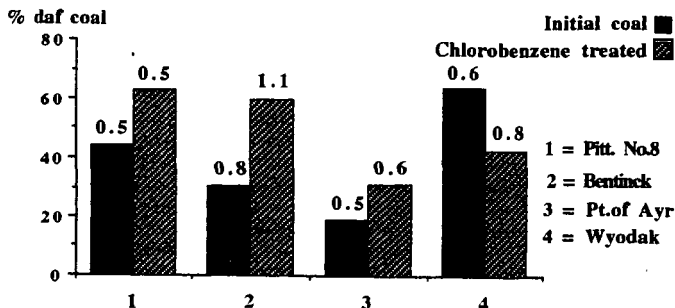


FIGURE 1 YIELDS OF DCM-SOLUBLES FROM TETRALIN EXTRACTIONS INDICATING %H TRANSFERRED (daf BASIS)

Table 1 Tetralin Extraction Results

Coal	DCM-solubles*	% daf coal Pyr sols/DCM- insols	Pyr. insols
Pitt. No. 8 (a) (15 min.)			
Initial coal	43.9	52.4	3.7
CB treated coal	62.8	31.0	6.2
Bentinck (15 min.)			
Initial coal	31.5	49.9	18.6
	28.9	46.9	24.4
CB treated coal	59.9	25.2	14.9
	56.6	28.9	14.5
Pt. of Ayr, 15 min.			
Initial coal	18.0	52.9	29.1
	20.1	48.8	31.1
CB treated coal	28.9	27.9	43.2
-one week	33.6	25.1	41.3
-3 hours	29.2	22.3	48.5
Pt. of Ayr, 60 min.			
Initial coal	37.3	36.2	26.5
CB-treated coal	46.7	29.7	23.6

* = 100 - %DCM-insols, includes DCM soluble liquid product + gas + water.

(a) = mean of duplicate runs from ref. 11.

Table 2 HAO and Naphthalene Extraction Results

Solvent/coal (15 min. extraction time)	DCM-solubles*	% daf coal Pyr sols/DCM- insols	Pyr. insols
HAO, Pt. of Ayr			
Initial coal	18.5	31.1	50.4
CB-treated coal	29.9	30.2	39.9
Naphthalene, Pt. of Ayr^(a)			
Initial coal	13.6	15.9	70.5
CB-treated coal	21.0	19.2	57.8
Naphthalene, Bentinck^(a)			
Initial coal	21.7	24.8	53.5
CB-treated coal	22.1	20.6	57.3

(a) = mean of duplicate runs

THE STRUCTURAL ALTERATION OF HUMINITE BY LOW SEVERITY LIQUEFACTION

Kurt A. Wenzel, Patrick G. Hatcher, George D. Cody, and
Chunshan Song

Fuel Science Program
The Pennsylvania State University
University Park, Pa 16802

Keywords: low severity liquefaction, coal structure, huminite

Introduction

Hydrous pyrolysis experiments were performed on low-rank coalified wood to investigate the chemical transformations that occur in huminite (vitrinite) during low severity liquefaction. The coal chosen for the experiments was of lignite rank. It consists of a single maceral huminite which consists predominantly of guaiacol- and catechol-like structures. These structures are believed to be responsible for many of the retrogressive reactions during liquefaction (1). Tubing bomb reactions were varied with reaction times ranging from 30 minutes to 240 hours and temperatures ranging from 100°C to 350°C. Structural characterization of the reacted residues were quantified by solid state ¹³C NMR and flash pyrolysis/gas chromatography/mass spectrometry. The combined analytical techniques show there is a progressive loss of oxygen which corresponds with the loss of catechols and guaiacols with increasing thermal stress. Further, dehydration of these catechol structures involves the transformation to phenol, and alkyl phenol structures that make up the macromolecular structure of the altered coalified wood. Dealkylation is also a dominant reaction pathway, as revealed by a decrease in alkyl substituents in the residue.

Detailed studies using NMR spectroscopic and pyrolysis GCMS techniques indicate that the natural evolution of humic coals proceeds through several fundamental stages (2-6). The transformation of huminite to vitrinite is characterized by reactions which result in complete demethylation of methoxy phenols to catechols and a concomitant reduction in catechols (and alkylated catechols), presumably through reaction, to form phenols and cresols; the details of the catechol reaction are so far unknown. Low severity hydrous pyrolysis of lignite parallels many of the natural coalification reactions.

Recently, Siskin et al. (7) have demonstrated that many of the reactions which typify coalification are facilitated, if not initiated, in the presence of water. They recognized that since coalification occurs in a water saturated system, water may play an integral role in the geochemistry of coalification. From their study of an enormous number of reactions with model compounds, several mechanisms with direct bearing on the chemical structural evolution of coal during liquefaction under hydrous conditions are clear. The demethylation reaction, for example, has been shown to be acid catalyzed yielding phenol as the predominant product (8). The mechanism by which the alkyl-aryl ether linkage (beta-0-4) of the modified lignin is rearranged to the beta-C-5 linkage may reasonably be expected to parallel the mechanism that Siskin et al. (7) demonstrated for their model compound study of the aquathermolysis of benzyl phenyl ether in which they observed significant yield of 2 benzyl phenol; this product is a perfect analog for the rearrangement necessary to yield the beta-C-5 linkage.

To date there is no mechanism proposed for the reduction of catechols and their alkylated analogs, through conversion, to phenol and cresols. This reaction appears to be a principal means by which the oxygen content of coal is reduced during the transformation through the subbituminous range (2-6). Although Siskin et al. (7) have not investigated the chemistry of catechols specifically, it appears reasonable to assume that the reactions of catechols may be ionic as well as thermolytic.

Experimental

A crushed sample of a coalified log described previously as the Patapsco lignite (2) was heated under hydrous conditions in a 22 ml autoclave reactor. The reactor was charged with approximately 1 gram of coal and 7 milliliters of deionized, deoxygenated water following a procedure similar to that of Siskin et al. (7). The tubing bomb reactor was consecutively pressurized to 1000 psi and depressurized with nitrogen three times to ensure all the oxygen was removed from the reactor. Finally it was depressurized to atmospheric pressure before heating. The bomb was inserted into a heated fluidized sand bath for different reaction periods, ranging from 30 min. to 10 days, and at various temperatures, ranging from 100°C to 350°C. After the elapsed heating times the reactor was removed and immediately quenched in water and then allowed to cool to room temperature. The liquids and solids were collected and analyzed. Only trace amounts of gases were detected. The bombs were opened and the liquid content pipetted off. The organic matter dissolved in the water was separated by extraction with diethyl ether. The residual lignite was removed, extracted in a 50:50 mixture of benzene:methanol, dried in a vacuum oven at 45° C for 24 hours, and then weighed.

The original lignite and solid residue from the reactors were analyzed by flash pyrolysis and by solid state NMR. The flash pyrolysis technique used was that published by Hatcher et al. (4). Solid-state ¹³C NMR spectra were obtained by the method of cross polarization and magic angle spinning (CPMAS) using the conditions previously given (2). The spectrometer was a Chemagnetics Inc. M-100 spectrometer operating at 25.2 MHz carbon frequency. Cycle times of 1 sec and contact times of 1 msec were chosen as the optimal conditions for quantitative spectroscopy.

Results and Discussion

Aquathermolysis of the Patapsco lignite was conceived as a means to trace the chemical changes that occur to the dominant maceral in low rank coals during liquefaction. Accordingly, our goal was to examine the coal before and after thermal treatment and to infer liquefaction pathways. Conversions ranged from 29 to 40 percent for the different experiments (Table I). This mass loss probably reflects low molecular weight products formed, water, and partial solubilization of lignitic structures originally of low molecular weight. The GC/MS analysis of the water soluble materials indicates the presence of lignin phenols and catechols, all of which are components of the lignite prior to thermolysis. Cleavage of a few bonds on the macromolecule could conceivably produce a catechol or methoxyphenol which would be soluble in water. Another water soluble product identified was acetic acid. This product is most likely derived from thermolysis of the side-chain carbons associated with the original lignin and coalified lignin in the sample. The content of evolved gases was not measured, because the amount of gas evolved was negligible.

The NMR data of the thermolysis residues (Figure 1) indicates clearly the evolutionary path during thermolysis. Comparing the NMR data for the residues with the original lignite and with gymnospermous wood coalified to higher rank (2) there appear to be several changes which describe the average chemical alteration. First, the most obvious change is the loss of aryl-O carbons having a chemical shift at 145 ppm. From previous studies (2) this peak has been assigned to aryl-O carbons in catechol-like structures in the coalified wood, based on chemical shift assignments and pyrolysis data. These are thought

to be originally derived from demethylation of lignin during coalification (2-6). The NMR spectrum of the aquathermolysis residue has clearly lost most of the intensity at 145 ppm but now shows a peak at 153 ppm which is related to aryl-O carbons in monohydric phenols. These are the primary constituents of subbituminous and high volatile bituminous coalified wood as depicted in the NMR spectra for such woods. It is obvious that the catechol-like structures of the lignitic wood have been transformed to phenol-like structures somewhat similar to those in higher rank coal. Thus, the aquathermolysis has reproduced, to some degree, the coalification reactions acting on aromatic centers.

The second most apparent change to occur during aquathermolysis is the loss of aliphatic structures. The methoxyl groups at 56 ppm are lost from the lignitic wood as are the other alkyl-O carbons at 74 ppm, consistent with demethylation reactions and dehydroxylation of the three carbon side chains of lignin which occur naturally during coalification of woods. However, the loss of alkyl-C carbons (those aliphatic carbons not substituted by oxygen) is the most significant change in the aliphatic region in the aquathermolysis residue. Loss of substantial amounts of aliphatic carbon is not observed during coalification of wood from lignite to high volatile bituminous coal. In fact, in most coalified wood samples, loss of alkyl-C carbon occurs only at higher ranks, above that of medium volatile bituminous coal. The lack of retention of aliphatic carbon during aquathermolysis is an indication that this treatment probably does not reproduce well the low-rank coalification reactions associated with aliphatic structures. It is important to note that the alkyl-C carbons in the aquathermolysis residues become dominated by methyl carbons with increasing thermal stress.

The pyrolysis data (Figure 2) provide confirmation for the average changes in structure observed by NMR. The loss of catechol-like structures is documented with the significant diminution of catechols in the pyrolyzate of the aquathermolysis residue compared to that of the original lignite. This loss of catechols is the singular most significant change in pyrolysis products. The pyrolyzate of the residue mimics somewhat the pyrolysis data for subbituminous coalified wood (3), being dominated by phenol and alkylphenols. Another difference between aquathermolysis residues and the original lignitic wood is in the abundance of methoxyphenols derived from lignin-like structures. The aquathermolysis has apparently reduced the relative yields significantly, consistent with the NMR data showing loss of methoxyl carbons. Some of the methoxyphenols may have been transformed to water soluble phenols and washed out of the residue in the aqueous phase; others may have undergone demethylation reactions, converted to catechols and then transformed to phenols.

The pyrolysis of the residue yields mostly phenol and the cresol isomers; other alkylated phenols, the C₂ and C₃ phenols, are not as abundant relative to phenol and cresols as the C₂ and C₃ phenols are in the pyrolysis of original lignite or the subbituminous log. This is probably related to the fact that alkyl substituents are not as abundant in the residue and the alkyl substituents are probably mostly methyl substituents as was deduced from the NMR data. Thus, the lack of significant relative amounts of C₂ and C₃ phenols in the thermolysis residue's pyrolyzate further supports the conclusion that thermolysis does not reproduce coalification reactions with regard to the aliphatic structures in the residue. The relatively high temperatures used in this study may force proportionally more thermolytic pathways over ionic pathways. The potential for such a situation has been recognized by Siskin et al. (7).

Acknowledgments

Financial support for this work was provided by the U. S. Department of Energy, Pittsburgh Energy Technology Center, under contract No. DE-AC22-91PC91042.

References

- 1) Song, C.; Schobert, H. H.; Hatcher, P.G.; *Am. Chem. Soc. Div. Fuel Chem. Prepr.* **1992**, *37*, 638.
- 2) Hatcher, P. G.; *Energy Fuels* **1988**, *2*, 40
- 3) Hatcher, P. G.; Lerch, H.E.; Verheyen, T. V.; *Int. Jour. Coal. Geol.* **1989**, *13*, 65.
- 4) Hatcher, P. G.; Lerch, H. E.; Kotra, P.K.; Verheyen, T. V.; *Fuel* **1988**, *67*, 106.
- 5) Hatcher, P. G.; Wilson, M.A.; Vassallo, A. M.; *Int. Jour. Coal. Geol.* **1989**, *13*, 99.
- 6) Hatcher, P. G.; Lerch, H. E.; Bates, A. L.; Verheyen, T. V.; *Org.Geochemistry* **1989**, *14*, 145.
- 7) Siskin, M.; Brons, G.; Vaughn, S.N.; Katritzky, A.K.; Balasubramanian, M.; *Energy & Fuels* **1990**, *4*, 488.
- 8) Katritzky, A. K. and Siskin, M. *Energy Fuels*, **1990**, *4*, 475-584.
- 9) Katritzky, A.K.; Murugan, R.; Balasubramanian, M.; Siskin, M.; *Energy Fuels* **1990**, *4*, 482.
- 10) Hatcher, P. G.; *Org. Geochem.* **1990**, *16*, 959.

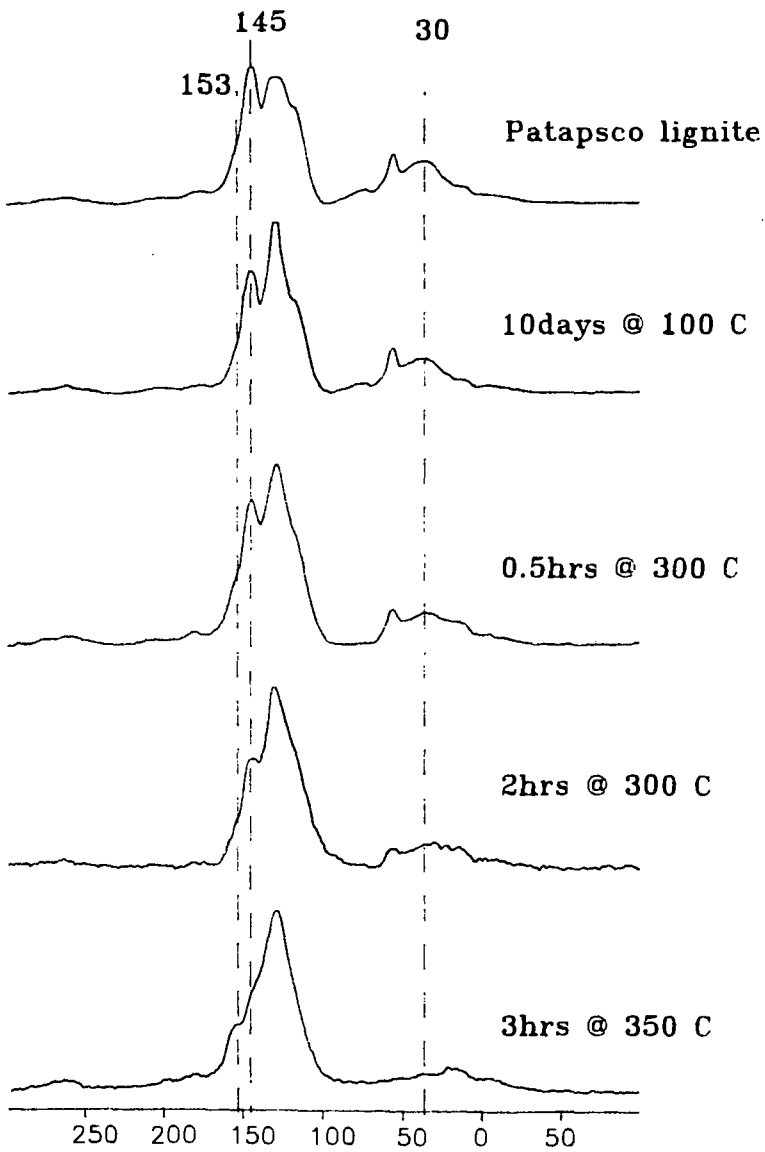


Figure 1. CPMAS ^{13}C NMR of the Patapsco lignite and the thermally altered residues.

Table I. Conversion data for hydrous pyrolysis experiments.

#	time	temperature	conversion, %
1	240 hrs	100°C	29.3
2	.5 hrs	300°C	29.8
3	2 hrs	300°C	30.6
4	3 hrs	350°C	39.7

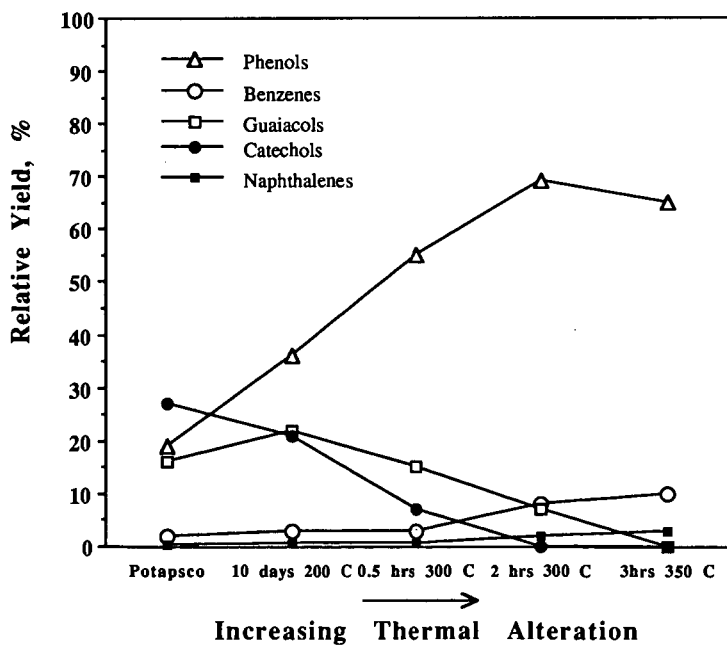


Figure 2. Relative Yields of Flash Pyrolysis Products from Aquathermolysis Residues

THE EFFECTS OF MOISTURE AND CATIONS ON LIQUEFACTION OF LOW RANK COALS

M.A. Serio, E. Kroo, H. Teng, and P.R. Solomon
Advanced Fuel Research, Inc.
87 Church Street
East Hartford, CT 06108

Keywords: Coal liquefaction, Cations, Low rank coals

INTRODUCTION

The role of calcium in reducing liquefaction yields from low rank coals has been suggested in previous work by Whitehurst et al. (1) and Mochida et al. (2). It is also consistent with work which shows an effect of calcium on reducing pyrolysis tar yields (3-7). The role of calcium may be to provide a nascent crosslink site in the coal by allowing coordination of groups like carboxyl and hydroxyl which are prone to such reactions. Otherwise, these sites would be more likely to coordinate with water (through hydrogen bonding) than with each other. There have been no studies of the effects of cation type and the associated moisture on liquefaction yields.

Studies were done on samples of Argonne Zap Lignite and Wyodak subbituminous coals which have been demineralized and then exchanged with calcium, barium or potassium cations. Two sets of samples were prepared: 1) vacuum-dried; 2) exposed to water vapor until an equilibrium moisture content was reached. The samples were characterized by FT-IR transmission analysis in KBr pellets, programmed pyrolysis in a TG-FIR system and liquefaction in donor solvent. The pyrolysis and liquefaction results are discussed in the current paper.

EXPERIMENTAL

In order to subject coals to a variety of modifications and avoid exposure to the ambient air, an apparatus for continuous-flow, controlled-atmosphere demineralization and controlled pH ion-exchange of coals was designed and constructed. A closed system is used, where instead of stirring the batch reactor contents, a continuous flow of solvent through the sample is used. By utilizing valves, it is possible to change solvents without opening the reactor. The different solvents are held in separate reservoirs which are all equipped with sparge valve systems to deoxygenate the solvents before use (with N₂ or He as needed).

Demineralization - The procedure is similar to that described in the work of Bishop and Ward (8). The coal samples used in this study are the Zap lignite and Wyodak subbituminous coals from the Argonne premium sample bank (9). The sample sizes were all -100 mesh. Before starting the acid treatment, the samples were thoroughly wetted by mixing with de-ionized water under a nitrogen environment. Demineralization involved washing the coal with a flow of 2M HCl for 45 minutes, 50% HF for 45 minutes, 2M HCl for 45 minutes, and de-ionized water for 120 minutes. The process was performed at 80 °C. After demineralization, the sample was dried in vacuum for at least 20 hours at room temperature. The vacuum dried samples were kept in a nitrogen box for subsequent analysis and liquefaction experiments.

Ion-Exchange of Carboxyl Groups with Metal Cations - The acidity constant (k_a) of carboxylic acids is around 10^{-5} , and that of phenols is around 10^{-10} . Theoretically, almost all carboxyl OH can be exchanged with cations at pH 8, whereas the phenolic-OH can remain in the acid form, according to the equation: $[A^-] / [HA] = k_a / [H^+]$, where HA is either the carboxyl or phenolic group in acid form. At pH 8, $[A^-] / [HA]$ would be a value of order 10^3 for carboxyl groups, and 10^2 for phenols. Schafer's experimental results also suggest that the carboxyl groups in coal can be completely exchanged with cations at pH around 8-8.5, along with ortho-dihydroxy groups (10). In the case of barium, a 1N barium acetate solution, which has a pH value around 8.2, was used for ion-exchange with carboxyl groups. Roughly 3 g of demineralized coal was

mixed with 300 ml of 1N barium acetate in a cell under a nitrogen environment. After 5 minutes of mixing, the pH value of the mixture dropped to less than 7.5. The mixture was filtered through a Teflon membrane by increasing the nitrogen pressure, and the mixing cell was refilled with another 300 ml of barium acetate. The pH value of the solution dropped again after mixing. The filtration and refilling procedure was repeated, usually 15-20 times, until the pH value of the mixture in the cell reached 8.0 ± 0.1 and remained constant with mixing. The drop of the pH value was probably due to the release of H^+ from carboxylic acids in the coal.

The mixture was kept under continuous mixing conditions in a nitrogen environment for at least 20 hours before the acetate solution was purged out, and the cell was refilled with a final 300 ml charge of 1N barium acetate. After 10 minutes of mixing, the acetate solution was purged out, and the coal sample was washed with 150-200 ml of de-ionized water. The coal sample was then removed from the cell for vacuum drying, which lasted for at least 20 hours. The sample was kept in a nitrogen box after drying. A similar procedure was used for exchanging calcium and potassium cations, starting with the metal acetate.

Ion-Exchange of Phenolic and Carboxyl Groups with Metal Cations - In theory, both phenolic and carboxyl groups can be totally exchanged with cations at pH around 12.5. Schafer (10) also reported that the exchange of -OH groups was complete at pH 12.6. In this study, a solution, recommended by Schafer, of 0.8 N $BaCl_2$ and 0.2 N $Ba(OH)_2$ having a pH of 12.7, was used for ion-exchange of barium cations. A similar procedure was used for calcium and potassium cations.

Approximately 3 g of a demineralized coal sample was stirred with 300 ml of the pH 12.7 solution in a nitrogen environment. After 5 minutes of mixing, the mixture was filtered through a membrane and the cell was refilled with another 300 ml of the pH 12.7 solution. The purging and refilling procedure was repeated 3 times, and the pH value of the final mixture was around 12.6. The mixture was continuously mixed under a nitrogen environment for at least 20 hours for exchange. After this long-time exchange period, the solution was purged out, and the cell was refilled with the pH 12.7 solution.

After 10 minutes of mixing, the solution was purged out, and the coal sample was washed with a solution of 0.1 N $BaCl_2$ and 0.03 N NaOH, which has a pH around 12.7, to avoid hydrolysis of the exchanged coal. The coal sample was then removed from the cell for vacuum drying. After drying, the sample was kept in a nitrogen box for further study.

It was noticed, in the process of ion-exchange that part of the coal structure was dissolved in the high pH value solution, since the filtrate had a yellowish color. This is most likely due to hydrolysis of the ester linkage in coal. The amount of the coal structure (so called humic acids) dissolved in the high pH value solutions during complete ion-exchange was estimated to be about 6.6 wt% daf of the demineralized Zap and 17 wt% daf of the demineralized Wyodak.

Preparation of Moisturized Coal Samples - A procedure for restoring the moisture level of modified coal samples was developed. The moisturized samples were prepared by enclosing the vacuum-dried modified samples in a box with a nitrogen purge of 100% humidity. The sample exposure to moisture was performed for several days (~6 days) until no further moisture uptake was observed.

RESULTS AND DISCUSSION

The modified coal samples were characterized by FT-IR transmission analysis in KBr pellets, programmed pyrolysis in a TG-FTIR system and liquefaction in donor solvent. The results are discussed below.

Effect of Cations on Pyrolysis Tar and Liquefaction Yields - The results of sample analysis by programmed pyrolysis in the TG-FTIR are shown in Figures 1 and 2, and summarized in Table

1 for the Zap lignite. These results show that demineralization tends to increase the tar yield, whereas both the gas and char yields were reduced. Similar results were observed for the Wyodak coal (11). Table 1 also shows a decrease of the tar yield with the extent of ion-exchange with the metal cations, and a corresponding increase in the total amount of gas evolution. The liquefaction results for different samples are shown in Table 2. The data in Tables 1 and 2 show that the yields of both the pyrolysis tar and toluene solubles from liquefaction decrease with the extent of ion-exchange, i.e., in the order of (demineralized) > (ion-exchanged at pH 8) > (ion-exchanged at pH 12.5). This result indicates that having the carboxyl or phenolic groups in the salt form makes it easier to crosslink the coal structure during pyrolysis or liquefaction reactions.

It is realized that this is a more difficult comparison for the samples exchanged at pH 12.5, since considerable amounts of humic acids were observed to dissolve in the high pH value solutions. The dissolution of coals in the aqueous alkaline solutions may be due to the breaking of ester bonds in coal, i.e., $\text{RCOOR}' + \text{OH}^- \rightarrow \text{RCOO}^- + \text{R}'\text{OH}$. This coal dissolution mechanism was also proposed by other workers (12). The solubility of coal in alkaline solutions varies with the cations contained in the solution. The color difference of the calcium and potassium solutions after ion-exchange at high pH is striking, in that the potassium solution has a much darker color, indicating much more coal dissolved in the monovalent cation (K^+ here) solution than the bivalent cation (Ca^{++} here) solution. The results also show that the barium solution extracted more coal than the calcium solution, but not as much as the potassium solution. A possible reason is the fact that Ca^{++} and Ba^{++} ions can act as cross-links between two acid groups of different coal fragments (12), whereas K^+ can only interact with one acidic site. The ability of bivalent cations to act as initial crosslinks in the structure at high pH is supported by data on the pyridine volumetric swelling ratios (VSR) and pyridine extractables, shown in Table 3. The values of the VSR are lower for the bivalent cations at high pH for both the dry and moist coals. It can be seen in Table 1, for the pyrolysis of vacuum dried samples, that the tar yield was higher for the potassium-exchanged coals than the calcium and barium-exchanged samples at high pH, suggesting that bivalent cations tighten the coal structure by cross-linking coal fragments and making it more difficult for tar molecules to form (7). At pH 8; the values of the tar yield and VSR for the monovalent and bivalent cations are more similar, though lower than the values for either the raw or demineralized coals. Consequently, it appears that the monovalent cations help to hold the structure together, although this must occur through electrostatic rather than covalent interactions. It makes sense that valency would be less important in the normal state of the coal or at pH=8 since, for steric reasons, cations are unlikely to be exchanged on more than one carboxyl or ortho-dihydroxy site.

It is likely that coal solubility in aqueous alkaline solutions increases with the size of the cations of the same valence. If this is true, the dissolution of coal in sodium solution would be expected to be less than that in the potassium solution. Preliminary results show that this is the case. However, this requires further confirmation. In summary, at similar pH values (~12.5), the amounts of Zap lignite extracted by 1 liter of the cation solutions in 20 hours increases in the order of $\text{Ca}^{++} < \text{Ba}^+ < \text{K}^+$.

In considering the size effect of the cations on the pyrolytic tar and liquefaction yields, one should compare the data for the barium- and calcium-exchanged samples. It is interesting that the size of the cations has an opposite effect on the tar and liquefaction yields. In pyrolysis, the tar yield for the barium-exchanged samples is lower than that of the calcium-exchanged samples, while in liquefaction, the yield was higher for the barium-exchanged samples. This could be due to increased extraction of tar precursors during ion-exchange in the case of barium which subsequently makes the coal more accessible to the liquefaction solvent.

Effect of Cations on Gas Yields from Pyrolysis and Liquefaction - It is of interest to note that the gas yields from liquefaction and pyrolysis do not always follow the same trend. Table 1 shows that, in pyrolysis, the total yield of oxygen-containing gases (i.e., CO_2 , CO , and H_2O) always increases with decreasing tar yield. Table 2 shows the expected increase of the

liquefaction yields with tar yield. However, the gas yields in liquefaction show an irregular variation with pH and with cation type. For example, the CO₂ yield is high for the partially barium exchanged Zap lignite, and is significantly reduced for the completely barium exchanged sample. The Wyodak subbituminous coal shows the opposite trend. For the ion-exchanged Zap lignite, the decrease of the CO₂ yield in liquefaction can be explained by the loss of some organic components, which contain CO₂-forming functions, during the barium exchange at high pH. Some of these variations could be due to catalysis of secondary gas-phase or gas-solid reactions.

For CO evolution in pyrolysis, the demineralized samples show the major evolution at temperatures between 400 and 800 °C. CO evolution also occurs in a similar temperature range for fresh and ion-exchanged samples. However, the evolution is depressed at temperatures lower than about 750 °C, but elevated above this temperature by comparing with that of the demineralized samples. It was also noted that the fraction of CO evolving before 750 °C increases with increasing tar yield, as shown in Fig. 3a for the Zap lignite. This observation is significant. The higher CO evolution at temperatures lower than 750 °C for demineralized samples could be due to more oxygen functions evolving as CO without crosslinking. For ion-exchanged samples, the depressed CO evolution at lower temperatures is probably caused by oxygen retention through crosslinking between oxygen functions, and the CO evolved at 750 °C or above, is likely from the decomposition of the metal carboxylate groups which can produce carbonates as a decomposition product. The raw and cation exchanged samples have a sharp evolution peak in the TG-FTIR analysis, as shown in Figs. 1 and 2. This occurs in the same temperature range as the decomposition of carbonates and could be the result of catalytic gasification of the CO₂ produced to CO. The correlation of the total CO evolution in coal pyrolysis with pyrolytic tar and liquefaction yields was studied, as shown in Fig. 3b for the Zap lignite. The data shows that both tar and liquefaction yields increase with decreasing total (pyrolysis) CO yield. Therefore, both the relative amount of CO evolved before 750 °C and the total CO evolution are indicators of the extent of crosslinking.

Figures 1 to 2 also show that CO₂, H₂O, and low temperature CO evolve in a similar temperature range. This might imply that these products are derived from a consecutive mechanism. The CO₂ evolution curve does not show as much shape variation with changes in cation content. However, the yield is basically a decreasing function of tar yield. In previous work, the relationship between CO₂ evolution and crosslinking events has been noted (13-15). This has been explained by the mechanism that elimination of CO₂ would create aryl radicals to enhance crosslinking. The CH₄ yield also showed a trend opposite to that of the tar yield for the ion-exchanged samples. This has been generally reported in coal pyrolysis studies. By reincorporation into the solid matrix by more stable bonds, the tar precursors can yield volatiles only by cracking off of small side groups, hence the increased CH₄ yields with decreasing tar yields.

One aspect of the H₂O evolution data revealed in Figs. 1 and 2 merits further comment. For samples which contain acidic functions in the salt form, including fresh and barium exchanged samples, there is always a water evolution peak present at around 200 °C. This 200 °C peak is obscure for demineralized samples. It is very likely that this peak is due to the evolution of moisture which is ionically bonded on the salt structure. For vacuum dried samples, it can be seen that the moisture content increases with the amount of barium in the samples, as shown in Table 3. This indicates that the acidic functions in the salt forms attract polar water molecules. These attracted water molecules cannot be removed by vacuum drying, but only by raising the temperature of the sample.

Analysis of Carboxyl and Phenolic Groups by Barium Titration - In theory, all of the carboxyl groups of demineralized samples can be exchanged with barium at pH 8. Consequently, it follows that one could determine the concentration of carboxyl groups in coal by knowing the amount of barium ion exchanged at pH 8. The chemical composition of ash formed by combustion of the barium exchanged sample is predominantly BaO. Therefore, from the ash

content of the samples ion-exchanged at pH 8, one can estimate the concentration of carboxyl groups in the coal. Similarly, the total concentration of carboxyl and phenolic groups can be determined by the ash content of the sample ion-exchanged at pH 12.6. The concentration of phenolic groups can be obtained from the difference of the above two measurements. The concentrations of carboxyl and phenolic groups determined in this manner for Zap and Wyodak are shown in Table 4. The results shown in Table 4 are similar to those determined by Schafer (10, 16) for Australian low-rank coals, using barium titration methods. However, our FT-IR results indicate that not all of these groups can be exchanged and that the cations can interact with additional sites in the coal. This will be the subject of a separate publication.

Pyrolysis and Liquefaction of Moisturized Coal Samples - Remoisturization of vacuum dried Zap and Wyodak was done in the attempt to understand if moisture uptake for low rank coals is a reversible process and to see if moisture influences the role of the cations. The remoisturized samples were analyzed by programmed pyrolysis with TG-FTIR. Preliminary results show that the moisture content can reach that of the raw samples by remoisturization for Zap, but not for Wyodak. The results for the Zap lignite are shown in Table 3. Furthermore, the chemical structure of the coal samples seems to have been changed by remoisturization, since different CO₂ evolution behaviors were observed. A comparison of the CO₂ evolution behavior for raw and remoisturized coal samples is given in Fig. 4. The detailed liquefaction and pyrolysis results are presented in Ref. 11.

In almost every case, the asphaltene yield was increased with moisturization except for the pH 8 Zap, in which case the asphaltene yield was slightly reduced. Interestingly enough, the oil yield was reduced for most of the modified samples with moisturization, except for the demineralized Zap and the pH 12.6 Wyodak. The indication from the above results is that moisturization favors the formation of the larger molecular weight asphaltenes in liquefaction, while the formation of the smaller molecular weight oils is less favored.

It is usually shown that the trends for improved liquefaction yields parallel those for improved tar yields in pyrolysis. However, it was found in this study that the influences of moisturization on the yields of pyrolytic tars and liquefaction toluene soluble yields are different in that moisturization does not appear to have a significant effect on pyrolysis tar yields. This indicates that moisture plays different roles for the formation of tars in pyrolysis and coal liquids in liquefaction. A possible explanation for the difference is that most of the moisture is depleted early in the pyrolysis process, whereas the moisture is retained in the reactor during liquefaction and can exist in a liquid phase. This aspect requires further investigation.

The results also show that the moist samples have higher gas yields in liquefaction than the vacuum dried samples. The increase in gas yield is mainly from CO₂ and CO (especially CO₂), whereas the yields of hydrocarbon gases decrease with moisturization. One possible explanation for this result is that moisture may react with side chain structures in coal, which are the sources for the formation of oils and hydrocarbon gases during liquefaction, to form oxygen functions. The subsequent reaction of these oxygen functions produces more CO₂, CO and asphaltenes in the liquefaction of moist coals.

CONCLUSIONS

The conclusions from this study are as follows:

- The tar yields and liquefaction yields are reduced for all three cations tested (K⁺, Ca⁺⁺, Ba⁺⁺) and are lower for the fully exchanged coals. The ability of cations to act as initial crosslinks is an important aspect of their role in retrogressive reactions.
- The previously observed correlation between pyrolysis tar and liquefaction yields for coals and modified coals appears to hold for the vacuum-dried cation-exchanged coals, but not always for the re-moisturized coals.

always for the re-moisturized coals.

- The total evolution of CO₂ and CO from pyrolysis is changed significantly by cation-exchange. However, only in the case of CO does the evolution profile change significantly.
- After careful demineralization, a calcium form Zap or Wyodak coal can be prepared at pH = 8, which is similar to the raw coal with regard to pyrolysis and liquefaction behavior.
- At pH=8, cations are most likely to be coordinating multiple oxygen functionalities around themselves through electrostatic type interactions, which diminishes the importance of valency.
- Some of the moisture in a coal is associated with the cations. The moisture content has a larger role in liquefaction than in pyrolysis because it is present for a longer period of time.

ACKNOWLEDGEMENTS

This work was supported by the U.S. D.O.E. Pittsburgh Energy Technology Center under Contract No. DE-AC22-91PC91026.

REFERENCES

1. Whitehurst, D.D., Mitchell, T.O., and Farcasiu, M., Coal Liquefaction, The Chemistry and Technology of Thermal Processes, Academic Press, NY (1980).
2. Mochida, I., Shimohara, T., Korai, Y., Fujitsu, H., and Takeshita, K., *Fuel* **62**, 659, (1983).
3. Tyler, R.J. and Schafer, H.N.S., *Fuel*, **59**, 487, (1980).
4. Morgan, M.E. and Jenkins, *Fuel*, **65**, 757, (1986).
5. Morgan, M.E. and Jenkins, *Fuel*, **65**, 764, (1986).
6. Morgan, M.E. and Jenkins, *Fuel*, **65**, 769, (1986).
7. Wornat, M.J., and Nelson P.F., *Energy and Fuel*, **6** (2) (1992).
8. Bishop, M., and Ward, D.L., *Fuel*, **37**, 191, (1958).
9. Vorres, K.S., *Energy and Fuel*, **4** (5), 420 (1990).
10. Schafer, H., *Fuel*, **49**, 197, (1970).
11. Serio, M.A., Kroo, E., Teng, H., Charpenay, S., and Solomon, P.R., "The Dual Role of Oxygen Functions in Coal Pretreatment and Liquefaction: Crosslinking and Cleavage Reactions," Fifth Quarterly Report, U.S. DOE Contract No. DE-AC22-91-PC91026 (1992).
12. van Bodegom, B., van Veen, J.A., van Kessel, G.M.M., Sinnige-Nijssen, M.W.A., and Stuiver, H.C.M, *Fuel*, **63**, 346 (1984).
13. Suuberg, E.M., Lee, D., and Larsen, J.W., *Fuel*, **64**, 1668, (1985).
14. Suuberg, E.M., Unger, P.E., and Larsen, J.W., *Energy & Fuels*, **1**, 305, (1987).
15. Solomon, P.R., Serio, M.A., Deshpande, G.V., and Kroo, E., *Energy & Fuels*, **4** (1), 42, (1990).
16. Schafer, H., *Fuel*, **51**, 4, (1972).

Table 1. Pyrolysis Results of Vacuum Dried Modified Zap Samples.

Coal (type/preparation)	Pyrolysis Products (wt.% daf)					
	Tars	CO ₂	CO	H ₂ O	CH ₄	Char
Fresh	7	8.9	14.7	14.3	2.2	57
Demin.	20	4.8	10.4	8.4	2.7	54
Demin. + K ⁺ (pH8)	11	8.6	9.9	16.0	1.9	57
Demin. + Ca ⁺⁺ (pH8)	10	8.6	13.5	10.3	2.4	58
Demin. + Ba ⁺⁺ (pH8)	6	11.7	15.8	18.6	2.6	55
Demin. + K ⁺ (pH12.5)	5	9.9	12.4	13.5	1.6	57
Demin. + Ca ⁺⁺ (pH12.5)	4	8.2	22.6	12.6	2.0	51
Demin. + Ba ⁺⁺ (pH12.5)	3	10.5	24.1	15.5	2.6	52

Table 2. Liquefaction Results of Vacuum Dried Modified Zap Samples.

	Toluene Solubles			Gas		
	Total	Oils	Asphaltenes	CO ₂	CO	CH ₄
Fresh	26	12	14	4.3	0.24	0.25
Demin.	52	26	26	1.1	0.43	0.27
Demin. + K ⁺ (pH8)	30	11	19	7.7	0.27	0.17
Demin. + Ca ⁺⁺ (pH8)	25	13	12	2.7	0.30	0.22
Demin. + Ba ⁺⁺ (pH8)	37	25	12	7.3	0.40	0.20
Demin. + K ⁺ (pH12.5)	17	5	12	5.0	0.24	0.27
Demin. + Ca ⁺⁺ (pH12.5)	*	*	3	0.7	0.04	0.08
Demin. + Ba ⁺⁺ (pH12.5)	15	15	0.5	0.3	0.27	0.02

* Yields Calculated by Difference were Negative. Solvent Incorporation is Suspected.

Table 3. Characterization of Cation-Exchanged Zap Samples.

Coal Type	Dry			Moist			
	V.S.R	P _s	Moisture	V.S.R.	P _s	Moisture	
Zap Raw	2.7	5	NM	1.9	15	32	
Zap Demin.	3.1	20	4	2.6	22	16	
pH 8	K ⁺	2.0	10	6	1.9	9	20
	Ba ²⁺	1.8	3	5	1.5	4	22
	Ca ²⁺	2.1	6	5	1.6	6	21
pH 12	K ⁺	1.7	2	6	1.4	2	29
	Ba ²⁺	1.1	2	7	1.2	2	22
	Ca ²⁺	1.1	1	9	1.2	1	25

Notes: V.S.R. = Volumetric Swelling Ratio in Pyridine; P_s = Pyridine Solubles (daf)
Moisture was Determined by TG-FTIR and is Reported on an As-received Basis.
NM = Not Measured.

Table 4. The Carbonyl and Phenolic Contents of Zap and Wyodak Coals Determined by Barium Titration. (meq g⁻¹ daf basis)

	Carboxyl Groups	Phenolic Groups	Total Acidity
Zap Lignite	2.52	6.74	9.26
Wyodak Sub.	2.40	5.76	8.16

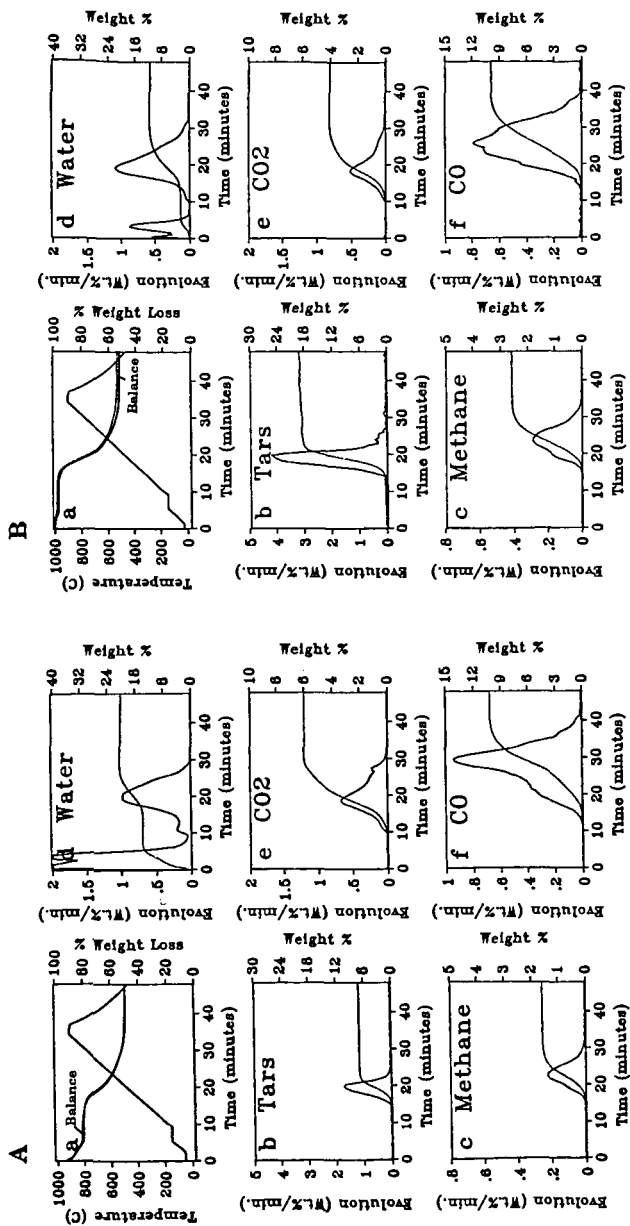


Figure 1. TG-FTIR Analysis of A) Raw and B) Demineralized Argonne Zap Lignite.

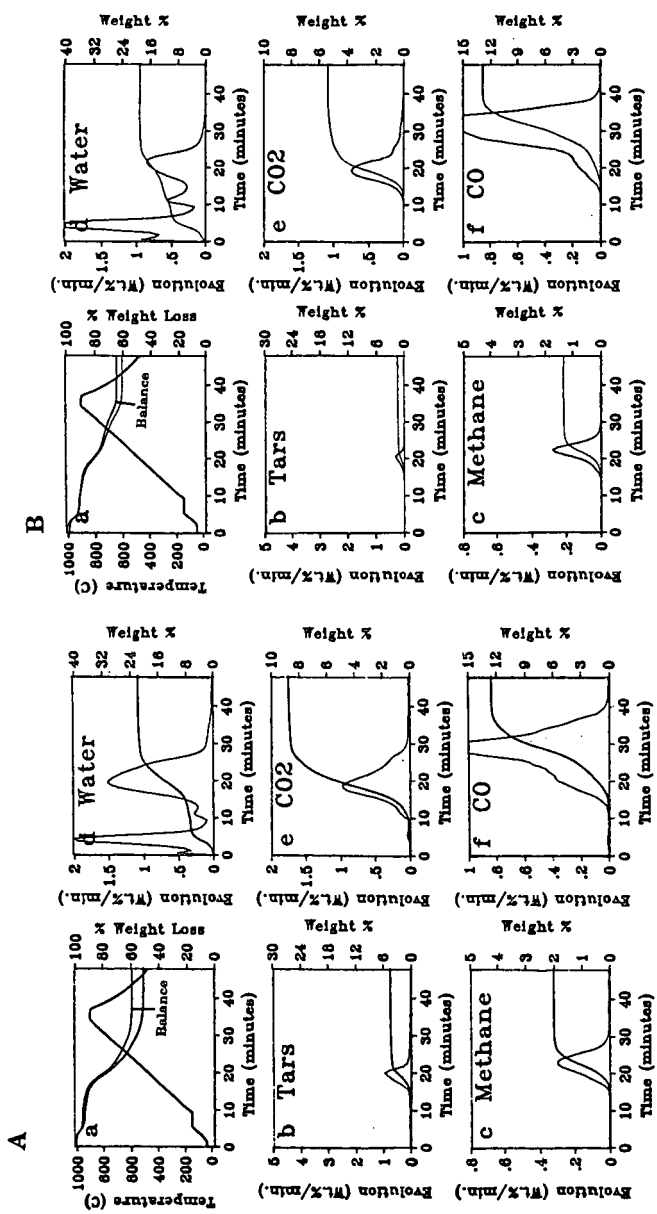


Figure 2. TG-FTIR Analysis of Zap Samples which A) have had Carboxyl Groups Exchanged with Barium; B) have had Carboxyl and Phenolic Groups Exchanged with Barium.

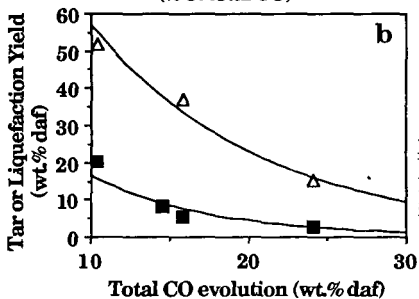
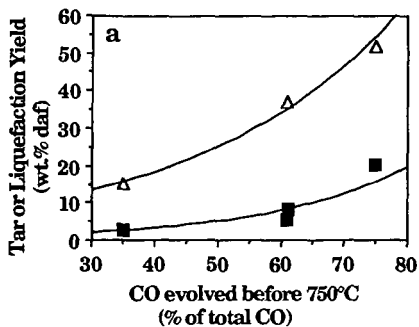


Figure 3. Correlation of Pyrolysis Tar Yield (■) and Toluene Solubles from Liquefaction (Δ) for Zap Lignite with a) Pyrolysis CO Evolution Before 750°C; b) Total Pyrolysis CO Evolution.

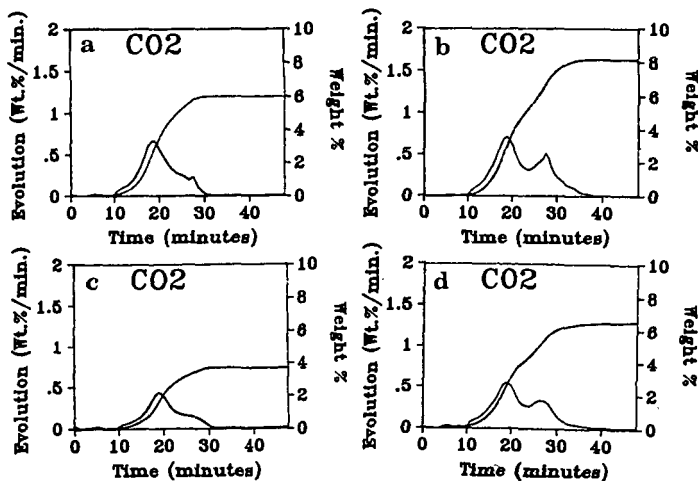


Figure 4. CO₂ Evolution During Coal Pyrolysis. a) Raw Zap; b) Remoisturized Zap; c) Raw Wyodak; d) Remoisturized Wyodak.

**EFFECT OF TEMPERATURE, SAMPLE SIZE AND GAS FLOW RATE ON
DRYING OF BEULAH-ZAP LIGNITE AND WYODAK SUBBITUMINOUS COAL**

Karl S. Vorres
Chemistry Division, Building 211
Argonne National Laboratory
Argonne, IL 60439

Keywords: drying, liquefaction, TGA

ABSTRACT

Beulah-Zap lignite and Wyodak-Anderson (-100 and -20 mesh from the Argonne Premium Coal Sample Program) were dried in nitrogen under various conditions of temperature (20-80°C), gas flow rates (20-160 cc/min), and sample sizes (20-160 mg). An equation relating the initial drying rate in the unimolecular mechanism was developed to relate the drying rate and these three variables over the initial 80-85% of the moisture loss for the lignite. The behavior of the Wyodak-Anderson subbituminous coal is very similar to that of the lignite. The nitrogen BET surface area of the subbituminous sample is much larger than the lignite.

INTRODUCTION

Economical production of synthetic coal liquids suitable for transportation fuels is a continuing goal of a number of coal conversion programs. The vast reserves of low rank coals in the western part of the U. S. provide a plentiful supply of input for potential processes. The low rank coals generally possess a high reactivity in many chemical reactions which also make them attractive feedstocks. One of the major detractors, however, is the high moisture content associated with many of these fuels, ranging up to 40%. An economical means of removing the moisture without sacrificing the reactivity or oil yields would be desirable.

A number of studies have been carried out on the drying behavior of coals from a fundamental viewpoint (1,2,3,4,5). The drying behavior has been found (1,2,3,4) to follow a unimolecular mechanism in a flow of dry gas (nitrogen or carbon dioxide) over a range of temperatures, gas flow rates and sample sizes). The mechanism proceeds through two stages. The initial stage accounts for about 80-85% of the moisture loss, while the second accounts for all but about 1% of the rest of the loss.

EXPERIMENTAL

Coal drying was done with a modified Cahn model 121 thermobalance or thermo-gravimetric analyzer (TGA) attached to an IBM PC/XT microcomputer. Vendor-supplied software was used to monitor the progress of individual runs, and convert data files to a form that could be further studied with Lotus 123.

The data were obtained as files of time, temperature and weight at 10 second intervals. Run times varied from 7-23 hours. Sample sizes typically started at about 80 mg, but varied from

20-165 mg. Runs were typically isothermal, with temperatures selected from 20 to 80°C. The gas velocity moving upward past the sample was typically 80 cc/min (but ranged from 20 to 160) in the 25 mm diameter tube. The thermobalance was modified so that all of the gas flow passed around the sample, rather than partly through the weighing mechanism. The sample was placed in a quartz flat bottom bucket about 10 mm internal diameter. The samples were the -100 mesh Argonne Premium Coal Samples: Beulah-Zap lignite and Wyodak-Anderson subbituminous (6).

Samples were quickly transferred from ampoules which had been kept in constant humidity chambers with water at room temperature (20°C or 293 K). In the thermobalance system a period of about 5 minutes was used to stabilize the system and initiate data acquisition. A condenser was made to replace the usual quartz envelope and furnace that surrounds the sample. Water was circulated from a constant temperature bath through the condenser to maintain constant temperature during the experiments. This was more stable than the original furnace and provided uniform temperature control during the experiments.

The atmosphere for the nitrogen gas runs was cylinder nitrogen (99.99%) or "house" nitrogen from the evaporation of liquid nitrogen storage containers used without further purification.

Data were analyzed on a separate microcomputer as reported earlier (1-4). Regression analysis was used to obtain the kinetic constants in terms of mg of water lost/gm sample per 10 second time interval. Lotus 123 was used for analysis of individual run data. In some runs, approximations to a first and second derivative of the rate expressions were made in Lotus 123 by averaging over a number of the 10 second time intervals before and after the point of interest. These derivatives were plotted with the rate data to aid in identifying the beginning of the transitions from an initial phase of drying to a second, slower phase. The initial drying kinetic data from a run at a temperature different from room temperature were collected over a time in which the sample was reaching the temperature of the system. These runs indicated that the initial rate increased for about 10-30 minutes until a constant value for the first phase was reached. Figure 1 indicates typical weight changes over the duration of a run for the Beulah Zap lignite and the Wyodak-Anderson subbituminous samples. Note that the lignite has a higher initial moisture content and therefore can lose more water.

Surface area measurements were carried out to complement the drying kinetic runs. The surface area was assumed to be important in that it determines the amount of exposure to the gaseous phase. The greater the surface area the greater the overall reaction rate will be, assuming a similar reactivity per unit of surface and comparable access to exterior and interior surface.

The Quantasorb Jr. instrument was used for nitrogen BET (Brunauer-Emmett-Teller) measurements of the surface. A series of values were obtained on samples which were prepared by drying in the vacuum oven at a range of temperatures as well as a set of nitrogen dried samples, prepared both in the vacuum oven with a flow of nitrogen at atmospheric pressure, and also the products

of some of the thermobalance runs. The typical run gives the data from the desorption cycle. Samples of nitrogen in helium (10, 20 and 30% nitrogen) were allowed to interact with the surface of the sample. Adsorption was carried out at liquid nitrogen temperatures. The amount of adsorbed nitrogen was determined by calibration of a thermal conductivity bridge.

RESULTS AND DISCUSSION

A typical run indicates a rapid initial moisture loss, followed by significantly reduced rates. A plot of the logarithm of the water left as a function of time gives two straight line segments followed by a downward slope for the loss of the last 1%. See Figure 2 for typical lignite and subbituminous coal runs. The first line segment has been correlated with the loss of "freezable" water, while the latter has been associated with "non-freezable" water as identified by Mraw and co-workers (7,8). The rate constants for the initial rate loss can be correlated with an Arrhenius plot to give an activation energy for the initial stage of water loss, but the second stage could not be correlated. A multiple regression analysis of the initial rate with the values of the absolute temperature, gas flow and sample weight was carried out with the data from 51 runs made with -100 mesh material in dry nitrogen. For an equation of the form:

$$\text{Log Initial Rate (mg water left/gm sample/10 second interval)} = c_1 * \text{Temperature (K)} + c_2 * \text{Gas flow (cc/min)} + c_3 * \text{Sample Weight (mg)} + c_4$$

The best fit was given for:

$$\begin{aligned} c_1 &= .0248 & c_2 &= .00376 \\ c_3 &= -.00528 & c_4 &= -3.295 \end{aligned}$$

with an R^2 value of .867. These values cover experiments in the range of 20-80°C, 20-160 cc/min gas flow and 20-169 mg sample weight.

A smaller series of runs (6) made with the -100 mesh Wyodak subbituminous sample at gas flow rates of 80 cc/min were analyzed with multiple regression. The best fit over the range of 20-60°C and weight of 40-80 mg were given by:

$\log k_1$ (initial rate in mg water left/gm sample /10 second interval) = .0242 * Temperature (K) - .00673 * Sample weight (mg) - 9.315. The R^2 value = .983. There is a similarity in the coefficients for the temperature and the weight for the two coals. The similarity in the two curves in Figure 2 would also indicate this.

The surface area measurement data are given in Table 1.

Table 1, Surface Area Measurements

Run #	Drying Method	Temp. °C.	Surface area m ² /gm
ND173	Nitrogen	22	1.993

RM-59-1	Vacuum	22	3.221	
RM-59-1	Vacuum	22	2.889	reproducibility check
RM-68-2	Vacuum	22	2.969	repro. different sample
ND175	Nitrogen	40	1.811	
RM-67-1	Vacuum	40	2.141	
ND177	Nitrogen	60	1.887	
ND178	Nitrogen	70	1.286	Questionable value
RM-62-1	Nitrogen	110	1.819	
RM-63-1	Vacuum	110	1.768	
RM-65-1	Nitrogen	150	1.865	
RM-65-1	Vacuum	150	1.900	
RM-66-1	Vacuum	150	1.764	repeat above after heating overnight in N2 at 150°C.

For comparison a run was made using Wyodak subbituminous coal:

RM-68-1 Vacuum 25 10.61

Clearly the subbituminous coal has a much larger surface area, reflecting a greater order in the coal particles, and better developed pore structure.

CONCLUSIONS

Generalizations on Lignite Drying

1. A complete understanding of the rate of lignite drying must include the effects of a number of variables. Some of these are inherent in the material itself, others depend on the processing given to the material, and still others have to do with mass transfer effects.

2. The rate of drying is affected by the temperature, gas flow, sample thickness and history. For the experiments conducted in this study the rate of drying from the 10 mm diameter container can be expressed by:

$$\text{Log rate} = .0248 * \text{Temp. (K)} + .00376 * \text{gas flow (cc/min)} - .00528 \text{ sample wt (mg)} - 3.295.$$

3. There is a unimolecular mechanism for the initial 60-85% of the weight loss. A transition occurs to a slower mechanism until about 1% of the water remains.

4. There are at least two kinds of water present in the low rank coals. The terms "freezable" and "non-freezable" have been applied to these. The kinetic data support this concept, and extend the perception to exchange between the two forms. The initial water loss corresponds to "freezable" water, while the later loss corresponds to "non-freezable" water.

Generalizations on Subbituminous Drying

1. The behavior of subbituminous coal on drying is very similar to that of lignite.

2. The mechanism of drying is a unimolecular process. There is a transition after about 80% of moisture loss to a slower unimolecular process.

3. The rate of drying is affected by the temperature, sample thickness or weight and history. For the experiments conducted in this study the rate of drying from the 10 mm diameter container can be expressed by:

$$\text{Log rate} = .0242 * \text{Temp. (K)} - .00673 \text{ sample wt (mg)} - 9.315.$$

4. The subbituminous coal has a larger nitrogen BET surface area, but the rate of drying is not enhanced by this larger area.

ACKNOWLEDGMENTS

The author is grateful for the support of the Office of Fossil Energy, U. S. Department of Energy in this work.

REFERENCES

1. Vorres, K. S., R. Kolman, and T. Griswold, Am. Chem. Soc. Preprints Fuel Chem. Div. 33 (2), 333 (1988).
2. Vorres, K. S. and R. Kolman, Am. Chem. Soc. Preprints Fuel Div. 33 (3), 7 (1988).
3. Vorres, K. S., Wertz, D. L., Malhotra, V. M., Dang, Joseph, J. T. and Fisher, R. Fuel, 71 (9) 1047-1053 (1992)
4. Vorres, K. S. Am. Chem. Soc. Preprints Fuel Chem. Div. 37 (2), 928 (1992). See also Vorres, K. S., Wertz, D., Joseph, J. T., and Fisher, R., Am. Chem. Soc. Preprints Fuel Chem. Div. 33 (3), 853 (1991) and Vorres, K. S., Molenda, D., Dang, Y., and Malhotra, V. M. Am. Chem. Soc. Preprints Fuel Chem. Div. 36 (1), 108 (1991).
5. Abhari, R. and L. L. Isaacs, Energy & Fuels 4, 448 (1990).
6. Vorres, K. S. Energy & Fuels 4 (5) 420-426 (1990)
7. Mraw, S. C. and B. G. Silbernagel, Am. Inst. Physics Proceedings 70, 332 (1981).
8. Mraw, S. C. and Naas-O'Rourke, D. F., Science, 205 901 (1979) and J. Coll. Int. Sci., 89 268 (1982)

Fig. 1: Wyodak and Beulah-Zap Dried in N₂, 40 C.
 WY13 & ND86, -100 mesh, 80 cc/min, 80 mg, fbb

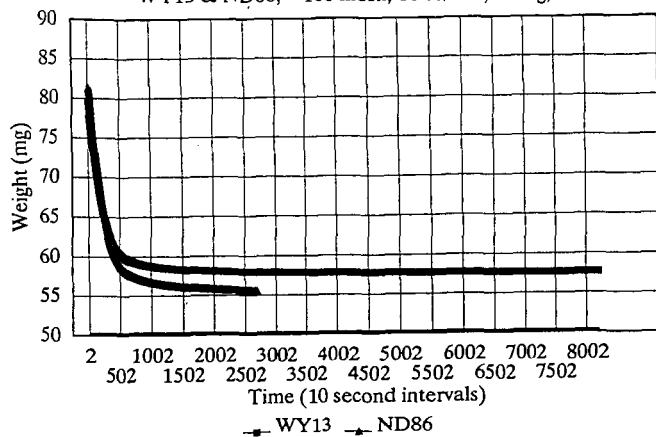
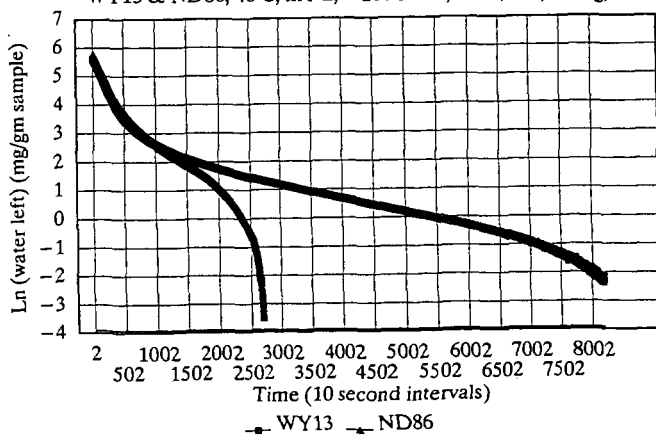


Fig. 2 Wyodak & Beulah-Zap Dried in N₂, 40 C.
 WY13 & ND86, 40 C, in N₂, -100 mesh, 80 cc/min, 80 mg, fbb



Influence of Drying and Oxidation of Coal on its Catalytic and Thermal Liquefaction.

1. Coal Conversion and Products Distribution.

Ajay K. Saini, Chunshan Song and Harold H. Schobert

Department of Material Science and Engineering, 209 Academic Projects Building, Fuel Science Program, The Pennsylvania State University, University Park, PA 16802.

Keywords: Drying, Oxidation, Coal liquefaction.

INTRODUCTION

Most of the subbituminous coals contain more than 25 wt % of moisture and it is considered an economic necessity to dry these coals prior to liquefaction. The drying of coal can have significant effect on the conversion reactivity of coal. Atherton (1) reported that the drying of low rank subbituminous coal in a gas atmosphere did not effect the total conversion except in air. The air-drying gave somewhat lower conversion, which may be a result of the adverse effect of preoxidation. The best conversion was obtained by vacuum and microwave drying. The oxidation of coal has been known to have an adverse effect on the coal conversion. Neavel (2) reported a significant reduction in the yield of benzene soluble products from hvc bituminous coal as a result of oxidation. Cronauer et al. (3) reported that partial drying of subbituminous coal in a mixture of nitrogen and oxygen or even in nitrogen alone reduced the conversion as compared to that of the raw coal. On the other hand, Vorres et al. recently reported that drying improves the oil yield in liquefaction of lignite samples (4)

In the present study we report the influence of drying Wyodak subbituminous coal in air and vacuum on the THF-conversion in thermal and catalytic liquefactions. From our results it appears that the drying of coal in air to some extent, which has been considered to be worse for liquefaction, may give a better conversion with dispersed Mo catalyst compared to the vacuum-dried coal in the presence of a liquefaction solvent. The raw coal was also subjected to liquefaction. Best conversion was obtained from the raw coal in the thermal and catalytic solvent-free run. In presence of solvents during catalytic runs the raw coal did not show any improvement over the thermal runs.

EXPERIMENTAL

The coal used was Wyodak subbituminous coal (DECS-8). This coal contains 32.4 % volatile matters, 29.3% fixed carbon, 9.9 % ash and 28.4 % moisture, on as-received basis; 75.8% C, 5.2% H, 1.0% N, 0.5% S and 17.5% O, on dmmf basis. The coal was dried under vacuum for 2 h at 100 °C. The drying of coal in air was done in an oven maintained at 100 and 150 °C with the door partially open. At 100 °C the coal was dried for 2, 20 and 100 hours and at 150 °C it was dried for 20 hours. The liquefaction was carried out at 350 °C for 30 minutes under 7 MPa (cold) H₂ in 25 ml tubing bomb. Ammonium tetrathiomolybdate (ATTM) was used as precursor for molybdenum sulfide catalyst. It was loaded on to coal by incipient wetness impregnation method from aqueous solution with 1 wt % Mo on dmmf basis. The impregnated coal samples were dried in a vacuum oven at 100 °C for 2 h. The experimental details about the liquefaction and the product work up is given elsewhere (5). The total conversion (TC) of the coal into soluble products have been calculated on the basis of the THF-insoluble residues. The analysis of the gases evolved during liquefactions at 350 °C show that the major components of the gases are CO and CO₂. The total yield of the hydrocarbon gases produced is less than 1wt % dmmf coal, in all the liquefaction runs.

RESULTS AND DISCUSSION

Solvent-free Liquefaction

The products distribution for the solvent-free thermal liquefactions are given in Table 1. As compared to the vacuum-drying the air-drying of coal at 100 °C for up to 100 h did not effect the total conversion on the basis of THF-insoluble residue. But the total gas yield increased with the drying time in air. This increase is mainly due to the increase in the CO and CO₂ yields (Table 3) at the expense of other products which is undesirable. The drying in air, oxidizes the coal, increasing the carboxylic and carbonyl functionalities which upon thermolysis produce CO₂ and CO gases. Upon excessive oxidation at 150 °C for 20 h the coal conversion slightly decreased but the gas yield increased considerably, which was accompanied by the decrease in the oil, asphaltene and preasphaltene yields. Since the main constituent of the gas is CO₂ which is associated with air-oxidation, it would be more appropriate to see the effect of drying on the desirable products. Figure 1 shows the distributions of the liquid and solid products in the

solvent-free thermal liquefaction experiments. It is clear that compared to the vacuum-drying, the air-drying of coal at 100 °C for up to 20 h increases the oil yield with no significant effect on the total conversion into THF-soluble products in thermal runs. But oxidative drying for the extended period of time decreases the total conversion as well as the oil yield because of the extensive degradation of the coal.

As with the vacuum-dried coal, the presence of catalyst in the solvent-free runs of the air-dried coal increases the total conversion compared to that of the thermal runs on the basis of THF-insoluble residues (Table 2). Similar to the thermal runs, in catalytic liquefactions the drying of coal in air at 100 °C for up to 100 h does not show any significant effect on the total conversion as compared to that of the vacuum-dried coal. The gas yields in the catalytic runs are lower than in the corresponding thermal runs with the most contribution from CO₂ and also increases with the drying time. If the conversion is calculated excluding the gas yield, the air-dried coal at 100 °C for up to 20 h does not show any effect but for the drying time of 100 h and at 150 °C for 20 h there is a considerable decrease in the conversion compared to that of the vacuum-dried coal (Figure 1). Over all, the increase in total conversion for the air-dried coal in catalytic runs over the thermal runs is similar to that for the vacuum-dried coal (Table 2 and Figure 1).

As-received coal (raw) was also subjected to thermal and catalytic liquefactions. The products distribution is given in Tables 1 and 2. Surprisingly, best values for the total conversions are obtained in the solvent-free thermal (25.0 wt%) and catalytic (43.3 wt%) runs on the basis of THF-insoluble residue compared to the vacuum- (12.5 and 29.8 wt%, respectively) and air-dried coal (14.8 and 29.2 wt%, respectively, for 2 h drying time). Significant increase in the oil yield is also observed from the raw coal compared to the dried coal. There is also a higher gas yield from the raw coal in thermal run compared to the vacuum- and air-dried coal at 100 °C for upto 20 h (Table 3). The increase in the gas yield is mainly due to the remarkable increase in the CO and CO₂ yields. The increase in the CO and CO₂ gases is due to the presence of water in the coal. It has been reported that the presence of water in the oxidized coal may enhance the removal of oxygen-containing groups (6). It appears that the presence of water during liquefaction removes the carbonyl functionalities from the coal network which makes the coal less refractory for liquefaction and hence improved conversion. The total-conversions excluding the gas yield shown in Figure 1, are the best in the case of the raw coal both in the solvent-free thermal and catalytic runs.

Liquefaction in Presence of Tetralin

It is known that the presence of a hydrogen donor solvent during liquefaction, enhances the total conversion of a coal to THF-soluble products as compared to the solvent-free runs. In the presence of tetralin during thermal runs the increase in total conversion of the vacuum-dried and air-dried coal is quite remarkable but, relatively, air-dried coal shows more increase in conversion (Table 1 and 2). The vacuum-dried coal shows an increase of 13.4 % (12.5% excluding gas yield) while the total conversion for the air-dried coal for 2 h at 100 °C increases by 20.3 % (19.9% excluding gas yield). The coal dried in air for 20 and 100 h at 100 °C also show a remarkable increase in conversion in the presence of tetralin but the increase is not as much as for the coal dried for 2 h. The oil yield for the air-dried coal for 2 h at 100 °C increases from 3.3 % to 11.7% with an increase of 8.4% in presence of tetralin, correspondingly, the increase in the oil yield for the vacuum-dried coal is only 2.0%. The oil yield for the coal dried at 100 °C in air for 20 h is also better than that of the vacuum-dried coal. The increase in the asphaltene and preasphaltene yields in presence of tetralin as compared to that of the solvent-free runs for the air-dried for 2 h and vacuum-dried coal are not significantly different. As the coal was dried in air for longer periods of time at 100 °C the increase in the oil production declined. The coal dried in air for 20 h at 150 °C showed only an increase of 1.5%. These results show that in thermal runs with tetralin the air-dried coal at 100 °C for up to 20 h gives better conversion and oil yield compared to the vacuum-dried coal (Figure 2). This suggests that the oxidation of a coal to some extent may enhance the oil yield and the total conversion but excessive oxidation of coal may have a negative effect.

The total conversion for the raw coal is 43.3% (37.5%, excluding gases) in thermal liquefaction in the presence of tetralin (Table 1). This conversion is undoubtedly better than the air-dried or vacuum-dried coal runs. Raw coal liquefaction gives an oil yield of 15.8% with an increase of 10.4% over the solvent-free run. Increasing the oil yields in liquefaction experiments is most desirable. Compared to the air-dried or vacuum-dried coal the oil yield is better in the case of raw coal run (Figure 2).

In the catalytic liquefactions also there is a remarkable increase in the total conversion from that of the solvent-free runs in presence of tetralin. This increase is similar to that in the thermal runs for the air-dried coal at 100 °C and vacuum-dried coal (Tables 1 and 2). In the catalytic runs in presence of tetralin the air-dried coal at 100

°C gives better total conversion compared to the vacuum-dried coal, on the basis of THF-insoluble or the total yields of oil, asphaltene and preasphaltene (Table 2 and Figure 2). It seems that the extent of drying at 100 °C also does not decrease the total conversion. Unexpectedly, the liquefaction of the raw coal in presence of tetralin does not show any significant catalytic improvement in total conversion (Figure 2). In the catalytic liquefaction in presence of tetralin of the raw coal the total conversion is 42.2% (39.4% excluding gas yield) and is 43.3% (37.5% excluding gas yield) in the thermal runs with tetralin. The products distribution of the raw coal experiments are also quite similar. As seen before in the thermal runs the raw coal showed a remarkably higher conversion in presence of tetralin, compared to the air-dried coal (Table 1). In the catalytic runs the raw coal and the air-dried coal showed a very similar conversions (Table 2 and Figure 2). It seems that during liquefaction of the raw coal in presence of tetralin the catalyst is less active. The decrease in the H₂-consumption by the raw coal during catalytic liquefaction in presence of tetralin from that in the solvent-free run is much higher than that for the dried coal (Figure 4).

Liquefaction in the Presence of 1-Methylnaphthalene

It has been seen before that the presence of a non-donor solvent such as 1-methylnaphthalene (1-MN) also enhances the total conversion to some extent compared to that of the solvent-free runs. In the thermal liquefaction of the vacuum-dried coal the total conversion increases from 12.5% in the solvent-free run to 18.3% with 1-MN (Table 1). The difference is significantly high. The liquefaction of the air-dried coal in presence of 1-MN also show a considerable increase as compared to that of the solvent-free runs. Total conversions for the coal dried at 100 °C for 2 and 20 h in air increases from 14.8 and 15.5% to 22.4 and 24.1% respectively, in presence of 1-MN. These conversion figures are better than that of the vacuum-dried coal (Table 1). Even after excluding the gas yields, the conversion is better if the coal was dried at 100 °C for up to 20 h in air. (Figure 3). Upon drying coal for 100 h at 100 °C in air the total conversion decreases and it is worse for the extensively oxidized coal at 150 °C for 20 h.

The total conversion of the raw coal in the thermal liquefaction increases from 25.0% (17.3% excluding gas) in solvent-free run to 39.9% (34.0%, excluding gas) with 1-MN (Table 1). This increase is significantly higher than that of the air- or vacuum-dried coal. In the thermal runs with 1-MN the raw coal gives 19.7% more THF-soluble products excluding gas yield, compared to the vacuum-dried coal, which is remarkably higher than that of the air-dried coal. The most importantly the increase in the total conversion of the raw coal is due to the significant increase in the yield of the most desirable product, oil. The oil yield increases from 1.1% in the vacuum-dried coal to 15.9% in the raw coal.

The catalytic liquefaction of vacuum- or air-dried coal in presence of 1-MN improves the conversion. The best conversion is obtained in the case of air-dried coal at 100 °C. The extent of drying at this temperature does not seem to make any considerable difference in the conversion (Table 2 and Figure 3). The catalytic liquefaction of the raw coal in presence of 1-MN gives a total conversion of 35.9% on the THF-insoluble residue basis. This conversion is rather lower than that of the thermal liquefaction under similar conditions. The unusual decrease in the oil yield for the raw coal in the catalytic run compared to that in the thermal run may be an artifact which needs to be reconfirmed. As in the presence of tetralin, the liquefaction of the raw coal in the presence of 1-MN in the catalytic runs there is no improvement in the total conversion compared to the thermal runs. In the catalytic liquefaction in presence of 1-MN the best conversion obtained is with the coal-dried in air at 100 °C with a significantly higher oil yields compared to the vacuum-dried coal.

Hydrogen Consumption

Figure 4 shows the H₂-consumption profile for the thermal and catalytic liquefactions from H₂-gas and from tetralin.. There is a significant decrease in the H₂-consumption during thermal liquefaction if the coal is pre-dried. In the solvent-free thermal run the H₂-consumption increases with the drying time in air at 100 °C and also the consumption increases as the coal is dried at 150 °C for 20 h. With tetralin and 1-MN there is an initial decrease in the H₂-consumption from 2 h to 20 h drying time and then it increases with the increased oxidative drying of coal. This suggests that the oxidative drying of coal increases the H₂-consumption during liquefaction and the consumption is higher if no solvent is used. In the catalytic runs the oxidative drying of coal at 100 °C for up to 100 h does not seem to have any significant effect on H₂-consumption. When the coal is dried at 150 °C for 20 h a slight decrease in the H₂-consumption in the solvent-free catalytic liquefaction is observed otherwise in presence of a solvent the H₂-consumption is essentially the same. These results suggest that the H₂-consumption increases with the extent of oxidation in thermal liquefaction and in catalytic liquefactions the oxidation does not make any considerable difference.

The vacuum-dried coal shows a similar H₂-consumption value as that of the coal dried in air for 2 h in thermal as well as catalytic runs. But during thermal liquefaction of the raw coal the H₂-consumption is higher than that of the vacuum- and air-dried coal for 2 h. In the catalytic liquefaction of the raw coal in presence of solvents the H₂-consumption is not much different from that of the vacuum- or air-dried coal for 2 h, but in the solvent-free catalytic run the H₂-consumption is remarkably higher. These results may account for the better conversions in the case of raw coal liquefaction compared to that of the vacuum- or air-dried coal.

Hydrogen-transfer from tetralin (Figure 4) increases (in the thermal liquefactions) with the extent of oxidation of coal. Vacuum-dried and the raw coal show a lower H-transfer compared to that of the air-dried coal. In the catalytic runs the H-transfer from tetralin is relatively lower than that in the corresponding thermal run and does not make any noticeable difference as the coal is dried at 100 °C in air up to 100 h. When the coal is dried at 150 °C for 20 h the H-transfer is slightly higher. The vacuum-dried coal shows a lowest value for the H-transfer from tetralin in the catalytic run.

CONCLUSIONS

The air-dried coal at 100 °C for up to 20 h gave similar conversions as the vacuum-dried coal in the solvent-free thermal and catalytic liquefactions. In the presence of solvents, better conversions were obtained from the coal dried in air at 100 °C for 2 h compared to the vacuum-dried coal. The extensive oxidation of coal decreased the coal conversions in thermal as well as catalytic runs. These results suggests that air-drying of coal to some extent may be beneficial for liquefaction. The raw coal gave the best conversions in the solvent-free runs. The improved conversion seems to be due to the presence of water, which enhances the removal of carbonyl functionalities during liquefaction making coal network less refractory for liquefaction.

ACKNOWLEDGEMENTS

This work was supported by the U.S. DOE Pittsburgh Energy Technology Center.

REFERENCES

1. Atherton, L.F.; Proc. 1985 Int. Conf. Coal Sci., p.553.
2. Neavel, R.; Fuel 1976, 55, 237.
3. Cronauer, D.C., Ruberto, R.G., Silver, R.S., Jenkins, R.G., Davis, A., and Hoover, D.S.; Fuel, 1984, 63, 77.
4. Vorres, K.S., Wertz, D.L., Malhotra, V., Dang, Y., Joseph, J.T., and Fisher, R.; Fuel, 1992, 71, 1047.
5. Saini, A.K., Song, C., Schobert, H.H., and Hatcher, P.G.; ACS Fuel Chem. Div. Prepr. 1992, 37(3), 1235.
6. Petit, J.C.; Fuel, 1991, 70,1053.

Table 1. Products distributions (dmmf wt %) for the thermal liquefactions of the raw and dried coal at 350 °C with different solvents.

Drying Conditions.	Gas*	Oil	Asphal.	Preasp.	Total Conv.
Solvent-free					
Raw-undried	7.7 (9.5)	5.4	2.8	9.1	25.0
Air-dried,2h,100°C	5.0 (6.3)	3.3	0.7	5.8	14.8
Air-dried,20h,100°C	5.7 (7.3)	6.0	0.6	3.2	15.5
Air-dried,100h,100°C	8.5 (12.0)	1.2	0.7	3.3	12.7
Air-dried,20h,150°C	9.8 (13.2)	0.6	0.2	0.4	10.9
Vac.-dried,2h,100°C	3.3 (5.9)	2.1	2.6	4.5	12.5
Tetralin					
Raw-undried	5.8 (7.7)	15.8	9.3	12.4	43.3
Air-dried,2h,100°C	5.4 (6.3)	11.7	7.4	10.6	35.1
Air-dried,20h,100°C	5.9 (8.7)	11.1	6.5	8.9	32.4
Air-dried,100h,100°C	8.7 (11.6)	6.1	6.3	9.7	30.8
Air-dried,20h,150°C	11.8(16.6)	2.1	2.8	3.2	19.9
Vac.-dried,2h,100°C	4.2 (5.4)	4.1	7.6	10.0	25.9
1-Methylnaphthalene					
Raw-undried	5.9 (8.4)	15.9	6.6	11.4	39.9
Air-dried,2h,100°C	5.1 (7.6)	4.2	4.0	9.4	22.7
Air-dried,20h,100°C	6.2 (7.5)	8.0	5.6	4.7	24.5
Air-dried,100h,100°C	9.0 (12.7)	1.7	4.1	6.3	21.1
Air-dried,20h,150°C	11.4(16.5)	1.8	2.2	2.5	18.0
Vac.-dried,2h,100°C	4.0 (5.7)	1.1	5.8	7.4	18.3

* The figures in parenthesis give the total gas yields calculated from GC analysis.

Table 2. Products distributions (dmmf wt %) for the catalytic liquefactions of the raw and dried coal at 350 °C with different solvents.

Drying Conditions.	Gas*	Oil	Asphal.	Preasp.	Total Conv.
Solvent-free					
Raw-undried	2.2 (4.3)	16.9	9.2	14.9	43.3
Air-dried,2h,100°C	3.3 (6.2)	12.6	3.2	10.1	29.2
Air-dried,20h,100°C	4.8 (6.8)	14.6	3.1	8.7	31.2
Air-dried,100h,100°C	7.6 (9.3)	13.3	2.4	5.1	28.4
Air-dried,20h,150°C	11.2(11.2)	5.1	0.5	1.7	18.5
Vac.-dried,2h,100°C	3.0 (2.9)	10.0	5.4	11.4	29.8
Solvent Tetralin					
Raw-undried	2.8 (4.9)	16.0	11.5	11.9	42.2
Air-dried,2h,100°C	3.9 (5.5)	15.7	11.1	14.9	45.6
Air-dried,20h,100°C	5.6 (7.4)	18.6	8.6	10.7	43.5
Air-dried,100h,100°C	6.7 (9.7)	16.5	10.8	11.0	45.0
Air-dried,20h,150°C	11.8(13.2)	9.6	2.3	5.7	29.4
Vac.-dried,2h,100°C	3.0 (2.9)	10.2	12.9	10.6	36.4
Solvent 1-MN					
Raw-undried	3.2 (5.0)	10.4	10.4	11.9	35.9
Air-dried,2h,100°C	3.0 (5.8)	10.3	8.1	16.0	37.4
Air-dried,20h,100°C	6.4(10.0)	14.1	8.7	10.5	39.7
Air-dried,100h,100°C	5.2(10.3)	14.4	8.7	11.1	39.4
Air-dried,20h,150°C	12.1(13.0)	5.3	2.8	4.3	24.5
Vac.-dried,2h,100°C	2.6 (3.7)	6.1	10.1	12.3	31.1

* The figures in parenthesis give the gas yields calculated from GC analysis.

Table 3. Gas yields (dmmf wt %) for the thermal and catalytic liquefactions.

Drying Conditions.	Thermal				Catalytic			
	CO	CO ₂	C ₁ -C ₄	Total	CO	CO ₂	C ₁ -C ₄	Total
Solvent-free								
Raw-Undried	0.37	8.90	0.25	9.52	0.24	3.52	0.35	4.26
Air-dried,2h,100°C	0.26	5.93	0.14	6.33	0.38	5.18	0.59	6.15
Air-dried,20h,100°C	0.39	6.70	0.16	7.25	0.42	5.67	0.71	6.79
Air-dried,100h,100°C	0.66	11.18	0.17	12.01	0.65	8.01	0.63	9.29
Air-dried,20h,150°C	0.80	12.32	0.09	13.21	0.94	9.76	0.54	11.24
Vac.-dried,2h,100°C	0.24	4.50	0.19	5.93	0.19	2.30	0.29	2.88
Tetralin								
Raw-Undried	0.11	7.41	0.19	7.72	0.14	4.45	0.35	4.94
Air-dried,2h,100°C	0.24	5.91	0.19	6.35	0.21	4.83	0.43	5.47
Air-dried,20h,100°C	0.28	7.18	0.28	8.74	0.17	6.86	0.36	7.39
Air-dried,100h,100°C	0.46	10.95	0.22	11.63	0.36	8.80	0.51	9.67
Air-dried,20h,150°C	0.59	15.87	0.11	16.58	0.41	12.43	0.38	13.20
Vac.-dried,2h,100°C	0.19	4.10	0.15	5.44	0.13	2.58	0.28	2.99
1-Methylnaphthalene								
Raw-Undried	0.14	7.02	0.18	8.45	0.14	4.48	0.34	4.96
Air-dried,2h,100°C	0.25	6.18	0.15	7.59	0.19	5.23	0.37	5.79
Air-dried,20h,100°C	0.28	7.04	0.15	7.48	0.18	9.26	0.51	9.95
Air-dried,100h,100°C	0.50	11.95	0.21	12.67	0.32	9.50	0.44	10.26
Air-dried,20h,150°C	0.65	15.69	0.12	16.47	0.33	12.36	0.32	13.01
Vac.-dried,2h,100°C	0.16	4.34	0.16	5.66	0.11	3.37	0.25	3.73

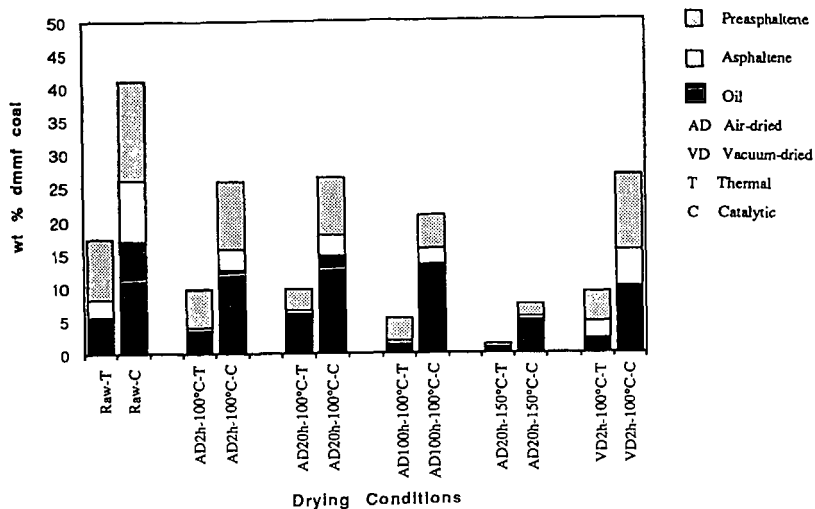


Figure 1. Products distribution from solvent-free thermal and catalytic liquefactions at 350 °C of the raw and coal dried in different conditions.

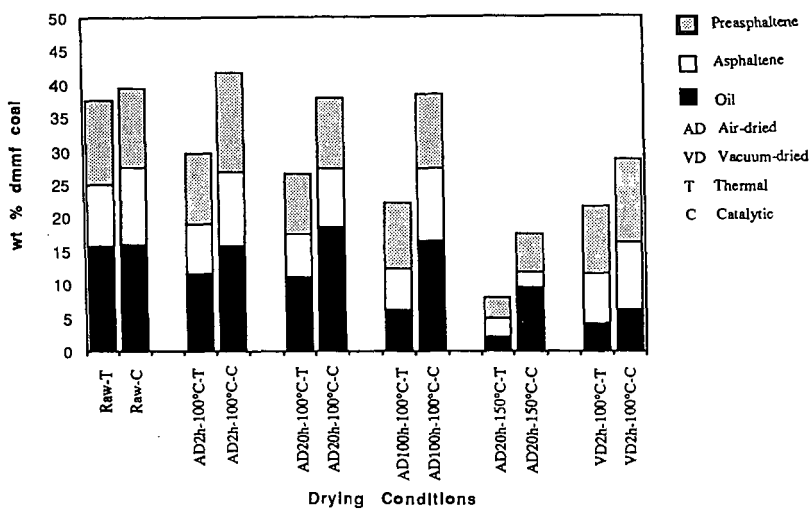


Figure 2. Products distribution from the thermal and catalytic liquefactions in the presence of tetralin at 350 °C of the raw and coal dried in different conditions.

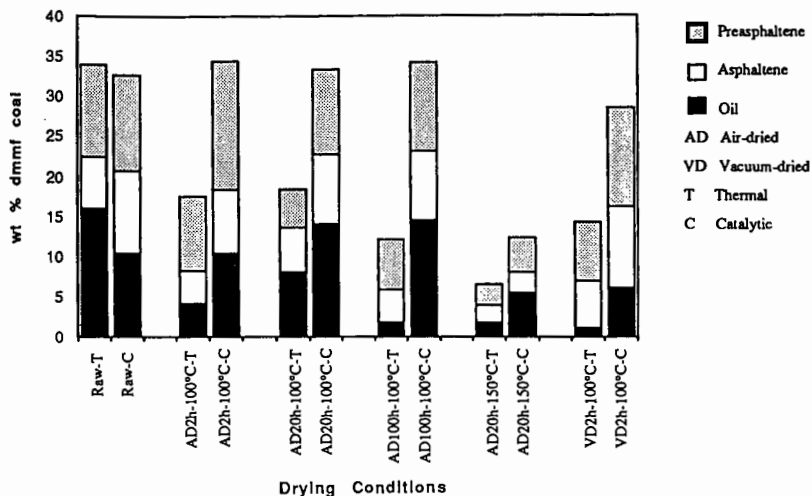


Figure 3. Products distribution from the thermal and catalytic liquefactions in the presence of 1-methylnaphthalene at 350 °C of the raw and coal dried in different conditions.

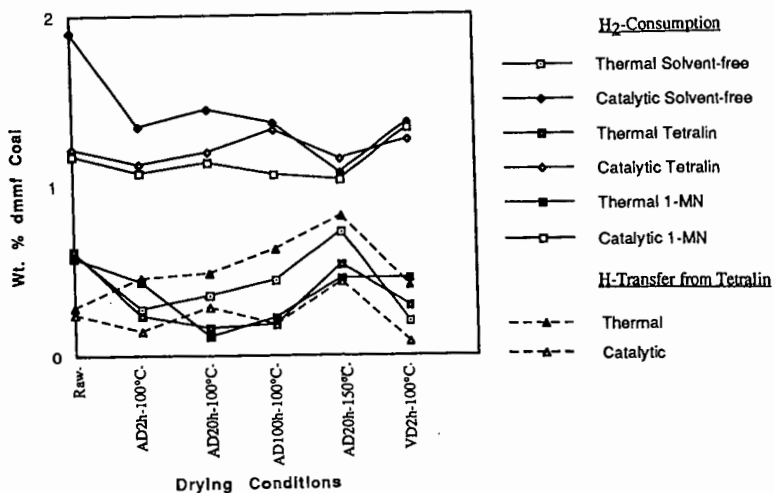


Figure 4. Hydrogen consumption profiles during thermal and catalytic liquefactions from H₂ and tetralin.

Influence of Drying and Oxidation of Coal on Its Catalytic and Thermal Liquefaction. 2. Characterization of Dried and Oxidized Coal and Residues.

Ajay K. Saini, Chunshan Song and Harold H. Schobert

Department of Material Science and Engineering, 209 Academic Projects Building, Fuel Science Program, The Pennsylvania State University, University Park, PA 16802.

Keywords: Drying, Oxidation, Structural characterization.

INTRODUCTION

Because of the high moisture content of the low rank coals it is desirable to dry coal before liquefaction. It has been recognized that drying of coal could adversely affect the reactivity of subbituminous coal for liquefaction (1,2). This study has been carried out with a view to understand the effect of low temperature oxidative and non-oxidative drying on coal structure and liquefaction residues. In the preceding paper the impacts of coal drying on the liquefaction have been discussed (3).

Several papers have been devoted to understanding the oxidation of coal (4-10) but very little has been reported on the effect of oxidation on the structures of liquefaction residues which could lead to an insight of the oxidative effect on liquefaction. In the present work we have analyzed the residues from thermal as well as catalytic liquefactions of the raw and dried coal under vacuum and in air. The analysis of the residues reveal that although there is a significant decrease in the aliphatics upon oxidative drying of coal compared to the vacuum dried coal the residues from the air-dried coal are more aliphatic rich, and as the oxidation proceeds more longer-chain aliphatics are lost during liquefaction. The raw coal shows an enhanced loss of carbonyls during liquefaction, which may be the cause of its higher conversion.

EXPERIMENTAL

The coal used was Wyodak subbituminous obtained from the Penn State Sample Bank (DECS-8). The characteristics of coal are given elsewhere (11). For the raw coal liquefaction it was used as received. For the drying experiments the coal was dried under vacuum at 100 °C for 2 h and in air at 100 °C for 2, 20 and 100 h. At 150 °C coal was dried for 20 h. The air-drying of coal was done in a preheated oven at desired temperature with the door slightly open to ensure the sufficient air supply. The thermal and catalytic liquefactions of coal were carried out at 350 °C under 6.9 MPa (cold) H₂ pressure for 30 minutes. Ammonium tetrathiomolybdate (ATTM) was used as catalyst. It was loaded on to coal by incipient wetness impregnation method from aqueous solution, with 1 wt % Mo on dmmf coal. After the reaction, the liquid and solid products were separated by sequential extraction with hexane, toluene and THF. After the extraction the THF-insoluble residues were washed first with acetone and then pentane in order to remove all the THF, followed by drying at 110 °C for 6 h under vacuum. The coal and residues were analyzed by Py-GC-MS, solid state CPMAS ¹³C NMR and FTIR techniques discribed elsewhere (12, 13).

RESULTS AND DISCUSSION

Characterization of the Raw and Dried Coal

CPMAS ¹³C NMR

Figure 1 compares between the CPMAS ¹³C NMR spectra of the raw coal and the vacuum and air-dried coal. The raw coal and the dried coal show similar NMR features. The region between 0-80 ppm consists of aliphatic carbons which may include methoxy carbons and the second region between 90 to 170 ppm is due to the aromatic carbons including two shoulders due to catechol-like and phenolic carbons (11). The carboxylic band appears at 170-190 ppm and carbonyl group between 190-230 ppm. Upon drying coal under vacuum there was no noticeable difference in the NMR spectrum as compared to that of the raw coal. When the coal was dried in air a slight difference seems to be apparent but not very significant until the coal was dried at 100 °C for 100 h or at 150 °C for 20 h. It appears that as the coal was dried under oxidative conditions there was a decrease in the intensity of the catechol shoulder. The other change seems to be the broadening in the carboxyl and carbonyl bands. These changes in the coal structure becomes apparent when the coal was dried in air under severe conditions. After drying coal at 150 °C for 20 h the CPMAS ¹³C NMR shows a complete disappearance of the catechol peak and the

carboxyl and carbonyl peaks also show significant broadening, seems to be merging into the aromatic band. The oxidation of coal significantly decreases the aliphatics from the coal. From NMR the decrease in aliphatics is not apparent when coal is dried at 100 °C, but after drying at 150 °C the aliphatic band shows a significant decrease.

FTIR

Obvious difference in the FTIR spectrum of the dried coal compared to that of the raw coal is the decrease in the broad water band between 3000-3600 cm^{-1} which is apparent from the direct comparison of the spectra. The drying of coal in air is known to oxidize the coal causing increase in the ketone, carboxyl and ester type functionalities and decrease in the aliphatic groups. Such changes in the functionalities of the coal upon oxidation at 100 °C were not apparent from direct comparison of the spectra. The difference FTIR technique was utilized to detect the minute spectroscopic changes in the coal structure. Vacuum-dried coal was used as a reference for the difference spectra. The differences in coal structure arising due to oxidative drying of coal apparent from the difference FTIR spectra are consistent with the literature (4-10). The difference spectra show a prominent peak at 1720 cm^{-1} due to carbonyl which increases in intensity with the severity of drying. There is another shoulder on the high energy side of the 1720 cm^{-1} band near 1770 cm^{-1} which also increases with the severity of drying. This band could be assigned to the ester groups. The band at 1640 cm^{-1} in the difference spectra can be assigned to the highly conjugated carbonyls formed by the oxidation of the methylene bridges linking aromatic units (Ar-CH₂-Ar) which are highly susceptible to autooxidation forming Ar-CO-Ar groups. As the oxidative drying at 100 °C proceeds the band at 1720 cm^{-1} due to carboxyl carbonyls seem to be increasing at a faster rate than 1640 cm^{-1} band. This band may also contain carbonyls in unconjugated ketones. After drying coal at 150 °C for 20 h in air the 1720 cm^{-1} band becomes more intense relative to the 1640 cm^{-1} band. A broad band between 1500 and 1590 cm^{-1} also becomes apparent in the difference spectra of the dried coal. This band is assigned to the carboxylate (COO⁻) groups which increase upon oxidative drying of coal. After drying coal at 150 °C the broad band at 1550 cm^{-1} in the difference spectrum due to the carboxylate carbonyls (-COO⁻) which is just a broad shoulder in the case when coal was dried at 100 °C, becomes an independent peak. The increase in the intensity of the 1550 cm^{-1} band could be related to the increase in the carboxylic functional groups upon oxidation followed by exchange with cations present in the coal to give COO. The region between the range 1000 and 1300 cm^{-1} consists of the bands due to C-O type of linkages in ethers, esters and phenols. Upon oxidative drying at 100 °C there is a slight increase in the intensity of the ether region.

Pyrolysis-GC-MS

The major aromatic components of wyodak subbituminous coal obtained upon pyrolysis have been reported previously (3). Low rank coals are known to have higher oxygen functionalities. The major oxygen compounds are phenol, methylphenol, ethylphenol, C₂-phenols and catechol and these are the most abundant components in the pyrogram of the raw coal. Among the alkylbenzenes the most abundant compounds identified are toluene, xylenes and C₃-benzenes. The other aromatic compounds such as naphthalene and alkyl-naphthalenes are also found but in a very low concentrations. There are many other peaks appearing over the whole pyrogram of the raw coal. These peaks have been identified as alkanes and alkenes ranging from C₄-C₃₁. The most abundant of these are C₄-C₆ alkanes and alkenes which appear in the early part of the pyrogram and are not very well resolved.

Upon drying coal under vacuum or in air the pyrogram is similar to that of the raw coal from which one can find identical peaks. The only difference is in the relative intensities of the peaks. Table 1 shows the ratios between the total area of the major phenolic and the alkylbenzene compounds in the pyrograms of the raw and the dried coal samples. The vacuum drying of coal did not change the phenolics to alkylbenzene ratio but oxidative drying of coal seems to have a significant effect on these ratios. For first two hours of drying coal in air at 100 °C the change is not very significant but as the extent of drying increases the ratio seems to be decreasing as if the phenolic structures are being consumed from the coal as the air-drying proceeds. After drying coal at 150 °C for 20 h the phenolic to alkylbenzene ratio decreases remarkably.

Using the selective ion chromatogram (SIC) technique for the 71 m/z ion the pattern of the abundances of the alkanes and alkenes can be recognized in the pyrogram of the coal. The SIC for the raw and the vacuum-dried coal using 71 m/z ion show a similar pattern. The most abundant are the C₄-C₆ alkanes and alkenes. Upon air-drying, coal shows a decrease in the intensities of the short chain aliphatic compounds. The extent of air-drying did not change overall pattern of the aliphatics, the SIC of aliphatics for all the air-dried samples looked similar.

Characterization of the Liquefaction Residues

FTIR

To investigate the differences in the structure of the residues from the raw and air-dried coal and to understand the liquefaction behavior of the coal dried under different conditions, the residues from the vacuum dried coal were used as reference for the FTIR difference spectra. The vacuum dried coal residues were subtracted from that of the raw and the air-dried coal. The subtraction factors were calculated on the basis of the amount of organic matters left in the residues after liquefactions and calculated by the ratio of the amount of dmmf coal per mg of the pellet keeping the diameter of the pellet constant. Before discussing the differences in coal structure using difference technique, it should be noted that the frequencies of the bands in the difference spectra are not well defined and also the apparent frequencies of different bands can often be affected by the degree of subtraction and residual band overlap (8).

The difference spectra of the residues from the thermal runs show a significant differences in the coal structure as a consequence of air-drying (Figure 2). The major differences are in the carbonyl region (1500-1800 cm^{-1}). The raw coal shows a negative band at 1740 cm^{-1} which could be assigned to the ester and ketone groups. This band is negative, also in the case when tetralin or 1-methylnaphthalene was used as solvent suggesting that during liquefaction the raw coal losses more of carbonyl structures compared to the vacuum-dried coal. The enhanced loss of carbonyls from the raw coal can also be accounted by the relative increase in the CO_2 and CO gas yields compared to the vacuum-dried coal. The residues from the air-dried coal also show a significantly higher loss of ester groups as indicated by the negative dip in the ester region of the difference spectra. But, there is also a positive band at 1700 cm^{-1} which could be assigned to the carboxylic groups. The carboxylic band increases with the extent of oxidation. The increase in the carboxylic functionalities in the residues could also be noticed by the broad band centered at 1590 cm^{-1} . This band is assigned to the carboxylate (COO^-) groups. The increase in these functionalities is the consequence of increase in the carboxylic groups upon oxidation of coal. This band may also have slight contribution from the aromatic $\text{C}=\text{C}$ stretching which appears at 1610 cm^{-1} .

In the aliphatic region between 2700-2950 cm^{-1} the raw coal shows no significant change in the band (Figure 2). But, relative to the vacuum-dried coal the residues from the air-dried coal show a significantly higher aliphatic content shown by the positive aliphatic bands. This is only true when coal was dried in air at 100 °C but for the coal dried at 150 °C for 20 h the aliphatic region shows a negative change. The increase in the aliphatics in the residues from air-drying at 100 °C is interesting because the unreacted air-dried coal show a decrease in the aliphatics because of the oxidation of some of the aliphatic groups. It appears that during liquefaction, the air-dried coal at 100 °C has retained more of the aliphatic components of the network as compared to that of the vacuum-dried coal. The negative aliphatic band in the case of the coal dried at 150 °C could be due to the extensive loss of these groups initially during air-drying. In the presence of tetralin or 1-MN also the air-dried coal showed an increase in the aliphatics.

Same criteria was adopted, as for the thermal runs, to obtain the FTIR difference spectra for the residues from the catalytic runs. Compared to the thermal runs, the difference spectra for the catalytic runs did not show any significant differences. Similar to the thermal runs, the residues from the air-dried coal at 100 °C were found to be more aliphatic and carbonyl rich compared to the vacuum dried coal. The residues from the tetralin and 1-MN runs also showed similar difference spectra except that the raw coal seemed to be aliphatic richer in the catalytic runs.

More significant differences in the thermal and catalytic runs were observed when the difference spectra were obtained between the residues from thermal and catalytic runs (Figure 3). The FTIR spectra of the catalytic runs were subtracted from that of the thermal runs. The negative mineral matter bands (1010 and 1035 cm^{-1}) in the difference spectra of the thermal and catalytic runs are the signs for more conversion of coal during catalytic runs. In the case of the raw coal the mineral matter bands are negative only in the solvent free runs may be because in the presence of solvents the raw coal did not show any significant difference in conversions between thermal and catalytic runs. The negative aliphatic bands in the difference spectra of the solvent-free runs clearly showed that during thermal runs more aliphatic compounds were lost in all the cases except when coal was oxidized at 150 °C. The differences in the aliphatic contents in the solvent runs were not very clear probably due to the differences in the adduction of solvents during liquefaction. In the carbonyl region positive bands near 1700 and 1550 cm^{-1} were observed in the solvent-free as well as solvent runs. The first band could be due to ketone and carboxylic groups and the second band could be assigned to the carboxylate ions. It suggests that the residues from the thermal runs are

richer in such functionalities. The ether region between 1100-1300 cm^{-1} also showed significantly intense positive bands which clearly suggests that more of ether type bonds are broken during catalytic liquefaction compared to that of the thermal runs. At the high oxidation level the ether region did not show any noticeable difference in the ether contents of the thermal and catalytic residues. The most significant difference was observed in the coal dried at 100 °C.

Pyrolysis-GC-MS

Compared to the raw coal the residues from the thermal solvent-free liquefactions show similar pyrolysis compounds, that is one can identify the same compounds in the raw coal as well as in residues. The differences in the pyrograms appear to be in the relative abundances of the compounds. Table 1 gives the ratios between phenolic and alkylbenzene compounds. For these ratios same compounds have been used as for the raw coal mentioned above. These ratios indicate the variations in the chemical composition of the aromatic compounds in the coal network as a consequence of different treatments to coal. After solvent-free thermal liquefaction of the raw coal the phenolic to alkylbenzene ratio decreases remarkably compared to that of the unreacted coal. Similar decrease is observed for the air-dried coal at 100 °C for 2 h and the vacuum-dried coal. For the coal dried at 100 °C for 20 and 100 h and dried at 150 °C there is no significant change in this ratio. From the catalytic solvent-free liquefaction the phenolic to alkylbenzene ratios of the residues are slightly higher than that of the corresponding residue from the thermal run but it is still lower than that of the unreacted coal. It appears that as the oxidative drying proceeds the difference in the phenolic to alkylbenzene ratio between the unreacted coal and the liquefaction residue decreases. Eventually at extensive oxidation of coal this ratio becomes same for the unreacted coal and its liquefaction residue.

Figure 4 compares of the pattern of the aliphatics present in the pyrogram of the residues from solvent-free thermal runs. Noticeable differences can be seen in the relative intensities of the aliphatics compared to that of the corresponding unreacted coal. In the residues from the raw and vacuum dried coal there is an appreciable decrease in the intensities of the shorter chain relative to the longer chain aliphatics, which has been noticed before with different coals too. For the air-dried unreacted coal, as mentioned before the pattern of the aliphatics in the pyrogram remains similar with the extent of drying, but for the residues the pattern is quite different. By comparing the residues from the air-dried coal at different extent of oxidation it appears that as the extent of oxidation increases more and more of longer chain aliphatics are lost during thermal liquefaction (Figure 4). It seems that for the air-dried coal the shorter chain aliphatics are strongly retained upon liquefaction. This phenomena was not observed for the catalytic runs.

All the pyrolysis compounds found in the pyrogram of the raw coal can also be identified in the pyrogram of the residues from the liquefactions in presence of solvents. Besides, there are several new bands which are known to have come from the addition of solvent used during liquefaction (11). Some of these compounds are in most abundances. From the liquefaction runs in presence of tetralin the peaks due to the solvent are tetralin, dihydronaphthalene, naphthalene and 1 and 2-methylnaphthalenes. C2-naphthalenes may also be due to tetralin but are in a very low abundances. From the runs with 1-methylnaphthalene two solvent adduction bands are observed, naphthalene and 1-methylnaphthalene. In our previous work (11) we reported that the adduction of solvents could be either due to the formation of chemical bond between the solvent molecules and coal network or the solvent molecules could be physically entrapped in the micropores. From Figure 5 the adduction of solvent is apparent by the presence of tetralin, dihydronaphthalene, naphthalene and 1 and 2-methylnaphthalene peaks. It is clear that the extent of adduction of the solvents is remarkably effected by the extent of initial oxidation of the coal. Apparently, as the oxidation proceeds the relative intensities of the adducted compounds increases. Similar trend was observed in the case when 1-MN was used as solvent. The residues from the catalytic runs also show a similar trends in the adduction of solvents with the drying of coal but during catalytic runs the adduction seems to be lower as compared to the thermal run.

Not much difference is observed between the pyrograms qualitatively in Figure 5. All the pyrograms for the raw and dried coal under different conditions have the same compounds but there relative intensities are significantly different. Table 1 gives the phenolic to alkylbenzene ratios. These ratios have increased significantly for residues from the raw coal and for the coal dried in air at 100 °C for 2 h and under vacuum, compared to that of the solvent-free runs. But, for the 1-MN runs these ratios seems to be similar to that of the thermal runs. It seems that during solvent-free runs or in the presence of 1-MN more phenolic type units which produce phenolic compounds upon pyrolysis are lost. This phenomena seems to be true for raw, vacuum-dried coal and for the coal dried in air at 100 °C for 2 h. At the higher oxidative drying of coal the change in the ratios of the phenolic to alkylbenzene is not significant.

CONCLUSIONS

The characterization of the liquefaction residues reveal that the residues from the air-dried coal are more aliphatic and carbonyl rich compared to the vacuum-dried coal. The increase in the carbonyls is due to the oxidation of the coal upon air-drying. It appears that upon oxidation of coal at 100 °C more shorter chain aliphatics are retained in the coal network as compared to the vacuum-dried coal. The enhanced conversion of the unoxidized raw coal may be due to the enhanced loss of carbonyls upon reacting with water. The enhanced loss of carbonyls with water can make coal less refractory for liquefaction. The Py-GC-MS analysis of the residues suggests that the extent of oxidation can enhance the solvent adduction during liquefaction.

ACKNOWLEDGEMENTS

This work has been supported by the U.S. Department of Energy, Pittsburgh Energy Technology Center. We wish to thank Dr. P. G. Hatcher, Mr. K. Wenzel and Mr. L. Hou for their instrumental support with Py-GC-MS and CPMAS ¹³C NMR instruments and Dr. M. Sobkowiak for her help with FTIR instrument.

REFERENCES

1. Cronauer, D.C., Ruberto, R.G., Silver, R.S., Jenkins, R.G., Davis, A., and Hoover, D.S.; *Fuel*, 1984, 63, 71-77.
2. Atherton, L.F.; *Proc. 1985 Int. Conf. Coal Sci.*, p.553.
3. Saini, A.K., Song, C., and Schobert, H.H.; *ACS Fuel Chem. Prepr.*, 1993, Preceding Paper.
4. Cronauer, D.C., Ruberto, R.G., Jenkins, R.G., Davis, A., Painter, P.C., Hoover, D.S.; Starsinic, M.E., and Schlyer, D.; *Fuel*, 1983, 62, 1124-1132.
5. Calemma, V., Iwanski, P., Rausa, R., and Girardi, E.; *ACS Fuel Chem. Prepr.* 1992, 730.
6. Calemma, V., Rausa, R., Margarit, R., and Girardi, E.; *Fuel*, 1988, 67, 764.
7. Clemens, A.H., Matheson, T.W., and Rogers, D.; *Fuel*, 1991, 70, 215.
8. Rhoads, C.A., Senftle, J.T., Coleman, M.M., Davis, A., and Painter, P.C.; *Fuel*, 1983, 62, 1387.
9. Painter, P.C., Snyder, R.W., Pearson, D.E., and Kwong, J.; *Fuel*, 1980, 59, 283.
10. Chamberlain, E.A.C., Barrass, G., and Thirlaway, J.T.; *Fuel*, 1976, 55, 217.
11. Saini, A.K., Song, C., Schobert, H.H., and Hatcher, P.G.; *ACS Fuel Chem. Prepr.*, 1992, 37(3), 1235.
12. Sokowiak, M. and Painter, P.; *Fuel*, 1992, 71, 1105.
13. Song, C., Schobert, H.H. and Hatcher, P.G.; *ACS Fuel Chem. Prepr.*, 1992, 37(2), 638-645; *Energy & Fuels*, 1992, 6, 326-328.

Table 1. Ratios of the amounts of the phenolic compounds to the alkylbenzenes.

Drying Conditions	Unreacted Coal	Residues	
		Thermal	Catalytic
Solvent-Free			
Raw			
Air-dried, 2h, 100	3.8	1.9	2.8
Air-dried, 20h, 100°C	3.5	2.0	2.8
Air-dried, 20h, 100°C	2.5	2.4	2.6
Air-dried, 100h, 100°C	2.3	2.0	2.2
Air-dried, 20h, 150°C	1.1	1.2	1.6
Vacuum-dried	3.6	2.2	2.4
Tetralin			
Raw		2.5	2.9
Air-dried, 2h, 100		3.3	3.7
Air-dried, 20h, 100°C		2.8	3.3
Air-dried, 100h, 100°C		2.2	2.6
Air-dried, 20h, 150°C		1.4	1.5
Vacuum-dried		3.1	3.1
1-Methylnaphthalene			
Raw		2.2	2.0
Air-dried, 2h, 100		2.4	2.7
Air-dried, 20h, 100°C		2.4	2.8
Air-dried, 100h, 100°C		1.5	2.3
Air-dried, 20h, 150°C		1.3	1.1
Vacuum-dried		1.8	2.3

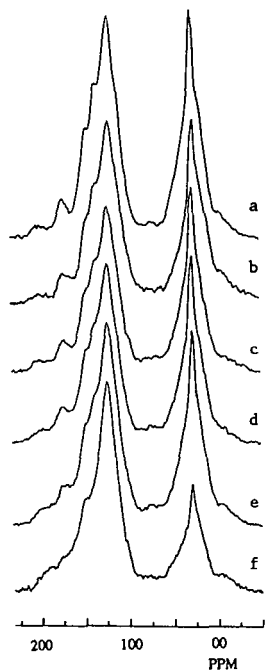


Figure 1. CPMAS ^{13}C NMR spectra of the coal a) raw, b) vacuum-dried at 100°C , dried in air at 100°C for c) 2 h, d) 20 h, e) 100 h, and f) dried at 150°C for 20 h.

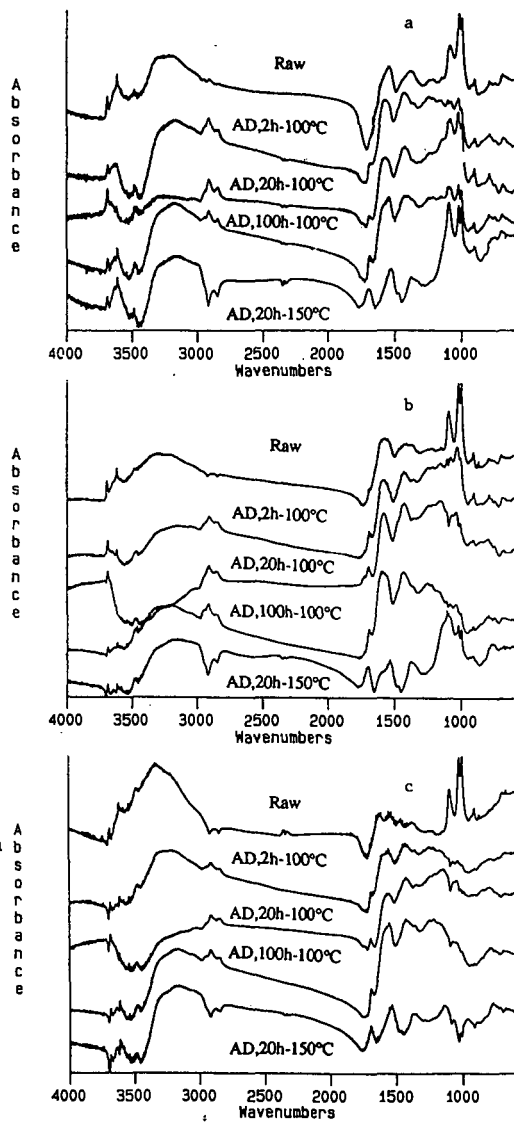


Figure 2. FTIR difference spectra for the residues from thermal liquefactions in a) solvent-free, b) tetralin, and c) 1-methylnaphthalene runs for the raw and air-dried (AD) coal.

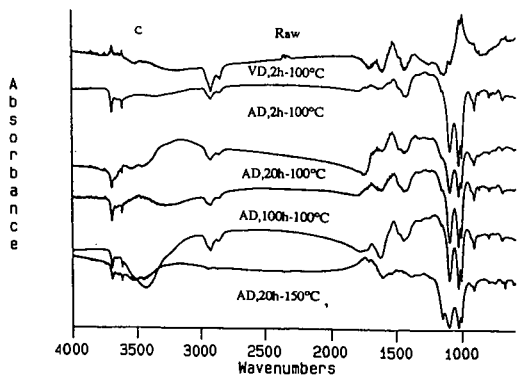
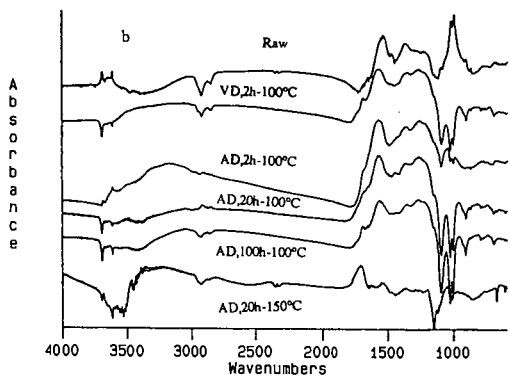
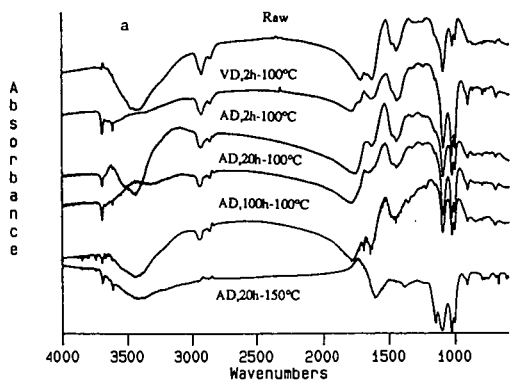


Figure 3. FTIR difference spectra between the residues from the thermal and catalytic a) solvent-free, b) tetralin and 1-methylnaphthalene runs for the raw, vacuum-dried (VD) and air-dried (AD) coal.

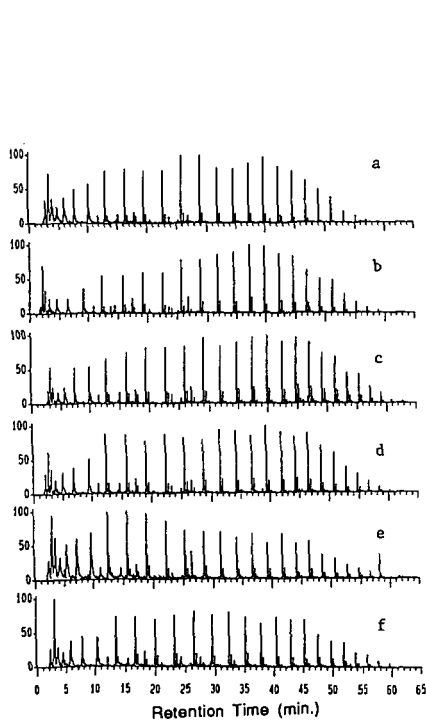


Figure 4. Selective ion monitoring of paraffins at m/z 71 from Py-GC-MS profiles of residues from thermal liquefactions of the coal a) raw, b) vacuum-dried at 100°C , dried in air at 100°C for c) 2 h, d) 20 h, e) 100 h, and f) dried at 150°C for 20 h.

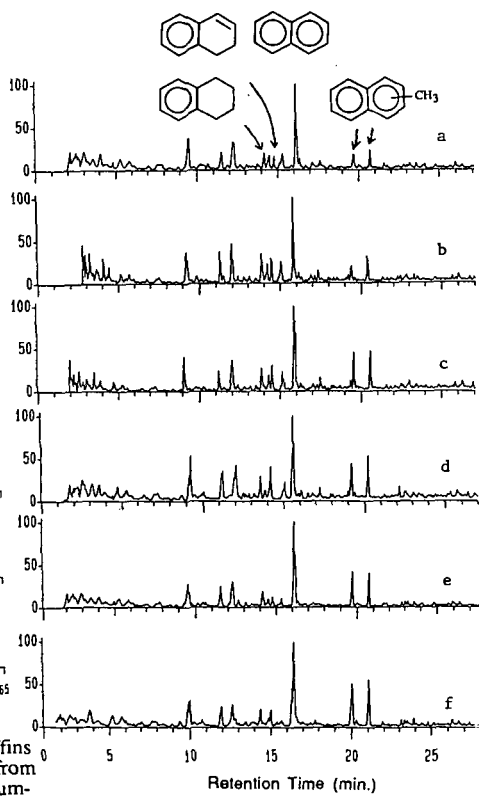


Figure 5. Py-GC-MS profiles of the residues from the thermal liquefactions in presence of tetralin of the coal a) raw, b) vacuum-dried at 100°C , dried in air at 100°C for c) 2 h, d) 20 h, e) 100 h, and f) dried at 150°C for 20 h.

An NMR Investigation of the Effects of Different Drying Methods on Coal Structure.

Francis P. Miknis, Daniel A. Netzel and Thomas F. Turner,
Western Research Institute, Box 3395, Laramie, WY 82071-3395

Keywords: Microwave and chemical drying, solid-state NMR, subbituminous coals

INTRODUCTION

One area for improvement in the economics of coal liquefaction is coal drying. This is particularly true for subbituminous coal and lignites of which the US reserves are huge. These coals contain significant amounts of water so that simply drying these materials before transportation to their final destination can represent a sizable reduction in cost. There is considerable evidence to show that drying has a detrimental effect on the liquefaction behavior of coals (1,2,3). As coals have both a physical and chemical structure, it is conceivable that drying affects one, the other, or both of these structures.

There do not appear to have been any systematic studies of different methods of coal drying on coal structure, and the role that water plays in enhancing, or lessening coal reactivity toward liquefaction. The overall objectives of this work are to investigate the effects of different drying methods on the liquefaction behavior of coal. Different methods for coal drying are being investigated to determine if drying can be accomplished without destroying coal reactivity toward liquefaction, thereby making coal drying a relatively economical and efficient method for coal pretreatment. Coal drying methods include conventional thermal and microwave drying at elevated temperatures, and chemical drying at low temperature. Solid-state nuclear magnetic resonance (NMR) techniques of cross polarization with magic-angle spinning (CP/MAS) are employed to measure changes in coal structure brought about by the different methods of drying and by low temperature oxidation. The initial work on the project has focused on development of standardized procedures for thermal, microwave, and chemical methods of coal drying. Results of this aspect of the project are reported in this paper.

EXPERIMENTAL

Coal Preparation

In order to study the effects of different methods for drying coal on moisture removal, a master batch sample (~500 g) of Eagle Butte subbituminous coal from the Powder River Basin, Wyoming was prepared by grinding and screening to -20, +100 mesh particle size. This sample was placed in a wide mouth jar and allowed to equilibrate in an oven with a beaker of water at 40°C for 24 hrs. The sample was then removed from the oven and placed in a humidifier until aliquots were taken for the different drying tests. The moisture values for all the coal drying tests were determined from the weight loss at 105°C for 24 hrs. The

moisture values for 2-gram aliquots from the master batch of Eagle Butte coal were 18-20% using this method.

Thermal Drying

Samples of the Eagle Butte subbituminous coal were heated to different final temperatures in order to determine at what temperature, significant structural changes begin to occur that might affect the liquefaction behavior. These heating experiments are referred to as ballistic heating experiments. The ballistic heating experiments were performed with a small, vertically aligned furnace. The furnace has a 12-centimeter long heated section which accepts a 1.4-centimeter i.d. quartz liner. A stainless steel screen provides support for the coal and a steel wool pack heats the nitrogen sweep gas which is introduced at the bottom of the quartz liner. In a typical experiment, the furnace is preheated to about 10°C above the desired final coal temperature. A 2-gram coal sample is then poured into the quartz liner and a thermocouple is inserted into the coal sample bed. When this thermocouple reaches the desired temperature, the quartz liner is removed from the furnace and allowed to cool. Nitrogen flow is maintained at all times. When the sample temperature is below 60°C the coal is poured into a sample vial, capped with nitrogen, and sealed. Heatup times with this system are typically from 15 to 20 minutes.

Microwave Drying

A number of microwave drying experiments were conducted using Eagle Butte subbituminous coal. The experiments were conducted using a CEM model MDS 81-D laboratory microwave oven that is equipped with facilities to introduce different gaseous environments, or using a commercially available microwave oven. Microwave drying tests were conducted in the following manner: ~ 2 grams of coal were placed in 25 mL beakers, and the beakers placed at the center of the microwave oven. Samples were exposed to microwave radiation for different periods of time and at different power levels, after which the samples were removed from the oven and a thermocouple inserted into the coal bed to determine an average temperature.

Chemical Drying

Chemical drying experiments were conducted on the Eagle Butte subbituminous coal, and also a Usibelli subbituminous coal from Alaska using 2,2-dimethoxypropane as a drying agent. One-half gram of coal was weighed into a 10 mL centrifuge tube followed by 2 mL of 0.2 N $\text{CH}_3\text{SO}_3\text{H}$ in CH_3OH and 1 mL of the reference standard cycloheptane. Four mL of dimethoxypropane were then added to the mixture. The total mixture was stirred, then centrifuged for 10 minutes. After 2, 4, 6, and 8 hours, one-half mL aliquots were removed, diluted with one-half mL CDCl_3 , and the ^1H NMR spectrum recorded. The solution was stirred and centrifuged prior to removing the aliquots.

A ^1H NMR method was developed to rapidly measure the amount of water in coal. The ^1H NMR spectra of the reaction products, methanol and acetone, give single resonances for the methyl groups, which are easily identified. These resonances do not overlap the hydrogen NMR resonances of DMP. Integration of the methyl resonances from acetone is used to measure directly the moles of water reacted. The average relative error using the ^1H NMR method is < 3% for standard solutions with a known amount of water. A curve-fitting routine

for determining the area of the peaks increases the precision and accuracy of the NMR method by eliminating instrumental and other artifacts which contribute to the peak shape.

RESULTS AND DISCUSSION

Thermal Drying

Samples of the Eagle Butte coal were ballistically heated to final temperatures of 100, 150, 200, and 250 °C. Solid-state ^{13}C NMR measurements were made on the heated samples, and are shown in Figure 1 for the starting coal, and coal heated to 150, and 250 °C. The spectra indicate that under this method of heating, there are no significant changes in carbon functionality up to temperatures of 250 °C, except for some deterioration in resolution of branched aromatic carbons (~140 ppm), phenolic carbons (~155 ppm), and carboxyl carbons (~180 ppm).

Microwave Drying

Microwave drying is an alternative thermal method of drying coals. However, the mechanism of drying with microwaves is different from that of simply heating the coal. In order for a substance to absorb microwaves and become heated, it must have a permanent dipole moment. Therefore, the functional groups that are the most efficient absorbers of microwaves are those that are highly polar, such as the -OH group in water.

When a substance containing water molecules is exposed to microwaves of the proper frequency (2,450 MHz) the water molecules attempt to align and realign with the alternating electric field of the microwaves. This causes friction at the molecular level, which becomes manifested as heat. Because the water in coals can be distributed on the surface, in pores, or as part of the coal structure as in a gel, depending on rank, microwaves might be used to provide some selectivity for coal drying without appreciably affecting the overall coal structure and liquefaction behavior of the coal.

The objective of the microwave drying subtask is to determine whether microwave drying alters the structure and composition of the coal, and hence its behavior toward liquefaction. This work was prompted by earlier work of Silver and Frazee (1) that showed that drying coal with microwaves beyond ~75% moisture removal actually had a detrimental effect on the reactivity toward liquefaction. However, there has not been a systematic study of changes in coal structure induced by microwave drying.

At full power (600 watts), 75 % or greater of the moisture was removed in ~2 min., and removal of the remaining moisture caused the temperatures to increase rapidly (Figure 2). Because of the rapid moisture removal at full power, different levels of microwave power were used in order to obtain a more complete drying curve. At power levels of 300 watts, 25 -75 % moisture could be removed for irradiation times of up to 15 min.

The general features of the coal drying curves using microwave radiation are shown in Figure 2. In general, there is a very rapid temperature rise after ~10 % of the moisture is removed. This is followed by removal of the bulk of the moisture (10-80%) at temperatures close to the

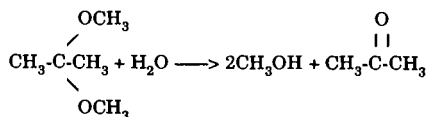
boiling point of water, which is ~ 93 °C at the 7,200 ft elevation in Laramie, WY. The rapid increase in temperature after >75% of the moisture is removed seems to be a general characteristic of microwave heating of subbituminous coals. This behavior was also observed by Silver and Frazee (1), who also noted a decreased reactivity toward liquefaction for greater than 75% moisture removal. We speculate that beyond this level of moisture removal, the additional moisture that is removed is an integral part of the gel or pore structure of the coal. These water molecules have a more difficult time aligning and realigning with the radiation field, and thus would cause heating to higher temperature, and possible disruption of part of the coal matrix enabling some retrograde reactions to take place that diminish the reactivity toward liquefaction.

It was possible to remove greater amounts of moisture than that determined by thermal drying, by microwave drying for extended periods of time (180 min) using lower power levels (300 watts). These results are shown in Figure 3. Solid-state ¹³C CP/MAS NMR spectra of the microwave heated coals are shown in Figure 4. The spectra do not show any significant carbon structural changes as a result of moisture removal using microwaves, even though the temperatures were greater than 100 °C and greater than 100% of the moisture removable by thermal drying at 105 °C was removed using microwaves. In general, there is a slight degradation in the resolution of some of the carbon functionality during heating, as evidenced by the smoothing of the resonance bands at -140, 155, 180 ppm, similar to what was observed in the ballistically heated samples (Figure 1).

Chemical Drying

Chemical drying of coals is a relatively unexplored technique for removing water at low temperature. Thermal methods of drying can alter the physical structure of coal as well as promote undesirable chemical reactions. Low-temperature drying of coal, on the other hand, should preserve the structural integrity, reduce retrograde reactions, reduce thermal degradation, and provide information on nonbonded, chemisorbed, and physisorbed water. This method of dehydrating coal should provide a baseline for studying initial stages of retrograde/condensation reactions. That is, decarboxylation and low-temperature oxidation reactions can then be studied in the presence and absence of water and gases and as a function of temperature.

Pore water and surface adsorbed water on coal can be effectively removed by the use of chemical dehydration agents which react with water to form volatile reaction products. We are investigating the use of a unique chemical dehydrating agent, 2,2-dimethoxypropane (DMP), for chemically drying coals. The reaction of DMP with water is as follows:



This reaction is rapid (<10 min) and endothermic. The use of DMP to dehydrate coal accomplishes two things: (1) the removal of water at ambient temperature by chemical means rather than by physically forcing exchange by mass action preserves the structural integrity

of the coal components and (2) the reaction products can easily be measured quantitatively to determine the amount of water in coal.

The results of the chemical drying experiments are summarized in Figure 5. As expected, the measured moisture content increased with time and reached a maximum after about 8 hrs. The data suggest that two types of water are removed sequentially. Free or surface sorbed water is rapidly removed upon contact with the drying agent, followed by removal of more tightly bound water as the reagents diffuse into the micropore structure. There appears to be an induction period of about 4 hrs for the Eagle Butte coal before the moisture content increases more rapidly due to removal of the more tightly bound water.

The chemical drying experiment was repeated twice for the Usibelli subbituminous coal. In the first experiment, aliquots were removed sequentially, and in the second experiment, separate coal samples were prepared and allowed to stand until the appropriate time for acquisition of the ^1H NMR spectrum. The data show excellent reproducibility.

Both coals were thermally dried at 110°C for 1 hour. The moisture content was determined by weight loss. Eagle Butte coal had an as determined moisture content of 16.6 wt% and the Usibelli had an as determined moisture content of 14.1 wt%. These values are close to the early time moisture contents determined by chemical drying.

ACKNOWLEDGMENT

This work was supported by DOE contract DE-AC22-91PC91043 and DOE grant DE-FG22-91PC91310. The solid-state NMR analyses were provided, in part, by a DOE University Research Instrumentation grant No. DE-FG05-89ER75506. Such support does not, however, constitute endorsement by DOE of the views expressed in this paper.

REFERENCES

1. Silver H.F., W.S. Frazee, Integrated Two-Stage Coal Liquefaction Studies, University of Wyoming, Laramie, WY, August 1985, EPRI report AP-4193, 460 p.
2. Silver H., P.J. Hallinan, W.S. Frazee, Amerf. Chem. Soc. Div. Petrol. Chem. Preprints, 1986, 31(3), 755.
3. Serio M.A., P.R. Solomon, E.Kroo, R. Bassilakis, R Malhotra, D. McMillen, Amer. Chem. Soc. Div. Fuel Chem. Preprints, 1990, 35(1), 61.

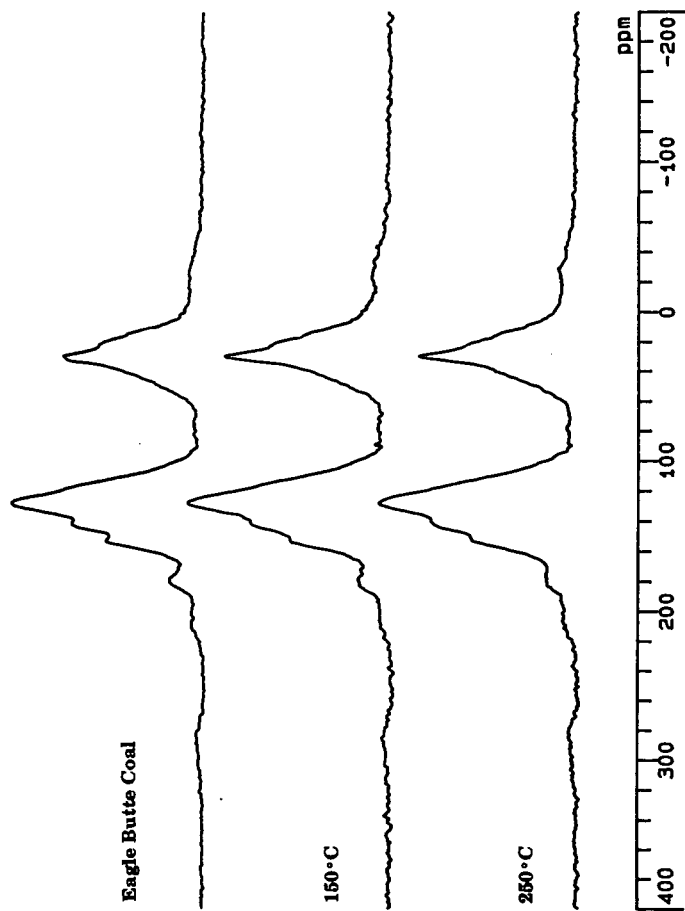


Figure 1. CP/MAS ^{13}C NMR spectra of ballistically-heated Eagle Butte subbituminous coal.

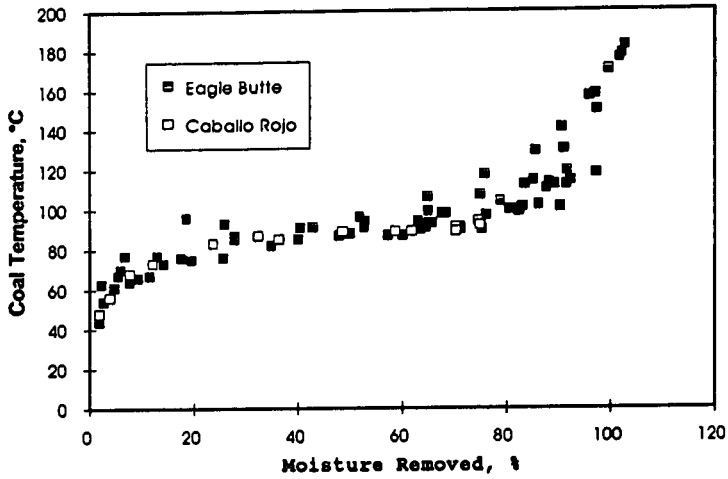


Figure 2. Coal temperature as a function of moisture removal for microwave drying.

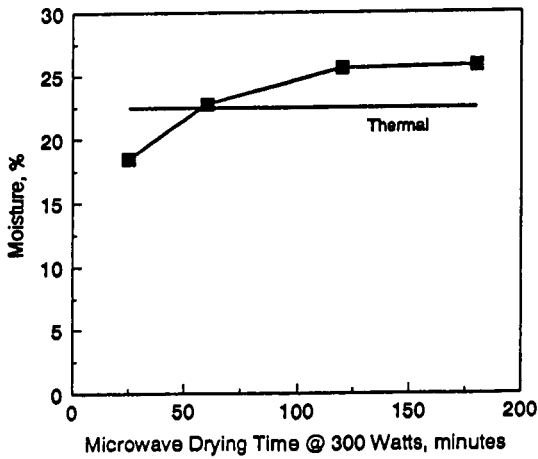


Figure 3. Moisture removal as a function of microwave drying time at 300 watts.

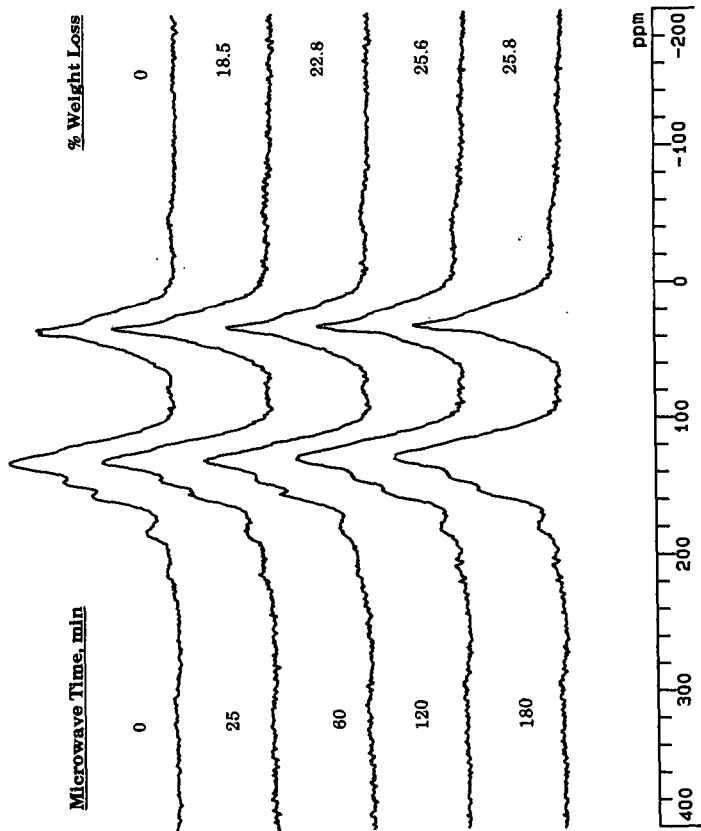


Figure 4. CP/MAS ^{13}C NMR spectra of microwave-dried Eagle Butte coal (weight loss from thermal drying = 22.5%).

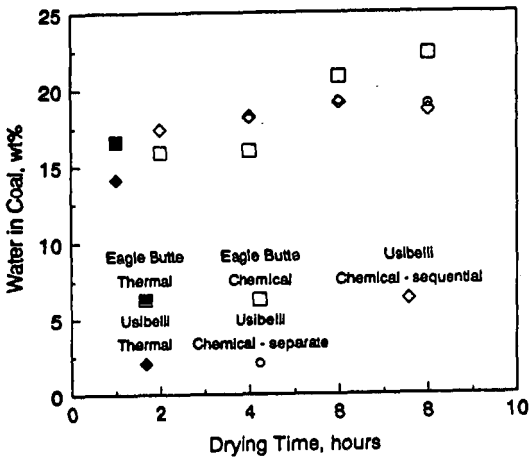


Figure 5. Moisture removal as a function of time for chemical drying.

CO PRETREATMENT AND LIQUEFACTION OF SUBBITUMINOUS COAL

S. C. Lim, R. F. Rathbone, E. N. Givens and F. J. Derbyshire,
University of Kentucky Center for Applied Energy Research,
3572 Iron Works Pike, Lexington, KY 40511-8433.

Keywords: Coal liquefaction, Pretreatment, Carbon Monoxide, Water

Abstract

A Wyodak subbituminous coal was pretreated at 300°C at various CO partial pressures in aqueous NaOH. Up to one-third of the oxygen is removed both in the presence and absence of CO. Oxygen-rich, water soluble humic acids are formed in the absence of or at low CO pressures; at 800 psig CO, water soluble product is absent. Higher CO conversions to hydrogen via the water gas shift (WGS) reaction was observed at lower pressures with higher H₂ consumption occurring at the higher pressures. Pyridine solubility and optical microscopy of the pretreated material indicate major reconstruction of the coal structure. Liquefaction of the pretreated material at 400°C in hydrogen/tetralin indicates that pretreated coal reacts faster giving higher conversion and lower hydrogen consumption than raw coal.

INTRODUCTION

Pretreating coal prior to liquefaction has been shown to result in higher yields of product through a net reduction of retrograde reactions. The methodology can vary from treatment of coal through demineralization,^{1,2} acid-washing, solvent swelling,^{3,4} alkylation,⁵⁻⁷ dissolution with strong acids and bases,^{8,9} catalytic reactions,¹⁰ or by the presence of hydrogen.¹¹ Solomon et al.¹² identified at least two distinct cross-linking events when coals are heated; one applies primarily to low-rank coals and occurs at lower temperatures simultaneous with CO₂ and H₂O evolution¹³ that correlates with loss of carboxyl groups and occurs prior to bridge breaking or depolymerization reactions. A second event that is exhibited by higher rank coals occurs at moderate temperatures simultaneous with methane formation subsequent to the initial bridge breaking reactions and correlates best with methane formation. For lignites, these cross-linking reactions begins at about 200°C while the corresponding reaction for higher rank coals begin at temperatures above 400°C.¹²

Aqueous treatment around the supercritical temperature of water, i.e. ~372°C, is also known to cause significant changes in coal which enhance coal conversion under a variety of process conditions.^{14,15} Illinois No. 6 coal, pretreated with steam at 50 atm between 320-360°C, provided a two fold increase in liquid yields and a 20% increase in total volatile yields when pyrolyzed at 740°C.¹⁶ Pretreated coal had lower oxygen content, exhibited reduced hydrogen bonding, had increased pore volume,¹⁷ and had twice as many hydroxyl groups than the starting coal.¹⁸ Steam inhibited retrograde reactions of the phenolic groups that were evolved.^{17,19}

Generally, coal conversion in aqueous systems to which CO and base are added, is higher than in straight aqueous systems or in hydrogen/donor solvent,²⁰ especially for lower rank coals.²¹⁻²⁵ In the CO/H₂O/base system the water-gas shift conversion occurs²⁶ (CO+H₂O→H₂+CO₂) which involves the intermediacy of the formate anion, HCO₂⁻.²⁷ In the study reported here the effect of this reaction system on subbituminous coal at temperatures around 300°C has been investigated. Substantial changes to the coal

substructure have been identified and the liquefaction of the pretreated coal in hydrogen donor solvent has been evaluated.

EXPERIMENTAL

Materials - Reagents were purchased as follows: 99% purity UV grade tetralin, high purity tetrahydrofuran (THF), and high purity pentane were Burdick & Jackson Brand from Baxter S/P; UHP 6000# hydrogen was supplied by Air Products and Chemicals, Inc. A sample of Wyodak Clovis Point coal was supplied by the Wilsonville Advanced Coal Liquefaction Research and Development Facility and had been ground to -200 mesh, riffled and stored in a tightly sealed container. Analysis of the coal is presented in Table 1.

Procedures - Pretreatment experiments were conducted by adding the specified amounts of coal, distilled water, and NaOH to a 25 ml vertical reactor which was sealed and pressurized with CO. The pH of the starting solution was between 13-14. After leak testing, the reactor was submerged in a fluidized sandbath at 300°C and shaken at a rate of 400 cycles per minute. At the end of the reaction period, the reactor was rapidly quenched to room temperature. Gaseous products were vented into a collection vessel and analyzed by gas chromatography. Solid and liquid products were scrapped and washed from the reactor using water and then filtered, and 'freeze dried'. The pH of the aqueous layer was between 5 and 6. Subsequently the sample was dried at 80°C/25 mm Hg for 60 min. In several experiments the insoluble material was placed in a Soxhlet thimble, extracted with THF for 18 hours, and dried overnight at 80°C/25 mm Hg. Ashing of the water and THF insolubles indicated >95% of the Na fed as NaOH reported to the aqueous layer. Soluble material was concentrated by removing excess THF to which was added a 50:1 excess volume of pentane and the mixture placed in an ultrasonic bath for 3 min. The insolubles were removed by filtering and the solubles recovered after evaporating the pentane. The water soluble fraction was acidified with HCl to precipitate humic acids which were centrifuged, collected and dried. The aqueous layer was extracted with ether. Recoveries and products are reported on an maf basis calculated by subtracting the coal ash from the total THF insolubles. Na product is assumed to report completely to the aqueous phase.

Liquefaction experiments were performed by placing raw or pretreated coal and tetralin (2:1 tetralin:coal) in the reactor described above and submerging the reactor in a sandbath at 400°C for periods from 15 to 60 min in 800 psig (cold) H₂. The reactor was rapidly cooled and gaseous products collected. The solid/liquid products were separated into THF insoluble (IOM plus ash), THF soluble/pentane insoluble (PA+A) and pentane soluble (oils) fractions. Conversions and product yields are reported on an maf basis by assuming complete recovery of the ash in the THF insolubles.

Analyses - FTIR transmittance spectra were obtained on a Nicolet Model 20SXC spectrometer using KBr pellets of the parent and demineralized coals. Carbon, hydrogen and nitrogen were determined on a Leco Model 600 combustion analyzer. Total sulfur was determined according to ASTM D4239-84 with a Leco Model SC32 combustion-IR analyzer.

Optical Microscopy - Samples of coal, pretreated coal, and liquefaction residues were prepared for microscopical examination by mixing with epoxy resin, placing the mixture into a small cylindrical mold, and allowing the epoxy to harden. A sample surface was then ground and

polished on a polishing wheel using a series of SiC grits and alumina polishing compounds. Microscopical observations were conducted using a Leitz MPV Compact polarizing microscope-photometer. As a qualitative measure of the acidic oxygen functional groups in the feedstock and pretreated coal, a freshly polished surface of the coal-epoxy pellet was immersed in aqueous KOH (pH = 13), rinsed, and then placed in a Safranin-O (a cationic dye) water solution. This procedure has been used as a petrographic method for detecting weathering in coals.^{28,29} This provides a measure of the number of carboxyl and phenolic groups in the coal; the more intense the staining of the polished coal surface, the greater the proportion of acidic oxygen functional groups.

RESULTS AND DISCUSSION

CO Pretreatment of Coal - The yields on an maf basis ranged from 75-92 wt% for water insoluble products and up to 7 wt% for water soluble products as presented in Table 2. All of the unaccounted for organic matter plus water and CO+CO₂ produced from the coal is lumped into Oil+Gas+Water. Total elemental recoveries based upon analysis of the water-insoluble material, or the subdivided PA+A and THF insoluble fractions, and humic acids indicate generally complete carbon recovery, especially at the higher CO pressures. The minor amounts of carbon associated with direct elimination of CO and CO₂ from the coal, which would be less than 1 wt%, plus the ether extract, which was formed only at the lower CO pressures, are not included in these values. Combined hydrogen recoveries ranged from 81% in the absence of CO to greater than 100% at higher CO pressures, and parallel the higher H₂ gas consumptions. Because of the small magnitude of the nitrogen and sulfur contents in the coal these numbers show greater scatter. A rather uniform 40 ± 4 wt% oxygen loss was observed. Based upon ash measurements, Na, added as NaOH, reported exclusively to the water phase.

The highest yield of water soluble product occurs in the complete absence of added CO with its yield steadily decreasing as CO concentration increases. At 800 psig it is completely absent. On the other hand, water insoluble product, as well as the PA+A portion of that product, is higher at higher CO pressures. Significantly, in the absence of CO, the PA+A fraction is completely absent. The yield and H/C atomic ratios of water insoluble product increase simultaneously.

The WGS reaction was approximately 80% complete at the lower CO concentrations versus only 39-53% complete at the higher pressures. Based upon the 4 fold greater CO concentration present at the higher pressure, twice as much H₂ is present at this concentration at which much higher levels of H₂ are consumed. At the lower CO concentrations the observed lower PA+A yields, the higher water insoluble product yields, and the generally higher oil+gas+water yields may be due, in part, to pyrolysis processes which dominate the competing hydrogenation reactions in the more hydrogen deficient environment. Data from the run in the complete absence of CO, where PA+A is absent and the highest yield of water soluble product was obtained, supports this view.

In each of the runs sufficient water is present to maintain a liquid phase at reaction temperature. The results suggest that increasing water concentration gives higher coal conversion at both 200 and 800 psig CO. The WGS reaction appears to show no sensitivity to water concentration in these runs probably because of similar water partial pressures. At this point whether water concentration affects the reaction remains unclear.

Pyridine extraction showed that 60 wt% of pretreated coal prepared at 800 psig CO pressure was soluble versus only 4.5 wt% solubility of the starting coal (Table 3). Pyridine solubility was lower for water insoluble products prepared either at low CO concentrations or in the absence of CO. Pyridine solubility qualitatively reflects the degree of cross-linking in the sample. This value plus the increased H₂ consumption and the absence of any significant reaction in a H₂ environment under these conditions,³⁰ suggest that coal depolymerizes into smaller fragments which are stabilized by the *in-situ* hydrogen generated during the WGS reaction. The poorer result observed at lower CO concentrations suggest rapid depletion of the CO which converts to CO₂ and H₂ before any significant coal upgrading takes place. This is consistent with a reaction path in which the coal structure is stabilized and hydrogenated by the active WGS intermediate.

Optical microscopy showed significant morphological changes in the coal structure of the water insoluble product prepared at the higher CO pressure (Run 45). The structure was completely melted and agglomerated to form large, coherent masses as compared to the original coal (Figure 1). The treated material contained abundant pores ranging from submicron to tens of microns in size, some of which were filled with solid homogeneous bitumen-type material which was fluorescent under ultraviolet illumination, suggesting a high-hydrogen content. The reflectance of the surrounding more abundant altered vitrinite (0.43%) was close to the original coal (0.39%) and showed no visible fluorescence. Staining of the samples with Safranin-O indicates that some of the oxygen functional groups were removed during pretreatment which agrees with the elemental analysis.

FTIR data indicate partial decarboxylation occurred during pretreatment. The intensity of the carbonyl absorption, which appears as a shoulder at 1703 cm⁻¹ on the relatively intense aromatic stretching vibration at 1600 cm⁻¹, is reduced in the pretreated coal.

Liquefaction of Pretreated Coal - THF conversions for liquefaction of pretreated coal in hydrogen and tetralin were 60.8 wt.% at 15 min and 83.2 wt.% at 60 min. The corresponding values for raw coal were higher: 49.4 wt.% at 15 min and 74.8 wt.% at 60 min (see Table 4). The increase in THF conversion at 15 min reported mainly to the PA+A fraction while in the 60 min run the improvement in conversion reported to the oil fraction. The CO+CO₂ yields for pretreated coal were significantly reduced for both 15 and 60 min runs suggesting significant elimination of carbon oxides during pretreatment.

Both gaseous H₂ and total hydrogen consumption, the latter which includes the sum of gaseous H₂ and hydrogen from tetralin, were determined. Hydrogen consumed in liquefaction of the pretreated coal over the reaction period from 15 to 60 min is nearly constant even though THF conversion increases by 22 wt%. By contrast, raw coal showed a larger increase in total hydrogen consumption over the period.

CONCLUSIONS

Low temperature CO pretreatment of coal promotes formation of a material through hydrogenation and modification of the coal structure which is more reactive than the starting coal. Retrogressive reactions competing for hydrogen during liquefaction apparently have been quenched leading to a more effective utilization of hydrogen.

REFERENCES

1. Serio, M. A., P. R. Solomon, E. Kroo, R. Bassilakis, R. Malhotra and D. McMillen, Preprints, Am. Chem. Soc. Div. of Fuel Chem., 1990, 35(1), p. 61.
2. Deshpande, G. V., P. R. Solomon and M. A. Serio, Preprints, Am. Chem. Soc., Div. of Fuel Chem. 1988, 33(2), p. 310.
3. Matturo, M. G., R. Liotta, and R. P. Reynolds, Energy and Fuels, 1990, 4, p. 346.
4. Warzinski, R. P., and G. D. Holder, Preprints, Am. Chem. Soc., Div. of Fuel Chem. 1991, 36(1), p. 44.
5. Schlosberg, R. H., R. C. Neavel, P. S. Maa and M. L. Gorbarty, Fuel, 1980, 59, p. 45.
6. Baldwin, R. M., O. Nguanpraesert, D. R. Kennar, and R. L. Miller, Preprints, Am. Chem. Soc. Div. of Fuel Chem. 1990, 35(1), p. 70.
7. Solomon, P. R. and K. R. Squire, Preprints, Am. Chem. Soc. Div. of Fuel Chem. 1985, 30(4), p.346
8. van Bodegom, B., J. A. Rob van Veen, G. M. M. van Kessel, M. W. A. Sinnige-Nijssen and H. C. M. Stuiiver, Fuel, 1984, 63, p. 346.
9. Kasehegen, L., Ind. Eng. Chem., 1937, 29, p.600
10. Solomon, P. R., M. A. Serio, G. V. Deshpande, E. Kroo, H. Schobert, and C. Burgess, Preprints, Am. Chem. Soc. Div. of Fuel Chem. 1989, 34(3), p. 803.
11. Bockrath, B. C., E. G. Illig and W. D. Wassell-Bridger, Energy and Fuels, 1987, 1, p.227.
12. Solomon, P. R., M. A. Serio, G. V. Deshpande and E. Kroo, Energy and Fuels, 1990, 4, p.42.
13. Suuberg, E.M., D. Lee, and J. W. Larson, Fuel, 1985, 64, p.1669.
14. Towne, S. E., Y. Shah, G. D. Holder, G. V. Deshpande and D. C. Cronauer, Fuel, 1985, 64, p883.
15. Bienkowski, P. R., R. Naragan, R. A. Greenkorn, K. C. Chao, Ind. Eng. Chem., 1987, 26, 202.
16. Graff, R. A., S. D. Brandes, Energy and Fuels 1987, 1, p 84.
17. Tse, D. S., A. Hirschon, R. Malhotra, D. F. McMillan and D. S. Ross, Preprints, Am. Chem. Soc., Div. of Fuel Chem., 1991, 36(1), p. 23.
18. Khan, M. R., W, Y, Chen, and E. Suuberg, Energy and Fuels 1989, 3, p. 223.
19. Trehwella, M. J. and A. Grint, Fuel, 1988, 67, p.1135.
20. Lim, S.C., Ph.D Thesis, Monash University, 1990.
21. Appell, H. R. et al., Preprints, Am. Chem Soc., Div. of Fuel Chem., 1968, 12(3), p. 220.
22. Appell, H. R. , Energy, 1976, 1(4), p.24.
23. Jackson, W. R. et al., 1987 International Conference on Coal Science, Maastricht, Coal Science and Technology 11 (J. A. Moulijn, K.A. Nater, H.A.G. Chermin. Eds.), p.45.
24. Oelert, H.H et al., Fuel, 1976, 55, p.39.
25. Takemura, Y. et al., Fuel, 1983, 62, p.1133.
26. D. C. Elliott and L. J. Sealock, Jr., Ind. Eng. Chem. Prod. Res. Dev. 1983, 22, p 426.
27. Ross, D. S., in "Coal Science," (M.L. Gorbarty, J.W. Larsen and I. Wender, Eds.) Academic Press, Inc., New York, NY.
28. Gray, R. J., A. H. Rhoads and D. T. King, Trans. Society Mining Engineers, 1976, 260, p. 334.
29. Marchioni, D. L., Int. J. Coal Geol., 1983, 2, p. 231.
30. D. S. Ross, J. E. Blessing, Q. C. Nguyen and G. P. Hum, Fuel, 1984, 63, p 1206.

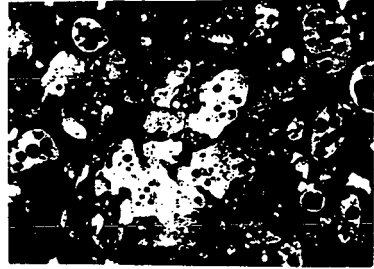


Figure 1. Reflected white-light photomicrographs of Wyodak coal (left) and CO-pretreated coal (right), at 625X. Width of each field of view is approximately 165 microns.

Table 1. Analysis of Wyodak Clovis Point Coal

Composition, wt % maf	
Carbon	71.0
Hydrogen	4.9
Nitrogen	1.3
Sulfur	1.1
Oxygen (by difference)	21.7
Ash, wt% dry coal	6.94
H/C Ratio	0.83

Table 2. Product Distribution from CO Pretreatment of Coal^a

CO, psig cold	200	200	400	800	800	800 ^b
Added water, ml	2	6	4	2	6	6
Products, wt% maf coal						
Water Insoluble	80.8	74.7	90.0	91.7	89.7	80.0
PA+A ^c	2.2	5.5	17.2	17.6	18.0	-
THF Insoluble	78.6	69.2	72.8	74.1	71.7	80.0
Water Soluble						
Humic Acids ^d	5.1	5.5	2.7	-	-	7.0
Ether Extract ^e	1.1	0.5	-	-	-	-
Oil+Gas+Water ^f	13.0	19.3	7.3	8.3	10.3	13.0
Elemental Recovery ^g						
Carbon	93	-	101	101	97	97
Hydrogen	84	-	99	103	107	81
Nitrogen	79	-	120	99	91	115
Sulfur	62	-	60	67	97	51
Oxygen ^h	64	-	66	60	59	56
WGS Conversion ⁱ	78	82	47	39	53	-
H ₂ Gas Consumed ^j	-	8	13	22	26	-
H/C Atomic Ratio ^k	0.75	-	0.83	0.85	0.92	0.71
Run Number	52	48	46	49	45	69

^a 2 g dry coal, 4.4 wt% NaOH on maf coal

^b 100% Nitrogen

^c THF soluble-pentane insoluble

^d Precipitated from acidified aqueous phase

^e Ether extract from acidified aqueous phase

^f Oil+Gas+Water=100-[water soluble (maf)+water insoluble (maf)]

^g Total in combined water soluble + water insoluble

^h Oxygen analysis by difference

ⁱ WGS = H₂O gas shift; % WGS Conv = $[(CO_{in}-CO_{out})/CO_{in}] \times 100$

^j H₂ Consumed is [mg H₂(from WGS)-mg H₂(final)]/g maf coal

^k Ratio for water insoluble product.

Table 3. Pyridine Extraction

Sample ^a	Pyridine Soluble, wt% maf
Wyodak Coal	4.5
N ₂ /6 ml H ₂ O/NaOH	6.4
200 psi CO/6 ml H ₂ O/NaOH	9.0
800 psi CO/6 ml H ₂ O/NaOH	60.0

a. 1.0 g water insoluble product extracted with 300 ml of pyridine in Soxhlet apparatus for 18 hours.

Table 4. Liquefaction of Raw and CO Pretreated Coal^{a,b}

Coal	Raw	Pretreated	Raw	Pretreated
Time, min	15	15	60	60
THF Conv, wt% maf coal	49.4	60.8	74.8	83.2
Products, wt% maf coal				
PA+A	34.3	47.0	42.8	41.8
Oils+Water	9.9	11.6	26.3	38.9
CO+CO ₂	5.0	2.0	5.4	1.9
HC Gases	0.2	0.2	0.3	0.6
H ₂ Gas Consumed ^c	11	19	17	18
Total H ₂ Consumed ^d				
Run Number	79	81/82	85	86

a. Pretreatment: 800 psig CO cold, 6 ml water, 4.4 wt% NaOH on dry coal, 300°C, 1 hr.

b. Liquefaction conditions: 400°C, 800 psig H₂ cold, 2 g pretreated coal, 2 g tetralin.

c. H₂ Gas Consumed = $[H_{2\text{ in}} - H_{2\text{ out}}]/\text{coal}$ (mg/g maf coal); excludes H₂ consumed by tetralin.

d. Includes both gaseous H₂ and hydrogen consumed from tetralin.

REACTOR SYSTEM DEVELOPMENT TO REDUCE COAL LIQUEFACTION SEVERITY

H.G. Sanjay, Arthur R. Tarrer
Department of Chemical Engineering
Auburn University, Auburn, ALA 36849

Keywords: Loop Reactors, Coal Liquefaction, Hydrogenation

INTRODUCTION

The hydrogenation of aromatic hydrocarbons is of interest not only because of the commercial interest of the reaction, but also because the liquefaction of coal and the subsequent product upgrading involves the hydrogenation of aromatic rings [1]. A number of reactions of industrial importance, such as the hydrogenation of various organic compounds and the hydrodesulfurization of petroleum fractions, involve reactions between two fluids in the presence of a solid catalyst. Coal liquefaction is one such reaction in which coal slurried in a solvent reacts with hydrogen to yield liquid products. The goal in a coal liquefaction process is to convert coal into a clean liquid fuel by increasing the hydrogen content of coal derived liquids and removal of heteroatoms such as sulfur, nitrogen and oxygen.

The efforts to improve yield and selectivity from coal liquefaction have focussed on the development of improved catalysts [2-4] and the use of different hydrogen donors [5-7]. These attempts have met with limited success due to the autocatalytic nature of the free radical propagation. The hydrogen supply rates are not sufficient to saturate the free radicals generated at longer residence times used in conventional reactors such as tubing bomb microreactors and stirred autoclaves. The development of new and improved reactor systems with better reaction control and improved mass transfer rates will reduce some of the problems associated with coal liquefaction.

REACTOR DESIGN CONCEPT

Coal liquefaction reactions proceed via a free radical propagation mechanism. The free radical propagation increases exponentially and very high gas-liquid mass transfer rates are necessary to saturate the free radicals and prevent retrogressive reactions. Commercial gas-liquid contactors are not capable of providing sufficiently high gas-liquid mass transfer rates to prevent hydrogen starvation and thus retrogressive reactions from occurring. An alternative approach to increase the yield and improve the product selectivity in free radical type reactions is to control the rate of free radical propagation so that only practically achievable mass transfer rates would be required. The reactor system used in this study is based on this alternative approach.

The approach used in developing the reactor system was two-fold: 1) a reactant flow pattern was developed which would allow versatility in reaction rate controllability and 2) a gas-liquid contactor design was sought that would provide the highest mass transfer rates per unit volume. The higher the mass transfer rate can be made per unit reactor volume via gas-liquid contactor design, the farther the operational range of the reactor system over which the rate of retrogressive reactions would be low.

A bang-bang control strategy was used to regulate the reaction rate. A cyclic switching from high to low reaction temperatures was used to control the free radical propagation rate. The adjustable control parameter selected was the frequency of the cyclic switching of the reaction temperature. Physically, this was accomplished using a recycle loop type reactor in which the temperature in part of the loop was kept high (reaction zone) and that in the remainder of the loop it was lower (quenching zone). The frequency of cyclic switching of the reactant temperature could be varied simply by changing the reactant recycle flow rate. The mass transfer requirements per reaction cycle could be maintained within a range that could be satisfied by practical gas-liquid contactors, simply by optimizing the recycle flow rate. This type of reactor flow arrangement is similar to jet loop type reactors, which have been employed when reaction rates are very high and the reactions are mass transfer limited.

REACTOR SYSTEM

The conventional slurry reactor designs are modified in industrial reactors to achieve specific objectives such as higher heat and mass transfer capabilities, higher catalyst efficiency, better reactor performance and selectivity, etc [8]. The high heat and mass transfer rates, easy control over the degree of backmixing, and simple design have made loop reactors very attractive for both industrial and academic purposes. A jet loop type reactor was designed and used in this study.

Jet loop reactors with hydrodynamic jet flow drive are suitable for gas-liquid-solid processes which require rapid and uniform mass distribution and high mass transfer rates. The reactor system developed for this study operates in a semi-batch mode with the gas being supplied continuously. The liquid and the solid constituting the slurry are recycled through the reactor system.

The reactor system employs stainless steel columns measuring eight inches in length and one inch in outer diameter (O.D.) as reactors. The reactors were connected with 0.5 inch O.D. tubing and were placed in a fluidized sand bath for efficient temperature control. The reactor tubes were filled with stainless packing rings, as heat transfer in a packed column with metal rings is highly efficient due to a large surface area per unit volume of liquid. The slurry was recycled through the closed loop reactor system by a pump. The slurry passes through a preheater before entering the reactor system. The slurry is heated to the desired temperature in the preheater by using ethylene glycol as the heating fluid. The glycol was heated in a cylindrical tank fitted with three electric heaters. A centrifugal pump was used to circulate the ethylene glycol between the preheater and the tank. The slurry passes through the preheater into the reactor tubes and through the reactors into a chiller. The slurry is cooled in the chiller using tap water as the coolant. A gas-liquid decoupling chamber separates the gas and the liquid coming out of the chiller. The liquid flows into the suction side of the pump to be recycled. The gas flows into a gas recirculation unit. The unit consists of three gas-liquid separators and an air driven gas compressor. The gas is drawn from the decoupling chamber into the separators in succession. The gas is fed to the compressor and pumped into the slurry along with fresh gas at the gas-liquid contactor on the discharge side of the pump. Any vapors in the gas condense in the separators and are drained after the run.

The reactant gas is fed into the reactor system through a gas-liquid contactor before the slurry enters the preheater. A number of gas-liquid contacting devices are available to increase the gas-liquid mass transfer rates. These include motionless mixers, column packings, high shearing mechanical agitators and different kinds of nozzles. An improvement in the gas-liquid mass transfer will result in stabilization of free radicals and could result in improved product selectivity.

Different types of nozzles are being used increasingly to enhance mass transfer during gas-liquid contacting. Two phase nozzles, where both the phases come into contact inside the nozzle, were used in this study due to their high mass transfer capabilities and their ease of use in a closed system. A very efficient type of two phase nozzle employed in the present study is the slot injector introduced by Zlokarnik [9]. In a slot injector, the mixing chamber which is circular becomes slot shaped gradually keeping the cross-sectional area constant. The slot shape results in a lower pressure drop, because the shear rate increases along the convergent surface. This produces a fine gas dispersion with the free jet retaining a large portion of its kinetic energy. In addition, the free jet leaves as a flat band and mixes rapidly with the surrounding liquid, reducing bubble coalescence. The reactor system is shown in Figure 1.

EXPERIMENTAL

Naphthalene hydrogenation experiments in the reactor system were conducted using tetralin as the solvent. A predetermined quantity of naphthalene and catalyst (5% Pd on carbon) was mixed with the solvent in a beaker. The mixture was sonicated for about ten minutes to effectively disperse the catalyst. The slurry was charged into the reactor system when the desired reaction temperature was reached (130-160°C). The system pressure was then increased to 125 psig by feeding in hydrogen. The pressure was monitored and the system was charged back to 125 psig after a 10 psig drop. A sample was withdrawn for analysis approximately a minute after gas recharging. The reaction was allowed to proceed until no drop in pressure was observed. The system was then drained and the product mixture was filtered before sampling for analysis. The system was flushed with toluene or tetralin after every run.

RESULTS AND DISCUSSION

The model reaction used in the present study to evaluate the reactor system was the hydrogenation of naphthalene. This is a very important reaction during the liquefaction of coal to regenerate the hydrogen donor solvent (tetralin). The catalyst used in the study was a commercial 5% Pd on carbon. Palladium is the most active hydrogenation catalyst, but is strongly inhibited by the presence of sulfur compounds [10]. However, the use of palladium in model compound studies (without the presence of sulfur) will facilitate evaluation of new and improved reactor systems under conditions which are not severe. This helps to reduce the "bugs" in the reactor system and, in addition, will also demonstrate improvements in conversion and selectivity.

The results of naphthalene hydrogenation in the present reactor system and in tubing bomb microreactors (TBMR) are shown in Tables 1 & 2. It appears from the tubing bomb results that the catalyst is deactivated very rapidly when the temperature is

increased from 120°C to 135°C, resulting in no conversion. The catalyst requirement in the tubing bomb was very high (35% based on naphthalene) at 120°C to obtain 93% conversion. There was no conversion in the TBMR at 165°C with 10% catalyst loading, but when the tubing bomb experiments were conducted with repeated heating and cooling every three minutes, 86% conversion was obtained in 7.5 minutes. The repeated heating and cooling is similar to the conditions in the reactor system, where the reactants are exposed to the high temperature for a very short time (6-10 seconds). The naphthalene conversion in the reactor system was nearly complete (Table 1) under similar conditions with much lower catalyst loading and less time. In the TBMR, the reactants are exposed to high temperature throughout the reaction time resulting in an exponential increase of free radicals. The mass transfer rates are not adequate to saturate all the radicals and this leads to polymerization of free radicals resulting in the deactivation of the catalyst. In the reactor system however, the reactants are subjected to high temperature for a very short time per pass, reducing the probability of free radical polymerization.

The effect of catalyst loading on naphthalene hydrogenation in the reactor system (Table 1) was used to determine if gas-liquid mass transfer was controlling the reaction. A plot of reciprocal reaction rate vs reciprocal catalyst loading indicated that gas-liquid resistance is about 25% of the total resistance at the lowest catalyst loading and about 50% at the highest loading, indicating that the reactor is operating in a regime where gas-liquid mass transfer is only partially controlling. The mass transfer coefficient K_a determined from the experimental results was 6.0/min.

A limitation of the reactor system for use with severe reaction conditions was the performance of the mechanical pump. The pump was not capable of handling slurries under these conditions and suitable custom made pumps were prohibitively expensive. To overcome this limitation, a gas driven pumping system was developed and integrated to the reactor system. The reactor system with the gas-driven pumping system has been used for naphthalene hydrogenation under elevated pressures (800-1000 psig). Attempts are being made at present to use the system for coal liquefaction.

CONCLUSIONS

A loop reactor system has been developed for use with reaction systems such as coal liquefaction that are gas-liquid mass transfer limited. The reactor system has the ability to process slurries and permits better control of free radical generation/reaction and provides higher mass transfer rates than conventional reactors. The reactor system was tested using naphthalene hydrogenation as a model reaction and performed much better than the conventional tubing bomb microreactors. The amount of catalyst required was considerably less than that required in the microreactors. A unique gas-driven pumping system was developed and integrated to the system because of the prohibitive cost of a suitable mechanical pump that could withstand coal liquefaction conditions. The reactor system will be used to coprocess coal with waste oil. Improvements in coal conversion/selectivity will be compared with those obtained in conventional reactors.

REFERENCES

1. Satterfield, C.N., *Heterogeneous Catalysis in Industrial Practice*, McGraw Hill, Inc, New York, 1991.
2. Pradhan, V. R., Tierney, J. W., Irving, W., *Energy & Fuels* 1991, 5, 497-507.
3. Suzuki, T., Yamada, O., Takehaski, Y., Watanabe, Y., *Fuel Process. Technol.* 1985, 10, 33-43.
4. Zielke, C. W., Struck, R. T., Evans, J. M., Costanza, C. P., Gorin, E., *I & EC Process Des. Dev.* 1986, 5(2), 151, 158.
5. Bedell, M. W., Curtis, C. W., *ACS Fuel Div. Preprints* 1990, 2, 577.
6. Curtis, C. W., Guin, J., Kwon, K., *Fuel* 1984, 63, 1404.
7. Neavel, R. C., *Fuel* 1984, 63, 237.
8. Chaudhari, R.V., et al *Catalysis Review-Science and Engineering* 1986, 28(4)
9. Zlokarnik, M., *Chemical Engineering Science* 1979, 34, 1265
10. Boitiaux, J.P., et al., *Hydrocarbon Processing* 1985, 3, 51,

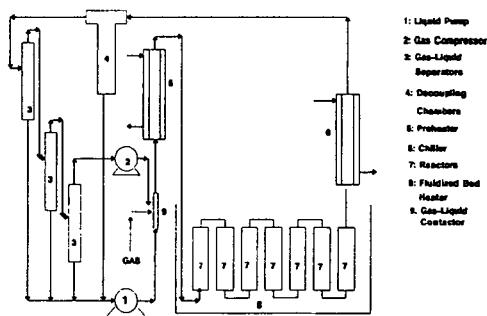


Figure 1. Jet Loop Reactor System

Catalyst (5.0%)		Catalyst (7.5%)	
Time (min)	Conversion (%)	Time (min)	Conversion (%)
7.0	17.07	3.5	24.75
9.0	31.20	6.5	33.13
14.0	47.22	9.0	45.14
20.0	64.30	10.75	54.50
27.0	85.44	15.0	69.62
37.0	98.81	20.50	88.88
		30.0	99.21
Catalyst (10.0%)		Catalyst (15.0%)	
Time (min)	Conversion (%)	Time (min)	Conversion (%)
4.0	35.34	3.5	39.92
6.5	40.18	5.0	44.55
8.75	54.14	7.25	63.94
11.25	70.82	9.50	78.89
14.50	86.57	15.0	99.14
19.00	98.41		

* wt% based on the amount of naphthalene used

Tetralin: 750 ml

Naphthalene : 129.9 gm (18% of Tetralin)

Average reactor inlet Temperature: 123°C;

Average reactor outlet Temperature: 153°C;

Pressure: 120 psig

Table 2.
Naphthalene Hydrogenation (Tubing bomb reactor)

10% Naphthalene*, 10% Catalyst**			
Temperature (°C)	Pressure (psig)	Time (min)	Conversion (%)
90	150	30	0
105	300	60	20
120	300	60	36
126	300	60	0
18% Naphthalene*, 10% Catalyst**			
Temperature (°C)	Pressure (psig)	Time (min)	Conversion (%)
90	150	30	0
165	150	30	0
165	300	30	0
10% Naphthalene*, 35% Catalyst**			
Temperature (°C)	Pressure (psig)	Time (min)	Conversion (%)
120	300	30	93
18% Naphthalene*, 14.57% Catalyst**, Cooling frequency 3 min			
Temperature (°C)	Pressure (psig)	Time (min)	Conversion (%)
165	100	3.0	38.26
165	100	6.0	73.85
165	100	7.5	86.09

* Wt% based on the amount of tetralin used

** Wt% based on the amount of naphthalene used

Use of Biocatalysts for the Solubilization/Liquefaction of Bituminous Coal in a Fluidized-Bed Bioreactor

Eric N. Kaufman, Charles D. Scott, Timothy C. Scott, and Charlene A. Woodward

Chemical Technology Division
Oak Ridge National Laboratory
Oak Ridge, TN 37831

Keywords: coal liquefaction, enzymes, fluidized-bed reactor

Abstract

Biocatalysts allow the solubilization/liquefaction of coal at near-ambient temperatures. This research has focused on the chemical modification of enzymes to enhance their solubility and activity in organic media and on optimal reactor design for a biocatalyst coal-liquefaction process. Modification of hydrogenase and cytochrome *c* using dinitrofluorobenzene has effected increased solubilities up to 20 g/L in organic solvents ranging from dioxane to benzene. Use of these modified enzymes in a small fluidized-bed reactor (with H₂ sparge) resulted in greater than 35% conversion of coal. A new class of continuous columnar reactors will be necessary to achieve the high throughput and low inventory necessary for biocatalyst processes. The controlling mechanisms in fluidized-bed systems using very small coal particulates are being studied. This investigation has included the hydrodynamic modeling of coal segregation in fluidized-bed reactors, with direct microscopic visualization using fluorescence microscopy.

Introduction

Biocatalysts allow the solubilization/liquefaction of coal at near-ambient temperatures. In such applications, it is apparent that enzymes must retain solubility and activity in organic media. This work summarizes our previous efforts on the modification of enzymes using dinitrofluorobenzene (DNFB) to enhance enzyme solubility and activity in organic media.¹ The ability of DNFB-modified hydrogenase and cytochrome *c* to solubilize lignite and bituminous coals in a fluidized-bed bioreactor is demonstrated. Optimal reactor design and scaleup will require detailed knowledge of coal segregation in the fluidized-bed bioreactor. A fluorescence visualization method is introduced to enable direct *in situ* observation of coal particles in operating fluidized bed reactors.² This information will be combined with a predictive mathematical model of coal fluidization³ to enable efficient reactor design and operation.

Methods

Techniques for Enzyme Modification

Modification of hydrogenase and cytochrome c with DNFB was achieved by a significant revision of the method originally developed by Sanger.⁴⁻⁷ Typically, the reaction solution was a mixture of water and ethyl alcohol, with the ethanol fraction varying from 28 to 65% that contained 0.1 to 3 vol% DNFB buffered to a pH of approximately 8.5 with a 7 mM phosphate buffer and/or NaHCO₃. The reaction was carried out in shake flasks at ambient temperature ($25 \pm 1^\circ\text{C}$) in the presence of air for reaction times of 0.5 to 2 h. After the primary reaction, the pH was reduced to 7 by the addition of HCl, and the reaction mixture was dialyzed overnight against 50 times the volume of the same ethanol-water-buffer mixture (without DNFB) at a pH of 7, using a cellulose membrane. After dialysis, the modified enzymes were converted to the reduced state by the addition of 5 mg/mL sodium dithionite and then lyophilized and stored under N₂ until used.

Fluidized-Bed Tests

Tests with coal were made with a small, tapered fluidized-bed bioreactor that was fabricated from glass. The reaction chamber was a 15-cm-long column in the form of an inverse cone with a diameter varying from 1.25 cm at the entrance to 2.5 cm at the exit, and the reactor was temperature-controlled at 30°C by circulating fluid in a surrounding jacket. The 0.5- to 1.0-g samples of coal particles (North Dakota lignite and Illinois No. 6 bituminous coal, -270+325 mesh fraction) were fluidized by pumping the reaction fluid containing the biocatalyst through the column at the rate of 2 to 3 mL/min. The system operated with continuous liquid recycle, and there was a H₂ sparge in the upper part of the column. The course of the reaction was followed by periodically measuring the spectrophotometric properties of the liquid phase. There appears to be a broad increase in light absorption in the range of 250 to 450 nm as the coal disappears, although it is usually convenient to choose a single wavelength for the presentation of results. At the end of tests for coal conversion, the solid residue was removed by successive centrifugation and washing. The first wash solution was the same solvent as that used in the tests, and this was followed by acetone and, finally, water. The supernatants were removed by siphoning, and spectral measurements were made. Coal conversion was reported on a moisture and ash-free basis.

Results

Enzyme Modification with Dinitrofluorobenzene

Modification of enzymes with DNFB resulted in higher solubilization in organic solvents, which increased as the hydrophobicity of the solvent decreased. The solubility of the unmodified enzyme also increased as the hydrophobicity of the solvent decreased, but it varied from undetectable in benzene and toluene to barely detectable in pyridine and dioxane. Appreciable enzyme deactivation was noted in the solvent of lowest hydrophobicity, dioxane, although significant enzyme solubilization occurred in that solvent.

The degree of dinitrophenylation affects the solubilization of the modified enzyme in organic solvents. For example, with a 0.5-h reaction time, as the concentration of DNFB in the reaction solution was increased from 0 to 0.67 vol %, there was a corresponding increase in the dinitrophenyl (DNP) content and solubilization in benzene that reached a maximum value of 9.2 mg/ml.⁷ However, there was also a corresponding decrease in the enzyme activity, presumably due to the addition of DNP in the region of the active sites. At the higher DNFB concentration, the activity was only 40% of the original value.⁷ This could be partially alleviated by the adsorption of an appropriate substrate, such as benzyl viologen, to the enzyme mixture prior to the addition of the DNFB. For example, when 0.17% DNFB was used to react with hydrogenase for 30 min, the biocatalytic activity was only 86.5% that of the starting material. But, when 20 mM benzyl viologen was added to the reaction mixture, the resulting activity of the modified hydrogenase was increased to the original value. The preadsorption of the substrate apparently partially protected the active site from interaction with the phenylizing reagent.

Coal Liquefaction/Solubilization Tests in Fluidized Beds

Two types of tests were made in small fluidized bed reactors: one in which the initial charge was maintained throughout the test, with periodic measurements of spectrophotometric changes in the organic solution, and one in which the solvent with modified enzymes was periodically replenished while the coal residue was maintained in the reactor. The latter type of test was somewhat representative of a continuous system in which some fresh biocatalyst was continuously introduced. Tests were made with pyridine as the solvent in contact with either bituminous or lignite coal.

In fluidized-bed tests with a single charge of the solvent containing DNP-enzymes, an apparent rapid conversion of the coal occurred during the first few hours, followed by a more gradual process throughout the remaining 24 h. This observation could be due to an initial use of the included reducing agent (DNP-cytochrome c) for the hydrogenation reaction, followed by the use of molecular H₂ for the succeeding hydrogenation at a lower rate. Without treatment for removing enzyme precipitation, the liquefaction/solubilization of the lignite was 23.9% and that of bituminous coal was 8.5%. The results were

somewhat higher than comparable shake-flask tests for both types of coal without HCl treatment.¹ Thus, the fluidized bed appears to be a more efficient contacting system.

One test was made with bituminous coal in pyridine in which the solvent containing DNP-mixed enzymes was replaced after 4 and 8 h in order to determine whether appreciable interaction could be induced throughout the course of the 24-h run. This was apparently the case since there was a significant increase in absorbance at 376 nm throughout a greater portion of the 24-h test. Apparent coal conversion without acid leaching of the residue to remove precipitated enzymes was 35.3%. This is the largest amount of biocatalyzed liquefaction/solubilization of a higher-rank coal that has been observed; it is a threefold increase over the fluidized-bed test in which there was a single charge of the solvent mixture.

Fluorescence Visualization of Coal Particles in a Fluidized Bed

Effective modeling, design and implementation of fluidized-bed reactors rely upon knowledge of bed expansion and segregation tendencies with particles of varying size and density. We have recently introduced a fluorescence method for the visualization of coal particles within a fluidized bed-reactor.² In this method, the dye fluorescein is added to the liquid phase and serves as a contrast agent. A modified fluorescence microscope abuts the column and is used to image the fluorescence emission in response to epi-illumination. The resulting image (dark particles on a bright field of fluorescent liquid) may be digitized and analyzed by using edge-detection algorithms to provide particle-area fraction and size distributions. The microscope may be positioned at any height relative to the column, thus producing particle segregation and expansion statistics as a function of bed height. Unlike previous attempts to visualize segregation in fluidized beds which require direct sampling, use of a modified ultra-thin column, low particle volume fraction, or radiation, the proposed method is non-invasive and may be conducted in an operational reactor at standard flow rates and particle loading. Further, unlike our previous attempts to directly label a bimodal distribution of coal particles,⁸ the current method may be applied to any distribution of particle sizes and densities, without possible alteration of particle hydrodynamics.

Preliminary results have been obtained on a small (1-ft) column in which a bimodal distribution (53-63 and 150-250 μm) of coal was fluidized. Digitized images clearly show that particle segregation is occurring and that both large and small particles are present throughout the column. Figure 1 demonstrates the current abilities in bed visualization. Figure 1a is a view near the top of the column while Figure 1b displays conditions near the bottom. In these figures, the round, darker regions are coal particles fluidized by fluorescein/water. Even from these preliminary data, it is evident that more large particles reside at the bottom of the column. Digital filtering and edge-detection algorithms have been developed to convert such images into particle area fraction and size distribution data as a function of axial position. These data will be of use in the development of predictive mathematical models of bed expansion and segregation³, and will also be useful in assessing the accuracy of current models.

Conclusions

Reducing enzymes can be chemically modified by the addition of dinitrophenyl groups so that they will be soluble in organic solvents while still maintaining biocatalytic activity. A hydrogenase has been shown to enhance the liquefaction/ solubilization of bituminous and lignite coals in both pyridine and benzene at 30°C when a reducing reagent such as reduced cytochrome c and/or molecular H₂ is used. A less polar organic solvent such as benzene may be more effective, and a small fluidized-bed has been shown to be an efficient contactor, especially with sequential addition of the reaction liquids. Coal conversions of up to 35.3% have been observed. A fluorescence method has been introduced to enable the visualization of coal-particle segregation and degradation in a fluidized bed-reactor. This technique will greatly enhance the ability to design and efficiently utilize this reactor scheme.

Acknowledgments

Research supported by the Fossil Energy Advanced Research and Technology Program, managed in part by the Pittsburgh Energy Technology Center, U.S. Department of Energy, under contract DE-AC05-84OR21400 with Martin Marietta Energy Systems, Inc. "The submitted manuscript has been authored by a contractor of the U.S. Government under contract DE-AC05-84OR21400. Accordingly, the U.S. Government retains a nonexclusive, royalty-free license to publish or reproduce the published form of this contribution, or allow others to do so, for U.S. Government purposes."

REFERENCES

- 1 Scott, C. D., Scott, T. C. and Woodward, C. A., *Fuel*. In Press
- 2 Kaufman, E. N. and Scott, T. C., *Powder Technology*. Submitted for Publication.
- 3 Asif, M., Petersen, J. N., Scott, T. C. and Cosgrove, J. M., *Fuel*. In Press.
- 4 Scott, C. D., Faison, B. D., Woodward, C. A., and Brunson, R. R. in "Proceedings: 1991 Second International Symposium on the Biological Processing of Coal," (Ed. S. Yunker), Electric Power Research Institute, Palo Alto, CA, 1991, pp. 4-29 - 4-39.
- 5 Sanger, F. *Biochem. J.* 1945, **39**, 507.
- 6 Sanger, F. *Biochem. J.* 1949, **45**, 563.
- 7 Scott, C. D., Scott, T. C., and Woodward, C. A. *Appl. Biochem. Biotechnol.* In Press.
- 8 Scott, T. C., Cosgrove, J. M., Asif, M. and Petersen, J. N., *Fuel*. In Press.

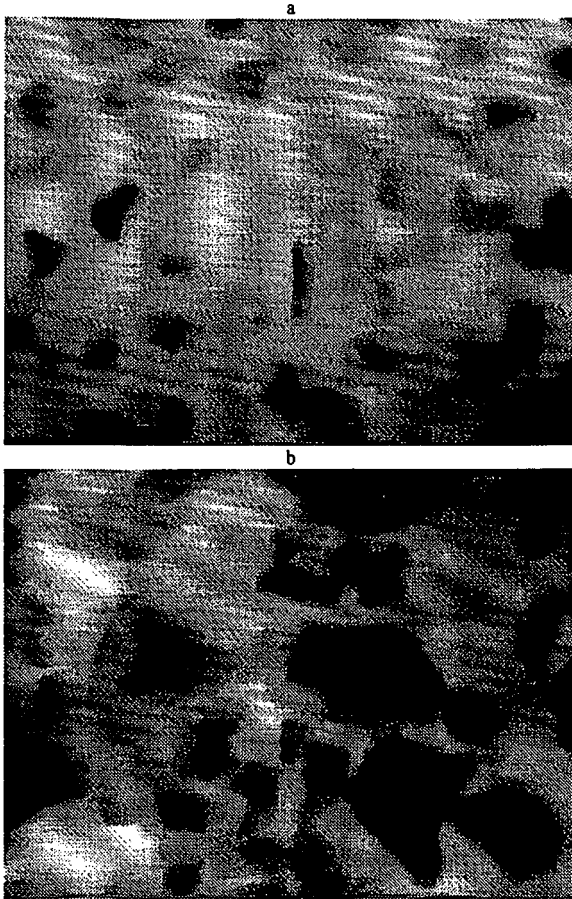


Figure 1: Visualization of fluidized coal particles using fluorescence microscopy. Coal particles appear dark on the otherwise bright background of fluorescent liquid. (a) Near top of column, the bed consists of only smaller particles (b) near bottom of column, the bed is a mixture of large and small coal particles. Video digitization, filtering and edge detection algorithms will be implemented to provide area fraction and particle size information from such images.

**Dynamics of the Extract Molecular-Weight Distribution
in Supercritical Thermolysis of Coal:
Continuous-Mixture Kinetics**

Chunjie Zhang, Ming Wang,
J. M. Smith, Ben J. McCoy

Department of Chemical Engineering
University of California
Davis, CA 95616

Keywords: coal, thermolysis, kinetics

Introduction

In this paper experimental molecular-weight distribution data for coal thermolysis at 340 °C and 360 °C in a differential flow reactor are interpreted by assuming that decomposition reaction rate expressions are continuous with molecular weight. Three groups of chemical species, representing polyaromatic compounds bound in the coal network by one, two, or more chemical linkages, are extracted simultaneously during the thermolysis reaction. The three groups are gamma distributions in molecular weight (Darivakis et al., 1990). The data support the hypothesis that the first-order rate coefficient is independent of molecular weight, and that as a consequence the MWD has a similar shape during the time of extraction.

When the number of chemical species involved in a chemical process reaches a large number, e.g., 10^2 - 10^3 , it is convenient to consider a property of the components to be a continuous variable. For example, the molecular weight, the number of carbon or oxygen atoms, or the boiling point of the different species can be considered a continuum of values, rather than discrete numbers. One line of inquiry is to formulate and solve the equations governing the chemical kinetics, or thermodynamics, of the continuous mixture, and to test the theory by experimentally measuring the frequency of occurrence of the continuous variable (e.g., the molecular weight distribution). Another possible program is to average the governing equations to obtain relations for lumped variables that can be measured experimentally for the bulk mixture. Both these approaches have been explored for continuous-mixture thermodynamics. The theoretical issues of continuous mixture and lumping kinetics for chemical reactions have been addressed in numerous mathematical studies, but their use to interpret experimental data has been limited. In the present work we wish to apply concepts from continuous-mixture kinetics to thermolytic coal extraction.

Some essential ideas of continuous-mixture kinetics provide a framework for the theoretical analysis of the data given below. The averaging, or lumping procedure shows how the kinetics governing the MWDs can lead to overall, lumped rate expressions used in most earlier studies of coal thermolysis. The overlapping groups of extractable compounds in the coal matrix present, in some cases, complications for lumping mathematics. The low temperature data ($T \leq 360$ °C) are readily explained by first-order expressions with rate coefficients that are independent of molecular weight and identical for the three groups of extractable compounds. The lumping in this case provides overall first-order rate expressions with the same rate coefficient.

Theory

In the present continuous-mixture approach the MW is considered to be a continuous variable. If x is the MW then the MWD is $c_i(x,t)$, where at time t , $c_i(x,t)dx$ is the concentration in the MW interval $(x, x+dx)$. The integral over all x is the lumped concentration, expressed in units of mass (kg) of extractables per mass (kg) of coal sample.

A central question of continuous-mixture kinetics is whether the reaction order is preserved by the lumping procedure. We follow Aris (1989) in answering this question for kinetics that describe coal thermolytic extraction when secondary reactions are negligible. For the flow reactor used here the residence time is too short for further (secondary) reactions of the extract molecules to occur. We generalize the earlier development by considering that several groups of chemical species are extracted simultaneously from the coal. If the process consists of parallel reactions of n th-order at each molecular weight, x , then the governing differential equation for the differential coal batch is

$$dc_i(x,t)/dt = -k_i(x) [c_i(x,t)]^n \quad (1)$$

with initial condition $c_i(x,t=0) = c_{i0}(x)$. The rate coefficient is $k_i(x)$ and the subscript i refers to the i th group of compounds that react. The solution is

$$c_i(x,t) = c_{i0}(x) [1 + (n-1) c_{i0}(x)^{n-1} k_i(x)t]^{1/(n-1)} \quad (2)$$

where in the limit as $n \rightarrow 1$, $c_i(x,t)$ approaches an exponential. The averaged, or lumped, concentration is given by

$$C(t) = \sum_i \int_0^\infty c_i(x,t) dx \quad (3)$$

and

$$C_0 = \sum_i \int_0^\infty c_{i0}(x,t) dx \quad (4)$$

The lumped n th-order kinetics equation corresponding to this system,

$$dC(t)/dt = -K [C(t)]^n \quad (5)$$

with initial condition $C(t=0)=C_0$ has the solution

$$C(t) = C_0 [1 + (n-1) C_0^{n-1} Kt]^{1/(n-1)} \quad (6)$$

where K is the rate constant. The solutions for $C(t)$ and the lumped expression of $c_i(x,t)$ are identical when

$$c_{i0}(x)^{n-1} k_i(x) = K C_0^{n-1} \quad (7)$$

Thus for first-order kinetics ($n=1$) we must have $k_i(x) = K$, independent of molecular weight, for the lumped expression to be first-order. If the rate coefficient is not constant with x , then the resulting lumped kinetics can be other than first-order.

Ho and Aris (1987) showed how lumping first-order continuous-mixture kinetics can lead to any reaction order between one and two, depending on the initial condition. We apply their reasoning here to the chemical groups extracted from coal. Consider that the rate coefficient is proportional to MW, i.e., $k_i(x) = k_{1i}x$, where k_{1i} is independent of x . A general initial MWD that covers many possible forms for $c_{i0}(x)$ is the gamma distribution (or Pearson Type III distribution; see Abramowitz and Stegun, 1968),

$$c_{i0}(x) = m_{oi} y_i^{\alpha_i - 1} \exp(-y_i) / \beta_i \Gamma(\alpha_i) \quad (8)$$

where $y_i = (x - x_{i0}) / \beta_i$. The zero moment of the distribution is m_{oi} . The average position of the peak, $x_{ai} = x_{oi} + \alpha_i \beta_i$, and its variance, $\sigma_i^2 = \alpha_i \beta_i^2$, are the first and second moments. The position of the peak maximum is $x_{pi} = x_{oi} + \beta_i(\alpha_i - 1)$. The distribution is equivalent to that used by Ho and Aris (1987) if $\beta = 1/\alpha$ and $m_{oi} = 1$. In the limit as $\alpha_i \rightarrow \infty$, $c_{i0}(x) = m_{oi} \delta(x - x_{i0})$, so that only components having a single molecular weight are reacting, and the rate coefficient has a constant value at that MW.

With the solution for $c_i(x,t)$, i.e., the case when $n=1$ in Eq. (2) above, we can integrate to obtain the lumped concentration,

$$C(t) = \sum \int_0^\infty c_{i0}(x) \exp(-k_{1i}xt) dx = \sum C_i(t) \quad (9)$$

with

$$C_i = m_{oi} (1 + \beta_i k_{1i} t)^{-\alpha_i} \quad (10)$$

The rate expression is obtained by differentiation,

$$dC/dt = \sum dC_i/dt \quad (11)$$

where

$$dC_i/dt = -m_{oi} \alpha_i \beta_i k_{1i} (C_i/m_{oi})^{\alpha_i + 1} / \alpha_i \quad (12)$$

In the special case that only one species group is reacting, this last equation simplifies to a power-law rate expression,

$$dC/dt = -KC^\phi \quad (13)$$

where $\phi = (1 + \alpha)/\alpha$. As α increases from one to infinity, the order of the lumped kinetics expression decreases from two to one. For the more general case when several groups react independently, however, no simple kinetics expression appears. One can perform the lumping operation numerically, and determine a reaction expression empirically.

For our experimental procedure, the extractable component MWD and concentration of coal, $c(x,t)$ and $C(t)$, are not measured directly. Rather, the concentrations of solubilized extract (both MWDs and lumped concentrations) in the solvent leaving the reactor are monitored with time. The time evolution of these concentrations is described by mass balances written for the reactor. The use of a differential bed of fine coal particles allows the reactor analysis to be simplified considerably. The convective term in the mass balance can be approximated as the volumetric flow rate multiplied by the gradientless concentration in the fixed bed. For the experimental conditions the residence time in the heated zone of the reactor is much less than the characteristic reaction time (reciprocal of the rate coefficient). Thus the accumulation term can be neglected, and the mass balance becomes simply

$$u_i(x,t) = k_{1i}(x) f[c_i(x,t)] / Q \quad (14)$$

where $u_i(x,t)$ is the MWD of extract in the solvent, Q is the volumetric flow rate of solvent, and $f[c_i(x,t)]$ represents the rate expression. The lumped extract concentration is

$$U(t) = \sum \int_0^\infty u_i(x,t) dx \quad (15)$$

Various rate expressions can be hypothesized for $f[\]$ and substituted into the equation for $U(t)$. Similar to the discussion above of the coal batch extraction, one concludes that only for special cases

will simple lumped mass balance expressions be found for $U(t)$. For example, at temperatures 360 °C and below, the rate is first-order with rate coefficients, k_0 , independent of x and identical for the extractable groups. For this case it is straightforward to demonstrate that the lumped rate is first-order with rate coefficient equal to k_0 ; thus,

$$u(x,t) = k_0 c_0(x) \exp(-k_0 t)/Q \quad (16)$$

and

$$U(t) = k_0 C_0 \exp(-k_0 t)/Q \quad (17)$$

which can be compared with the lumped reactor exit concentration.

Experiments

The experimental apparatus and procedure have been described previously (Zhang et al., 1992). Supercritical fluid thermolysis of Illinois No. 6 coal is conducted in a fixed-bed reactor with flowing solvent. The lumped, reactor-exit concentration is measured by spectrophotometric absorbance in a flow cuvette. Thus we select t-butanol as the solvent, since it does not interfere with the uv absorbance of aromatic coal extraction products. The thermolysis process is carried out at constant pressure, 6.8 MPa, and constant flow rate, 0.17 cm³/sec. Coal particles are small enough that intraparticle diffusion resistance is not significant, and the solvent flow rate is large enough that external mass transfer resistance is negligible (Zhang et al., 1992). The coal is pretreated by supercritical extraction at 300 °C to remove physically extractable constituents. Coal extract samples of 100 ml were collected during the thermolysis process, and concentrated by evaporation of t-butanol under vacuum. The MWDs of these samples, based on polystyrene molecular-weight standards, are determined by gel permeation chromatography with the uv detector set at 254 nm (Bartle et al. 1984).

Discussion of Results

The time evolution of extract MWDs for the temperatures 340 and 360 °C are provided in Figures 1. The two temperatures show MWDs whose shapes are similar at the different times, i.e., the ratio of peak heights, the position of peaks, and the average molecular weight are invariant with time. Such behavior can be described by assuming that the rate coefficient for the MWDs is independent of MW. The values of the first-order rate coefficients at the two temperatures, displayed in Table 1, give an energy of activation $E_1 = 58$ kJ/mol. The gamma distribution parameters, provided in Table 2, show that increasing the temperature changes only the zero moments. The concentrations for each group of extractable compounds, m_{0i} , shift due to the greater extraction at the higher of the two temperatures.

The comparison of the calculated and experimental MWDs is shown in Figure 2 for two samples. Only time changes during the course of the evolution of the MWDs; the parameters for the initial MWD in the coal and the rate coefficients are constant. The agreement between the experimental data and the model calculations is consistently good for all samples during the course of a run.

Figure 3 shows experimental data for total, lumped extract concentrations for the thermolytic extractions at two temperatures. The lumped concentrations are determined by the flow-through spectrophotometer at the reactor exit. The model calculations shown in Figure 3 are based on Eq. (17) and the same rate constant values (Table 1) determined from the time evolution of the MWDs. The

satisfactory agreement between theory and experiment, for both the lumped and MWD data, supports the validity of the explanation of coal thermolytic extraction that we have proposed.

Conclusion

A continuous-flow thrmolysis reactor, in which supercritical t-butanol contacts a differential bed of coal particles, provides sequential coal-extract samples that are analyzed by HPLC gel permeation chromatography to obtain time-dependent MWD data. The coal thermolysis experimental data support an interpretation of the results based on considering the molecular weight of extraction products as a continuous variable. This continuous-mixture theory suggests that three groups of coal components are extracted independently. At temperatures 340 °C and 360 °C the MWDs maintain a similar shape during the semibatch extraction. This indicates that first-order kinetics dominate, and that the rate coefficient is independent of molecular weight. The lumped extract concentration is monitored at the reactor exit by continuous uv-absorbance spectrophotometry. Both MWD and lumped concentration data are described by consistent expressions based on the same rate coefficient.

Acknowledgements

The financial support of Pittsburgh Energy Technology Center Grant No. DOE DE-FG22-90PC90288, and the University of California UERG is gratefully acknowledged.

References

- R. Aris, "Reactions in Continuous Mixtures," AICHE J. **35**, 539 (1989).
- Abramowitz, M. and I. A. Stegun, Handbook of Mathematical Functions, NBS, Chap. 26 (1968).
- Bartle, K. D., M. J. Mulligan, N. Taylor, T. G. Martin, C. E. Snape, "Molecular Mass Calibration in Size-Exclusion Chromatography of Coal Derivatives," Fuel, **63**, 1556 (1984).
- Darivakis, G. S., W. A. Peters, J. B. Howard, "Rationalization for the Molecular Weight Distributions of Coal Pyrolysis Liquids," AICHE J. **36**, 1189 (1990).
- Ho, T. C., R. Aris, "On Apparent Second-Order Kinetics," AICHE J. **33**, 1050 (1987).
- Zhang, C., J. M. Smith, B. J. McCoy, "Kinetics of Supercritical Fluid Extraction of Coal: Physical and Chemical Processes," ACS Symposium on Supercritical Fluids, in press (1992).

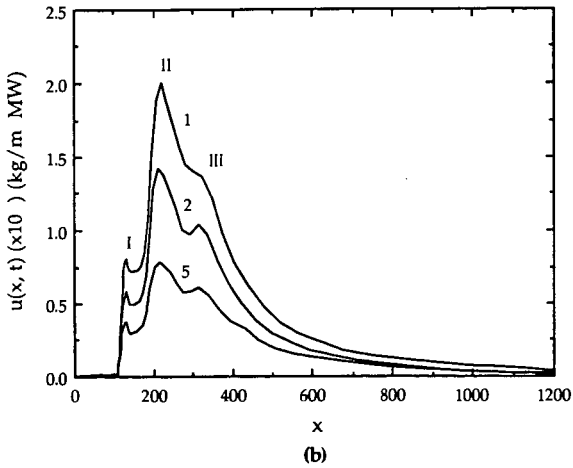
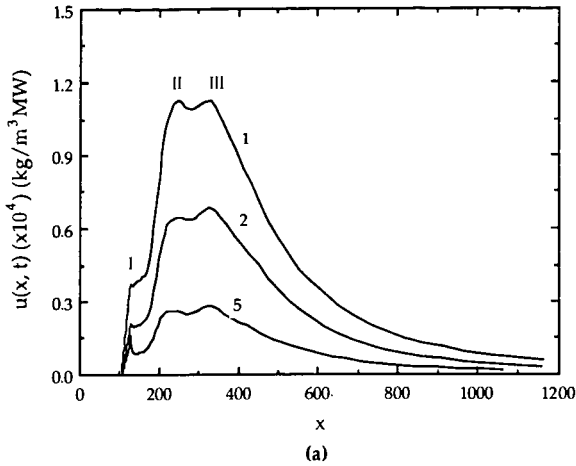


Figure 1. Time evolution of MWDs for thermolytic extractions of coal at 340 °C (a) and 360 °C (b). Samples 1, 2, and 5 were collected at the reactor effluent at times 30, 56, and 145 min for runs at 340 °C and 10, 30, and 70 min for runs at 360 °C.

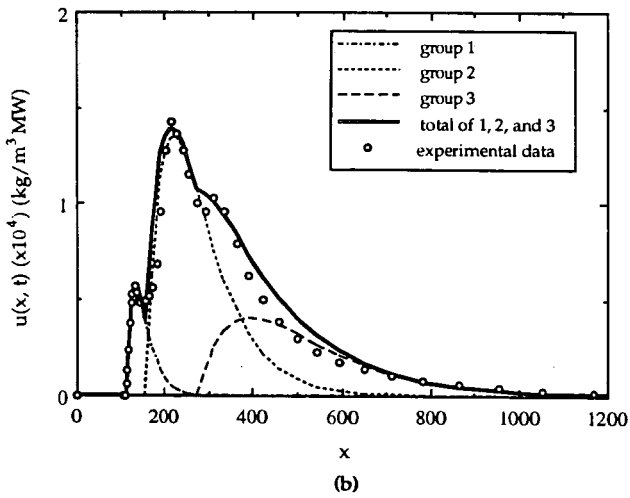
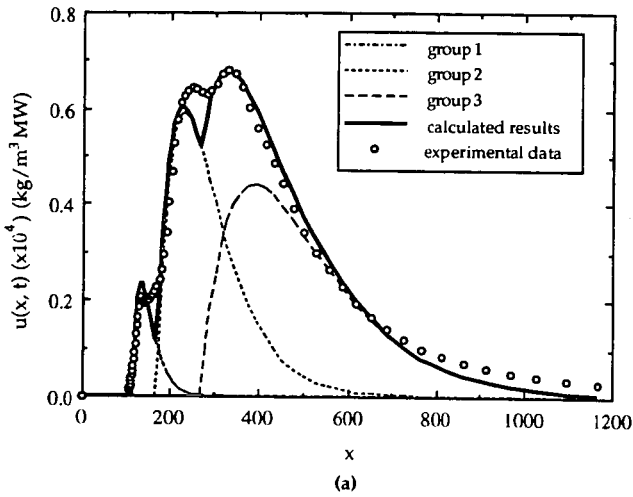


Figure 2. Comparison of model calculations and experimental data for MWDs for Sample 2 of runs at 340 °C (a) and 360 °C (b), respectively.

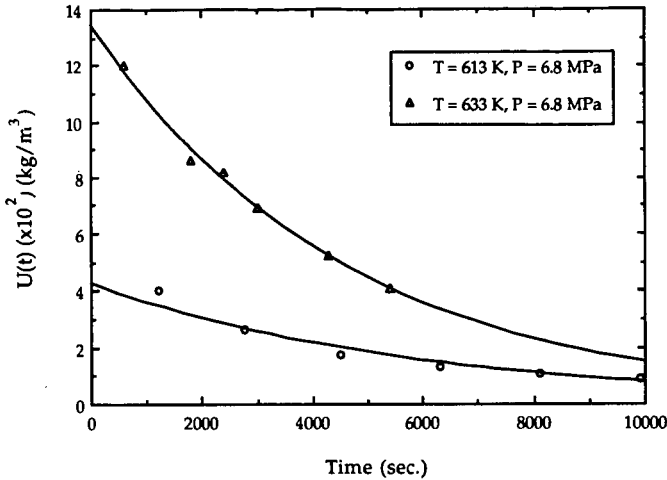


Figure 3. The experimental data of total extract concentrations at 613 K and 633 K and their exponential fit based upon kg of initial coal sample mass.

Table 1. The values of the first-order rate constants from the model

Temperature (K)	Rate Constant, k_i , sec ⁻¹	Activation Energy, kJ/mol
613	0.00015	58
633	0.00022	

Table 2. The parameter values for the gamma distributions

T = 613 K	$m_{01} = 0.0033$ kg/kg coal	$\alpha = 2$	$x_{01} = 120$
	$m_{02} = 0.032$ kg/kg coal	$\beta_1 = 20$	$x_{02} = 170$
	$m_{03} = 0.029$ kg/kg coal	$\beta_2 = 62$	$x_{03} = 275$
T = 633 K	$m_{01} = 0.0080$ kg/kg coal	$\beta_3 = 120$	$x_{01} = 120$
	$m_{02} = 0.049$ kg/kg coal	$\alpha = 2$	$x_{02} = 170$
	$m_{03} = 0.041$ kg/kg coal	$\beta_1 = 20$	$x_{03} = 275$

The Use of Solid State C-13 NMR Spectroscopy to Study Pyridine Extracted and Extraction Residues in the Argonne Premium Coals

R. J. Pugmire,* M.S. Solum, S. Bai, +
T.H. Fletcher,** S. Woods,+ and D.M. Grant****
Departments of Chemical & Fuels Engineering* and Chemistry**
University of Utah, SLC, UT 84112
and
Departments of Chemistry+ and Chemical Engineering**
Brigham Young University, Provo, UT 84602

INTRODUCTION

The relationship between coal structure and combustion behavior is a matter of on-going research in our laboratories. A great deal of effort has gone into obtaining data that is used for modeling studies of devolatilization behavior.¹ We have also carefully studied the process of char formation.²⁻³ Our past work has focused on trying to understand the relationship between coal/char/tar formation² as they relate to the devolatilization and char oxidation phenomena. The formation of metaplast during pyrolysis was studied by Fong and Howard⁵ in terms of extractable material obtained at different stages of the devolatilization process. We have recently turned our attention to metaplast formation in devolatilization and plan to conduct a series of experiments that will help define the formation and chemical structure of metaplast in coals of different rank.

Howard and Fong used pyridine extraction methods to quantify the amount of metaplast formed during pyrolysis of a Pittsburgh #8 coal. These experiments demonstrated that pyridine extractable material initially increased with pyrolysis temperature, passed through a maximum, and then decreased as retrogressive reactions became dominant at the higher temperatures. We have completed an initial study of the pyridine extraction of the Argonne Premium coal samples and the detailed study of the carbon skeletal structure of the extracts and the extraction residues from these coals. The ¹³C NMR data obtained from these extracts and extraction residues will be compared with the extracts and extraction residues formed at different stages of the pyrolysis process in these coals as our pyrolysis work develops.

EXPERIMENTAL

It is well known that a considerable amount of material is extracted by pyridine from bituminous coals. However, a significant part of the extract seems to form colloidal dispersions that can be disruptive to analytical techniques such as proton and carbon NMR spectroscopy. It is also known that pyridine is imbibed into the structure of coal and is very difficult to remove. This imbibed pyridine makes it difficult to quantify the structural features of coals. We adopted the technique of Buchanan⁶ in an effort to minimize the formation of colloidal dispersions. Extractions were carried out at room temperature after the manner of Buchanan's procedure with the extraction process taking as much as three days to complete. It was judged that extraction was complete at the point that the pyridine recycle solvent in the Abderhalden extraction apparatus was colorless. The samples were then washed as described by Buchanan and dried at room temperature in a vacuum to remove solvents. Proton NMR spectra were then obtained on the extract to determine the level of incorporation of pyridine into the extract material. In all cases only minor traces of pyridine were observed in the proton NMR spectra.

The carbon-13 NMR spectra of all extracts and extraction residues were obtained according to the procedure of Solum, et al.⁷ High resolution NMR data was obtained on a Varian VXR-500 spectrometer using dimethyl sulfoxide as solvent. It was noted that the solubility of the extracts varied with the coal and that solubilization was not complete for any of the coals. The NMR spectra exhibited the characteristics of high resolution with line widths that would be typical of compounds with molecular weights of several hundred daltons.

RESULTS

The amount of extract obtained from each of the 8 Argonne Premium coals is given in Table 1. The duplicate extractions were run in parallel and the reproducibility of the results appears to be quite adequate. It is noted that a mass closure of at least 94% was obtained on each sample. Figure 1 portrays the extract yield together with the fraction of total carbons that are protonated aromatic carbons in the pyridine extracts and residues. In each case this parameter is found to be higher in the extract than in the residue, indicating that the residue contains a higher fraction of substituted carbons than the extract. In Figure 2, the coordination number of the residues is higher than the extracts with the single exception of the Illinois #6 in which no distinction can be made. The number of bridges and loops in the residues and extracts are shown in Figure 3. This parameter is a measure of the cross link structure that exists between individual aromatic clusters. As one might expect, the residues exhibit a greater number of bridges than are found in the extracts. The single exception, again, is the Illinois #6 coal in which no distinction can be made between the two. In Figure 4, the average aromatic cluster size is given and in each case the size of the extract is less than that of the residue, with the single exception of Illinois #6 where no clear distinction can be made. Figure 5 portrays the number of side chains per cluster in the extracts and residues. From this data no consistent trend can be observed. Figure 6 contains the aromatic characteristics of the extracts from the Argonne coals. As expected, both the carbon and proton aromaticity of the extracts increase with rank with the single exception of the Pocahontas extract. The carbon aromaticity of the residue is also plotted for comparison purposes. Using the proton structural definitions reported by Fletcher, et al.,² it is possible to approximate the contributions 1, 2, and 3-ring aromatic species in the coal extracts. These data are also shown in Figure 6. In Figure 7, the contributions of total α -hydrogens, α -methyls, α -CH₂ groups, and γ -methyls for the pyridine extracts are given. It is interesting to note that the total α -hydrogen and α -CH₂ groups pass through a maximum, as a percent of the total hydrogen in the samples, in the high volatile bituminous coal. As expected, the contributions of γ -methyl groups decrease from lignite through the high volatile bituminous coal range and then increase slightly in the Upper Freeport and Pocahontas extracts.

CONCLUSIONS

Comparing the ¹³C NMR data on the extracts and residues, it becomes apparent why material is extracted from the parent coal. While the CP/MAS spectra of both the extracts and residues are quite similar, an examination of the details of the structure provide the subtle differences in structural detail that are important in describing the extraction process. While one must recognize that we are observing the averages of all the components present in the extracts, the extracted material appears to have many of the structural features that are observed in the macromolecular structure of the coal. The

differences lie in the fact that the number of cross links is reduced and the number of substituents on the aromatic rings is lower in the extracts than in the residues. Hence, these data are consistent with the fact that this material can be extracted since it is not extensively incorporated by means of covalent bonds into the macromolecular structure. The proton NMR data shows that the amount of 2- and 3-ring components present in the extracts increases with the rank of the coal. The aliphatic region of the proton NMR data indicates that: a) the amount of α -methyl groups is essentially the same in all extracts, b) the amount of γ -methyl groups decreases with rank, and c) the amount of α -hydrogen goes through a maximum at the high volatile bituminous rank range.

These data on the extracts will be used to compare the pyridine extractable material that is obtained as these coals are pyrolyzed. Experiments that are now underway in our laboratories together with the results presented herein will be useful in our future work on modeling the transformation that occur during devolatilization and char formation.

ACKNOWLEDGMENT

This work was supported by the National Science Foundation through the Advanced Combustion Engineering Research Center at Brigham Young University and the University of Utah.

REFERENCES

1. T.H. Fletcher, A.R. Kerstein, R.J. Pugmire, and D.M. Grant, A Chemical Percolation Model for Devolatilization: 3. Chemical Structure as a Function of Coal Type, *Energy & Fuels*, 1992, 6, 414.
2. T.H. Fletcher, M.S. Solum, D.M. Grant, S. Critchfield, and R.J. Pugmire, Solid State ^{13}C and ^1H NMR Studies of the Evolution of the Chemical Structure of Coal Char and Tar During Devolatilization, 23rd Symposium (International) on Combustion, The Combustion Institute, 1990, 1231.
3. R.J. Pugmire, M.S. Solum, D.M. Grant, S. Critchfield, and T.H. Fletcher, Structural Evolution of Matched Tar/Char Pairs in Rapid Pyrolysis Experiments, *Fuel*, 1991, 70, 414.
5. W.S. Fong, W.A. Peters, and J. Howard, *Fuel*, 1986, 65, 251.
6. D.H. Buchanan, *Am. Chem. Soc., Div. of Fuel Preprints*, 32, No. 4, p. 293.
7. M.S. Solum, R.J. Pugmire, and D.M. Grant, ^{13}C Solid State NMR of the Argonne Premium Coals, *Energy & Fuels*, 1989, 3, 187.

Table 1
Pyridine Extraction Yields

Coals	Extractable Yield (%)^a	Residue Yield (%)^a	Total Recovery
Stockton	13.8	80.2	94.0
	15.6	80.5	96.1
Pittsburgh #8	26.0	69.1	95.2
	27.0	70.5	97.5
Blind Canyon	31.1	65.3	96.4
	33.1	64.6	97.5
Illinois #6	27.3	67.3	94.6
	28.5	65.1	93.6
Upper Freeport	14.8	81.8	96.6
	15.0	82.7	97.7
Wyodak	6.1	92.4	98.5
	6.3	91.7	98.0
Zap	3.0	94.5	97.5
	3.2	94.7	97.9
Pocahontas	0.5	96.8	97.3
	0.5	97.2	97.7

^a Weight percent on a dry basis.

**PROTONATED AROMATIC CARBONS IN
PYRIDINE EXTRACTS AND RESIDUES FROM
ARGONNE COALS**

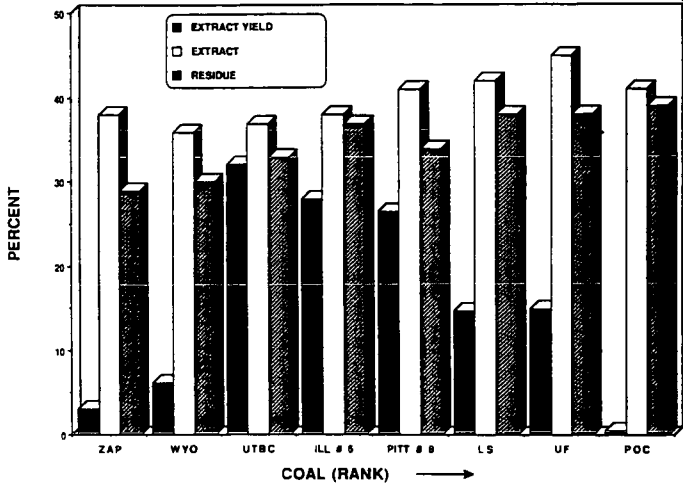


Figure 1. Extract yields and fraction of total aromatic carbons that are protonated (f_aH) in pyridine extracts and residues of the APCS coals.

**COORDINATION NUMBER IN PYRIDINE
EXTRACTS AND RESIDUES IN ARGONNE COALS**

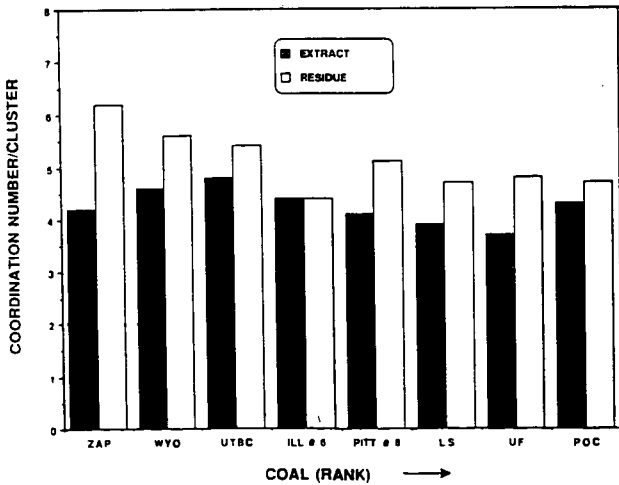


Figure 2. Coordination number in pyridine extracts and residues of the APCS coals.

**BRIDGES AND LOOPS IN PYRIDINE EXTRACTS
AND RESIDUES FROM ARGONNE COALS**

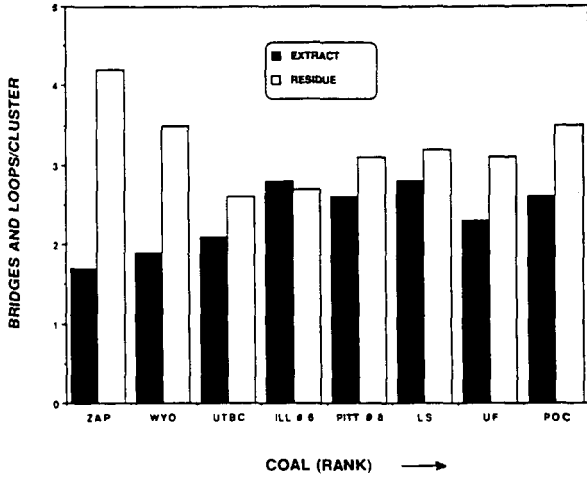


Figure 3. Number of bridges and loops per cluster in pyridine extracts and residues of the APCS coals.

**AVERAGE AROMATIC CLUSTER SIZE IN
PYRIDINE EXTRACTS AND RESIDUES
FROM ARGONNE COALS**

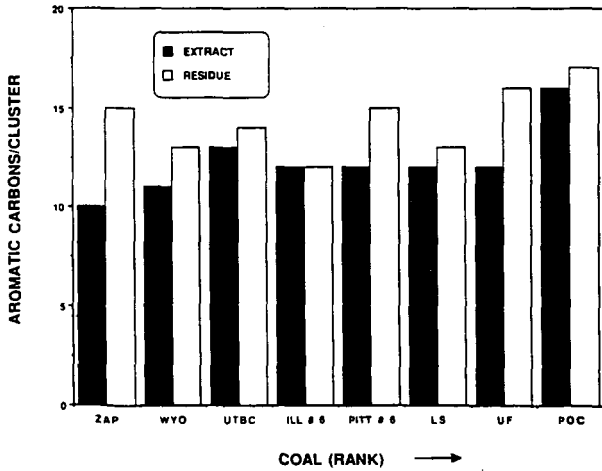


Figure 4. Average aromatic cluster size in the extracts and residues of the APCS coals.

SIDE CHAINS IN PYRIDINE EXTRACTS AND RESIDUES FROM ARGONNE COALS

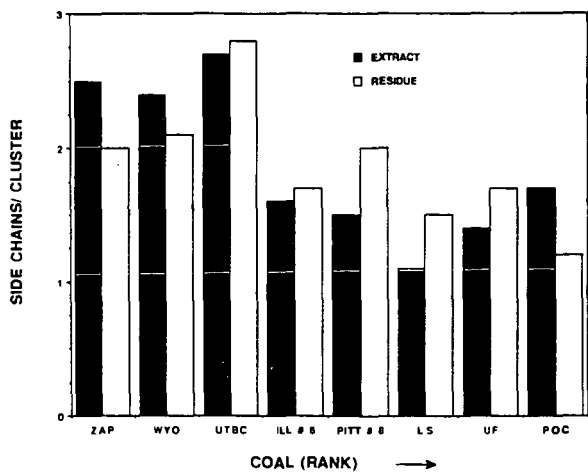


Figure 5. Number of side chains per cluster (coordination number) in the extracts and residues of the APCS coals.

AROMATIC CHARACTERISTICS OF PYRIDINE EXTRACTS FROM ARGONNE COALS

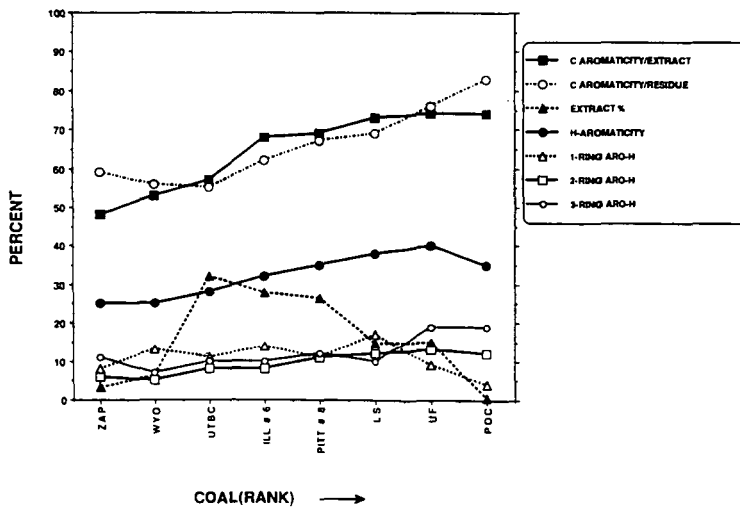


Figure 6. Aromatic characteristics in the extracts and residues of the APCS coals.

**ALIPHATIC PROTON STRUCTURAL PARAMETERS
IN PYRIDINE EXTRACTS FROM ARGONNE COALS**

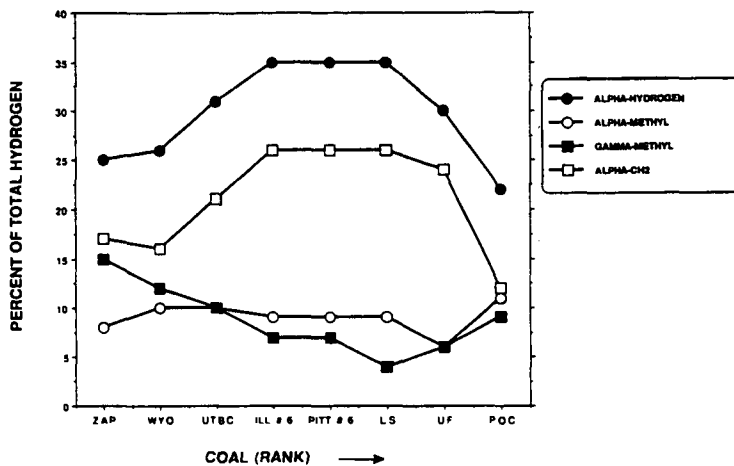


Figure 7. Aliphatic proton structural parameters of the APCS coals.

ORGANIC VOLATILE MATTER AND ITS SULFUR-CONTAINING COMPOUNDS PRODUCED BY COAL PYROLYSIS

M.-J.M. Chou, C.W. Kruse, and J.M. Lytle, Illinois State Geological Survey, Champaign, IL 61820
K.K. Ho, Illinois Clean Coal Institute, Carterville, IL 62918-0008

Keywords: coal, pyrolysis, volatile matter

INTRODUCTION

The types and distributions of the major components in the volatile matter produced from two types of coal pyrolysis were examined. Batch pyrolysis was used to produce coal tars for fractionation and characterization. Flash pyrolysis, in combination with gas chromatography (GC) analysis, showed a broad distribution of the volatile organics, including sulfur-containing compounds. Further characterization of these volatile sulfur compounds should provide the understanding needed of coal's behavior during thermal processing, an understanding critical for cleaning coal through flash pyrolysis or thermal pre-treatment processes.

EXPERIMENTAL

Tar Collection, Separation, and Characterization - Batch Pyrolysis: About 100 g of coal was pyrolyzed at 450 °C or 600 °C in a Parr reactor (1). The tar was delivered through a heated quartz tube to a collection flask containing a mixture of tetrahydrofuran and dimethoxypropane at -30 °C. After evaporation of the solvents, the tar was fractionated into acid, base, neutral-nitrogen, saturates, and aromatic fractions by ion-exchange, coordination, and adsorption chromatography (SARA) (2). The *n*-paraffins, separated from the saturates by a molecular sieve method (3), were analyzed by GC. Three solvents (5% benzene in pentane, 15% benzene in pentane, and 20% benzene/20% ethyl ether/60% methanol) were used to separate aromatic fractions into three subfraction by column chromatography on alumina. The fractions were designated monoaromatics, diaromatics and polyaromatics, and identified as SAF-1, SAF-2, and SAF-3, respectively (4). Elemental analyses were performed on each subfraction.

On-line Analysis of Volatile Matter from Flash Pyrolysis: A Perkin-Elmer 3920B gas chromatograph (GC) with a flame photometric detector (FPD) and a flame ionization detector (FID) and a Dexsil-300 column (programmed for 8 °C/min from 50 °C to 280 °C) was used. Coal volatile matter was produced by a Chemical Data System pyroprobe 190 pyrolyzer in the GC's injection port. Pulverized coal (5 mg to 15 mg) in a 25 mm by 2.4 mm quartz tube was heated at 75 °C/msec in the GC's helium carrier gas flowing at 30 mL/min. Samples were preheated at 100 °C for 30 seconds prior to the first analysis. A given sample was analyzed at 300 °C, 400 °C, 500 °C, 600 °C, 700 °C, and 800 °C. The pyroprobe temperature was held at each temperature for 20 seconds and then it was allowed to return to the injection port temperature during the 37 minutes required for the GC analysis of the volatile matter from each step using the FID. A new coal sample was analyzed at 600 °C with FPD for sulfur compounds.

RESULTS AND DISCUSSION

Batch Pyrolysis Products: The amount of tar obtained from the pyrolysis of six coals (Table 1) varied from 3 to 15 weight percent of the raw coal and the yields were approximately proportional to the H/C atomic ratio of the raw coal. Yields of fractions separated from each coal by the SARA method are also listed in Table 1. The aromatic fraction was generally the largest fraction in the tars. Elemental analysis of the SARA fractions from one coal sample (Table 2) showed most of the nitrogen to be in the base fraction. Sulfur was more evenly distributed but it too was highest in the base fraction.

The C, H, N, and S contents of the three aromatic subfractions are listed in Table 3. The H/C ratio decreased as expected for a progression of increasing aromaticity from monoaromatics (SAF-1) to the polyaromatics (SAF-3). Sulfur in the aromatic fractions was detected only in the polyaromatic subfractions, and this trend was observed both at 450 °C and 600 °C. The nitrogen content within the aromatic subfractions varied in a similar fashion, especially at 600 °C. The lack of sulfur and nitrogen in the monoaromatics and diaromatics fractions may be due a higher ratio of the functional group(s) to carbon atoms in the hydrocarbon portion of the molecule, or to having both sulfur and nitrogen in the same small molecule. Either factor might result in the partitioning of these aromatics into earlier SARA fractions,

possibly the basic fraction. Further study is needed to identify the S and N functional groups and learn more about their positions in the structure of molecules in order to understand the solvent partitioning properties seen in this study and other studies (3, 5). GC/FPD chromatograms of two SAF-3 fractions show most of the sulfur-containing compounds to be in the GC retention time range starting with dibenzothiophene and beyond as expected of a polyaromatic fraction. They also indicated that the distribution of sulfur-containing compounds of the high-sulfur Illinois coal (Figure 1, B) was much more complex than those of the low-sulfur Alabama coal (Figure 1, A).

Patterns among tars for the distribution of n -paraffins are indicated in Figure 2. The effect of different pyrolysis temperatures (450 and 600 °C) on n -paraffins distribution of the same coal sample was minor. Calkins et al. (6) who studied flash pyrolysis of pure n -paraffins and also low-temperature tar showed that n -paraffins in low temperature tar (<600 °C) were the precursors of light hydrocarbon gases, such as ethylene and propylene, that were produced when the low temperature tar was further subjected to a much higher temperature (700-800 °C) heating. The current results indicated that there was not much more cracking of n -paraffins at 600 °C than at 450 °C. The distribution of chain lengths appeared to be related to coal rank. As indicated in Figure 2, the major n -paraffins from lignite were distributed between C₁₄ and C₂₁. The distributions of the major n -paraffins produced from high volatile bituminous (hvCb) and medium volatile bituminous (mvb) coals were in a relatively narrow carbon number band compared to the broad band obtained from the lignite sample, and they peaked at C₁₇. The two pyrolysis temperatures (450 and 600 °C) appeared to induce a similar thermal extraction of n -paraffins in coal (7,8). The lower rank, less mature LigA contains more longer chain n -paraffins than the higher rank, relatively more mature hvCb and mvb coals.

Cross Polarization/Magic Angle Spinning (CP/MAS) solid state ¹³C NMR has been used to determine the aliphatic and aromatic compositions of the raw coals (9). In this study, three raw coals were analyzed by the CP/MAS NMR. The analysis condition and peak assignment are described elsewhere (10). The percent of total carbon in aliphatic positions was 48% for LigA coal, 54% for the hvCb, and 34% for the mvb coal. Comparison of the NMR data with the n -paraffins data from batch pyrolysis suggests that more paraffin, algae/resins-derived material (11) is found during the relatively early stages of coalification, and perhaps more branch/cyclic or aromatic associated aliphatic material occurs in coal at later stages of coalification. The NMR analysis does not distinguish among these aliphatic types.

Flash Pyrolysis Products: Typical step wise pyrolysis GC/FID chromatograms of LigA, hvCb and mvb coals are shown in Figure 3. The chromatograms of these coals indicated that volatilization of heavy hydrocarbons in coal took place mainly between 500 °C and 700 °C. The maximum production appears to be rank dependent. The maximum volatility appears to be lower than 600 °C for lignite, at 600 °C for hvCb coal, and higher than 600 °C for mvb coal (Figures 3a, 3b, and 3c, respectively). These observations are consistent with those of Barker (12) on programmed-temperature pyrolysis of vitrinite of various rank coals. His programs, showing the GC detector response as a function of temperature, indicated a single maximum at 660 °C for higher rank samples and 420 °C for lignite samples.

In the present study, through GC fingerprint analysis, volatile organics were examined in more detail in the C₁₅+ region. The components in this region appeared to be less branched for the lignite. The proportion of the long straight chain aliphatic components decreased as the rank of the coal increased from ligA, hvCb, to mvb. These results are consistent with the earlier suggestion that the low-rank coal contained a greater degree of longer chain aliphatic hydrocarbons.

GC chromatograms of volatile organic sulfur compounds produced from flash pyrolysis of three coals at 600 °C were compared. As indicated in Figure 4, the GC fingerprint of products from the high-sulfur Illinois coal (hvCb) was much more complex than those of the low-sulfur Alabama coal (mvb) and the low-sulfur North Dakota lignite (LigA). The GC chromatogram of sulfur compounds from high sulfur Illinois hvBb coal has material with retention times expected of aliphatic sulfides, thiophene, and alkylthiophene isomers. The large envelop fraction at 15 minutes to 40 minutes retention time corresponds to retention times expected of benzothiophene and dibenzothiophene having an array of side chains. Additional high-sulfur Illinois coals were analyzed. Their fingerprints (not shown) indicate that the types of volatile organic sulfur compounds in other Illinois coals were quite similar. They were present in a much greater variety and in larger quantities than those of either the Alabama coal or the North Dakota lignite. The GC/FPD chromatograms obtained from the flash pyrolysis of raw coal were consistent with those of SAF-3 fractions

(Figure 1). They indicated that the distribution of sulfur-containing compounds of the high-sulfur Illinois coal was much more complex than that of the low-sulfur coal. Flash pyrolysis of raw coal with on-line GC/FPD analysis of sulfur volatile matter (Figure 4) showed sulfur-containing compounds as a broad peak in the region corresponding to retention times for benzothiophene (two aromatic rings) and dibenzothiophene (three aromatic rings). The sulfur compounds in the SAF-3 fractions (Figure 1) are better resolved. The absence of sulfur in SAF-1 and SAF-2 (Table 3), despite the presence sulfur compounds in pyroprobe products corresponding to their molecular weight range (Figure 1), suggests that sulfur in this molecular weight range may be in basic nitrogen molecules separated by the SARA method into another fraction.

SUMMARY AND CONCLUSION

With one exception, the aromatic fraction was the largest fraction isolated. The sulfur-containing compounds were observed to concentrate in the polyaromatic subfraction of the three aromatic subfractions, and this tendency was observed for both 450°C and 600°C samples. This study indicated that the distribution of sulfur-containing organic compounds in the tar produced from the high-sulfur Illinois coal was much more complex than that of the low-sulfur coal. Although there are numerous sulfur compounds in flash pyrolysis products having molecular weights up through those of benzothiophene and dibenzothiophene, sulfur compounds did not appear in the monoaromatics and diaromatics subfractions. We postulate that sulfur in the molecular weight compounds below dibenzothiophene may be in compounds having a basic nitrogen as well. Sulfur as well as nitrogen were the highest in the SARA base fractions as would be expected by this postulate. This would account for the absence of this molecular weight range of sulfur compounds in the SARA aromatic fraction. The nitrogen compounds in batch pyrolysis tars partitioned mainly into the base fraction of the tar, whereas the sulfur-containing compounds were more evenly distributed between the base, neutral-nitrogen, and aromatic fractions. This study also indicated that flash pyrolysis in a pyroprobe is a fast method to screen and compare sulfur-containing compounds produced during thermal treatment of coals of different rank.

The observation that the distributions of *n*-paraffins in tars produced at 450°C or 600°C from a given coal were essentially the same supports the view that these *n*-paraffins are thermal extraction products, not cracking products. The variations in the distributions of the *n*-paraffins from coals of different rank show that the lower rank, less mature LigA contained more longer chain *n*-paraffins than the higher ranks. The NMR spectra of raw coal together with the batch pyrolysis *n*-paraffins GC analysis support the view that algae/resins-derived *n*-paraffinic material occurring during the relatively early stages of coalification may have been converted to branched/cyclic material and ultimately either eliminated as light hydrocarbons or converted to aromatics as coalification progressed toward anthracite. The preponderance of relatively long chain aliphatic hydrocarbons in low-rank coal was also seen in the GC spectra of flash pyrolysis products.

ACKNOWLEDGMENTS

Support for this research was provided by the Illinois State Geological Survey and the U.S. Environmental Protection Agency, Fuel Process Branch, Research Triangle Park, North Carolina, under Contract 68-02-2130 to the University of Illinois: "Characterization of Coal and Coal Residues." The current publication and continued research on coal desulfurization are supported by the Illinois Clean Coal Institute (ICCI). The authors are indebted to D.R. McKay, and J.S. Frye of the Colorado State University for NMR analysis and to two members of the ISGS staff, R.H. Shiley for coal tar generation by batch pyrolysis and D.D. Dickerson for the technical assistance in coal tar fractionation.

REFERENCES

1. Cahill, R.A., R.H. Shiley, and N.F. Shimp, 1982, "Forms and Volatiles of Trace and Minor Elements in Coal," Illinois State Geological Survey, EGN 102:6.
2. Jewell, D.M., J.H. Weber, J.W. Bunker, H. Plancher, and D.R. Latham, 1972, "Ion-Exchange, Coordination, and Adsorption Chromatographic Separation of Heavy-Petroleum Distillates," *Anal. Chem.*, 44:1391-95.
3. O'Connor, J.G., F.H. Burow, and M.S. Norris, 1962, "Determination of normal paraffins in C₂₀ to C₃₂ paraffins waxes by molecular sieve chromatography," *Anal. Chem.*, 34(1):82-85.
4. Selucky, M.L., Y. Chu, T. Ruo, and O.P. Strausz, 1977, "Chemical Composition of Athabasca Bitumen," *Fuel*, 56: 369-381.

5. Farcasiu, M., 1977, "Fractionation and Structural Characterization of Coal Liquid," *Fuel*, 56:9-14.
6. Calkins, W.H., and R.J. Tyler, 1984, "Polymethylene Compounds in Low-Temperature Flash Pyrolysis Tars," *Fuel*, 63:1119-1124.
7. Given, P.H., A. Marzec, W.A. Barton, L.J. Lynch, and B.C. Gerstein, 1986, "The Concept of a Mobile or Molecular Phase Within the Macromolecular Network of Coals: A Debate," *Fuel*, 65:155-164.
8. Yun, Y., H.L.C. Meuzelaar, N. Simmleit, and H.-R. Schulten, 1991, "Mobile Phase in Coal Viewed from a Mass Spectrometric Perspective," In *ACS Symposium Series*, 461:89-110.
9. Solum, M.S., R.J. Pugmire, and D.M. Grant, 1989, "¹³C Solid-State NMR of Argonne Premium Coals," *Energy and Fuels*, 3(2):187-193.
10. Chou, M.-I.M., D.R. Dickerson, D.R. McKay, and J.S. Frye, 1984, "Characterization of Coal Chars from a Flash Pyrolysis Process by Cross Polarization/Magic Angle Spinning ¹³C NMR," *Liquid Fuels Technology*, 2(4):375-384.
11. Colin, E.S., W.R. Landner, and K.D. Bartle, 1985, "Fate of Aliphatic Groups in Low-Rank Coals During Extraction and Pyrolysis Processes," *Fuel*, 64:1394-1400.
12. Barker, C., 1974, "Programmed-Temperature Pyrolysis of Vitrinites of Various Rank," *Fuel*, 53:176-177.

Table 1. Yields of pyrolysis products from six coal samples

Coal	(seam)	Blue Creek	Herrin (No. 6)	Herrin (No. 6)	Herrin (No. 6)	Springfield (No. 5)	Ft. Union Formation
Coal Sample Number		C-18848	C-18857	C-16501	C-18560	C-16264	C-18440
State		Alabama	Illinois	Illinois	Illinois	Illinois	N. Dakota
Rank		mvb	hvBb	hvBb	hvCb	hvCb	ligA
H/C Atom Ratio (mf)		0.67	1.05	0.85	0.85	0.85	0.78
Type of sample		composite face channel	face channel	composite face channel	column	composite face channel	face channel
Tar Yield (wt %)	450°C	3.2	14.5	10.4	12.1	11.9	7.3
	600°C	3.1	14.6	15.8	12.2	13.8	8.3
Tar Sample No.	450°C	T-18848	T-18857	T-16501	T-18560	T-16264	T-18440
Tar fraction recovered from chromatography (wt%)							
	Acid	10.4	11.7	26.0	11.1	52.2	10.4
	Base	2.5	2.7	1.0	8.6	2.3	5.1
	Neutral-Nitrogen	--	2.4	2.0	10.5	--	3.4
	Saturate	3.9	5.4	9.0	5.7	8.6	8.2
	Aromatic	57.1	24.9	35.0	46.9	27.6	29.9
Tar Sample No.	600°C	T-18848	T-18557	T-16501	T-18560	T-16264	T-18440
Tar fraction recovered from chromatography (wt%)							
	Acid	27.5	10.3	--	9.3	47.9	12.2
	Base	2.0	5.2	--	7.4	4.0	5.1
	Neutral-Nitrogen	--	5.4	--	0.5	--	3.9
	Saturate	3.5	5.6	--	6.1	7.5	14.5
	Aromatic	57.6	39.1	--	49.0	27.6	46.8

-- not determined

Table 2. Elemental analyses acid, base, and neutral-nitrogen, saturate, and aromatic fractions derived from coal sample C18440.

Fraction	Carbon	Hydrogen	Nitrogen	Sulfur	H/C Atom Ratio
Acid	78.75	7.81	0.12	0.56	1.18
Base	77.29	7.73	3.85	1.13	1.21
Neutral-Nitrogen	78.42	8.18	0.38	0.90	1.25
Saturate	79.75	12.22	--	--	1.84
Aromatic	79.50	9.22	0.30	1.05	1.39

-- not determined

Table 3. Elemental analysis of aromatic subfractions

Coal (seam)		Blue Creek	Herrin (No.6)	Springfield (No. 5)
Tar Sample Number		T-18848-450 °C	T-16501-450 °C	T-16264-450 °C
Aromatic Subfraction 1 monoaromatics (eluted with 5% benzene in n-pentane)	Carbon	89.64	87.06	84.24
	Hydrogen	9.77	10.70	11.60
	Nitrogen	trace	0.18	0.21
	Sulfur	--	--	--
	H/C Atom Ratio	1.30	1.46	1.64
Aromatic Subfraction 2 diaromatics (eluted with 15% benzene in n-pentane)	Carbon	89.97	87.26	84.91
	Hydrogen	8.02	8.21	9.03
	Nitrogen	0.23	0.07	0.25
	Sulfur	--	--	--
	H/C Atom Ratio	1.14	1.12	1.27
Aromatic Subfraction 3 polyaromatics (eluted with mixed solvent: 20% benzene, 20% ethyl ether and 60% methanol)	Carbon	85.81	82.48	84.41
	Hydrogen	7.30	7.32	7.44
	Nitrogen	0.53	0.14	0.24
	Sulfur	1.10	2.37	2.37
	H/C Atom Ratio	0.97	1.06	1.05
<hr/>				
Tar Sample Number		T-18848-600 °C	T-16501-600 °C	T-16264-600 °C
Aromatic Subfraction 1 monoaromatics (eluted with 5% benzene in n-pentane)	Carbon	87.25	87.74	86.71
	Hydrogen	9.55	10.20	10.70
	Nitrogen	--	--	--
	Sulfur	--	--	--
	H/C Atom Ratio	1.30	1.39	1.47
Aromatic Subfraction 2 diaromatics (eluted with 15% benzene in n-pentane)	Carbon	90.55	86.14	85.45
	Hydrogen	7.71	7.25	8.01
	Nitrogen	--	--	--
	Sulfur	--	--	--
	H/C Atom Ratio	1.01	1.01	1.12
Aromatic Subfraction 3 polyaromatics (eluted with mixed solvent: 20% benzene, 20% ethyl ether and 60% methanol)	Carbon	86.88	81.90	80.92
	Hydrogen	7.04	6.90	7.81
	Nitrogen	0.35	0.34	0.90
	Sulfur	0.80	3.93	4.29
	H/C Atom Ratio	0.97	1.01	1.15
-- not detectable				

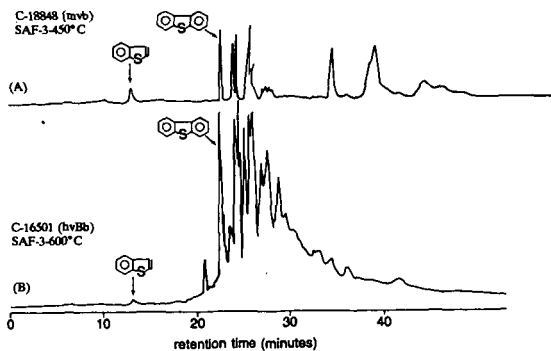


Figure 1. Typical GC/FPD chromatogram of SAF-3 fraction from a low-sulfur Alabama coal (A) and a high-sulfur Illinois coal (B).

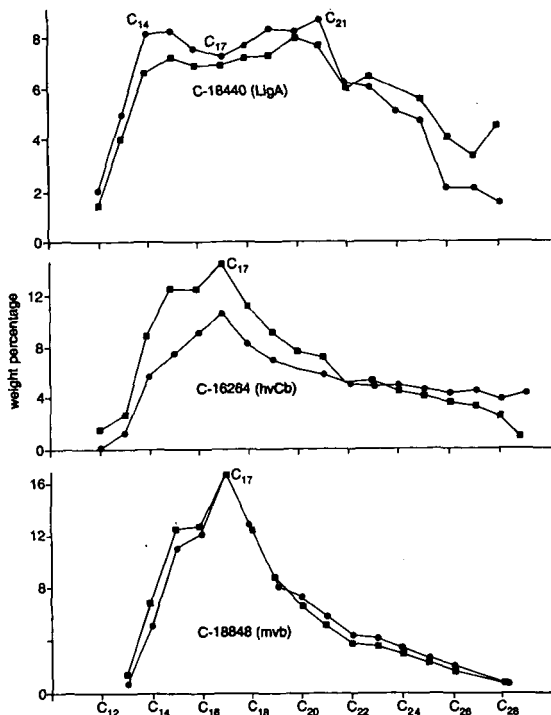


Figure 2. Distribution of n-paraffins obtained from batch pyrolysis three different ranks of coal at 450°C (●) and 600°C (■).

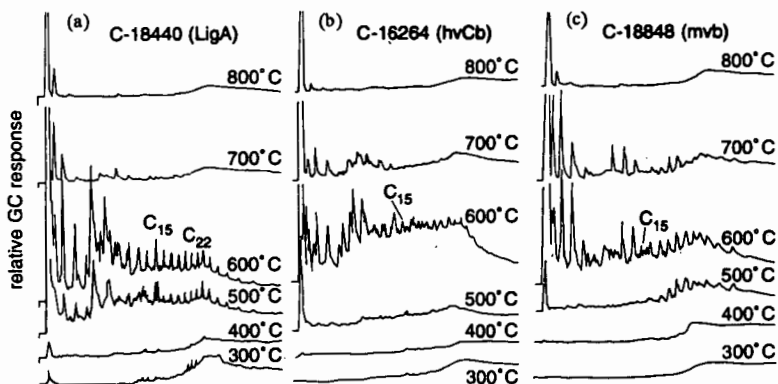


Figure 3. GC/FID chromatogram of organic compounds produced from stepwise flash pyrolysis of three different ranks of coal.

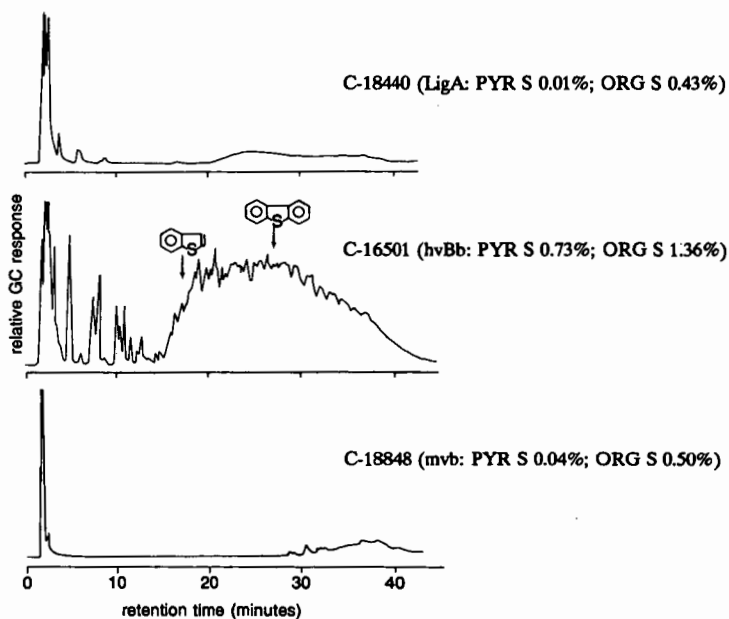


Figure 4. GC/FPD chromatogram of volatile sulfur compounds produced from flash pyrolysis of three different ranks of coal at 600°C.